ZooKeys 1152: 1–8 (2023)
doi: 10.3897/zookeys.1152.96447
https://zookeys.pensoft.net

RESEARCH ARTICLE

A peer-reviewed open-access journal
ZooKeys
Launched to accelerate biodiversity research

A new species of *Aleurolobus* Quaintance & Baker, 1914 (Hemiptera, Aleyrodidae) from China infesting *Murraya exotica* L.

Qing-Song Lin[1], Lin-Qian Lu[1], Ji-Rui Wang[1]

1 *College of Advanced Agricultural Sciences, Zhejiang Agriculture & Forestry University, Lin'an, Zhejiang 311300, China*

Corresponding author: Ji-Rui Wang (jrwang@zafu.edu.cn)

Academic editor: Colin Favret | Received 18 October 2022 | Accepted 13 February 2023 | Published 2 March 2023

https://zoobank.org/1DED8A3D-1715-4B4C-A1A4-C96BA5DE97C7

Citation: Lin Q-S, Lu L-Q, Wang J-R (2023) A new species of *Aleurolobus* Quaintance & Baker, 1914 (Hemiptera, Aleyrodidae) from China infesting *Murraya exotica* L.. ZooKeys 1152: 1–8. https://doi.org/10.3897/zookeys.1152.96447

Abstract

A new whitefly species, *Aleurolobus rutae* **sp. nov.**, collected on *Murraya exotica* (Sapindales, Rutaceae) leaves in the Maolan National Nature Reserve, Guizhou, China, is described and illustrated. Some of the individuals were infected with *Aschersonia placenta*, an entomopathogenic fungus. The insect is circular in shape and characterized by a very wide submarginal region, and the submarginal furrow is almost continuous, with only a small break at the caudal furrow. Anterior and posterior marginal setae are absent, but setae are present on the 8th abdominal segment. Thoracic and caudal tracheal folds are discernible.

Keywords

Aleyrodinae, morphology, new taxa, taxonomy

Introduction

The whitefly genus *Aleurolobus* was erected by Quaintance and Baker (1914), with *Aleurodes marlatti* Quaintance 1903, as its type species by original designation. The genus currently includes 90 species worldwide (Martin and Mound 2007; Dooley and Smith-Pardo 2013; Sundararaj and Vimala 2018); of these, only 16 species are known to occur in China (Dubey and Ko 2009; Yan and Bai 2017). The majority of

species are from the Oriental Region. Dubey and Ko (2009) reviewed the species of this genus from Taiwan, China. *Aleurolobus* is recognized by having the submargin separated from the dorsal disc by a prominent furrow, the presence of eye spots, and the abdominal segment VIII forming a trilobed figure anterolateral to the vasiform orifice (Dubey and Ko 2009).

Recently, heavy infestations of a new whitefly, *Aleurolobus rutae* sp. nov., were discovered on *Murraya exotica* L. trees in the Maolan National Nature Reserve, Guizhou Province, China. *Murraya exotica* (Sapindales, Rutaceae) is an economically and medicinally important woody tree in China. It is widely used in daily life, especially in medical treatment, spices, seasonings, and other industries (Chen et al. 2020). It is one of the main crude materials of a patented Chinese compound drug "Sanjiu Weitai", which is a traditional medicine for gastritis (Lu et al. 2021). The new species infesting *M. exotica* might affect the medicinal efficacy of the plant. We also found that some puparia were infected by *Aschersonia placenta*, an entomopathogenic fungus. Further studies of its biological characteristics are warranted to determine its potential as a biological control agent of the whitefly and its role in protecting this tree species.

Materials and methods

Puparia of the new species were collected on *Murraya exotica* trees in the Maolan National Nature Reserve, Guizhou, China; no adults were collected in the samples. The puparia were mounted following the method suggested by Dubey and David (2012). The terminology for morphological structures follows Bink-Moenen (1983), Martin (1985), and Gill (1990). The habitus images were taken using a digital camera Nikon D500 and Keyence VHX-6000 digital microscope from Guizhou University (**GZU**). Puparial measurements and microphotographs were taken using an Olympus (cx33) from Zhejiang Agriculture and Forestry University, Lin'an, China (**ZAFU**). The scanning electron microscope images were taken with a Hitachi SU8010 Scanning Electron Microscope (Hitachi, Japan) from Center of Electron Microscopy, ZAFU. Adobe Photoshop software was used to make small adjustments and to assemble the plates. The holotype is deposited in the Insect Collection of ZAFU.

Taxonomic account

***Aleurolobus rutae* Lin & Wang, sp. nov.**
https://zoobank.org/EB4E769E-5F38-4819-B2B6-9C7851D0645E

Type material. ***Holotype*** puparium: China, Guizhou, Qiannan state, Maolan National Nature Reserve, 25°28.98'N, 108°07.10'E, 1190 m, 1 puparium on slide, 7. vii. 2022, leg. ST Meng, on *Murraya exotica*, deposited in ZAFU, Lin'an, China.

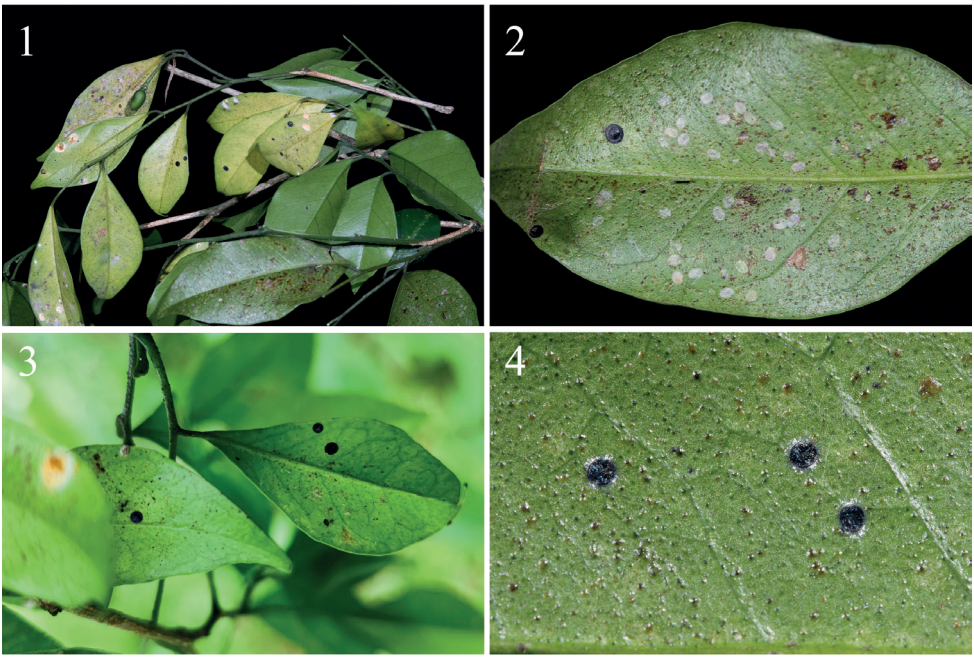

Figures 1–4. *Murraya exotica* leaves infested by nymphs of *Aleurolobus rutae* sp. nov. **1, 3** puparia with some individuals infected with *Aschersonia placenta* **2** *Dialeuropora murrayae* (pale nymphs) coexisting among *A. rutae* (dark nymphs) **4** third instar nymph of *A. rutae*.

***Paratypes*:** 17 paratype puparia with same collection data as the holotype; of these14 puparia on 14 slides are deposited in ZAFU, 2 on 1 slide are deposited in Guizhou University and 1 on 1 slide are deposited in Shanghai Entomological Museum, Chinese Academy of Sciences.

Diagnosis. *Aleurolobus* is recognized by having the submargin separated from the dorsal disc by a prominent furrow, the presence of eye spots, and the abdominal segment VIII forming a trilobed figure anterolateral to the vasiform orifice. The key characteristics that distinguish the new species from other *Aleurolobus* species is that it has a very wide submarginal region and lacks dorsal setae except the 8th segment abdominal. Puparium black, circular, surrounded by a fringe of transparent shiny white wax and some wax deposition on the dorsum of the thoracic and abdominal segments, as well as along the thoracic tracheal folds (Figs 5–7, 9). The submargin is very wide and flattened and is separated from the dorsal disk by an uninterrupted submarginal furrow which extends around the entire body (Figs 5, 6, 9, 13, 16). An elongate, rectangular area with many minute tubercles extends from the tracheal opening approximately halfway to the submarginal furrow (Figs 10, 13, 16). The submargin in some specimens has 85–89 lanceolate setae present on each side, arranged in three rows (Figs 13, 15). The longitudinal molting suture and transverse molting suture both reach the submargin

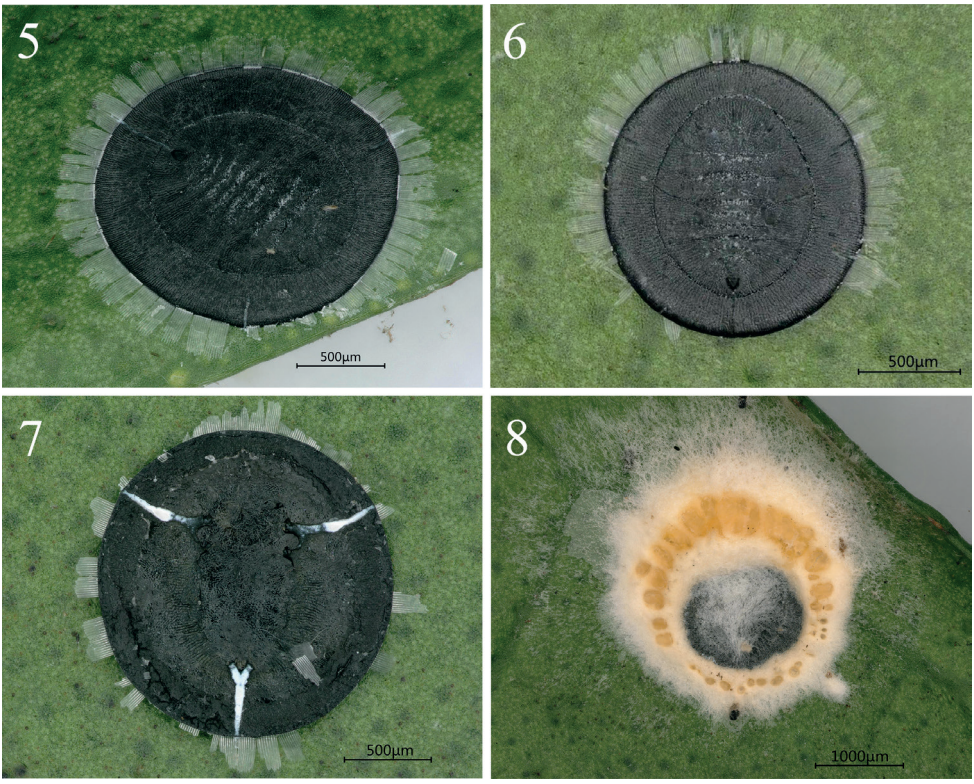

Figures 5–8. Live *Aleurolobus rutae* sp. nov. on *Murraya exotica* leaves **5, 6** puparia in dorsal view **7** puparium in ventral view **8** puparia infected with *Aschersonia placenta* fungus.

(Figs 9, 13, 16). The vasiform orifice is triangular, slightly longer than wide, lateral margins are rounded, with the basal ends curved to meet the basal margin; operculum triangular, almost covering the orifice and obscuring the lingual (Figs 11, 15, 18). Anterior and posterior marginal setae are absent. Caudal and dorsal setae, other than those in the submarginal region, are absent. The eighth abdominal segment setae is present (Fig. 11). Thoracic and caudal furrows are discernible (Figs 10, 12, 14, 15).

Description. ***Puparium*** black, large, 1.762–1.829 mm long, 1.725–1.833 mm wide, circular and nearly flat: the length–width ratio close to 1:1. Pupal margin surrounded by a fringe of transparent, shiny, white wax with some wax deposition on the dorsum of the thorax and abdominal segments, as well as along the thoracic tracheal fold (Figs 5–7, 9).

Margin (Figs 10, 14, 17) crenulate, with eight or nine crenulations in 0.1 mm, each one with an apical notch. Anterior and posterior marginal setae are absent.

Dorsum**:** submargin broad and flat, separated from the dorsal disc by an uninterrupted submarginal furrow which extends around the entire body and with 85–89 submarginal, lanceolate setae present each side arranged in three rows (Figs 13, 15). An elongate, rectangular area with many minute tubercles extends from the tracheal opening approximately halfway to the submarginal furrow (Figs 10, 13, 16). The longitudinal molting suture and transverse molting suture both reach the submargin

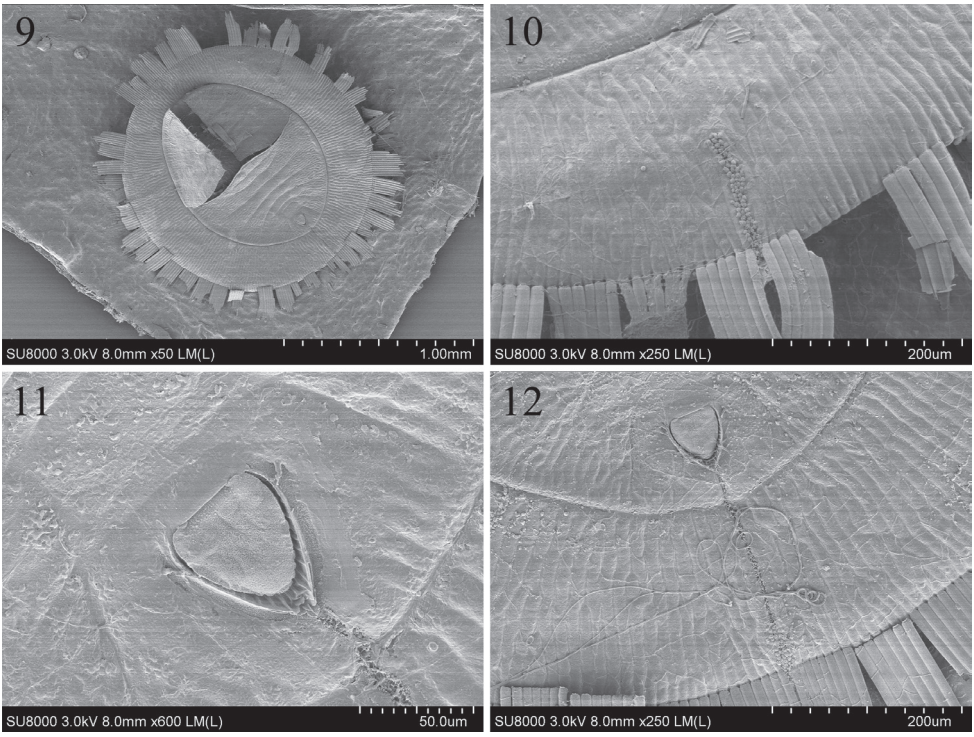

Figures 9–12. Scanning electron microscope photographs of *Aleurolobus rutae* sp. nov. **9** empty pupal case in dorsal view **10** thoracic tracheal fold and margin **11** vasiform orifice and operculum **12** caudal furrow.

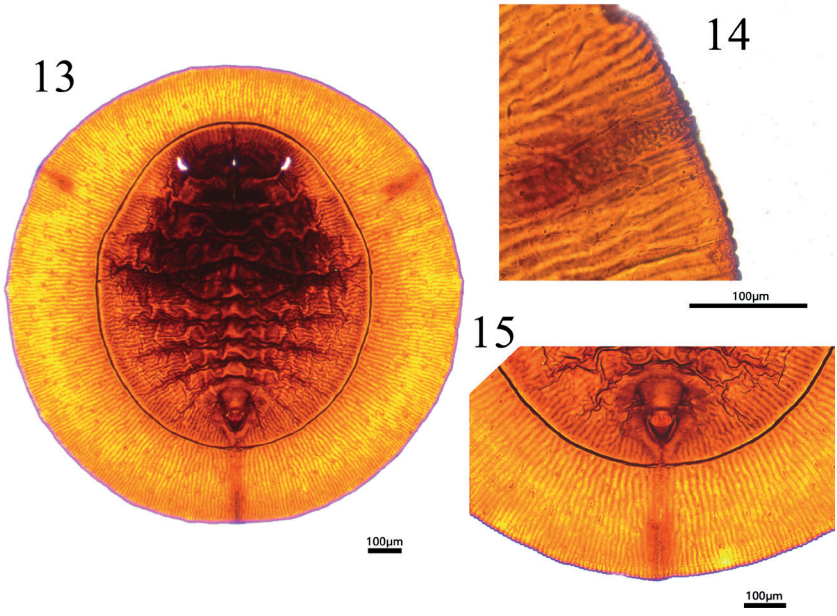

Figures 13–15. *Aleurolobus rutae* sp. nov., slide-mounted specimen **13** dorsum of puparium **14** lateral margin at tracheal opening **15** vasiform orifice, operculum, and caudal furrow.

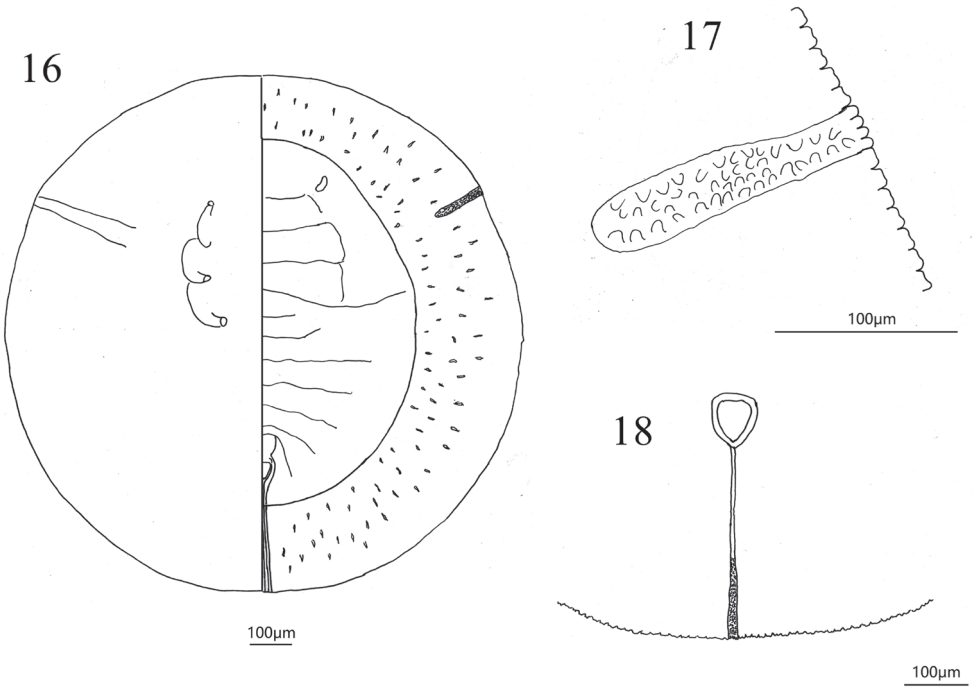

Figures 16–18. *Aleurolobus rutae* sp. nov., holotype puparium **16** puparium in dorsal (right) and ventral (left) views **17** margin **18** vasiform orifice.

(Figs 13, 16). Thoracic and abdominal segment sutures are well defined; length of abdominal segments as measured along the midline as follows: abdominal segment I ~ 77.1 μm; abdominal segment II ~ 68.9 μm; abdominal segments III–V each ~ 81.2 μm; abdominal segment VI ~ 70.2 μm; and abdominal segment VII ~ 38.5 μm. Some small pores are present on dorsum.

Vasiform orifice (Figs 11, 15, 18) triangular, slightly longer than wide, 78.8 μm long, 69.9 μm wide; operculum triangular, 58.4 μm long, 55.4 μm wide, almost covering the orifice and obscuring the lingual. Vasiform orifice set anterior to the caudal end of the puparium by nearly four times its length. Caudal furrow 304.5 μm long. A pair of eighth abdominal setae present, ~10.0 μm, near the anterolateral margin of the vasiform orifice (Fig. 11).

***Venter*:** thoracic and caudal tracheal folds discernible (Fig. 16). Ventral abdominal setae absent.

Third instar nymph (Fig. 4). 0.82 mm long, 0.81 mm wide; the other morphological characteristics are basically identical with those of the puparium.

Host Plant. *Murraya exotica* (Sapindales, Rutaceae).

Distribution. China (Guizhou).

Biology. Three to five specimens were found per leaf (Figs 1, 3, 4), distributed on both sides of leaves, but especially on the upper side. This new species coexists with

Dialeuropora murrayae (Fig. 2). The puparium is covered by a thin layer of white wax, with highly characteristic secretions in the form of a broad, laterally directed, white fringe on each side of the body, 0.21–0.23 mm long (Figs 5, 6, 9). Some puparia were found infected with an entomopathogenic fungus (Figs 1, 8). Results of a polygenic sequencing analysis (ITS, *tef1- a*, SSU, LSU, RPB1, and RPB2; 100% similar to those in NCBI database respectively) identified the fungus as *Aschersonia placenta* Berk (Hypocreales, Clavicipitaceae), a highly effective pathogen of whitefly and scale insects (Wei et al. 2016). *Murraya exotica* is an important medicinal plant, and the research and development of this fungal preparation may be helpful in reducing the damage of whitefly on this plant. The fungal specimen (No. ZHA-ZNL01) and its isolated strain (No. GZ-ZNL01) are both preserved in the Herbarium of Guizhou Institute of Technology. No ants were observed attending the whitefly.

Etymology. The species is named for Rutaceae, the family of its host plant *M. exotica*. The specific epithet is a feminine genitive noun that does not change gender with respect to the genus.

Comments. The puparium of the new species resembles that of *Aleurolobus rubus* in being round in shape, black in color, and in having a broad submargin. It differs in that the puparium of *A. rubus* is smaller and subcircular in shape. Additionally, the vasiform orifice is set anterior to the pupal caudal margin by four times of its own length in the new species, compared to that in *A. rubus*, which is twice its own length. The new species also resembles *Aleurolobus shiiae* but can be easily distinguished from that species which has an elongate, oval shape and minute tubercles located within the thoracic tracheal furrows that almost reache the submarginal furrow. The new species is also similar to *Aleurolobus olivinus*, but it has a very wide submarginal region, and the submarginal furrow is almost continuous with only a small break at the caudal furrow. *Aleurolobus subrotundus*, which has been found on the same host plant, has 10 pairs of long setae along the submargin, as compared to the absence of long setae in *A. rubus* and many minute, submarginal setae in *A. rutae*.

Acknowledgements

We express our deep gratitude to the Shi-Tao Meng (Guizhou University) for offering the specimens. We also express our deep gratitude to the Ling-Sheng Zha (Huaibei Normal University) for the identification of *Aschersonia placenta*. This research was funded by the National Natural Science Foundation of China (31601884), the Research and Development Fund of Zhejiang A&F University (2017FR041).

References

Bink-Moenen RM (1983) Revision of the African whiteflies (Aleyrodidae). Monografieën van de Nederlandse Entomologische Vereniging. Amsterdam 10: 1–211.

Chen CY, Hou LY, Lin B, Zhan RT (2020) Study on genuineness and clinical application of Murrayae Folium et Cacumen. Liaoning Journal of Traditional Chinese Medicine 47(03): 161–164.

Dooley JW III, Smith-Pardo A (2013) Two new species of whiteflies (Hemiptera: Sternorrhyncha: Aleyrodidae: Aleyrodinae) intercepted in quarantine on plants from Asia. The Pan-Pacific Entomologist 89(2): 84–101. https://doi.org/10.3956/2012-61.1

Dubey AK, David BV (2012) Collection, preservation and preparation of specimens for taxonomic study of whiteflies (Hemiptera: Aleyrodidae). In: David BV (Ed.) The Whiteflies or Mealywing Bugs: Biology, Host Specificity and Management. Lambert Academic Publishing, Saarbrücken, 19 pp.

Dubey AK, Ko CC (2009) A review of the genus *Aleurolobus* Quaintance and Baker (Hemiptera: Aleyrodidae) from Taiwan, based mainly on pupal morphology with a description of a new species. Entomological Science 12(1): 51–66. https://doi.org/10.1111/j.1479-8298.2009.00304.x

Gill RJ (1990) The morphology of whiteflies. In: Gerling D (Ed.) Whiteflies, their Bionomics, Pest Status and Management. Intercept, Andover, 13–46.

Lu MQ, Liang HZ, Tu PF, Jiang Y (2021) Pharmacodynamic comparison of two different source plants of Murrayae Folium et Cacumen. Journal of Chinese Pharmaceutical Sciences 30(01): 49–57. https://doi.org/10.5246/jcps.2021.01.005

Martin JH (1985) The whitefly of New Guinea (Homoptera: Aleyrodidae). Bulletin of the British Museum (Natural History). Historical Series 50: 303–351. [Natural History]

Martin JH, Mound LA (2007) An annotated check list of the world's whiteflies (Insecta: Hemiptera: Aleyrodidae). Zootaxa 1492(1): 1–84. https://doi.org/10.11646/zootaxa.1492.1.1

Quaintance AL, Baker AC (1914) Classification of the Aleyrodidae part II. Technical Series Burlin Entomology, United States 27: 97–105. https://doi.org/10.5962/bhl.title.123077

Sundararaj R, Vimala D (2018) Description of two new aleyrodids of the genus *Aleurolobus* Quaintance & Baker (Hemiptera: Aleyrodidae) from India. Journal of Insect Biodiversity 7(2): 24–24. https://doi.org/10.12976/jib/2018.07.2.1

Wei XY, Song XY, Dong D, Keyhani NO, Yao LD, Zang XY, Dong LL, Gu ZJ, Fu DL, Liu XZ, Qiu JZ, Guan X (2016) Efficient production of *Aschersonia* placenta protoplasts for transformation using optimization algorithms. Canadian Journal of Microbiology 62(7): 579–587. https://doi.org/10.1139/cjm-2015-0770

Yan FM, Bai RE (2017) Whitefly Fauna of China. Henan Science and Technology Press, Zhengzhou, 59 pp.

ZooKeys 1152: 9–34 (2023)
doi: 10.3897/zookeys.1152.101100
https://zookeys.pensoft.net

RESEARCH ARTICLE

A peer-reviewed open-access journal
ZooKeys
Launched to accelerate biodiversity research

Androctonus tihamicus sp. nov. from the Mecca Province, Saudi Arabia (Scorpiones, Buthidae)

Abdulaziz R. Alqahtani[1*], Ersen Aydın Yağmur[2*], Ahmed Badry[3*]

1 *Department of Biology, College of Science, University of Bisha, P.O. Box 551, Bisha 61922, Saudi Arabia* **2** *Alaşehir Vocational School, Manisa Celal Bayar University, Manisa, Turkey* **3** *Department of Zoology, Faculty of Science, Al Azhar University, Nasr City, P.O. Box: 11751, Cairo, Egypt*

Corresponding author: Ahmed Badry (ahmedbadry@azhar.edu.eg)

Academic editor: Wilson Lourenço | Received 27 January 2023 | Accepted 18 February 2023 | Published 2 March 2023

https://zoobank.org/8EB9C6B9-2B40-426C-A20E-433B8A39A6F7

Citation: Alqahtani AR, Yağmur EA, Badry A (2023) *Androctonus tihamicus* sp. nov. from the Mecca Province, Saudi Arabia (Scorpiones, Buthidae). ZooKeys 1152: 9–34. https://doi.org/10.3897/zookeys.1152.101100

Abstract

We describe and illustrate a new scorpion species, *Androctonus tihamicus* **sp. nov.**, from the Mecca Province of southwestern Saudi Arabia. The new species is compared to the genus *Androctonus* Ehrenberg, 1828, which is distributed throughout the Middle East, and especially to *A. australis* (Linnaeus, 1758). We provide the molecular phylogeny for this species.

Keywords

Molecular phylogeny, mtDNA, new species, scorpion, Tihamah Plain

Introduction

Androctonus Ehrenberg, 1828 is one of the largest and most widely distributed genera of the family Buthidae (order Scorpiones) in North Africa, the Middle East, and western Asia (Fet and Lowe 2000). The genus has 36 valid species (Rein 2023), of which most species are known to deliver severe stings. *Androctonus* is also very taxonomically confused due to great intraspecific morphological and molecular variation (Ben Ali et al. 2000; Lourenço 2005; Lourenço and Qi 2006, 2007; Lourenço 2008; Othmen

* These authors contributed equally to this work.

et al. 2009; Alqahtani et al. 2022a, b). As already shown by Hendrixson (2006) and Alqahtani et al. (2019), several *Androctonus* species are widely distributed in Saudi Arabia, where they inhabit diverse habitats. Alqahtani et al. (2022c) found intraspecific variation among populations of *A. crassicauda* (Olivier, 1807) from different regions of Saudi Arabia and suggested the existence of cryptic taxa. Also, Hendrixson (2006) noted light-coloured *A. crassicauda*, and Alqahtani et al. (2019) questioned the existence of *A. australis* (Linnaeus, 1758) in Saudi Arabia.

In this study, we examined a *Androctonus* population from Mecca Province, which had been previously reported as *A. crassicauda* (Vachon 1979; Hendrixson 2006). We describe *A. tihamicus* sp. nov. and compare this new species with specimens of *A. australis* from Egypt (Sinai) and other *Androctonus* species from the Middle East. Additionally, we provide the first molecular phylogeny, supplemented by morphological comparisons, of the genus *Androctonus* in Saudi Arabia.

Materials and methods

We collected 21 specimens of *A. tihamicus* sp. nov. at night using ultraviolet light in Mecca Province between 1 September 2018 and 29 January 2022. The specimens were preserved in 96% alcohol. Photographs were taken as described by Yağmur (2021). The trichobothrial nomenclature follows Vachon (1974), and the morphological nomenclature follows Francke (1977), Stahnke (1971), and Hjelle (1990). The male holotype and a female paratype of *A. tihamicus* sp. nov. are deposited at Alaşehir Zoological Museum, Manisa Celal Bayar University, Alaşehir, Manisa, Turkey (**AZMM**) and at the Al-Azhar University Zoological Collection (**AUZC**), Nasr City, Cairo, Egypt.

Molecular analysis

The whole genomic DNA was isolated from four freshly preserved scorpion specimens using Qiagen DNA extraction kits following the manufacturer's instructions. The amplified 16S rRNA gene products were checked and purified (Qiagen) according to the manufacturer's instructions. A fragment of the 16S rRNA gene was amplified via a standard polymerase chain reaction (PCR) using the invertebrate universal primers, as determined and sequenced on an ABI 3500 automated sequencer (Applied Biosystems Inc., USA) and following Gantenbein et al. (1999). The chromatograms and sequences were examined and edited using BioEdit v. 7.2.5 (Hall 1999). Additional sequence data were retrieved from GenBank for *A. amoreux* (Audouin, 1825), *A. australis*, and *A. crassicauda* from Egypt, Iran, Turkey, and Saudi Arabia. A sequence of *Scorpio palmatus* Linnaeus, 1758 (AY156570.1) was downloaded as the outgroup. Sequence data were edited using Mega 6 (Tamura et al. 2013) and aligned using the default settings of ClustalW. Nucleotide composition was calculated from the ingroup sequences only. The genetic distances (*p*-distances) were calculated for the entire data set using Mega 6 (Tamura et al. 2013). Phylogenetic analyses of the 16S data set (n = 35) were

performed as proposed by Alqahtani and Badry (2020). Maximum-parsimony and neighbor-joining analyses were conducted with Paup v. 4 (Swofford 2003) combined with heuristic clustering based on TBR (tree bisection and reconnection) branch swapping. A character was considered missing when a gap was present in an alignment. In addition to 1000 bootstrapping replicates, random additions of taxa were used to assess the degree of confidence within the nodes (Felsenstein 2002). The best-fit nucleotide evolution models were preferred using Paup v. 4 (Swofford 2003) and MrModeltest v. 2.3 (Nylander 2004) based on the Akaike Information Criterion (Akaike 1973). To infer the geographic structure, MrBayes v. 3.1.2 (Ronquist et al. 2012) was used to implement Bayesian inference. The analyses were executed for a million generations, and output parameters were plotted with Tracer v. 1.7 (Rambaut et al. 2018).

Systematics

Family Buthidae C.L. Koch, 1837

Genus *Androctonus* Ehrenberg, 1828

***Androctonus tihamicus* sp. nov.**
https://zoobank.org/1E854848-8838-4EB8-807A-611AFD4A8E39
Figs 1–15; Table 1

Buthus australis citrina (incorrect spelling)–Gough and Hirst 1927: 4.
Androctonus crassicauda–Vachon 1979: 31–34, figs 1, 2, 4.
Androctonus australis–Levy and Amitai 1980: 36, 40; Alqahtani et al. 2019: 21: fig. 2a ; Al-Asmari et al. 2013: fig. 7.
Androctonus crassicauda–Hendrixson 2006: 38–43, figs 1, 2, pl. 1.
Androctonus amoreuxi–Al-Asmari et al. 2013: table 1.

Type materials. ***Holotype*** ♂: **Saudi Arabia**, Mecca Province, Al-Gunfuda, 1.xi.2018, 19.166389°N, 41.099806°E, 10 m a.s.l., Alqahtani A.R. leg. (AZMM/Sco-2018:01). ***Paratypes*** (10 ♀, 10 ♂): **Saudi Arabia**, Mecca Province, Al-Gunfuda, 19.1674°N, 41.0999°E, 8 m a.s.l., 1.xi.2018, 1♀, Alqahtani A.R. leg. (AZMM/Sco-2018:02). Mecca, Province, Al Baydayn, 19.1836°N, 41.2334°E 45 m a.s.l., xi.2018, 2♀, 1♂, Alqahtani A.R. leg. (AUZC/Sco-2018:3-5). Mecca Province, Keyad, xi.2018, 18°42'00.1"N 41°24'00.4"E, 40 m a.s.l., 1♀, 1♂, Alqahtani A.R. & Badry A. leg. (AUZC/Sco-2018:6-7). Mecca Province, Al-Gunfuda, 19.1674°N, 41.0999°E, 8 m a.s.l., 4.I.2022, 6♀, 8♂, Alqahtani A.R. & Badry A. leg. (AUZC/Sco-2022:8-21).

Comparative material. *Androctonus australis*, **Egypt**, Bir El-Abd, north of Sinai Peninsula, 31.0142°N, 32.7486°E, 1♀, 1♂ (AZMM/Sco-2003:03-04).

Etymology. The new species is named after the Tihamah Plain, the coastal plain along the Red Sea.

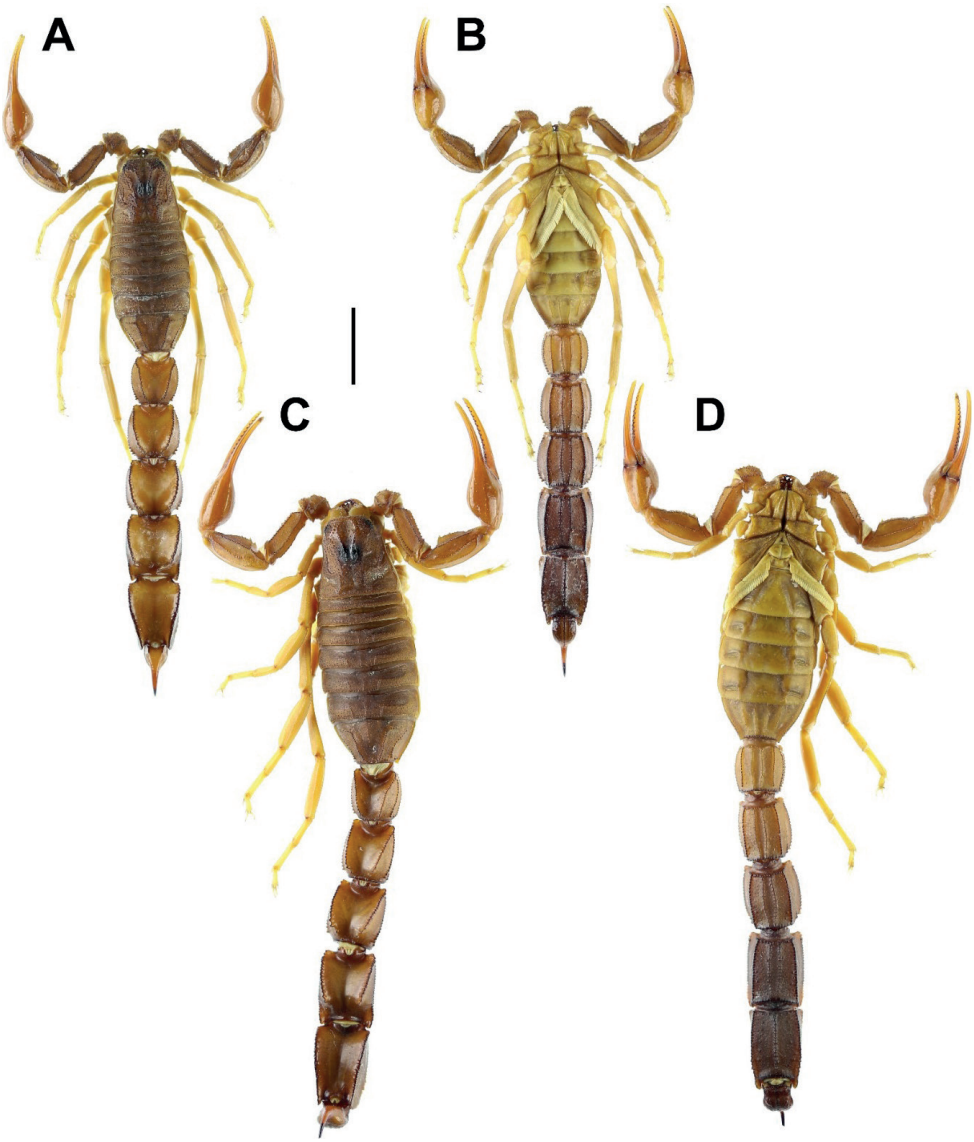

Figure 1. Habitus of *Androctonus tihamicus* sp. nov., male holotype and female paratype **A** male in dorsal view **B** male in ventral view **C** female in dorsal view **D** female in ventral view. Scale bar: 10 mm.

Diagnosis. Medium-sized scorpion with average length 76.15 mm in females and 77.06 mm in males. General color light brown to reddish brown; chela reddish yellow. Legs completely yellow, without any spots in both males and females. Fixed and movable fingers with 13–15 (mostly 14) and 13–15 (mostly 14) principal rows of denticles, respectively. Carapace coarsely granulose; granules at anterior corners larger. Posterior median and central median carinae coarsely granulose and strong. Ventrolateral carinae of metasomal segment V moderately developed, with granules gradually and

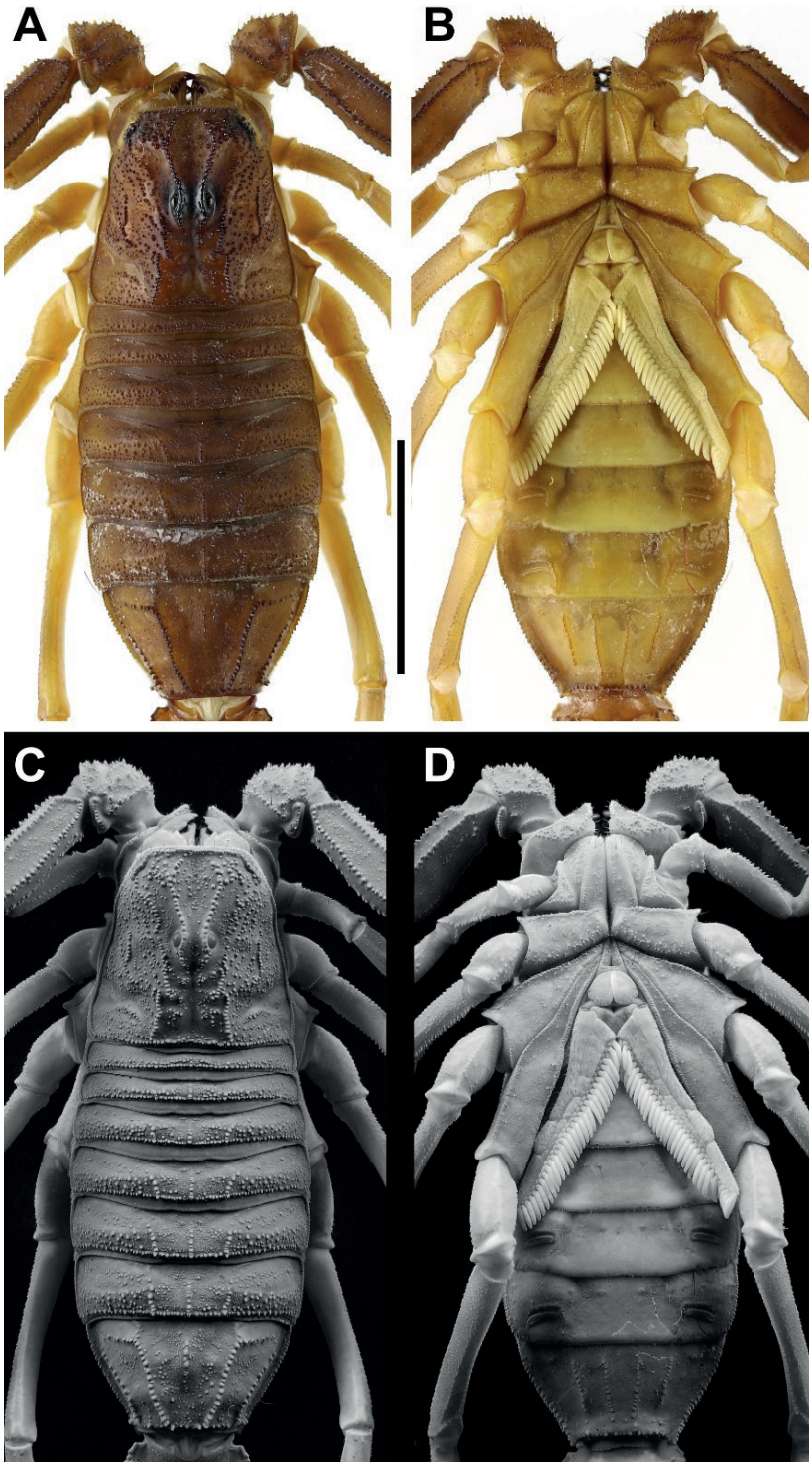

Figure 2. *Androctonus tihamicus* sp. nov., male holotype **A, C** carapace and mesosoma **B, D** sternopectinal area and ventral of mesosoma (**A, B** under white light; **C, D** under UV light). Scale bar: 10 mm.

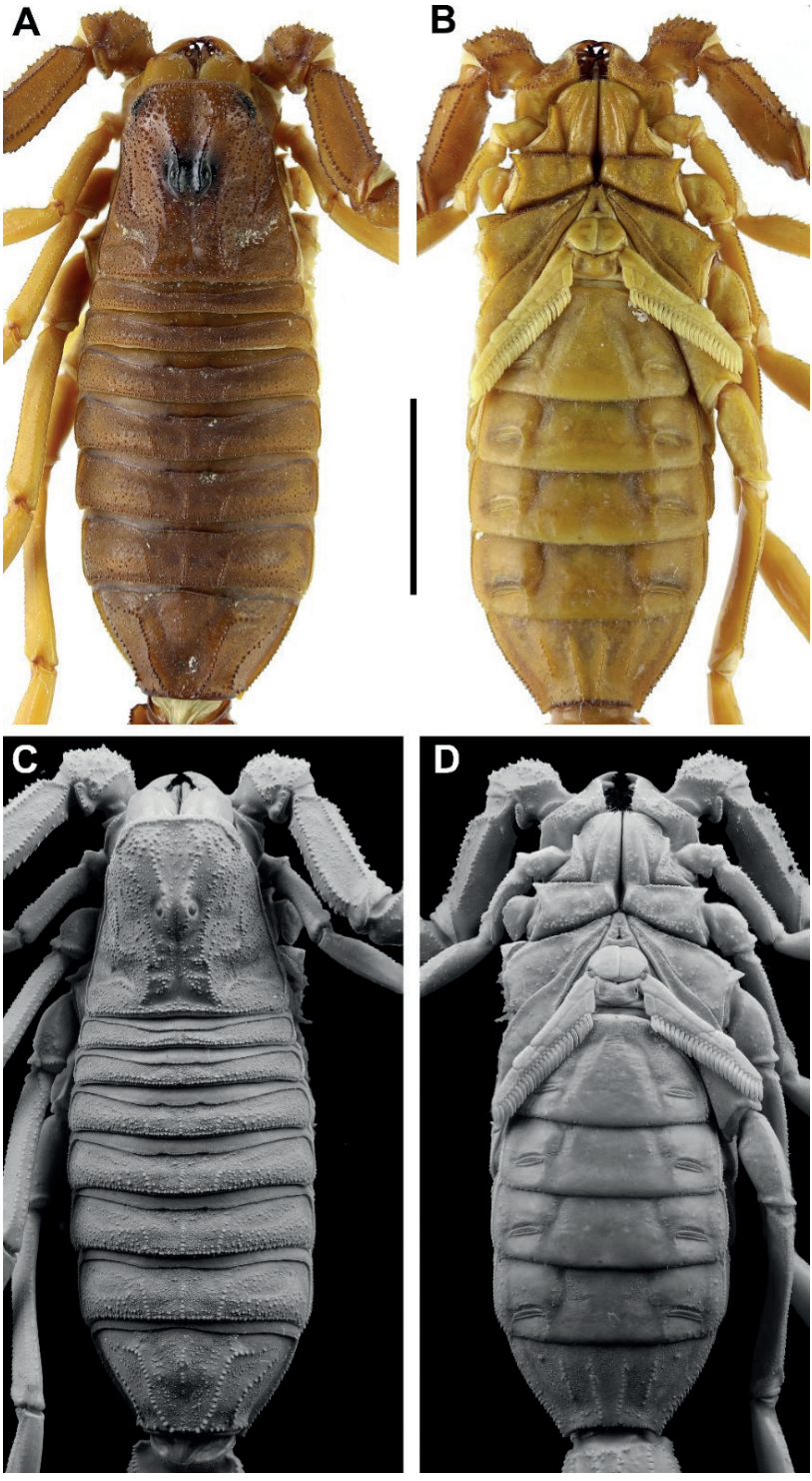

Figure 3. *Androctonus tihamicus* sp. nov., female paratype **A, C** carapace and mesosoma **B, D** sternopectinal area and ventral of mesosoma (**A, B** under white light; **C, D** under UV light). Scale bar: 10 mm.

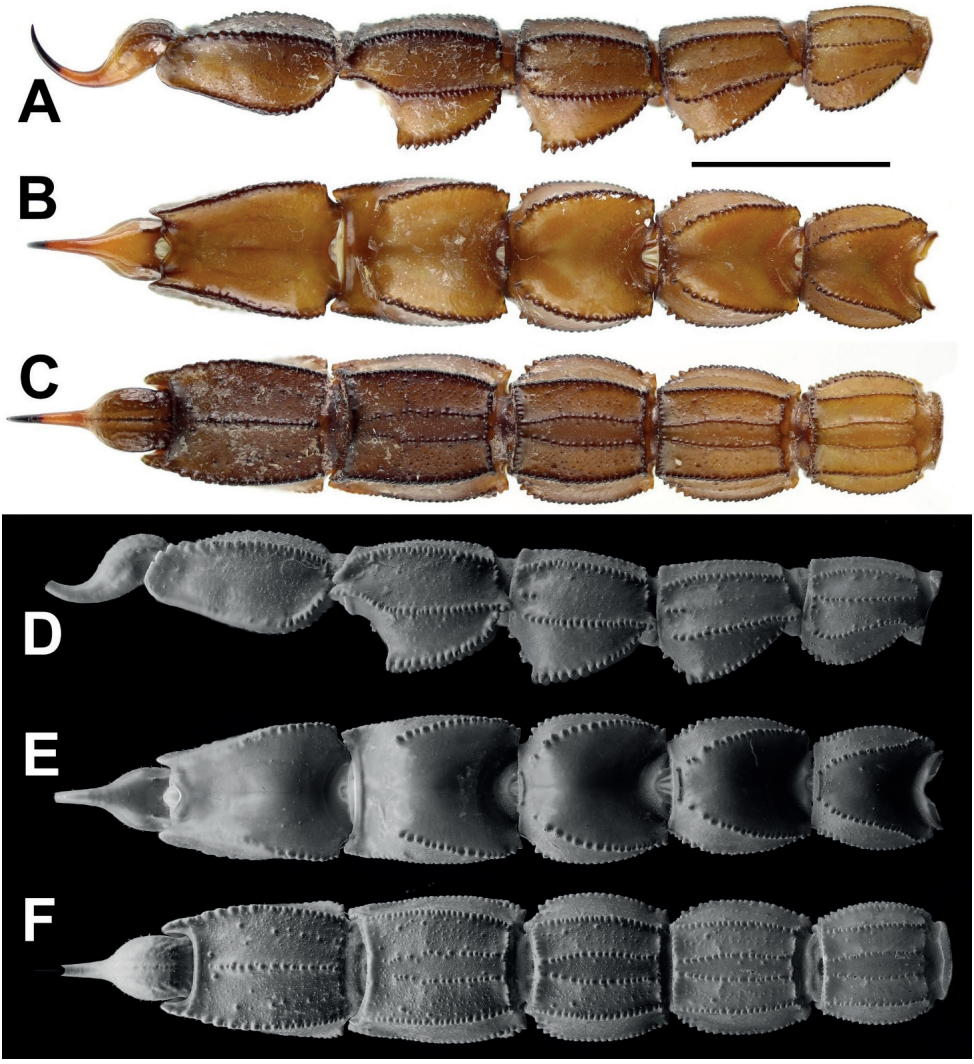

Figure 4. *Androctonus tihamicus* sp. nov., metasoma and telson of male holotype **A, D** lateral view **B, E** dorsal view **C, F** ventral view (**A–C** under white light; **D–F** under UV light). Scale bar: 10 mm.

slightly increasing in size posteriorly. Dorsolateral carinae of segments III–IV strong, with large, serrate, gradually increasing in size granules posteriorly and two large granules posteriorly. Dorsolateral carinae of metasomal segment V with rounded, distinct, large granules anteriorly, and without granules posteriorly. Pectines with 31–33 teeth in males and 23–31 in females.

Description based on holotype. *Coloration*: general color light brown to reddish brown. Prosoma: carapace reddish brown; carinae and surrounds of eyes marked by black pigmentation. Mesosoma: reddish brown, slightly lighter than carapace. Metasoma: segments I–V light brown, ventral surfaces of reddish brown; carinae marked with brown or black pigmentation; vesicle reddish brown anteriorly, light brown posteriorly; aculeus

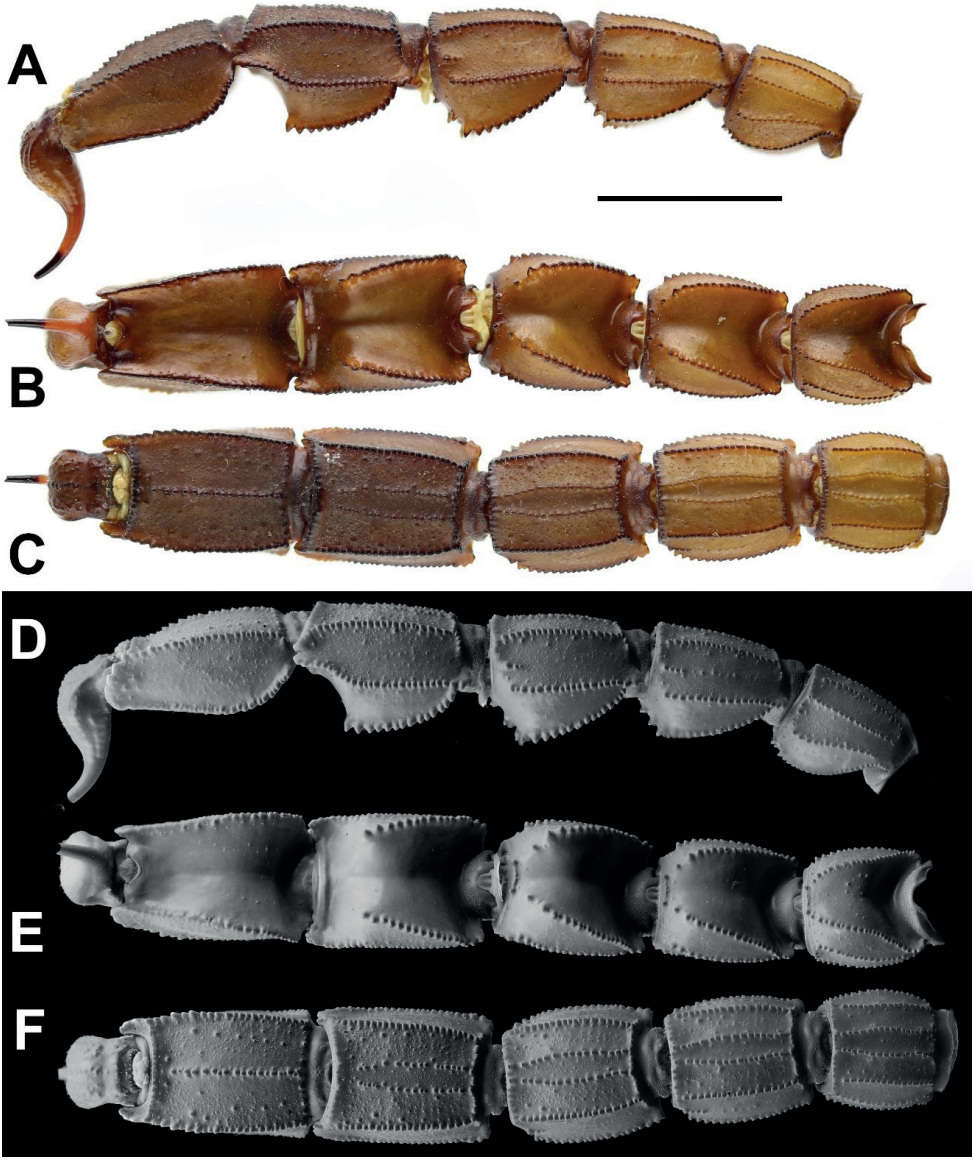

Figure 5. *Androctonus tihamicus* sp. nov., metasoma and telson of female paratype **A, D** lateral view **B, E** dorsal view **C, F** ventral view (**A–C** under white light; **D–F** under UV light). Scale bar: 10 mm.

reddish at base and blackish at extremity. Venter yellowish to reddish yellow; pectines pale yellow. Chelicerae yellowish, without variegated spots in male and with diffused variegated spots in females; fingers yellowish, with dark teeth. Pedipalps: femur and patella brownish yellow, with dark reddish brown carinae; chela reddish brown, fingers reddish brown but dark yellow posteriorly, denticles black. Legs uniformly dark yellow, without spots.

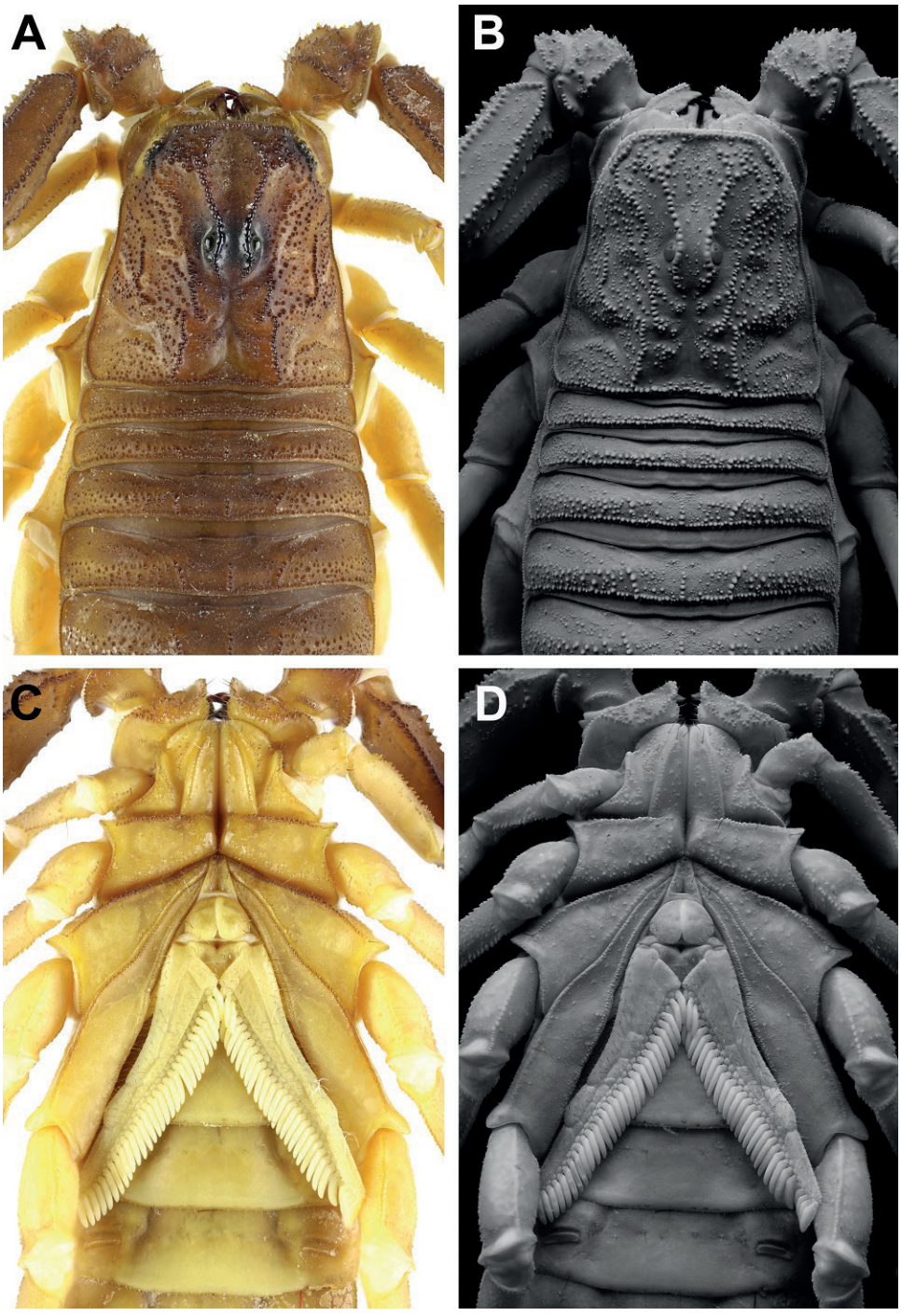

Figure 6. *Androctonus tihamicus* sp. nov., male holotype **A, B** carapace **C, D** sternopectinal area (**A, C** under white light; **B, D** under UV light).

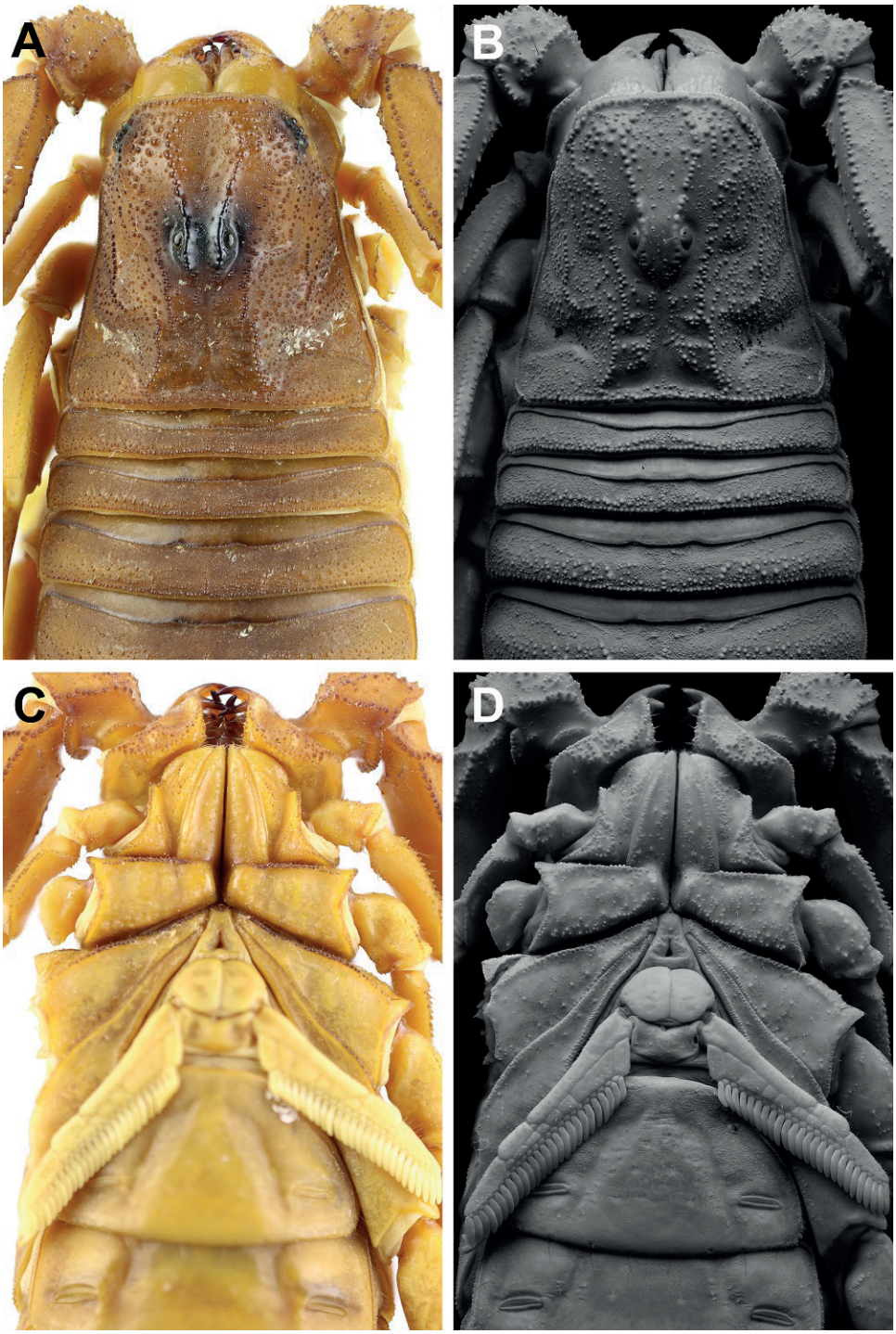

Figure 7. *Androctonus tihamicus* sp. nov., female paratype **A, B** carapace **C, D** sternopectinal area (**A, C** under white light; **B, D** under UV light).

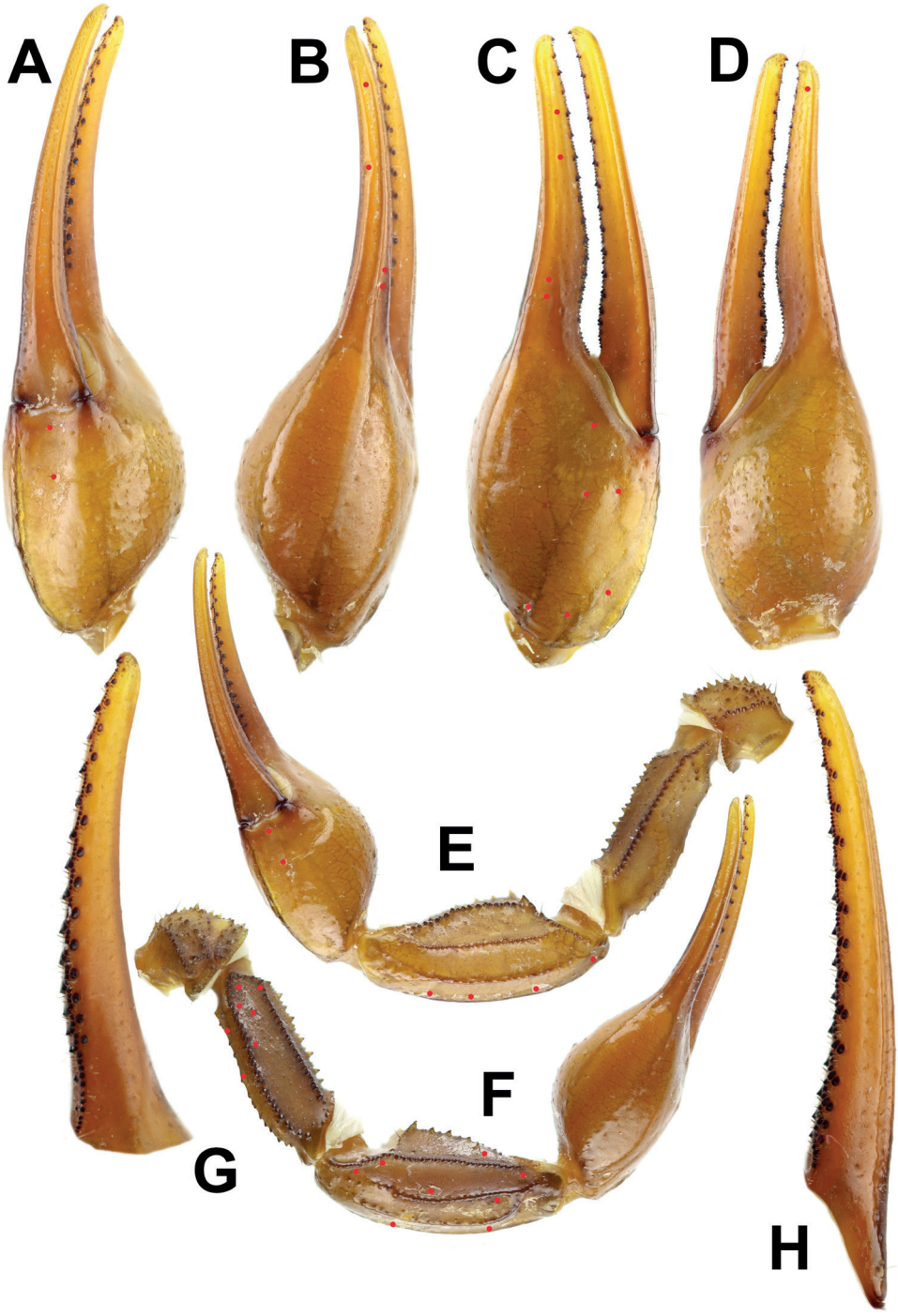

Figure 8. *Androctonus tihamicus* sp. nov., male holotype **A** ventral view of chela **B** dorsal view of chela **C** external view of chela **D** internal view of chela **E** ventral view of pedipalp **F** dorsal view of pedipalp **G** fixed finger dentition **H** movable finger dentition (trichobothrial pattern is indicated by red circles).

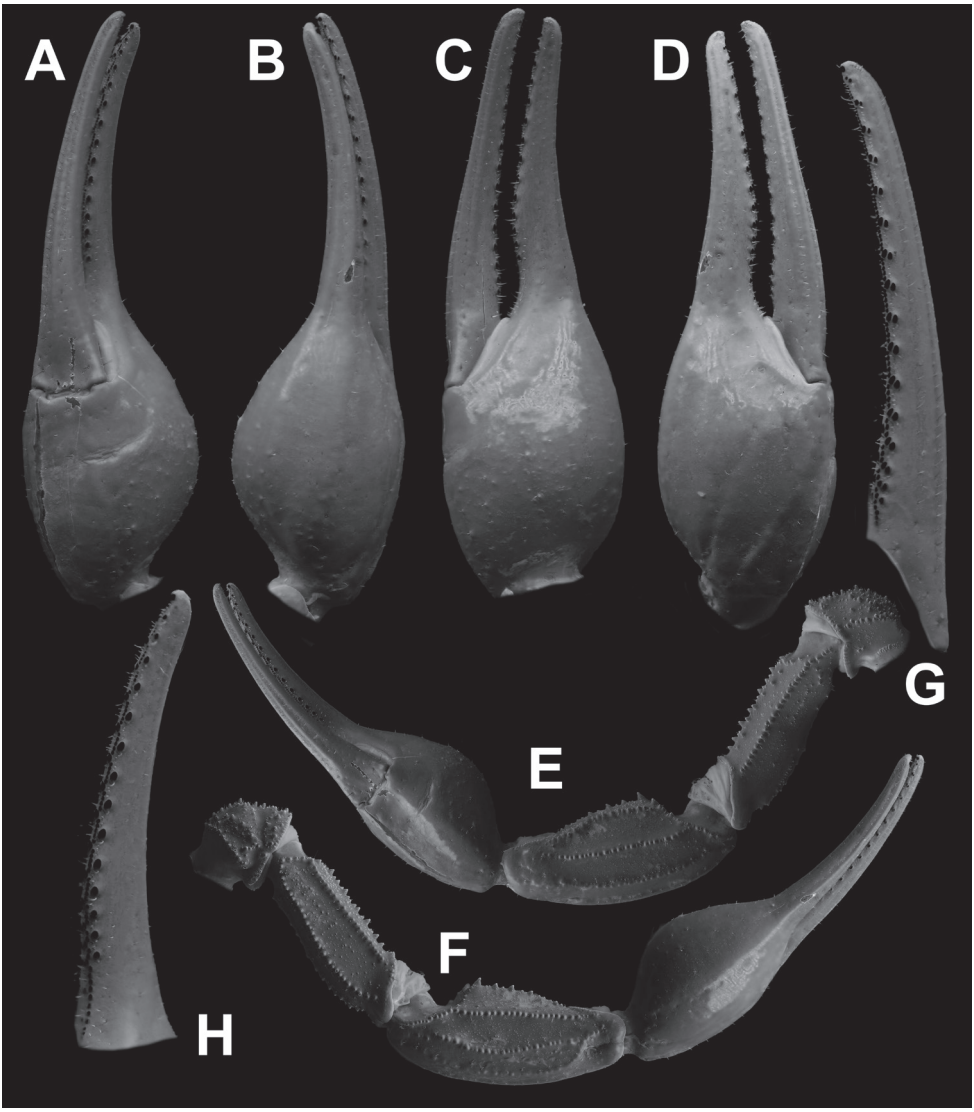

Figure 9. *Androctonus tihamicus* sp. nov., male holotype, under UV light **A** ventral view of chela **B** dorsal view of chela **C** internal view of chela **D** external view of chela **E** ventral view of pedipalp **F** dorsal view of pedipalp **G** fixed finger dentition **H** movable finger dentition.

***Prosoma*:** carapace trapezoidal, wider than long; all carinae strong and coarsely granular. Larger, anterior and posterior median and central median carinae coarsely granulose; strong intergranular area with medium-sized and large granules, anteriorly with very large granules; anterior margin nearly straight, with some stout macrosetae; all furrows moderate to weak; median ocular tubercle slightly anterior to center of carapace; eyes separated by two ocular diameters; five pairs of lateral eyes, first three pairs of

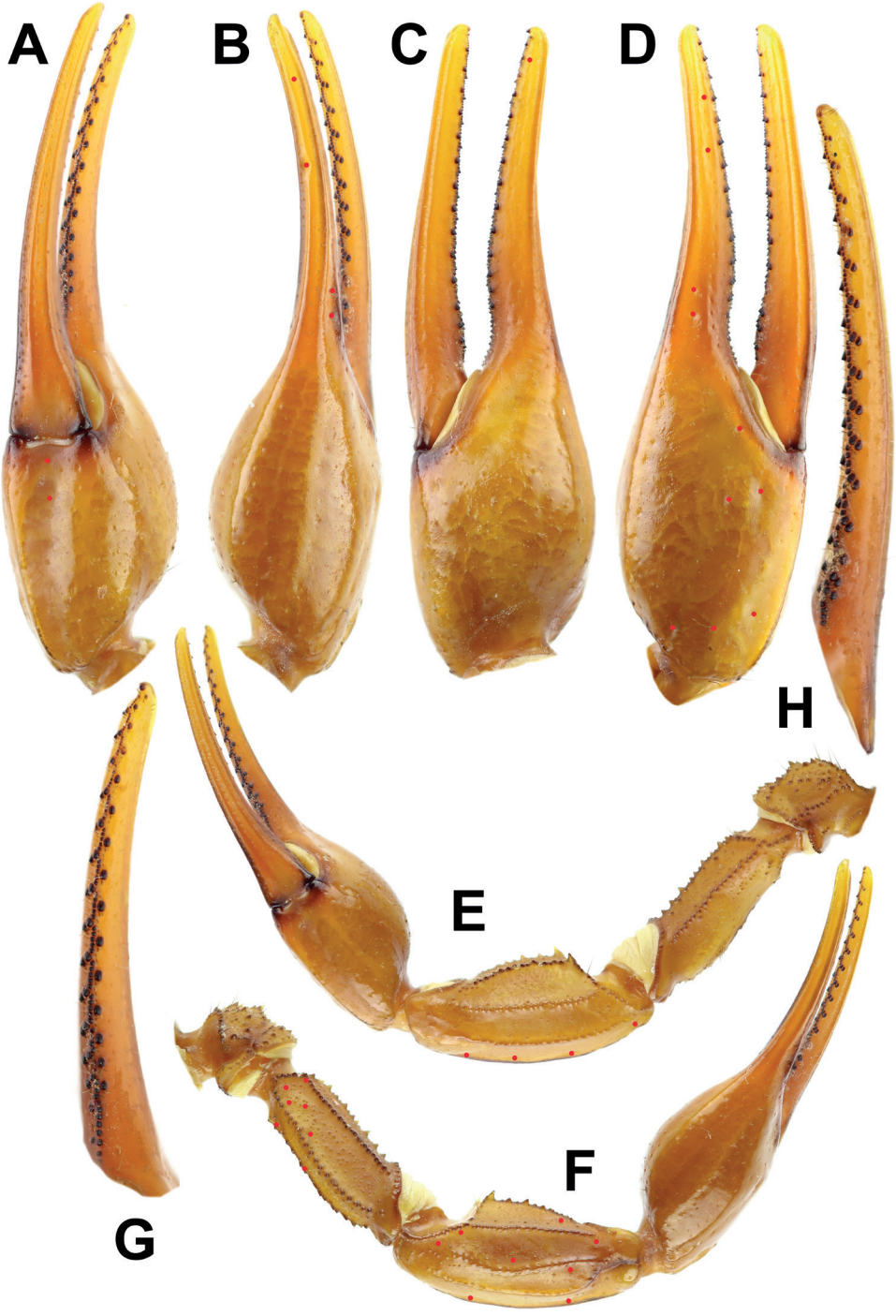

Figure 10. *Androctonus tihamicus* sp. nov, female paratype **A** ventral view of chela **B** dorsal view of chela **C** internal view of chela **D** external view of chela **E** ventral view of pedipalp **F** dorsal view of pedipalp **G** fixed finger dentition **H** movable finger dentition (trichobothrial pattern is indicated by red circles).

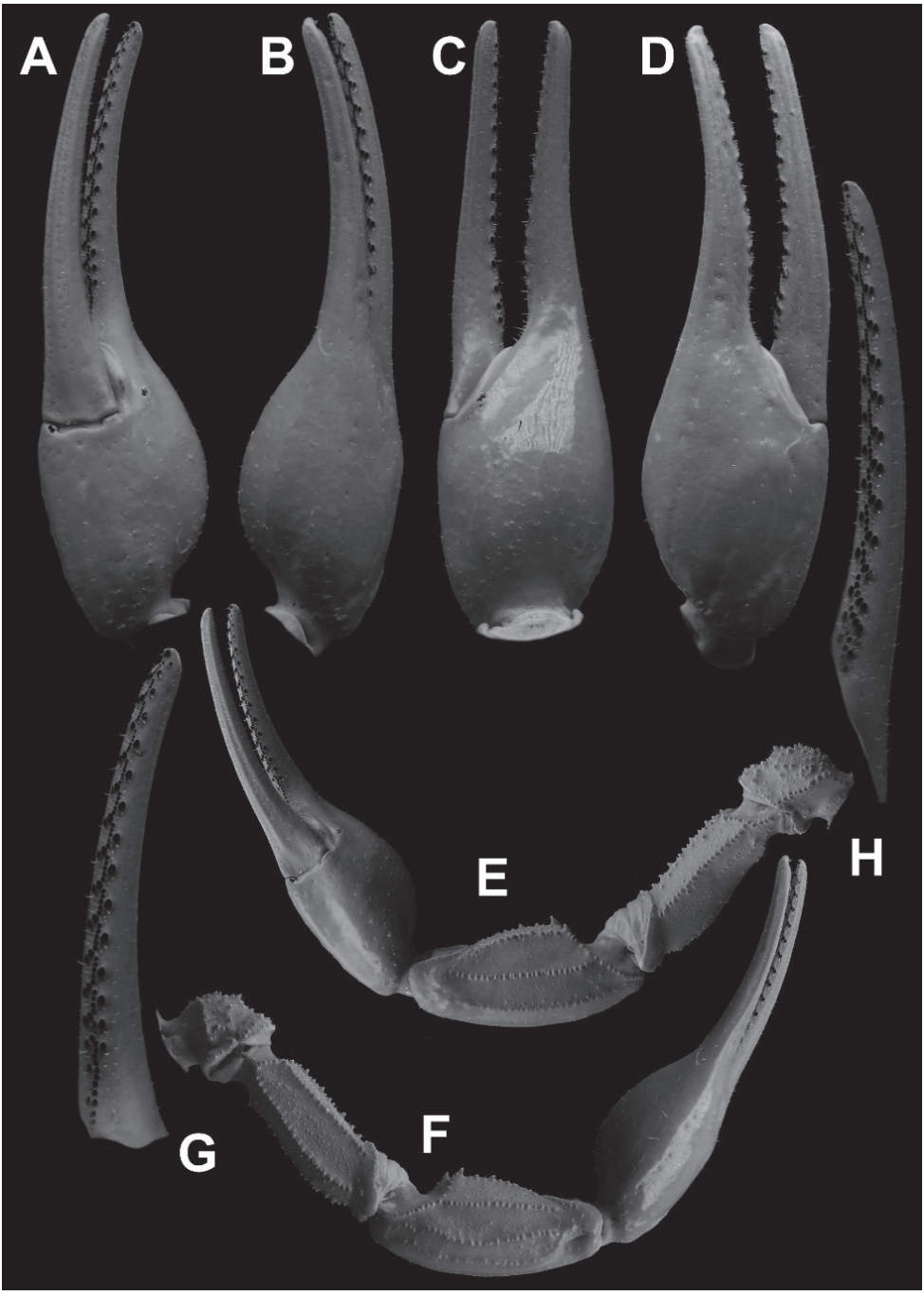

Figure 11. *Androctonus tihamicus* sp. nov., female paratype, under UV light **A** ventral view of chela **B** dorsal view of chela **C** internal view of chela **D** external view of chela **E** ventral view of pedipalp **F** dorsal view of pedipalp **G** fixed finger dentition **H** movable finger dentition.

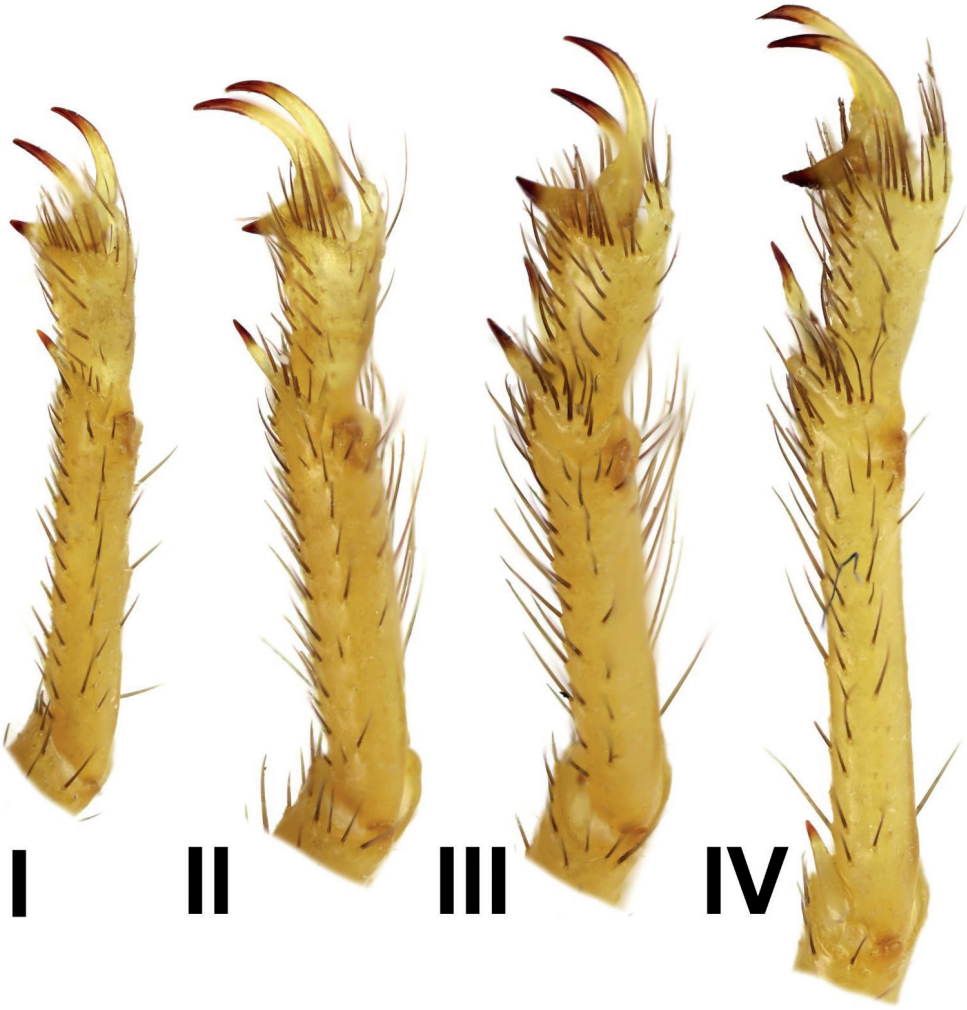

Figure 12. *Androctonus tihamicus* sp. nov., male holotype, right legs I–IV, retrolateral aspect.

moderate size and aligned, last two pairs vestigial; sternum triangular, narrow, slightly longer than wide. Cheliceral dentition typical for genus, as defined by Vachon (1963); surface smooth, with coarse granules arranged in longitudinal ridges.

***Mesosoma*:** tergites densely granular; pretergites finely granular, posttergites coarsely granular; posterior margins with a row of distinct strong granules; I–VI with three moderate to strong, granulose carinae (median and submedians), projecting beyond posterior margin. Tergite VII pentacarinate, with scattered fine granules (median, submedians, and laterals). Venter: sternum standard for the genus: type 1, triangular; genital operculum divided longitudinally, forming two semi-oval plates; pectines long, reaching leg IV coxa/trochanter joint, narrow, densely setose; tooth count 31/33; basal plate heavily

Figure 13. *Androctonus tihamicus* sp. nov., female paratype, right legs I–IV, retrolateral aspect.

sclerotized and wider than long, with anterior margin with strong, median indentation and posterior margin widely convex. Sternites sparsely setose, without granules, smooth with very elongated spiracles and slit-like without granulation; sternites III–VI carinate, with two vestigial furrows; sternite VI with fine, very scattered granules; sternite III without carinae; sternite VII with two pairs of strong granular carinae.

***Metasoma*:** very sparsely setose, with all segments robust. All segments longer than wide; segments I–III very slightly longer than wide; wider than deep; inter-carinal tegument of dorsal surface without granulation and smooth, lateral surface slightly roughened, with scattered fine and moderately sparse granules, ventral surface rough with moderately dense fine granules and scattered large granules on segments I–V; dorsal furrow moderately deep and wide on all segments; segment I with 10 carinae, lateral infra-median carinae complete and moderate, segment II with 10 carinae, lateral infra-median incomplete, present on posterior quarter, strongly granular, with three granules; segment III with 10 carinae, lateral infra-median incomplete with two granules; segment IV with eight, and segment V with five carinae. Dorsolateral carinae of segments I–IV strong, with serrate granules that gradually increase posteriorly.

Figure 14. Comparison of chela between male holotype and female paratype of *Androctonus tihamicus* sp. nov. and male and female of *A. australis* **A, C, E, G** *A. australis* **B, D, F, H** *A. tihamicus* sp. nov. **A–D** male **E–H** female **A, B, E, F** dorsal **C, D, G, H** external.

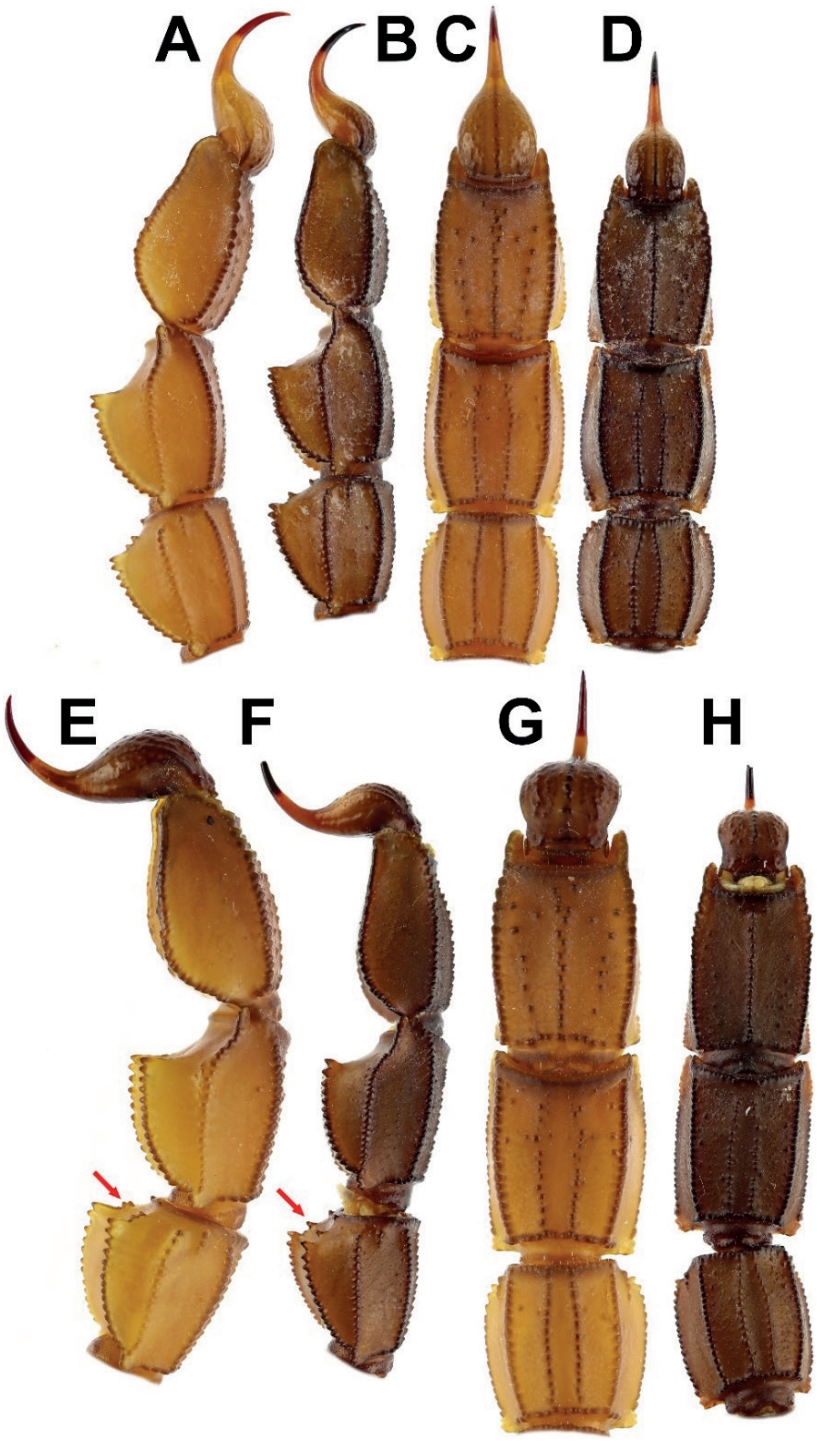

Figure 15. Comparison of metasoma III–V and telson between male holotype and female paratype of *Androctonus tihamicus* sp. nov. and male and female of *A. australis* **A, C, E, G** *A. australis* **B, D, F, H** *A. tihamicus* sp. nov. **A–D** male **E–H** female **A, B, E, F** lateral **C, D, G, H** ventral (arrows: see Comparisons in text).

Granules small on segment I, moderate on segment II, and large on segments III–IV. Segment V with strong, rounded carinae, posteriorly smooth with very rounded, shallow granules anteriorly. Lateral supra-median carinae strong on segment I–IV, with moderate, rounded and crenulate granules on segment I, large, rounded, crenulate granules on II–V, and more swollen and one very large, rounded granule at the posterior end of segment IV. Ventrolateral carinae on segments I–IV strong, with large, rounded granules; strong with gradually and slightly increased granules posteriorly on segment V. Ventral submedian carinae moderate on segments I–V, with moderately rounded granules. Anal arch laterally with three rounded lobes, the inferior lobe twice as large as the other two lobes. Telson slender, elongate, densely setose; vesicle small somewhat globose, tegument glossy and essentially smooth, with only some coarse granules and a coarse but very poorly defined ventro-median carinae; setal pair subaculear; aculeus very long and thick, as long as vesicle, and moderately curved.

***Legs*:** long, slender, covered by several macrosetae. Basitarsus of legs I–III bear bristle combs; basitarsus of leg IV without bristle comb. Proventral and retroventral basitarsal (pedal) spurs present but tibial spurs present on legs III and IV. Tarsus of legs I–IV ventrally with spine-like setae arranged in two rows: tarsal spurs basally bifurcate, bearing 1–3 macrosetae (four on legs I–II, eight or nine on leg III–IV). Basitarsus of legs I–III with bristle combs; basitarsus of legs IV without bristle combs.

***Pedipalps*:** stocky, moderately long, densely setose. Type A trichobothrial pattern; orthobothriotaxic. Dorsal trichobothria of femur arranged in beta-configuration with d_2 situated on dorsal surface. Femur pentacarinate, slender, straight; all carinae strong and moderately granulose; intercarinal tegument finely granulose, with irregular, coarse granules dorsally; inner surface with a few coarse granules; dorso-internal carinae with distinct spinoid granules. Patella with seven carinae, moderately slender and straight; surfaces smooth with scattered fine granules; all carinae moderately strong, dorsomedian, dorsoexternal, ventromedian, ventroexternal, ventrointernal carinae granulose, external smooth, dorsointernal with seven spinoid granules; dorsointernal and ventrointernal carinae distally terminate at one spinoid granule. Chela smooth, without carinae, stocky. Manus wider than patella (chela width/patella width = 1.13); internal surface of manus with scattered fine granules; fingers moderately elongate (movable finger length/manus length = 1.76), evenly curved. Movable fingers of pedipalps bear 15 rows of granules and external and internal granules; fixed fingers bear 14 rows of granules, with external and internal accessory granules and three distal granules.

Comparison. *Androctonus tihamicus* sp. nov. can be distinguished from other *Androctonus* species in the Middle East by following characters: *A. tihamicus* sp. n. has stocky chela whereas *A. bicolor* Ehrenberg, 1828 has elongate chela. Ventrolateral carinae of 5th segment of *A. tihamicus* sp. nov. lacks large granules and the general color is light to reddish brown, whereas ventrolateral carinae of the 5th segment of *A. turkiyensis* Yağmur, 2021 bears large granules, The general color is brown or black in *A. crassicauda*. The new species has stockier metasoma segments, whereas *A. amoreuxi* (Audouin, 1826) has elongated metasoma segments, and especially the 5th segment, which is remarkably more elongate. The length/width ratios of metasomal segments I–V from the measurements provided by Levy and Amitai (1980) are 0.90-1.12-1.15-1.38-1.71 in males and 0.91-1.12-1.19-1.38-1.71 in

Table 1. Comparative measurements of types of *Androctonus tihamicus* sp. nov. Abbreviations: length (L), width (W; for carapace, it corresponds to posterior width), depth (D).

Dimensions (mm)		*A. tihamicus* sp. nov.	*A. tihamicus* sp. nov.
		♂, holotype	♀, paratype
Carapace	L / W	8.79 / 8.91	10.36 / 10.38
Mesosoma	L	17.05	21.49
Tergite VII	L / W	5.36 / 9.68	5.97 / 11.13
Metasoma + telson	L	45.28	52.66
Segment I	L / W / D	5.68 / 6.21 / 5.29	6.08 / 6.10 / 5.73
Segment II	L / W / D	7.14 / 6.68 / 6.23	7.54 / 6.69 / 6.14
Segment III	L / W / D	7.25 / 7.08 / 6.59	8.46 / 7.25 / 6.76
Segment IV	L / W / D	9.34 / 7.38 / 6.61	10.02 / 7.28 / 6.74
Segment V	L / W / D	9.23 / 6.65 / 4.93	10.75 / 6.92 / 5.46
Telson	L / W / D	7.14 / 3.50 / 2.56	9.79 / 4.16 / 3.13
Pedipalp	L	31.34	34.31
Femur	L / W	7.49 / 2.61	7.96 / 2.84
Patella	L / W	8.89 / 3.66	9.58 / 4.09
Chela	L	14.96	17.39
Manus	L / W / D	5.1/ 4.82 / 4.87	5.88 / 4.36 / 5.26
Movable finger	L	9.60	11.50
Fixed finger	L	7.71	9.40
Total	**L**	**71.82**	**84.51**

females. These ratios in *A. tihamicus* sp. nov. are 0.91-1.06-1.02-1.26-1.38 in males and 0.99-1.12-1.16-1.37-1.55 in females (Table 1). Additionally, *A. amoreuxi* is yellow or olive-yellow. The new species can be distinguished from *A. australis* by the following characteristics: (a) general coloration light to reddish brown with legs uniformly yellow (vs yellow in *A. australis*); (b) pedipalp less robust and movable finger with a small recess and hump (vs more robust and movable finger with a larger recess and hump at base of the fingers in in *A. australis*) (Fig. 14); (c) metasomal segments smaller than *A. australis*; (d) dorsolateral carinae of metasomal segment III has one separate spinoid granule in posterior of segments IV (vs two rounded granules in *A. australis*; Fig. 15, indicated by arrows); (e) ventral carina of 5th metasomal segment without bifurcation (vs bifurcated in *A. australis*); and (f) anal arch with three lateral lobes (vs two lateral lobes in *A. australis*; Fig. 15A, B, E, F).

Ecology. *Androctonus tihamicus* sp. nov. is an arenicolous species of scorpion from the Tihamah plain in southwestern Saudi Arabia. The sampling sites are all at low elevations along the coast, where temperatures are high, around 40 °C daily. Southern sites are in the coastal fog desert zone, with high temperatures of 43 °C and a relative humidity of 40–60%.

Genetic analysis. *Androctonus tihamicus* sp. nov. forms a monophyletic clade distinct from *A. crassicauda* (from Saudi Arabia, Turkey, and Iran), and other related *Androctonus* species analyzed (Fig. 16). The new species differs from *A. crassicauda* by a raw genetic distance of 4.0–9.0%, and from *A. amoreuxi* by 13.0%; it differs from *A. australis*, *A. liouvillei* (Pallary, 1924), and *A. mauritanicus* (Pocock, 1902) by a raw genetic distance of 16.0% (Table 2).

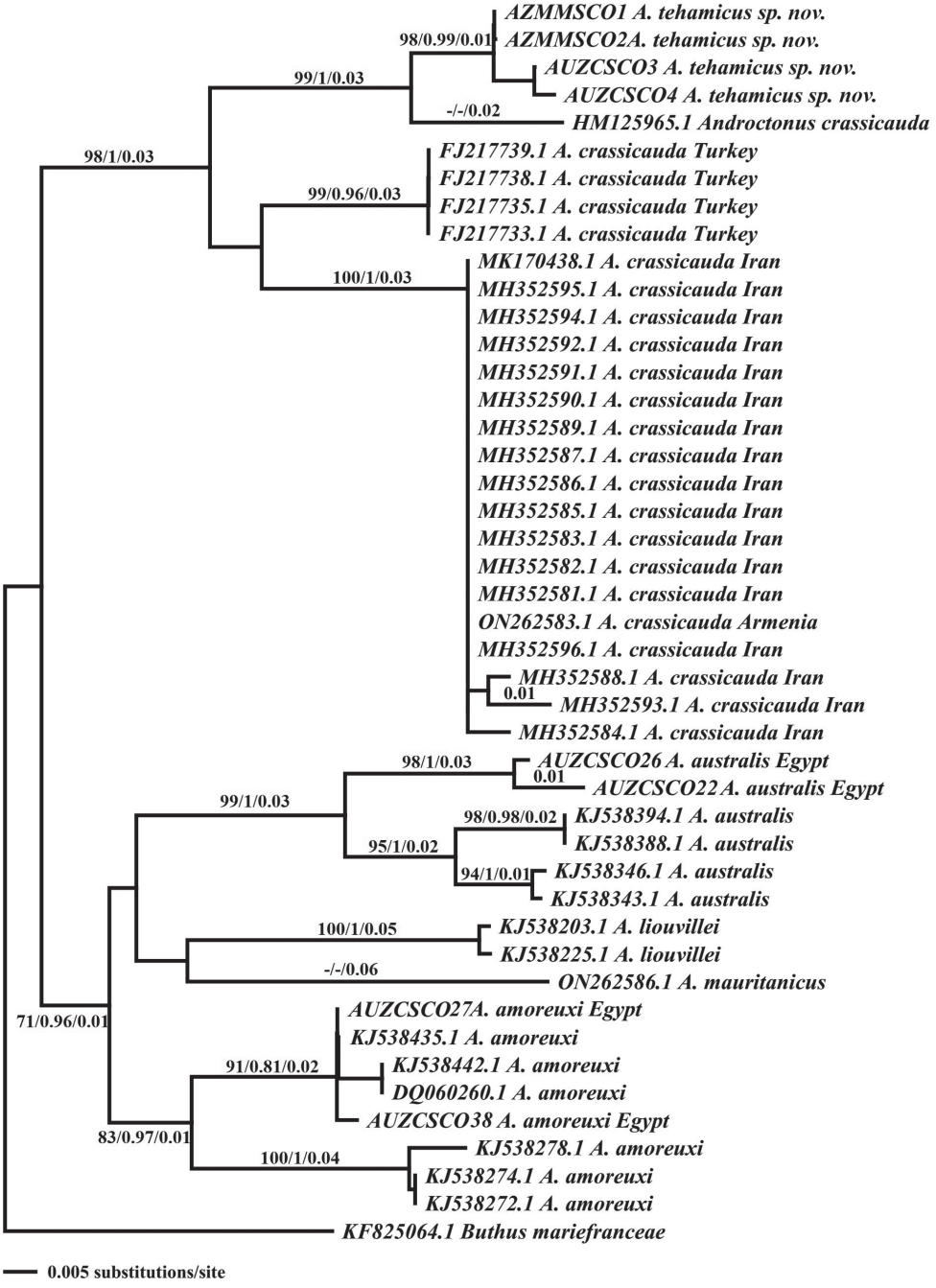

Figure 16. Neighbor-joining (NJ) phylogenetic tree of *Androctonus* species based on 16S rRNA sequences. Numbers above and below branches indicate maximum parsimony bootstrap values/Bayesian posterior probabilities/NJ distance values.

Table 2. The uncorrected *p*-distance of the sequence divergence of 16S mtDNA sequences between *Androctonus* samples included in this study.

	1	2	3	4	5	6	7	8	9
1. *A. tihamicus* sp. nov.		0.01	0.02	0.02	0.02	0.02	0.02	0.02	0.02
2. *A. crassicauda* Saudi Arabia	0.04		0.02	0.02	0.02	0.02	0.02	0.02	0.02
3. *A. crassicauda* Turkey	0.09	0.09		0.01	0.02	0.02	0.02	0.02	0.02
4. *A. crassicauda* Iran	0.09	0.10	0.06		0.02	0.02	0.02	0.02	0.02
5. *A. amoreuxi*	0.13	0.13	0.13	0.13		0.02	0.02	0.01	0.02
6. *A. australis*	0.16	0.17	0.15	0.15	0.12		0.02	0.01	0.02
7. *A. liouvillei*	0.16	0.17	0.13	0.14	0.10	0.12		0.02	0.02
8. *A. mauritanicus*	0.16	0.17	0.15	0.15	0.12	0.09	0.12		0.02
9. *Scorpio palmatus* (outgroup)	0.14	0.15	0.12	0.13	0.12	0.15	0.13	0.14	

Discussion

The 16S mitochondrial gene has been successfully used by several authors to delimit cryptic species of *Euscorpius* Thorell, 1876 and *Centruroides* Marx, 1890 (Gantenbein et al. 2001, 2002; Fet et al. 2003, 2016; Ponce-Saavedra et al. 2009; Quijano-Ravell and Ponce-Saavedra 2016). It was for this reason, that we conducted a molecular phylogenetic analysis using the mRNA 16S mitochondrial gene. Our results show a genetic divergence between *A. tihamicus* sp. nov. and populations of *A. crassicauda* from Saudi Arabia, Turkey, and Iran (*p*-distance = 0.04–0.09), and the new species was found to differ from *A. amoreuxi*, *A. australis*, *A. liouvillei* and *A. mauritanicus* by a raw genetic distance of 0.13–0.16 (Table 2). The phylogenetic trees obtained by different models were topologically consistent (Fig. 16). The phylogenetic tree shows that *A. tihamicus* sp. nov. appears most closely related to the *A. crassicauda* sequence from Hail, Saudi Arabia (GeneBank HM125965.1; Desouky and Alshammari 2010). Gough and Hirst (1927) reported *Buthus australis citrina* from Saudi Arabia, an incorrect spelling of the *A.* (*Prionurus*) *citrinus* Ehrenberg, 1828. Its type locality is in Sudan (Dunqulah, Nubia). This taxon was synonymized by Di Caporiacco (1932) with *A. amoreuxi* and the species does not occur in Saudi Arabia. Hendrixson (2006) reported *A. crassicauda* as the only species of *Androctonus* in Saudi Arabia.

Although Levy and Amitai (1980) reported *A. australis* from Saudi Arabia, Hendrixson (2006) re-examined the specimens used by Levy and Amitai and found no significant differences from *A. crassicauda* except color variation. Hendrixson (2006) mentioned that *A. crassicauda* can be distinguished from *A. australis* by dark coloration and the granules on the ventrolateral carinae of metasomal segment V increase in size posteriorly. Al-Asmari et al. (2013: fig. 7) reported *A. australis* from Al-Medina Al-Munawwara region. The morphology and coloration are similar to *A. tihamicus* sp. nov., and this record probably was the new species. In molecular and morphometrical investigations, Alqahtani et al. (2022a, b, c) referred to the existence of three distinct clusters of *A. crassicauda* populations collected from different ecogeographical regions in Saudi Arabia, and the Arabian clade is placed as a basal clade to Turkey and Iran sequences. Ozkan et al. (2010) referred to two genetic groups of *A. crassicauda* found in Turkey, based on the 16S

rRNA gene. Subsequently, Yağmur (2021) described a new species of *Androctonus* from the Şanlıurfa Province, Turkey, which had been previously identified as *A. crassicauda* (Fig. 16). Accordingly, seven species of the genus *Leiurus* Ehrenberg, 1828 in Arabia were described, transferred, or synonomized by Lowe et al. (2014) based on quantitative and qualitative morphological variations. Of these, *Leiurus brachycentrus* (Ehrenberg, 1829) occurs on the Tihamah Plain of western Yemen and southwestern Saudi Arabia. The observed diversity of scorpions is possibly a consequence of prominent geographical features, which contribute to an increased propensity for diversification in association with long-term processes such as geomorphological development and climatic cycles (Harzhauser et al. 2007; Lowe et al. 2014; Hou and Li 2018; Georgalis et al. 2020).

References

Akaike H (1973) Information theory and an extension of the maximum likelihood principle. In: Petrov BN, Caski F (Eds) 2nd International Symposium on Information Theory, Akademiai Kiado, Budapest.

Al-Asmari AK, Al-Saif AA, Abdo NM, Al-Moutaery KR, Al-Harbi NO (2013) A review of the scorpion fauna of Saudi Arabia. Egyptian Journal of Natural History 6(1): 1–21. https://doi.org/10.4314/ejnh.v6i1.1

Alqahtani AR, Badry A (2020) Interspecific phylogenetic relationship among different species of the genus *Buthacus* (Scorpiones: Buthidae) inferred from 16S rRNA in Egypt and Saudi Arabia. Zoology in the Middle East 66(2): 178–185. https://doi.org/10.1080/09397140.2020.1742991

Alqahtani AR, Elgammal B, Ghaleb KI, Badry A (2019) The scorpion fauna of the southwestern part of Saudi Arabia. Egyptian Academic Journal of Biological Sciences, B, Zoology 11(1): 19–29. https://doi.org/10.21608/eajbsz.2019.28565

Alqahtani AR, Badry A, Aly H, Amer SA, Al Galil FMA, Ahmed MA, Kadasah S, Amr ZS (2022a) Genetic diversity and population structure of *Androctonus crassicauda* (Scorpiones: Buthidae) in different ecogeographical regions of Saudi Arabia and Iran. Zoology in the Middle East 68(2): 171–179. https://doi.org/10.1080/09397140.2022.2051915

Alqahtani AR, Badry A, Abd Al Galil FM, Amr ZS (2022b) Morphometric and meristic diversity of the species *Androctonus crassicauda* (Olivier, 1807) (Scorpiones: Buthidae) in Saudi Arabia. PeerJ 10: e14198. https://doi.org/10.7717/peerj.14198

Alqahtani AR, Badry A, Amer SA, Abd Al Galil FM, Ahmed MA, Amr ZS (2022c) Intraspecific molecular variation among *Androctonus crassicauda* (Olivier, 1807) populations collected from different regions in Saudi Arabia. Journal of King Saud University-Science 34(4): e101998. https://doi.org/10.1016/j.jksus.2022.101998

Ben Ali Z, Boursot P, Said K, Lagnel J, Chatti N, Navajas M (2000) Comparison of ribosomal ITS regions among *Androctonus* spp. scorpions (Scorpionida: Buthidae) from Tunisia. Journal of Medical Entomology 37(6): 787–790. https://doi.org/10.1603/0022-2585-37.6.787

Desouky MM, Alshammari AM (2010) Scorpions of the Ha'il Region, northern Saudi Arabia, and molecular phylogenetics of two common species, *Androctonus crassicauda*

and *Scorpio maurus kruglovi*. Arachnology 15(6): 193–200. https://doi.org/10.13156/arac.2011.15.6.193

Di Caporiacco L (1932) Spedizione scientificaall' oasi di Cufra. (Marzo-Luglio 1931). Scorpioni e Solifugi. Annali del Museo Civico di Storia Naturale di Genova 55: 395–408.

Felsenstein J (2002) Bootstraps and testing trees. Transition 5(10): 1–20.

Fet V, Lowe G (2000) Family Buthidae C. L. Koch, 1837. In: Fet V, Sissom WD, Lowe G, Braunwalder ME (Eds) Catalog of the Scorpions of the World (1758–1998). The New York Entomological Society, New York, 54–286.

Fet V, Soleglad ME, Gantenbein B, Vignoli V, Salomone N, Fet EV, Schembri P (2003) New molecular and morphological data on the "*Euscorpius carpathicus*" species complex (Scorpiones: Euscorpiidae) from Italy, Malta, and Greece justify the elevation of *E. c. sicanus* (C.L. Koch, 1837) to the species level. Revue Suisse de Zoologie 110(2): 355–379. https://doi.org/10.5962/bhl.part.80189

Fet V, Graham MR, Blagoev G, Karataş A, Karataş A (2016) DNA barcoding indicates hidden diversity of *Euscorpius* (Scorpiones: Euscorpiidae) in Turkey. Euscorpius 216(216): 1–12. https://doi.org/10.18590/euscorpius.2016.vol2016.iss216.1

Francke OF (1977) Scorpions of the genus *Diplocentrus* from Oaxaca, Mexico (Scorpionida, Diplocentridae). The Journal of Arachnology 4: 145–200.

Gantenbein B, Fet V, Largiadèr CR, Scholl A (1999) First DNA phylogeny of *Euscorpius* Thorell, 1876 (Scorpiones: Euscorpiidae) and its bearing on taxonomy and biogeography of this genus. Biogeographica 75(2): 49–65.

Gantenbein B, Fet V, Barker MD (2001) Mitochondrial DNA reveals a deep, divergent phylogeny in *Centruroides exilicauda* (Wood, 1863) (Scorpiones: Buthidae). In: Fet V, Selden PA (Eds) Polis. British Arachnological Society, Burnham Beeches, Bucks, 235–244.

Gantenbein B, Soleglad ME, Fet V, Crucitti P, Fet EV (2002) *Euscorpius naupliensis* Caporiacco, 1950 (Scorpiones: Euscorpiidae): elevation to species level justified by molecular and morphology data. Revista Iberica de Aracnologia 6: 13–43.

Georgalis GL, Gawad MKA, Hassan SM, El-Barkooky AN, Hamdan MA (2020) Oldest co-occurrence of *Varanus* and *Python* from Africa-First record of squamates from the early Miocene of Moghra Formation, Western Desert, Egypt. PeerJ 8: e9092. https://doi.org/10.7717/peerj.9092

Gough LH, Hirst S (1927) Key to the identification of Egyptian scorpions. A method of identifying Egyptian scorpions from the fifth caudal segment and stings. Bulletin of Mini shy of Agriculture, Egypt. Technical Scientific Service 76: 1–7.

Hall TA (1999) BioEdit: A user-friendly biological sequence alignment editor and analysisprogram for Windows 95/98/NT. Nucleic Acids Symposium Series 41: 95–98.

Harzhauser M, Kroh A, Mandic O, Piller WE, Göhlich U, Reuter M, Berning B (2007) Biogeographic responses to geodynamics: A key study all around the Oligo-Miocene Tethyan Seaway. Zoologischer Anzeiger 246(4): 241–256. https://doi.org/10.1016/j.jcz.2007.05.001

Hendrixson BE (2006) Buthid scorpions of Saudi Arabia, with notes on other families (Scorpiones: Buthidae, Liochelidae, Scorpionidae). Fauna of Arabia 21: 33–120.

Hjelle JT (1990) Anatomy and morphology. In: Polis GA (Ed.) The Biology of Scorpions. Stanford University Press, Stanford, 9–63.

Hou Z, Li S (2018) Tethyan changes shaped aquatic diversification. Biological Reviews of the Cambridge Philosophical Society 93(2): 874–896. https://doi.org/10.1111/brv.12376

Levy G, Amitai P (1980) Scorpiones. Fauna Palaestina, Arachnida I. Israel Academy of Sciences and Humanities, Jerusalem, 130 pp.

Lourenço WR (2005) New taxonomic considerations on the species of the genus *Androctonus* Ehrenberg, 1828 and description of two new species (Scorpiones, Buthidae). Revue Suisse de Zoologie 112(1): 145–171. https://doi.org/10.5962/bhl.part.80291

Lourenço WR (2008) A new species of *Androctonus* Ehrenberg, 1828 from Togo (Scorpiones, Buthidae). Entomologische Mitteilungen aus dem Zoologischen Museum Hamburg 15(179): 37–44.

Lourenço WR, Qi JX (2006) A new species of *Androctonus* Ehrenberg, 1828 from Afghanistan (Scorpiones, Buthidae). Zoology in the Middle East 38(1): 93–97. https://doi.org/10.1080/09397140.2006.10638170

Lourenço WR, Qi JX (2007) A new species of *Androctonus* Ehrenberg, 1828 from Mauritania (Scorpiones, Buthidae). Boletin de la SEA 40: 215–219. https://doi.org/10.1080/09397140.2006.10638170

Lowe G, Yağmur EA, Kovařík F (2014) A review of the genus *Leiurus* Ehrenberg, 1828 (Scorpiones: Buthidae) with description of four new species from the Arabian Peninsula. Euscorpius 191(191): 1–129. https://doi.org/10.18590/euscorpius.2014.vol2014.iss191.1

Nylander JAA (2004) MrModeltest v2. Program distributed by the author. Evolutionary Biology Centre, Uppsala University.

Othmen AB, Said K, Mahamdallie SS, Testa JM, Haouas Z, Chatti N, Ready PD (2009) Phylogeography of *Androctonus* species (Scorpiones: Buthidae) in Tunisia: diagnostic characters for linking species to scorpionism. Acta Tropica 112(1): 77–85. https://doi.org/10.1016/j.actatropica.2009.07.001

Ozkan O, Ahmet C, Zafer K (2010) A study on the genetic diversity of *Androctonus crassicauda* (Olivier, 1807; Scorpiones: Buthidae) from Turkey. The Journal of Venomous Animals and Toxins Including Tropical Diseases 16(4): 599–606. https://doi.org/10.1590/S1678-91992010000400010

Ponce-Saavedra J, Francke OF, Cano-Camacho H, Hernández-Calderón E (2009) Evidencias morfológicas y moleculares que validan como especie a *Centruroides tecomanus* (Scorpiones: Buthidae). Revista Mexicana de Biodiversidad 80: 71–84.

Quijano-Ravell AF, Ponce-Saavedra J (2016) A new species of scorpion of the genus *Centruroides* (Scorpiones: Buthidae) from the state of Michoacán, Mexico. Revista Mexicana de Biodiversidad 87(1): 49–61. https://doi.org/10.1016/j.rmb.2016.01.022

Rambaut A, Drummond AJ, Xie D, Baele G, Suchard MA (2018) Posterior summarisation in Bayesian phylogenetics using Tracer 1.7. Systematic Biology 67(5): 901–904. https://doi.org/10.1093/sysbio/syy032

Rein JO (2023) The Scorpion Files. www.ntnu.no/ub/scorpion-files/ [January 16, 2023]

Ronquist F, Teslenko M, van der Mark P, Ayres DL, Darling A, Höhna S, Larget B, Liu L, Suchard MA, Huelsenbeck JP (2012) MrBayes 3.2: Efficient Bayesian phylogenetic inference and model choice across a large model space. Systematic Biology 61(3): 539–542. https://doi.org/10.1093/sysbio/sys029

Stahnke HL (1971) Scorpion nomenclature and mensuration. Entomological News 81: 297–316.
Swofford DL (2003) PAUP*. Phylogenetic Analysis Using Parsimony (*and Other Methods). Version 4. Sinauer Associates, Sunderland.
Tamura K, Stecher G, Peterson D, Filipski A, Kumar S (2013) MEGA6: Molecular Evolutionary Genetics Analyses version 6.0. Molecular Biology and Evolution 30(12): 2725–2729. https://doi.org/10.1093/molbev/mst197
Vachon M (1963) De l'utilité, en systématique, d'une nomenclature des dents des chélicères chez les scorpions. Bulletin du Muséum National d'Histoire Naturelle 35: 161–166.
Vachon M (1974) Étude des caractères utilisés pour classer les familles et les genres de scorpions (*Arachnides*). 1. La trichobothriotaxie en arachnologie. Sigles trichobothriaux et types de trichobothriotaxie chez les scorpions. Bulletin du Muséum National d'Histoire Naturelle 140: 857–958.
Vachon M (1979) Arachnids of Saudi Arabia: Scorpions. Fauna of Saudi Arabia 1: 30–66.
Yağmur EA (2021) *Androctonus turkiyensis* sp. n. from the Şanlıurfa Province, Turkey (Scorpiones: Buthidae). Euscorpius 341: 1–18.

ZooKeys 1152: 35–43 (2023)
doi: 10.3897/zookeys.1152.99290
https://zookeys.pensoft.net

RESEARCH ARTICLE

A peer-reviewed open-access journal
ZooKeys
Launched to accelerate biodiversity research

Discovery of the termitophilous genus *Trichopsenius* Horn, 1877 (Coleoptera, Staphylinidae, Aleocharinae) from China with description of a new species

Ri-Xin Jiang[1,2,3], Xiu-Dong Huang[1,2,3], Xiang-Sheng Chen[1,2,3]

1 *Institute of Entomology, Guizhou University, Guiyang 550025, Guizhou, China* **2** *The Provincial Special Key Laboratory for Development and Utilization of Insect Resources of Guizhou, Guizhou University, Guiyang, 550025, Guizhou, China* **3** *The Provincial Key Laboratory for Agricultural Pest Management of Mountainous Region, Guiyang 550025, Guizhou, China*

Corresponding author: Xiang-Sheng Chen (chenxs3218@163.com)

Academic editor: Jan Klimaszewski | Received 2 January 2023 | Accepted 18 February 2023 | Published 6 March 2023

https://zoobank.org/D9FCAD65-F187-4AC9-BA80-C99B30067B31

Citation: Jiang R-X, Huang X-D, Chen X-S (2023) Discovery of the termitophilous genus *Trichopsenius* Horn, 1877 (Coleoptera, Staphylinidae, Aleocharinae) from China with description of a new species. ZooKeys 1152: 35–43. https://doi.org/10.3897/zookeys.1152.99290

Abstract

The termitophilous genus *Trichopsenius* Horn, 1877 is recorded from China for the first time. A new species, *Trichopsenius huaxiensis* **sp. nov.** is described; it was collected in a nest of the termite genus *Reticulitermes* Holmgren from a dead and flattened pine tree.

Keywords

Guizhou, rove beetles, termites, termitophily, Trichopseniini

Introduction

The rove beetle genus *Trichopsenius* Horn, 1877 (Aleocharinae, Trichopseniini) is composed of 12 known species, and discontinuously distributed from Europe (one species from Spain; Kistner and Assing 1995) and North Africa (one species; Kanao and Maruyama 2019) to North America (five species; LeConte 1863; Seevers 1941, 1945, 1957; Pasteels and Kistner 1971). In Asia, five species are known from Japan, but there are not any records outside of Japan (Naomi and Terayama 1986, 1996).

All known members of the genus *Trichopsenius* are termitophiles and associated with the termite genus *Reticulitermes* Holmgren (Blattodea, Rhinotermitidae; Kanao and Maruyama 2019). Immature stages of *Trichopsenius* are known only for two American species, *T. depressus* (LeConte, 1863) and *T. frosti* Seevers, 1945 (Howard and Kistner 1978; Kistner and Howard 1980).

In the present paper, the genus *Trichopsenius* is reported from China for the first time, represented by the new species *Trichopsenius huaxiensis* sp. nov., described and illustrated herein. All adults of the new species were collected in a nest of termites of the genus *Reticulitermes* from a flattened dead pine tree.

Material and methods

Material examined is deposited in the Institute of Entomology, Guizhou University, Guiyang, China (**GUGC**).

Label data is quoted verbatim. The Chinese translation of each locality below the provincial level is included in parentheses at its first appearance in the text. Each type specimen bears the following label: 'HOLOTYPE (red) (or PARATYPE (yellow)), m# (or f#), *Trichopsenius huaxiensis* sp. nov., Jiang, Huang & Chen, 2023.'.

Images of habitus and morphological details were taken using a Canon 5D Mark IV digital camera with a Mitutoyo Plan NIR 10 lens, a Godox MF12 flash was used as the light source, or a Nikon SMZ25 stereoscopic microscope with a Nikon DS-Ri2 camera. Zerene Stacker (ver. 1.04) was used for image stacking. Adobe Illustrator CS5 was used to prepare the line-drawings. All images were modified and grouped into plates in Adobe Photoshop CS5 Extended.

The following abbreviations are applied: **AL**—length of visible abdomen (in dorsal view) along the midline, **HL**—length of head from the anterior clypeal margin to the occipital constriction; **HW**—width of head across eyes; **PL**—length of pronotum along the midline; **PW**—maximum width of pronotum; **EL**—length of elytra along the suture; **EW**—maximum width of elytra; **BL**—Length of the body is a sum of PL + EL + AL.

Taxonomy

***Trichopsenius huaxiensis* Jiang, Huang & Chen, sp. nov.**
https://zoobank.org/0D6CAF2E-7348-4216-85D5-88B47E9D920A
Figs 1–3

Type material. (10 exs: 7 ♂♂, 3 ♀♀): ***Holotype*:** China: ♂, labeled 'China: Guizhou, Guiyang City (贵阳市), Huaxi District (花溪区), South Campus of Guizhou University (贵州大学南校区), Songlinpo (松林坡), 26°25'40"N, 106°40'06"E, H: 1105 m, 22.XI.2022, Jiang Ri-Xin leg.' (GUGC). ***Paratypes*:** 6 ♂♂, 1 ♀, with same label data as the holotype (GUGC); 2 ♀♀, with same label data as the holotype, except '23. XI.2022, Jiang Ri-Xin & Huang Xiu-Dong leg.' (GUGC).

Diagnosis. Body reddish brown with elytra and lateral lobe of tergite IX darker. Pronotum transverse with anterior margin M-shaped at middle. Surface of visible sternites and tergites finely covered with short setae and modified with a row of long setae at posterior margin. Median lobe of aedeagus with apical lobe knife shaped; left paramere with apical lobe thin and strongly sinuous; right paramere with apical lobe curved and weakly sinuous, with a thin seta at base.

Trichopsenius huaxiensis sp. nov. is most similar with *T. crassicornis* Naomi & Terayama, 1996; they share similar habitus characters, such as the sinuated anterior margin of the pronotum and the form of the antennomeres. The new species can be adequately distinguished from *T. crassicornis* by the following characters: 1) anterior margin of the head weakly curved (cf. straight in *T. crassicornis*); 2) median lobe of the aedeagus hemispherical at the base, apex without setae (cf. median lobe bulbous at base, apex with a short setae in *T. crassicornis*); and 3) apical lobe of the parameres much shorter, about 1/2 length of basal lobe in the right paramere, about 1/3 length of basal lobe in the left paramere (cf. apical lobe more than half length of basal lobe in both right and left parameres in *T. crassicornis*).

Description. Male. ***Body*** (Fig. 1) glossy, reddish brown with elytra and lateral lobe of tergite IX slightly darker.

Head (Fig. 2A) transverse, widest across eyes, surface glossy, covered with sparse thin punctures, with a pair of long setae between eyes, and a pair of long setae located at middle of anterior margin. Antenna (Fig. 2C) 11-articled, antennomeres 1–3 shiny, only bearing sparse long setae, antennomere 4 covered with sparse long setae and several short setae, other antennomeres covered with dense short setae and sparse long setae. Antennomere 1 longer than wide, distinctly expanded at apical 1/2; antennomere 2 longer than wide, narrower than antennomere 1, expanded near middle; antennomere 3 slightly shorter than antennomere 2, longer than wide, widest near apex; antennomeres 4 and 5 similar in form, slightly longer that wide; antennomeres 6–10 similar, about as long as wide, near trapezoidal; antennomere 11 with apex moderately pointed, about 1.5 times as long as wide, widest at basal 2/5. Mandibles (Fig. 2A) simple and aduncous, apex cuspidal. Maxillary palpomere 3 (Fig. 2A) about twice as long as wide, palpomere 4 small and subulate.

Pronotum (Figs 1, 2F) transverse, about 1.5 times as wide as long, widest around posterolateral corners, surface covered with sparse long setae and thin and shallow punctures. Anterior margin protruded, M-shaped at middle, with three pairs of long setae (Fig. 2F, s1–s3) present subapically. Lateral margins finely curved, with several long setae. Posterior margin near straight, slightly concaved at middle, with two pairs of long setae. Disc of pronotum with four pairs of long setae, three pairs (Fig. 2F, s4–s6) located near median line, one pair (Fig. 2F, s7) located near lateral margin.

Elytron (Fig. 2B) longer than wide, with lateral margin near straight, and curved at posterior part, posterior margin curved. Surface of elytron finely covered with large punctures, each puncture bearing long setae.

Meso- and metaventrites (Fig. 2E) covered with several short setae and pores laterally. Surface of mesoventrite modified with thin polygonal microsculpture, mesocoxae almost contiguous. Surface of metaventrite covered with thin and longitudinal microsculpture; median sulcus longitudinal and thin, extending from posterior margin

Figure 1. Habitus of *Trichopsenius huaxiensis* sp. nov., male **A** dorsal view **B** lateral view. Scale bars: 0.5 mm (**A, B**).

to near anterior margin; metaventral plate sparsely covered with minute pores; hind trochanter large and near ovate, surface covered with sparse minute pores.

Legs (Fig. 2D–E) simple, surface finely covered with short setae. Outer margins of tibiae covered with long setae, setae on inner margins much shorter than on out margin, and only present in apical half. Apex of tibiae with several spurs, two of them long and strong, others shorter and thinner. Surface of tarsus densely covered with long setae. Front tarsaomere 1 (Fig. 2D) slightly expended near apex, about as long as sum of length of tarsomeres 2 and 3; tarsomeres 2–4 similar in form, short; tarsomere 5 elongate, about as long as sum of tarsomeres 2–4. Middle tarsomere 1 (Fig. 2E) elongate, slightly shorter than sum of other four tarsomeres; tarsaomeres 2–4 similar in form, tarsaomere 2 longer than tarsaomeres 3 and 4; tarsaomere 5 elongate, shorter than sum of length of tarsaomeres 2–4. Hind tarsomere 1 strongly elongate, longer than sum of other four members; tarsomere 2 shorter than sum of tarsomeres 3–4; tarsomere 3 slightly longer than tarsomere 4; tarsomere 4 shortest; tarsomere 5 about as long as sum of length of tarsomeres 2–3.

Abdomen (Fig. 1A) gradually narrowed posteriorly, surface finely covered with short setae, all visible sternites and tergites modified with a row of long setae at posterior margin. Tergite VIII (Fig. 3A) about as long as wide, disc with several small pores

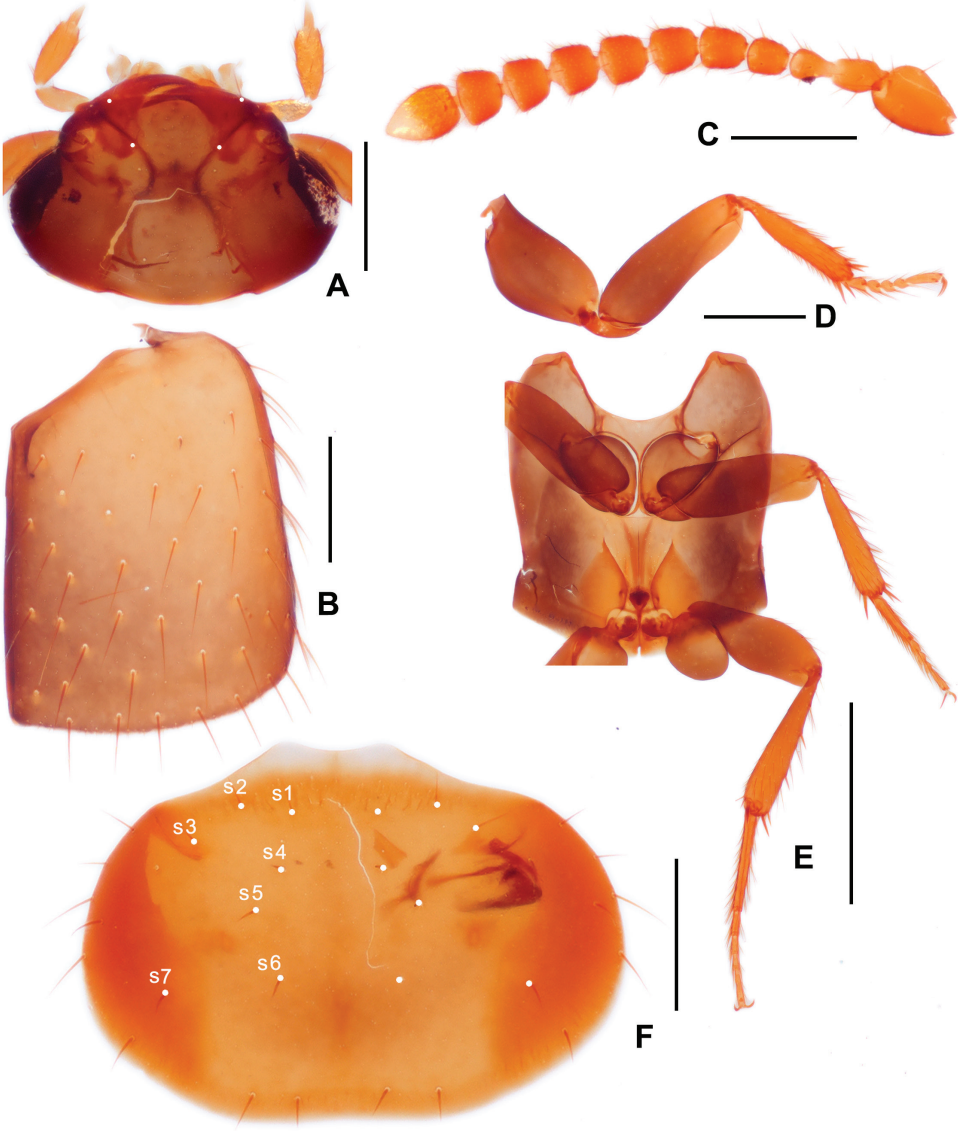

Figure 2. Diagnostic features of *Trichopsenius huaxiensis* sp. nov., male **A** head, dorsal view **B** elytra **C** antenna **D** front leg **E** meso- and metaventrites, with middle and hind legs **F** pronotum, dorsal view. Note: s1–s7, setae of pronotum. Scale bars: 0.2 mm (**A–D, F**); 0.5 mm (**E**).

and without setae, posterior margin rounded, margined by a row of long setae. Sternite VIII (Fig. 3B) longer than wide, disc with sparse small pores, without setae, posterior margin V-sharped, rounded at middle and margined by a row of long setae. Tergite IX (Fig. 3E) cylindrical, lobes long and slender, sparsely covered with setae of different lengths on posterior half; struts thin and long, finely curved, both ends narrower than middle part. Tergite X (Fig. 3E) membranous, inverted triangular, slightly concaved at

middle of posterior margin. Sternite IX (Fig. 3E) rhombic, with middle of posterior margin with several short setae.

Median lobe of aedeagus (Fig. 3G, H) with basal capsule longer than apical lobe; apical lobe knife shaped, with apex slightly expended, apex with a small zonal sclerite. Parameres (Fig. 3I, J) large, longer than median lobe, asymmetric. Left paramere (Fig. 3J) with apical lob shorter than in right paramere, thin and strongly sinuous, apex acute. Right paramere (Fig. 3I) with apical lobe curved and weakly sinuous, with a thin seta at base, apex acute.

Measurements**:** BL: 1.99–2.10 mm; HL: 0.30–0.35 mm, HW: 0.51–0.53 mm; PL: 0.38–0.40 mm, PW: 0.55–0.59 mm; EL: 0.41–0.44 mm; EW: 0.75–0.81 mm; AL: 1.20–1.26 mm.

Female (Fig. 3C, D, F, K), externally similar with male in habitus. Tergite VIII (Fig. 3C) transverse, disc with several small pores and sparsely covered with short setae; posterior margin curved with an apical rounded extension at middle, margined by a row

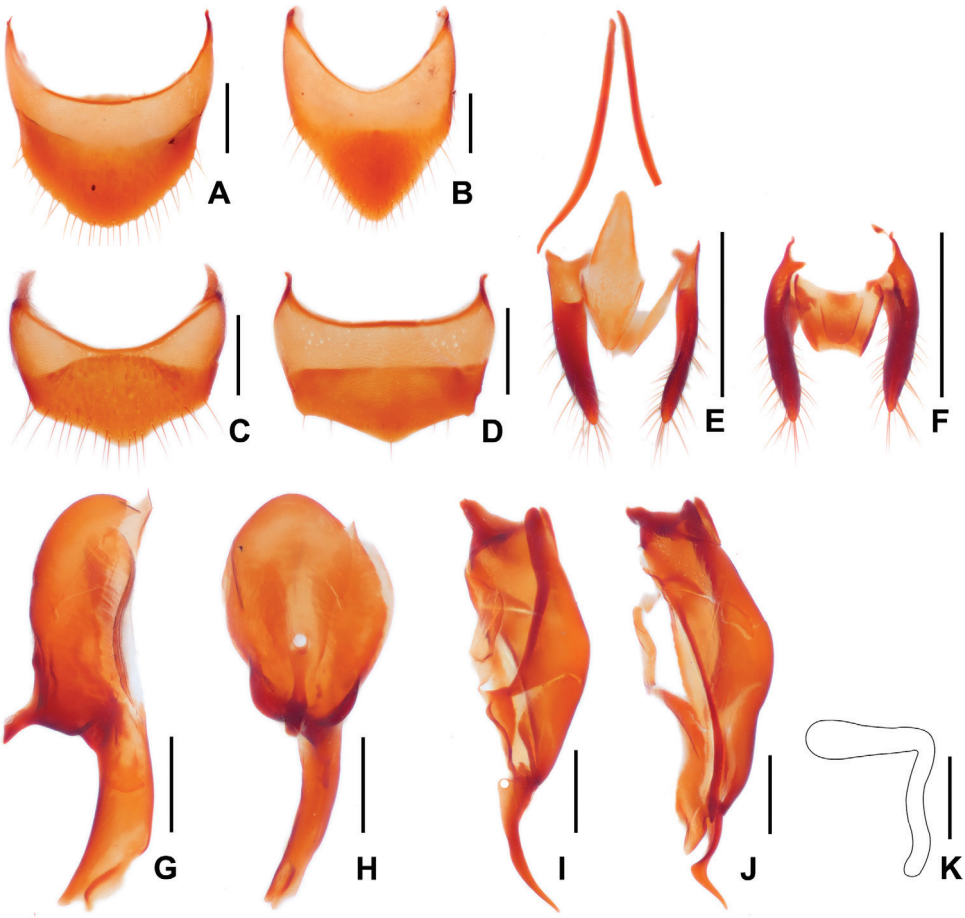

Figure 3. Diagnostic features of *Trichopsenius huaxiensis* sp. nov., **A, B, E, G–J** male; **C, D, F, K** female **A** tergite VIII, male **B** sternite VIII, male **C** tergite VIII, female **D** sternite VIII, female **E** tergite IX–X and sternite IX, male **F** ditto, female **G** median lobe of aedeagus, lateral view **H** ditto, ventral view **I** right paramere **J** left paramere **K** spermatheca. Scale bars: 0.05 mm (**K**); 0.2 mm (**A–D, G–J**); 0.5 mm in (**E, F**).

of long setae. Sternite VIII (Fig. 3D) generally similar with tergite VIII in form, posterior margin with only several long setae. Tergite IX (Fig. 3F) cylindrical, lobes long and slender, sparsely covered with setae of different lengths on posterior half. Tergite X (Fig. 3F) membranous, inverted trapezoidal, slightly concaved at middle of posterior margin. Sternite IX (Fig. 3F) rhombic, with posterior margin rounded. Spermatheca (Fig. 3K) with apical and basal part near perpendicular to each other, basal part narrower than apical part, distinctly sinuated, apical part near straight, with apical expanded and round.

***Measurements*:** BL: 1.98–2.10 mm; HL: 0.30–0.33 mm, HW: 0.50–0.55 mm; PL: 0.39–0.41 mm, PW: 0.55–0.58 mm; EL: 0.40–0.44 mm; EW: 0.78–0.82 mm; AL: 1.19–1.25 mm.

Distribution. China (Guizhou).

Symbiotic host. *Reticulitermes* sp. (Rhinotermitidae, Fig. 4).

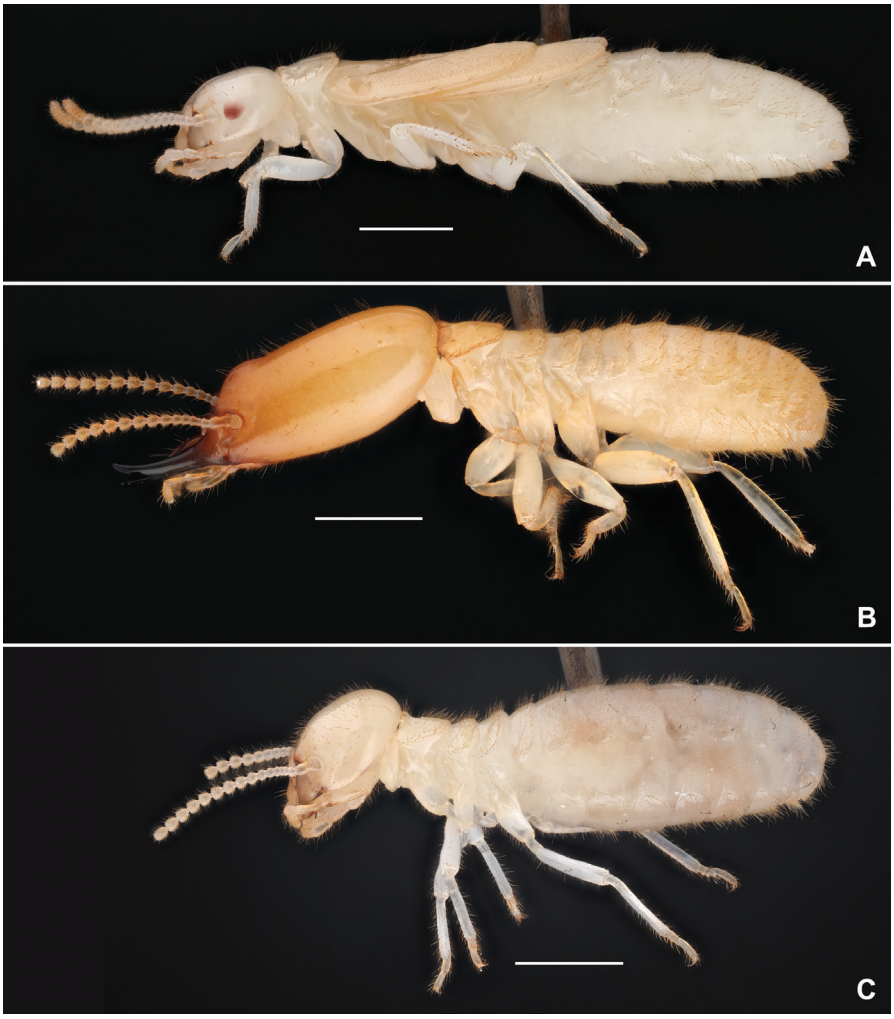

Figure 4. Host termite of *Trichopsenius huaxiensis* sp. nov., *Reticulitermes* sp. **A** neotenic reproductive **B** soldier **C** worker. Scale bars: 1 mm (**A–C**).

Etymology. The species is named after its type locality, Huaxi District (Guiyang City, Guizhou, China).

Biological notes. All adults of the new species were collected in November 2022, they were found in a dead and flattened pine tree where host termites were living (Fig. 5). There were obvious communications between the new species and its host termites after laboratory observation, including antennal touch at least. No attack behavior from their host termites was observed.

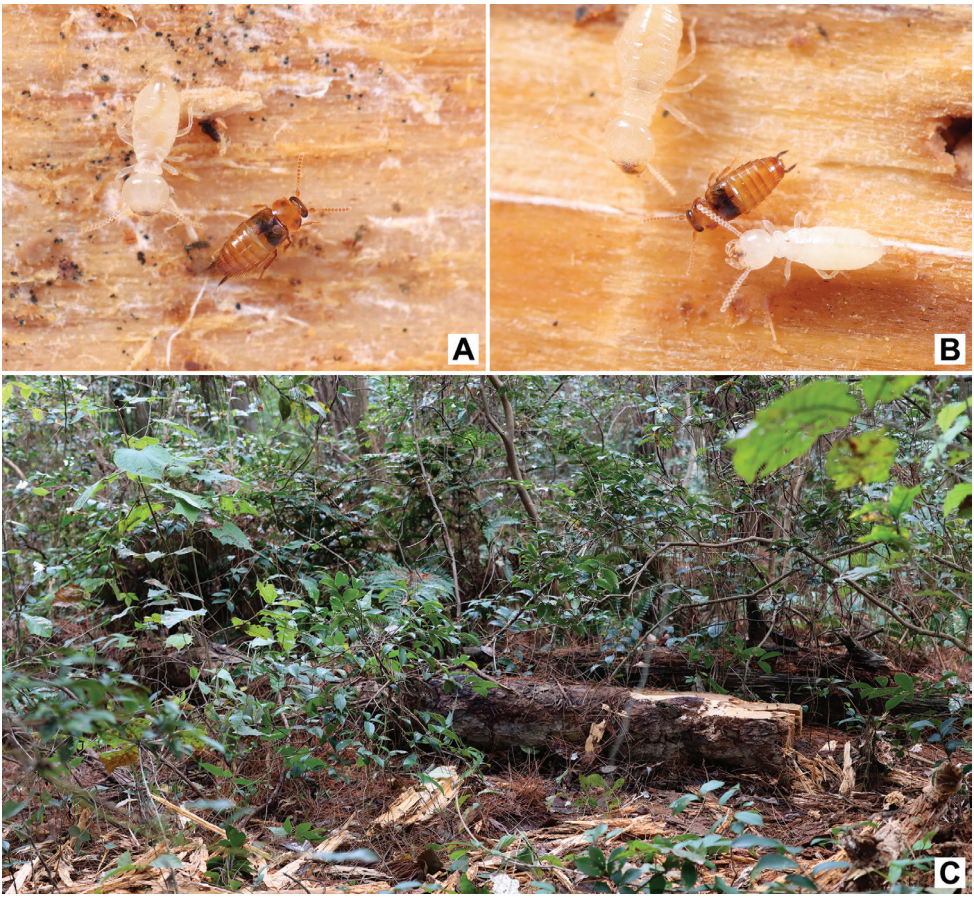

Figure 5. Habitat of *Trichopsenius huaxiensis* sp. nov. **A, B** adults with workers and larvae of *Reticulitermes* sp. **C** environment where *Trichopsenius huaxiensis* sp. nov. was found.

Acknowledgements

The authors express their sincere gratitude to Mr Xiao-Bin Song (Shanghai, China) for his support of this work. We also thank to Dr Taisuke Kanao (Yamagata, Japan) for kindly providing us indispensable references. Dr Michael S. Caterino (Clemson

University, Clemson, U.S.A.) kindly revised the English of this work. Appreciation is also given to two anonymous reviewers for providing constructive suggestions. Financial support was provided by the Program of Excellent Innovation Talents, Guizhou Province (No. 20154021).

References

Howard RW, Kistner DH (1978) The eggs of *Trichopsenius depressus* and *T. frosti* (coleoptera: Staphylinidae, Trichopseniinae) with a comparison to those of their host termites *Reticulitermes virginicus* and *R. flavipes* (Isoptera: Rhinotermitidae, Heterotermitinae). Sociobiology 3(2): 99–106.

Kanao T, Maruyama M (2019) A new species of the termitophilous genus *Trichopsenius* Horn, 1877 (Coleoptera, Staphylinidae, Aleocharinae) from Morocco. Elytra (n. ser.) 9: 297–303.

Kistner DH, Assing V (1995) A new species of Trichopseniinae from Europe (Coleoptera: Staphylinidae). Sociobiology 26: 299–304.

Kistner DH, Howard RW (1980) First report of larval and pupal Trichopseniinae: External marphology, taxonomy and behavior (Coleoptera: Staphylinidae). Sociobiology 5(1): 3–20.

LeConte JL (1863) New species of North American Coleoptera. Part I. Smithsonian Miscellaneous Collections 6(167): 1–92. https://doi.org/10.5962/bhl.title.51303

Naomi S, Terayama M (1986) Taxonomic study on the subfamily Trichopseniinae (Coleoptera, Staphylinidae) of Japan, with descriptions of three new species. Kontyû 54: 697–705.

Naomi S, Terayama M (1996) A new species of *Trichopsenius* Horn (Coleoptera: Staphylinidae) from Japan. New Entomologist 45: 84–86.

Pasteels JM, Kistner DH (1971) Revision of the termitophilous subfamily Trichopseniinae (Coleoptera: Staphylinidae). II. The remainder of the genera with a representative study of the gland systems and a discussion of their relationships. Miscellaneous publications of the Entomological Society of America 7: 351–399.

Seevers CH (1941) Taxomic investrigations of some temitophilous Staphylinidae of the subfamilies Aleocharinae and Trichopseniinae (new subfamily). Annals of the Entomological Society of America 34(2): 318–349. https://doi.org/10.1093/aesa/34.2.318

Seevers CH (1945) New genera and species of Trichopseniinae from American and Australian termite nests. The Pan-Pacific Entomologist 21: 63–72.

Seevers CH (1957) A monograph on the termitophilous Staphylinidae (Coleoptera). Fieldiana. Zoology 40: 1–334. https://doi.org/10.5962/bhl.title.3797

ZooKeys 1152: 45–95 (2023)
doi: 10.3897/zookeys.1152.98258
https://zookeys.pensoft.net

RESEARCH ARTICLE

A peer-reviewed open-access journal
ZooKeys
Launched to accelerate biodiversity research

Seven new "cryptic" species of Discodorididae (Mollusca, Gastropoda, Nudibranchia) from New Caledonia

Julie Innabi[1], Carla C. Stout[1], Ángel Valdés[1]

1 *Department of Biological Sciences, California State Polytechnic University Pomona, 3801 West Temple Avenue, Pomona, California 91768, USA*

Corresponding author: Ángel Valdés (aavaldes@cpp.edu)

Academic editor: Nathalie Yonow | Received 1 December 2022 | Accepted 15 February 2023 | Published 7 March 2023

https://zoobank.org/D20AFC88-0963-45FE-A8B0-74D00728424F

Citation: Innabi J, Stout CC, Valdés A (2023) Seven new "cryptic" species of Discodorididae (Mollusca, Gastropoda, Nudibranchia) from New Caledonia. ZooKeys 1152: 45–95. https://doi.org/10.3897/zookeys.1152.98258

Abstract

The study of a well-preserved collection of discodorid nudibranchs collected in Koumac, New Caledonia, revealed the presence of seven species new to science belonging to the genera *Atagema*, *Jorunna*, *Rostanga*, and *Sclerodoris*, although some of the generic assignments are tentative as the phylogeny of Discodorididae remains unresolved. Moreover, a poorly known species of *Atagema* originally described from New Caledonia is re-described and the presence of *Sclerodoris tuberculata* in New Caledonia is confirmed with molecular data. All the species described herein are highly cryptic on their food source and in the context of the present study the term "cryptic" is used to denote such species. This paper highlights the importance of comprehensive collecting efforts to identify and document well-camouflaged taxa.

Keywords

Molecular phylogenetics, species delimitation, systematics, taxonomy

Introduction

The systematics of sea slugs has benefited enormously from the introduction of molecular data analyses, which have dramatically improved species delimitation and phylogenetic reconstruction, facilitating the description and re-description of taxa belonging to notoriously difficult taxonomic groups (e.g., Jörger et al. 2012; Churchill et al. 2014; Ekimova et al. 2015; Martín-Hervás et al. 2021). In this context, the term "cryptic" is widely used to refer to taxa that are morphologically indistinguishable but can be identified or distinguished using molecular data (Jörger and Schrödl 2013). On the contrary, in ecological research, the term "cryptic" has long been used to denote organisms that are camouflaged on their environment or food source (Faulkner and Ghiselin 1983; Dalton and Godwin 2006; Cheney et al. 2014), and this is not uncommon in many sea slug lineages. But, while "cryptic" species of sea slugs and nudibranchs in the systematics sense have received a great deal of attention in recent years, resulting in the description and identification of numerous cryptic species (e.g., Epstein et al. 2019; Knutson and Gosliner 2022), "cryptic" sea slugs in the ecological sense have been somewhat neglected and have received significantly less attention compared to their often brightly colored, extravagantly shaped cousins.

"Cryptic" species of sea slugs in the ecological sense are difficult to collect, requiring a substantial effort by experienced collectors, or the collection and processing of substrate suspected to contain living specimens. With the exception of sacoglossans, for which substrate collection produces specimens relatively easily (Krug et al. 2016, 2018), few examples of papers describing ecologically cryptic sea slug species have been published in recent years (e.g., Pola et al. 2012; Donohoo and Gosliner 2020).

In this paper we examine a few ecologically "cryptic" species of dorid nudibranchs collected during three research expeditions to Koumac, New Caledonia. These expeditions included a multidisciplinary team of expert collectors and taxonomists, using a combination of a variety of collecting techniques and methods (direct collecting, substrate collecting, autonomous reef monitoring structures (ARMS), underwater vacuum-cleaners, brush baskets, dredging, ROVs, etc.), resulting in an exceptionally well-curated collection. Among the specimens collected were several extraordinarily cryptic species in the ecological sense that would have been difficult to detect without the collecting infrastructure of the Koumac expeditions.

All the species described or re-described herein belong to the family Discodorididae. While this group has been the subject of several monographic reviews (Valdés and Gosliner 2001; Valdés 2002; Dayrat 2010) there is no consensus on the taxonomic structure of the Discodorididae or the number of valid genera. Additionally, molecular phylogenies including substantial coverage of this group (e.g., Mahguib and Valdés 2015; Hallas et al. 2017) have failed to provide enough support to unravel the relationships among different clades. In the present study we use a newly generated molecular phylogeny, including a broad representation of Discodorididae genera, as well as morphological data to provide a framework of classification for the new species described. In some cases, this information is not sufficient to provide definitive generic placements and therefore they are left as tentative.

Materials and methods

Source of specimens

The material examined in this study was collected during three expeditions to Koumac, New Caledonia, organized by the Muséum national d'Histoire naturelle, Paris, France (**MNHN**). All collected specimens were individually photographed, labeled, preserved in 95% ethanol, and deposited at the MNHN. A total of 56 specimens was examined in this study, 46 of which were successfully sequenced (Table 1).

DNA extraction, amplification, and sequencing

From each specimen a small tissue sample (~ 1 mm^3) was taken from the foot using sterilized forceps. DNA extraction was conducted using a Chelex protocol using a mixture of 200 µL of 10% Chelex 100 (Bio-Rad.com), blotted tissue (to remove any remaining ethanol), and 4 µL of proteinase K. The 1.7 mL microcentrifuge tubes with the mixture were placed in a water bath for 20 min at 55 °C (cell lysis and protein digestion) followed by placement in a heat block at 100 °C for 8 min (protein denaturation). Then, the microcentrifuge tubes were centrifuged to separate the Chelex beads from the supernatant containing the DNA, and 100 µL of the supernatant was aliquoted and used for DNA amplification.

The Polymerase Chain Reaction (PCR) was conducted on all samples for three genes: cytochrome c oxidase subunit one (CO1, mtDNA), ribosomal RNA 16S (16S, mtDNA), and Histone H3 (H3, nuclear), using universal primers (Folmer et al. 1994; Palumbi 1996; Colgan et al. 1998) in a Thermal Cycler T100 (Thermo Scientific, Waltham, MA). Each reaction was conducted using 38.5 µL of ultra-pure water, 5 µL of 10× PCR Dream Taq Buffer, 1.25 µL of Bovine Serum Albumin (BSA 20mg/mL), 1 µL 10 mM dNTPS, 1 µL forward primer, 1 µL reverse primer, 0.25 µL of Dream Taq, and 2 µL of DNA extraction, which resulted in each microcentrifuge tube containing a total volume of 50 µL. Reaction conditions for 16S and H3 were are follows: initial denaturation at 94 °C for 2 min, denaturation at 94 °C for 30 sec, annealing at 50 °C for 30 sec, elongation at 68 °C for 1 min, 30 cycles from denaturation to elongation and a final elongation at 68 °C for 7 min. Reaction conditions for COI were are follows: initial denaturation at 95 °C for 3 min, denaturation at 94 °C for 45 sec, annealing at 45 °C for 45 sec, elongation at 72 °C for 2 min, 35 cycles from denaturation to elongation and a final elongation at 72 °C for 10 min. Gel electrophoresis was conducted using 1% agarose tris-borate-EDTA (TBE) buffer and ethidium bromide for 15 min, including a ladder and a negative control to verify successful amplification of the PCR products of the correct length and confirm the absence of contamination. DNA purification was conducted with E.Z.N.A Cycle Pure D6492-02 kits (Omega Bio-Tek, Inc., Norcross, GA) following the manufacturer's instructions. DNA concentration of purified samples was measured using a Nano Drop 1000 spectrophotometer (Thermo Scientific, Waltham, MA) prior to Sanger sequencing, which was outsourced to Retrogen Inc. (San Diego, CA).

Table 1. List of specimens examined in this paper, including isolate, voucher and GenBank accession numbers when available. Specimens labeled with an asterisk (*) were successfully sequenced for this study.

Species	Isolate	Voucher	GenBank Accession Numbers		
			COI	16S	H3
Aldisa albatrossae	JM153a	CASIZ 181288	KP871632	KP871679	KP871655
Asteronotus cespitosus	–	CASIZ 191163	MN720294	MN722441	MN720325
	–	CASIZ 191321	MN720296	MN722443	MN720327
Asteronotus hepaticus	–	–	MW559976	MW559976	–
	–	CASIZ 191310	MN720295	MN722442	MN720326
Asteronotus markaensis	–	CASIZ 192316A	MN720299	MN722446	MN720330
Asteronotus mimeticus	–	CASIZ 208221	MN720305	MN722452	MN720336
Asteronotus namuro	–	CASIZ 192297	MN720298	MN722445	MN720329
Asteronotus spongicolus	–	CASIZ 192317A	MN720300	MN722447	MN720331
	–	CASIZ 194597	MN720301	MN722448	MN720332
*Atagema spongiosa**	JI09	MNHN IM-2013-86190	OQ362153	OQ379356	OQ366207
	JI30	MNHN IM-2013-86189	OQ362156	–	OQ366210
	JI33	MNHN IM-2013-86188	OQ362154	–	OQ366208
Atagema spongiosa	JI02	MNHN IM-2013-86170	OQ362155	OQ379357	OQ366209
Atagema cf. *osseosa*	–	CASIZ 185142	MF958426	MF958296	–
Atagema notacristata	–	CASIZ 167980	KP871634	KP871681	KP871657
Atagema papillosa	JI42	MNHN IM-2013-86192	OQ362138	–	OQ366192
Atagema sobanovae sp. nov.*	JI16	MNHN IM-2013-86211	OQ362139	–	OQ366193
	JI05	MNHN IM-2013-86181	OQ362141	OQ379351	OQ366195
	JI06	MNHN IM-2013-86178	OQ362140	OQ379350	OQ366194
	JI08	MNHN IM-2013-86187	OQ362142	OQ379352	OQ366196
	JI19	MNHN IM-2013-86174	OQ362150	OQ379354	OQ366204
	JI21	MNHN IM-2013-86179	OQ362145	OQ379353	OQ366199
	JI23	MNHN IM-2013-86180	OQ362151	OQ379355	OQ366205
	JI28	MNHN IM-2013-86175	OQ362146	–	OQ366200
	JI29	MNHN IM-2013-86171	OQ362148	–	OQ366202
	JI41	MNHN IM-2013-86173	OQ362149	–	OQ366203
	JI44	MNHN IM-2013-86176	OQ362147	–	OQ366201
	JI45	MNHN IM-2013-86177	OQ362143	–	OQ366197
	JI46	MNHN IM-2013-86172	OQ362144	–	OQ366198
Atagema sobanovae sp. nov.	–	MNHN IM-2013-86229	–	–	–
Atagema kimberlyae sp. nov.*	JI43	MNHN IM-2013-86191	OQ362152	–	OQ366206
Carminodoris flammea	–	CASIZ 177628	MN720285	MN722433	MN720311
Diaulula greeleyi	TL286	LACM 3016	KU950017	KU949947	KU950060
Diaulula nayarita	TL176	LACM 153353	KU950018	KU949948	KU950061
Diaulula odonoghuei	TL178	CPIC 01073	KU950036	KU949967	KU950080
	TL179	CPIC 01074	KU950037	KU949968	KU950081
Diaulula sandiegensis	TL025	CPIC 00911	KU950057	KU949987	KU950103
	TL268	CPIC 01269	KU950058	KU949989	KU950105
Discodoris boholiensis	–	CASIZ 204802	MN720304	MN722451	MN720335
Discodoris cebuensis	–	CASIZ 185141	KP871639	KP871687	KP871663
	–	CASIZ 190761	MN720293	MN722440	MN720322
Discodoris coerulescens	–	CASIZ 182850	MF958421	MF958290	–
Doris kerguelenensis	H20	–	EU823146	EU823238	–
Doris pseudoargus	–	–	AJ223256	AJ225180	–
Hexabranchus sanguineus	JM70a	CPIC 00336	KP871644	KP871692	KP871668
Hoplodoris desmoparypha	–	CASIZ 070066	MN720283	MN722431	MN720309
	–	CASIZ 309550	MN720308	MN722455	–
Hoplodoris rosans	–	CASIZ 182837	MN720288	MN722436	MN720318
	–	CASIZ 182921	MN720290	MN722438	MN720320

Species	Isolate	Voucher	GenBank Accession Numbers		
			COI	16S	H3
Jorunna artsdatabankia	–	NTNU-VM 58891	MW784174	MW784486	MW810589
	–	ZMBN 125946	MW784173	MW784485	MW810590
	–	ZMBN 127749	MW784172	MW784487	–
Jorunna daoulasi sp. nov.	–	MNHN IM-2013-86230	–	–	–
	–	MNHN IM-2013-86220	–	–	–
Jorunna daoulasi sp. nov.*	JI22	MNHN IM-2013-86219	OQ362165	OQ379361	OQ366219
Jorunna hervei sp. nov.	–	MNHN IM-2013-86221	–	–	–
	–	MNHN IM-2013-86222	–	–	–
	–	MNHN IM-2013-86223	–	–	–
	–	MNHN IM-2013-86224	–	–	–
Jorunna hervei sp. nov.*	JI47	MNHN IM-2013-86225	OQ362163	–	OQ366217
	JI48	MNHN IM-2013-86226	OQ362164	–	OQ366218
Jorunna hervei sp. nov.	–	MNHN IM-2013-86227	–	–	–
	–	MNHN IM-2013-86228	–	–	–
Jorunna liviae	–	MNCN15.05/200187	OP948382	–	–
	–	MNCN15.05/200188	OP948383	–	–
	–	MNCN15.05/200189	OP948384	–	–
	–	MNCN15.05/94693	OP948385	–	–
Jorunna onubensis	–	ZMBN 125474	MW784171	MW784483	MW810587
Jorunna tomentosa	–	CASIZ 175752	MW784185	MW784508	MW810604
	–	CASIZ 175753	MW784202	MW784506	MW810610
	–	CASIZ 176820	MW784179	–	MW810602
	–	CASIZ 193035	MW784176	MW784491	MW810607
Montereina nobilis	–	CASIZ 182223	HM162684	HM162593	HM162499
Paradoris liturata	–	CASIZ 177510	KP871648	KP871696	–
	–	CASIZ 182756	MW223084	MW220951	MW415015
Peltodoris atromaculata	–	–	AF249784	AF430360	–
Platydoris sanguinea	–	CASIZ 177762	MF958416	MF958285	–
Rostanga byga	–	CASIZ 181157	MW223085	MW220952	MW415016
Rostanga calumus	EED-Phy-934	–	FJ917485	FJ917427	–
Rostanga elandsia	–	CASIZ 176110	KP871651	KP871699	KP871674
Rostanga poddubetskaiae sp. nov.*	JI01	MNHN IM-2013-86199	OQ362134	OQ379347	OQ366188
	JI03	MNHN IM-2013-86202	OQ362129	–	OQ366183
	JI07	MNHN IM-2013-86218	OQ362136	OQ379348	OQ366190
	JI12	MNHN IM-2013-86203	OQ362122	OQ379345	OQ366176
	JI13	MNHN IM-2013-86206	OQ362121	–	OQ366175
	JI15	MNHN IM-2013-86215	OQ362124	–	OQ366178
	JI17	MNHN IM-2013-86200	OQ362125	–	OQ366179
	JI18	MNHN IM-2013-86209	OQ362135	–	OQ366189
	JI20	MNHN IM-2013-86204	OQ362137	OQ379349	OQ366191
	JI24	MNHN IM-2013-86216	OQ362127	OQ379346	OQ366181
	JI25	MNHN IM-2013-86208	OQ362119	OQ379344	OQ366173
	JI26	–	OQ362132	–	OQ366186
	JI27	MNHN IM-2013-86205	OQ362130	–	OQ366184
	JI31	MNHN IM-2013-86212	OQ362126	–	OQ366180
	JI32	MNHN IM-2013-86201	OQ362133	–	OQ366187
	JI36	MNHN IM-2013-86213	OQ362120	–	OQ366174
	JI37	MNHN IM-2013-86214	OQ362123	–	OQ366177
	JI38	MNHN IM-2013-86217	OQ362128	–	OQ366182
	JI39	MNHN IM-2013-86207	OQ362131	–	OQ366185
Rostanga poddubetskaiae sp. nov.	JI40	MNHN IM-2013-86210	–	–	–
Rostanga pulchra	–	CASIZ 174490A	MW223086	MW220953	MW415017

Species	Isolate	Voucher	GenBank Accession Numbers		
			COI	16S	H3
Sclerodoris sp.	–	CASIZ 182866	MN720289	MN722437	MN720319
	–	CASIZ 191525	MN720297	MN722444	MN720328
Sclerodoris faninozi sp. nov.*	JI11	MNHN IM-2013-86198	OQ362161	OQ379359	OQ366215
Sclerodoris dutertrei sp. nov.*	JI04	MNHN IM-2013-86193	OQ362157	OQ379358	OQ366211
	JI14	MNHN IM-2013-86196	OQ362160	–	OQ366214
	JI34	MNHN IM-2013-86195	OQ362159	–	OQ366213
	JI35	MNHN IM-2013-86194	OQ362158	–	OQ366212
Sclerodoris tuberculata	–	CASIZ 190788	MF958417	MF958286	MN720323
*Sclerodoris tuberculata**	JI10	MNHN IM-2013-86197	OQ362162	OQ379360	OQ366216
Taringa sp.	–	CASIZ 172039	MN720284	MN722432	MN720310
Taringa telopia	–	CASIZ 182933	MN720291	KP871700	KP871675
Tayuva ketos	TL086	CPIC 00654	KU950019	KU949949	KU950062
Thordisa aff. *albomacula*	–	CASIZ 179590	MF958418	MF958287	MN720313
	–	CASIZ 181136	MN720286	MN722434	MN720314
	–	CASIZ 182834	MT454622	MT452888	MT454628
	–	CASIZ 220322	MT454620	MT452884	MT454624
Thordisa bimaculata	–	CASIZ 184516	MN720292	MN722439	MN720321
Thordisa nieseni	–	CASIZ 173057	MW223087	MW220954	MW415018

Data analysis

Forward and reverse sequences were assembled, edited, and consensus sequences were extracted using the computer program Geneious v. 11.1.5 (Kearse et al. 2012). Additional sequences were downloaded from GenBank for comparison (Table 1). Sequences were aligned using the MUSCLE (Edgar 2004) plug-in in Geneious. Gaps in the 16S alignment were removed manually, and concatenation of all three genes was performed in Geneious. Bayesian and maximum likelihood phylogenetic analyses were conducted on the concatenated sequences (partitioned by gene) and on each gene fragment individually. Bayesian analysis was implemented using MrBayes v. 3.2.1 (Ronquist et al. 2012) with the GTR model, using two runs of six chains for 10 million repetitions with a sampling interval of 1,000 repetitions and burn-in of 25% removed. The maximum-likelihood analysis was conducted in RaXMLGUI v. 1.0 (Silvestro and Michalak 2012) using the bootstrap + consensus option and the GAMMAGI model with 10,000 bootstrap repetitions. *Hexabranchus sanguineus* (Rüppell & Leuckart, 1830) was used to root the resulting trees. Nodes in the resulting phylogenetic tree with Posterior probabilities (PP) ≥ 90% and bootstraps values (MLB) ≥ 70% were interpreted as supported.

The Automatic Barcode Gap Discovery (ABGD) software (Puillandre et al. 2012) was used to provide statistical support to determine the number of species in the sample using COI sequences of 107 specimens. Pairwise p-distance values were calculated using MEGA v. 11.0.13 (Kumar et al. 2018) using the Kimura-2 model (Kimura 1980).

Morphological examination

At least two specimens (if available) from each species recovered in the ABGD analysis were dissected to study their reproductive system (including the penis), jaw (if present),

and radula. Dissections were performed by a dorsal incision from the middle of the nudibranch to the anterior end. The reproductive system was carefully removed from each specimen and drawn with a camera lucida. The penis was dissected and examined under a compound microscope. The buccal mass (including the radula and jaw) was removed from the anterior end of each animal and placed in a 10% NaOH solution to dissolve soft tissue and expose the radula and jaws. After 20 min to several hours, the radula and labial cuticle (housing the jaw) were rinsed in distilled water and mounted on a small copper plate for Scanning Electron Microscopy (SEM) examination. The samples were sputter-coated with gold and observed under a JSM- 6010PLUS/LA SEM at California Polytechnic State University, Pomona, California.

Results

The concatenated phylogenetic trees (BI and ML) recovered species of Discodorididae Bergh, 1891 + Cadlinidae Bergh, 1891 (represented by the genus *Aldisa* Bergh, 1878) as a monophyletic group (PP = 0.99, MLB = 70) (Fig. 1). Members of the genus *Atagema* Gray, 1850 are monophyletic (PP = 1, MLB = 100) and sister to the rest of Discodorididae + Cadlinidae (PP = 0.98, MLB = 96). The remaining Discodorididae (when *Aldisa* and *Atagema* are excluded) is monophyletic (PP = 1, MLB = 89) and contains a number of clades, most of which are not supported. The analyses recovered a clade containing species identified as *Sclerodoris* Eliot, 1904 (including the type species, *S. tuberculata* Eliot, 1904), as monophyletic (PP = 1, MLB = 100), which is sister to the single representative of *Platydoris* Bergh, 1877 (PP = 1, MLB = 92); these two groups appear to be related to another monophyletic group (PP = 1, MLB = 100), containing two species identified as members of *Diaulula* Bergh, 1878 [*D. nayarita* (Ortea & Llera, 1981) and *D. greeleyi* (MacFarland, 1909)], but the relationship between *Platydoris*, *Sclerodoris*, and these two species of *Diaulula* is not supported. Another monophyletic group includes species identified as *Rostanga* Bergh, 1879 (PP = 0.79, MLB = 94), with unresolved relationships to other Discodorididae clades. The genus *Discodoris* Bergh, 1877, including the type species *D. boholiensis* Bergh, 1877, is also monophyletic (PP = 1, MLB = 100) and sister to the single representative of *Carminodoris* Bergh, 1889 (PP = 1, MLB = 99), and these two groups appear to be related to some species identified as *Thordisa* Bergh, 1877, which also form a monophyletic group (PP = 1, MLB = 100). Although not supported in the ML analysis, *Discodoris*, *Carminodoris*, and *Thordisa* appear to be related to the monophyletic genus *Jorunna* Bergh, 1876 (PP = 1, MLB = 96), including the type species *J. tomentosa* (Cuvier, 1804). Another genus recovered as monophyletic is *Asteronotus* Ehrenberg, 1831 (PP = 1, MLB = 91), including the type species *A. cespitosus* (van Hasselt, 1824), which is sister (PP = 1, MLB = 94) to another monophyletic group including species identified as *Hoplodoris* Bergh, 1880 (PP = 1, MLB = 99), and together sister (PP = 1, MLB = 75) to another group of species identified as *Thordisa* (PP = 1, MLB = 99). Other traditional genus-level groups appear to be related but these relationships are not supported; these include *Paradoris liturata* (Bergh, 1905),

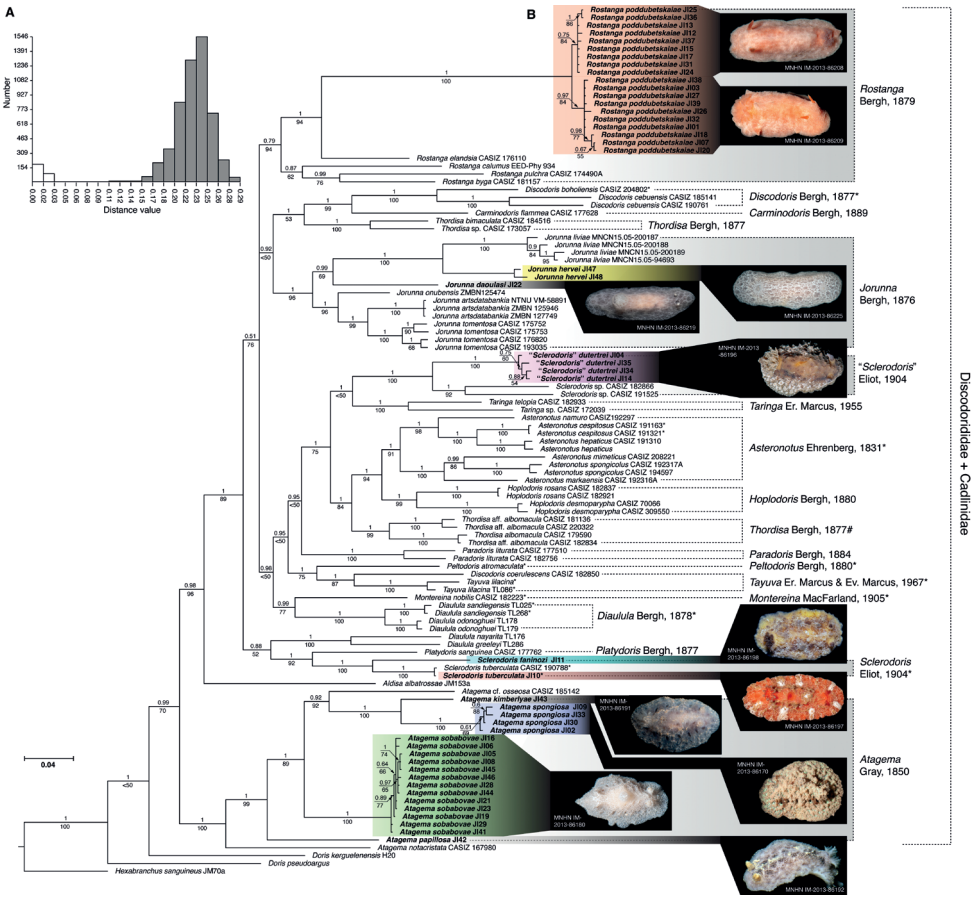

Figure 1. Graphic representation of the molecular analyses results **A** histogram represents the distance plot for the ABGD analysis using the COI gene showing pairwise *p*-distances (Kimura 2 model) among candidate species **B** Bayesian consensus tree of the concatenated 16S, COI and H3 gene fragments. Posterior probabilities from the Bayesian analysis are listed above each branch; bootstrap values from maximum likelihood analysis are listed below each branch.

the type species of *Peltodoris* Bergh, 1880 (*P. atromaculata* Bergh, 1880), *Discodoris coerulescens* Bergh, 1888, and specimens currently identified as *Tayuva lilacina* (Gould, 1852). Finally, the genus *Diaulula* including the type species *D. sandiegensis* (Cooper, 1863) is monophyletic (PP = 1, MLB = 100) and sister to *Montereina nobilis* MacFarland, 1905. Single gene fragment phylogenetic analyses provided similar results in general but with lower resolution (Suppl. materials 1–3).

The ABGD analysis recovered 52 distinct species in the sample, which matches the structure recovered in the phylogenetic analysis (Table 2). The species recovered include all the taxa described below in the systematics section and species currently recognized as valid in the literature. The only exceptions are *Diaulula sandiegensis* and *Diaulula odonohuei* (Steinberg, 1963), which ABGD failed to recover as distinct, and

Table 2. Candidate species (groups) recovered in the ABDG analysis of COI sequence fragments. Initial Partition with prior maximal distance $P = 2.15e^{-02}$; barcode gap distance = 0.088; distance simple distance minimum slope = 1.00.

Group	Species	Voucher # (Isolate #)
1	*Aldisa albatrossae*	CASIZ 181288 (JM153a)
2	*Asteronotus cespitosus*	CASIZ 191321, CASIZ 191163
3	*Asteronotus hepaticus*	n/a, CASIZ 191310
4	*Asteronotus markaensis*	CASIZ 192316A
5	*Asteronotus mimeticus*	CASIZ 208221
6	*Asteronotus namuro*	CASIZ 192297
7	*Asteronotus spongicolus*	CASIZ 192317A, CASIZ 194597
8	*Atagema* cf. *osseosa*	CASIZ 185142
9	*Atagema notacristata*	CASIZ 167980
10	*Atagema kimberlyae* sp. nov.	MNHN IM-2013-86191 (JI43)
11	*Atagema papillosa*	MNHN IM-2013-86192 (JI42)
12	*Atagema sobanovae* sp. nov.	MNHN IM-2013-86211 (JI16), MNHN IM-2013-86178 (JI06), MNHN IM-2013-86181 (JI05), MNHN IM-2013-86187 (JI08), MNHN IM-2013-86177 (JI45), MNHN IM-2013-86172 (JI46), MNHN IM-2013-86179 (JI21), MNHN IM-2013-86175 (JI28), MNHN IM-2013-86176 (JI44), MNHN IM-2013-86171 (JI29), MNHN IM-2013-86173 (JI41), MNHN IM-2013-86174 (JI19), MNHN IM-2013-86180 (JI23)
13	*Atagema spongiosa*	MNHN IM-2013-86190 (JI09), MNHN IM-2013-86188 (JI33), MNHN IM-2013-86170 (JI02), MNHN IM-2013-86189 (JI30)
14	*Carminodoris flammea*	CASIZ 177628
15	*Diaulula greeleyi*	LACM 3016 (TL286)
16	*Diaulula nayarita*	LACM 153353 (TL176)
17	*Diaulula sandiegensis/odonoghuei*	CPIC 00911 (TL025), CPIC 01269 (TL268), CPIC 01073 (TL178), CPIC 01074 (TL179)
18	*Discodoris boholiensis*	CASIZ 204802
19	*Discodoris cebuensis*	CASIZ 185141
20	*Discodoris cebuensis*	CASIZ 190761
21	*Discodoris coerulescens*	CASIZ 182850
22	*Doris kerguelenensis*	(H20)
23	*Doris pseudoargus*	n/a
24	*Hexabranchus sanguineus*	CPIC 00336 (JM70a)
25	*Hoplodoris desmoparypha*	CASIZ 070066, CASIZ 309550
26	*Hoplodoris rosans*	CASIZ 182837, CASIZ 182921
27	*Jorunna artsdatabankia*	NTNU-VM 58891, ZMBN 125946, ZMBN 127749
28	*Jorunna daoulasi* sp. nov.	MNHN IM-2013-86219 (JI22)
29	*Jorunna hervei* sp. nov.	MNHN IM-2013-86225 (JI47), MNHN IM-2013-86226 (JI48)
30	*Jorunna liviae*	MNCN15.05/200187, MNCN15.05/200188, MNCN15.05/200189, MNCN15.05/94693
31	*Jorunna onubensis*	ZMBN 125474
32	*Jorunna tomentosa*	CASIZ 175752, CASIZ 175753, CASIZ 176820, CASIZ 193035
33	*Paradoris liturata*	CASIZ 177510, CASIZ 182756
34	*Peltodoris atromaculata*	n/a
35	*Montereina nobilis*	CASIZ 182223
36	*Platydoris sanguinea*	CASIZ 177762
37	*Rostanga byga*	CASIZ 181157
38	*Rostanga calumus*	EED-Phy-934
39	*Rostanga elandsia*	CASIZ 176110
40	*Rostanga poddubetskaiae* sp. nov.	MNHN IM-2013-86208 (JI25), MNHN IM-2013-86213 (JI36), MNHN IM-2013-86206 (JI13), MNHN IM-2013-86203 (JI12), MNHN IM-2013-86214 (JI37), MNHN IM-2013-86215 (JI15), MNHN IM-2013-86200 (JI17), MNHN IM-2013-86212 (JI31), MNHN IM-2013-86216 (JI24), MNHN IM-2013-86209 (JI18), MNHN IM-2013-86218 (JI07), JI20 (MNHN IM-2013-86204), MNHN IM-2013-86217 (JI38), MNHN IM-2013-86202 (JI03), MNHN IM-2013-86205 (JI27), MNHN IM-2013-86207 (JI39), MNHN IM-2013-86201 (JI32), MNHN IM-2013-86199 (JI01)

Group	Species	Voucher # (Isolate #)
41	*Rostanga pulchra*	CASIZ 174490A
42	*Sclerodoris dutertrei* sp. nov.	MNHN IM-2013-86193 (JI04), MNHN IM-2013-861924 (JI35), MNHN IM-2013-86195 (JI34), MNHN IM-2013-86196 (JI14)
43	*Sclerodoris* sp.	CASIZ 182866
44	*Sclerodoris* sp.	CASIZ 191525
45	*Sclerodoris faninozi* sp. nov.	MNHN IM-2013-86198 (JI11)
46	*Sclerodoris tuberculata*	CASIZ 190788, MNHN IM-2013-86197 (JI10)
47	*Taringa* sp.	CASIZ 172039
48	*Taringa telopia*	CASIZ 182933
49	*Tayuva ketos*	n/a, CPIC 00654 (TL086)
50	*Thordisa* aff. *albomacula*	CASIZ 181136, CASIZ 220322
51	*Thordisa albomacula*	CASIZ 179590, CASIZ 182834
52	*Thordisa bimaculata*	CASIZ 184516
53	*Thordisa nieseni*	CASIZ 173057

specimens identified as *Discodoris cebuensis* Bergh, 1877, which ABGD recovered as two distinct species.

There are consistent interspecific morphological differences among representative specimens in the clades recovered in the phylogenetic analyses, which also correspond to the species from the species delimitation analyses. These differences included aspects of internal morphology such as radular morphology and reproductive system differences that are discussed in the Systematics section below.

Systematics

Family Discodorididae Bergh, 1891

Genus *Atagema* Gray, 1850

Atagema Gray 1842–50 [1850]: 104. Type species: *Doris carinata* Quoy & Gaimard, 1832 [= *Atagema carinata* (Quoy & Gaimard, 1832)], by monotypy.

Trippa Bergh 1877: 63. Type species: *Trippa ornata* Bergh, 1877 [= *Atagema ornata* Ehrenberg, 1831], by original designation.

Phlegmodoris Bergh 1878: 593. Type species: *Phlegmodoris mephitica* Bergh, 1878 [= *Atagema spongiosa* (Kelaart, 1858)], by subsequent designation by Valdés and Gosliner (2001).

Petelodoris Bergh, 1881: 227–228. Type species: *Petelodoris triphylla* Bergh, 1881 [?= *Atagema ornata* (Ehrenberg, 1831)], by monotypy.

Glossodoridiformia O'Donoghue, 1927: 87–89. Type species *Glossodoridiformia alba* O'Donoghue, 1927 [= *Atagema alba* O'Donoghue, 1927], by original designation.

Remarks. For an in-depth discussion of the characteristics of the genus *Atagema* and its synonyms see Valdés and Gosliner (2001).

***Atagema spongiosa* (Kelaart, 1858)**
Figs 2A, B, 3A, 4A–C

Doris spongiosa Kelaart, 1858: 97–98. Type locality: Inner Harbor, Trincomalie, Ceylon [= Trincomalee, Sri Lanka].

Doris areolata Alder & Hancock, 1864: 119, pl. 30, figs 1–3 [non *Doris areolata* Stuwitz, 1835]. Type locality: Waltair, Madras Presidency [= Visakhapatnam, Andhra Pradesh], India.

Phlegmodoris mephitica Bergh, 1878: 594–597, pl. 66, figs 8–20. Type locality: Lapinig Island, Ubay, Philippines.

Trippa (*Phlegmodoris*) *paagoumenei* Risbec, 1928: 87–90, text fig. 15, pl. B, fig. 3, pl. 3, fig. 1. Type locality: Paagoumene, New Caledonia.

Material examined. Pointe Pandop, Koumac, New Caledonia (20°34.9'S, 164°16.6'E), 0 m depth [Koumac 2.1 stn. KM100, rocky shore, rubble, sand, mud, seagrasses], 12 Sep 2018, 1 specimen 49 mm long (MNHN IM-2013-86170, isolate JI02). Koumac, New Caledonia (20°34.7'S, 164°16.5'E), 2–4 m depth [Koumac 2.1 stn. KR231, rocky bottom turning to mud, sponges, *Halimeda*], 25 Sep 2018, 1 specimen 27 mm long, dissected (MNHN IM-2013-86190, isolate JI09). Pointe Pandop, Koumac, New Caledonia (20°34.9'S, 164°16.6'E), 0 m depth [Koumac 2.2 stn. KM100, rocky shore, rubble, sand, mud, seagrasses], 1 Mar 2019, 1 specimen 29 mm long (MNHN IM-2013-86188, isolate JI33). Koumac, New Caledonia (20°35.1'S, 164°16.3'E), 7–8 m depth [Koumac 2.2 stn. KR231], 1 Mar 2019, 1 specimen 6 mm long (MNHN IM-2013-86189, isolate JI30).

Description. Body oval, flattened, covered with large, rounded tubercles decreasing in size towards the mantle margin (Fig. 2A, B). A central, longitudinal ridge runs between the rhinophores and gill. A series of depressions on each side of the central ridge, generally decreasing in size towards the mantle margin. Entire dorsal surface, except for the depressions, covered with caryophyllidia. Branchial sheath composed of three large lobes; gill composed of five tripinnate branchial leaves, arranged horizontally in the living animal. Rhinophoral sheaths elevated; rhinophores long, lamellated, with 24 lamellae. Juvenile specimens with less marked dorsal tubercles (Fig. 2B). Body color opaque greyish brown in adult specimens, except for the depressions, which are dark brown to black (Fig. 2A); juveniles translucent gray (Fig. 2B). Rhinophores and branchial leaves are the same color as the dorsum.

Reproductive system (Fig. 3A) with a long, narrow, simple ampulla that connects with the female gland complex and an elongated, convoluted prostate, with several folds. Prostate ~ 3× as long as the ampulla. The prostate narrows slightly before expanding into the long, simple, wide deferent duct. Deferent duct several times as wide as the prostate, but shorter in length. The penis is unarmed. The vagina is long and wide, as wide as the deferent duct, and connects directly to the small, oval bursa copulatrix. The small elongate seminal receptacle also connects to the bursa copulatrix next to the vaginal connection and the short uterine duct

that enters the female gland complex. The bursa copulatrix is ~ 2× as large as the seminal receptacle.

Radular formula 18 × 35.0.35 in a 27-mm long specimen (MNHN IM-2013-86190). Rachidian teeth absent. Inner and mid-lateral teeth hamate, having a small cusp and lacking denticles (Fig. 4A, B). Innermost teeth very small in comparison to mid-laterals (Fig. 4A). The teeth increase in size suddenly towards the medial portion of the half-row (Fig. 4A). Outermost teeth small, decreasing in size gradually, and hamate (Fig. 4C). No jaw was observed, labial cuticle smooth.

Biology. Geographic range including the Indian and Western Pacific oceans (see synonymy and remarks). In New Caledonia it is found under rocks during the day in shallow water, from 0–8 m depth. The specimens examined were obtained by direct collection during low tide and/or SCUBA diving; they were highly cryptic on rocks covered with sponges and other encrusting organisms.

Remarks. *Doris spongiosa* Kelaart, 1858 was originally described from Sri Lanka and re-described by Valdés and Gosliner (2001), who transferred it to the genus *Atagema*, and recognized two synonyms, *Doris areolata* Alder & Hancock, 1864 and *Phlegmodoris mephitica* Bergh, 1878. This species is common across the tropical Indo-Pacific region and is well characterized and illustrated in modern literature (Wells and Bryce 1993; Yonow 2008; Hervé 2010; Gosliner et al. 2018; Nakano 2018). The specimens here examined from New Caledonia match the original description as well as the common usage of the name in the references above (see Hervé 2010).

Trippa (*Phlegmodoris*) *paagoumenei* Risbec, 1928 was originally described based on a single specimen collected in Paagoumene, northern New Caledonia, but it was later reported from Nouméa, southern New Caledonia (Risbec 1930, 1953). Risbec (1928) described *T. paagoumenei* as having a rather tough notum, dark violet in color, except towards the edges of the foot and the mantle, where it has a yellowish tint, and completely covered with purplish green, irregular tubercles. One of the specimens from Nouméa was unusual as it was covered by a bright green deposit of metallic appearance (Risbec 1953). Rudman (2002) considered *T. paagoumenei* a member of the genus *Atagema* and a synonym of *A. spongiosa*, and we concur with this opinion.

Atagema spongiosa is clearly distinct from other species of *Atagema* recognized as valid in the modern literature, such as *Atagema ornata* (Ehrenberg, 1831) [= *Atagema intecta* Kelaart, 1858] and *Atagema carinata* (Quoy & Gaimard, 1832), illustrated and/or redescribed in Willan and Coleman (1984), Valdés and Gosliner (2001), and Rudman (2005), as well as *Atagema echinata* (Pease, 1860), illustrated by Tibiriçá et al. (2017) and Gosliner et al. (2018). None of these species possesses the characteristic dorsal pattern of tubercles, depressions with a central ridge present in *A. spongiosa*. *Atagema boucheti* Valdés & Gosliner, 2001, described based in a preserved specimen from New Caledonia deep water (405–411 m depth), is characterized by having the dorsum covered by large, irregularly scattered tubercles, not aligned to form ridges. Although the live color of this species is unknown, the external morphology is clearly different from other species of *Atagema* including *Atagema spongiosa* (see Valdés and Gosliner 2001).

***Atagema papillosa* (Risbec, 1928)**
Figs 2E, 3D, E, 4G–I

Phlegmodoris papillosa Risbec, 1928: 90–91, pl. 8, fig. 2. Type locality: Nouméa, New Caledonia [not indicated in the original description], see Risbec (1953).
?*Trippa albata* Burn, 1962a: 101–102, text fig. 5. Type locality: Sunderland Bay, Phillip Island, Victoria, Australia.
?*Atagema* sp. 11: Gosliner et al. 2018: 116.

Material examined. Koumac, New Caledonia (20°35.6'S, 164°16.2'E), 4–6 m depth [Koumac 2.3 stn. KD510, coral debris and coarse sand], 30 Oct 2019, 1 specimen 11 mm long, dissected (MNHN IM-2013-86192, isolate JI42).

Description. Body oval, flattened, covered with a complex network of small ridges with two levels of organization (Fig. 2E). The largest ridges cover the entire body, leaving some depressions in between. Smaller ridges occur in the depressions dividing them into smaller fragments. Entire dorsal surface, except for the depressions, covered with caryophyllidia. Branchial sheath composed of three large lobes; gill composed of five tripinnate branchial leaves, arranged horizontally in the living animal. Rhinophoral sheaths elevated; rhinophores long, lamellated, with 16 lamellae. Body color opaque grey with scattered yellow spots; depressions with gray ridges dividing dark grey to black fragments. Gill leaves are the same color as the dorsum. Rhinophores greyish to yellowish cream.

Reproductive system (Fig. 3D, E) with a large, folded ampulla that connects with the female gland complex and an elongate prostate. The prostate is much longer and ~ 2× as narrow as the ampulla. The prostate narrows substantially into a long, folded tube before expanding into the short, curved, wide deferent duct. The deferent duct is ~ 2× as narrow as the prostate. The penis is unarmed. The vagina is long and narrow, slightly narrower than the deferent duct, and connects directly to the oval bursa copulatrix. The elongate seminal receptacle also connects to the bursa copulatrix next to the vaginal connection, and the short uterine duct, which enters the female gland complex. The bursa copulatrix is several times as large as the seminal receptacle (Fig. 3E).

Radular formula 13 × 19.0.19 in a 11-mm long specimen (MNHN IM-2013-86192). Rachidian teeth absent. Inner and mid-lateral teeth hamate, having a small cusp and lacking denticles (Fig. 4G–I). Innermost teeth very small in comparison to mid-laterals (Fig. 4G), elongate, with an inconspicuous secondary cusp mid-length. The teeth increase in size suddenly towards the medial portion of the half-row (Fig. 4G). Outermost teeth small, decreasing in size gradually, and hamate (Fig. 4I). No jaw was observed, labial cuticle smooth.

Biology. Possibly a New Caledonia endemic, rare, 4–6 m depth. The single specimen was collected by dredging on coral debris and coarse sand bottoms.

Remarks. *Phlegmodoris papillosa* Risbec, 1928 was originally described based on a single specimen collected in Nouméa, New Caledonia, with a short description and an illustration of the live animal. Risbec (1928) described the species as having the notum

covered with large papillae and bearing spots with the appearance of black ocelli standing out against a yellowish background. Risbec (1928) also mentioned that the elongated, perfoliate rhinophores of *P. papillosa* are retractile in funnel-shaped sheaths with a well-marked ocelliform spotted papilla; and the gill is retractile in a cavity with a star-shaped orifice. The specimens here examined closely resemble the original description of *P. papillosa* with the exception that the notum is grey, not yellowish.

Atagema albata (Burn, 1962a) is a similar species, originally described as *Trippa albata*, based on three specimens collected in Victoria, Australia. The specimens were described as pure white, sometimes with cream pigment, and characterized by having a soft, broad, flat body, with the mantle covered with low caryophyllidia, all similar in size, and with a mid-dorsal crest, extending from between the rhinophores to the branchial cavity. Burn (1962a) also described the branchial cavity as having an irregular outline and the rhinophores as perfoliate, with small, raised sheaths. Burn (1962a) compared *T. albata* with the New South Wales species *T. intecta* Kelaart, 1859 (= *Goniodoris erinaceus* Angas, 1864), which according to Burn (1962a) is usually much larger than *A. albata* and is of an ashy-brown color. With the available information is it not possible to confirm if *A. albata* and *A. papillosa* are the same species, and sequence data from *A. albata* would be needed to confirm this potential synonymy.

Finally, the specimen from the Philippines illustrated by Gosliner et al. (2018) as *Atagema* sp. 13 presents a similar external appearance and could be the same species. Examination of specimens is needed to confirm this possibility.

***Atagema kimberlyae* sp. nov.**
https://zoobank.org/FFE42C3A-F0E3-486D-9376-DC999DE7F241
Figs 2C, D, 3B, C, 4D–F

Atagema sp. 2: Hervé 2010: 190.

Type material. *Holotype*: Koumac, New Caledonia (20°35.5'S, 164°16.4'E), 5 m depth [Koumac 2.1 stn. KR223, patch of sponges, small bits of sedimented coral, coarse sand and mud with algae], 19 Sep 2018, 20 mm long, dissected (MNHN IM-2013-86191, isolate JI43).

Description. Body oval, flattened, covered with small, irregular tubercles and short ridges decreasing in size towards the mantle margin (Fig. 2C, D). A central, longitudinal area devoid of tubercles or ridges runs between the rhinophores and gill. A series of depressions on each side of the central ridge, generally decreasing in size towards the mantle margin. Entire dorsal surface, except for the depressions, covered with caryophyllidia. Branchial sheath composed of three large lobes; gill composed of five tripinnate branchial leaves, arranged horizontally in the living animal. Rhinophoral sheaths elevated; rhinophores long, lamellated, with 20 lamellae. Body color opaque greyish brown, with pale brown pigment mainly on top of the tubercles and ridges and scattered opaque white pigment; depressions dark brown to black (Fig. 2C). Rhinophores and branchial leaves are the same color as the dorsum.

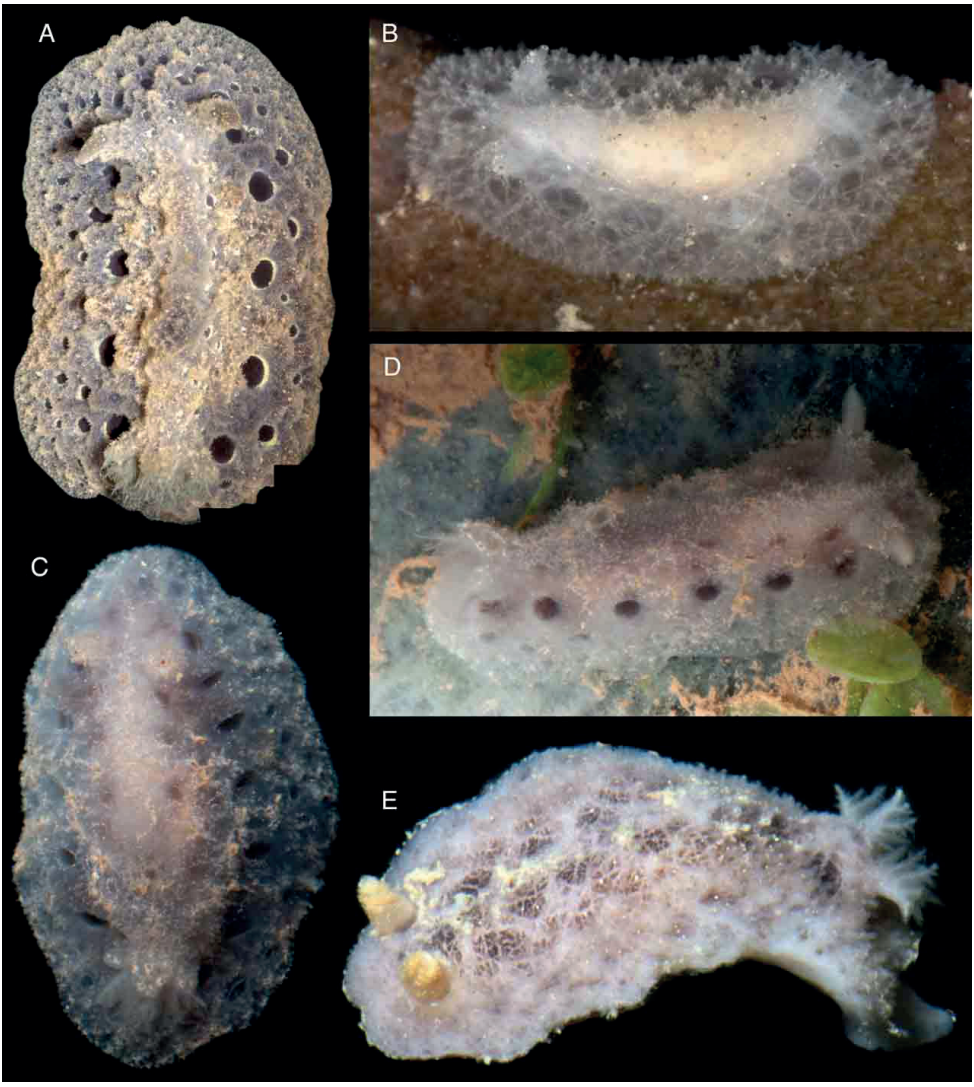

Figure 2. Photographs of live animals of the genus *Atagema* Gray, 1850 **A, B** *Atagema spongiosa* (Kelaart, 1858), MNHN IM-2013-86188 on black background (**A**), MNHN IM-2013-86189 in situ (**B**) **C, D** *Atagema kimberlyae* sp. nov., MNHN IM-2013-86191 on black background (**C**), MNHN IM-2013-86191 in situ (**D**) **E** *Atagema papillosa* (Risbec, 1928), MNHN IM-2013-86192 on black background.

Reproductive system (Fig. 3B, C) with a short, wide, simple ampulla that connects with the female gland complex and a convoluted prostate. The prostate has several folds and is approximately as wide as the ampulla. The prostate narrows slightly into a curved duct before expanding into the long, ovoid, wide deferent duct. At its widest point, the deferent duct is slightly wider than the prostate. The penis is unarmed. The vagina is long and narrow and connects directly to the spherical bursa copulatrix. The vagina is approximately as wide as the deferent duct. The small elongate seminal

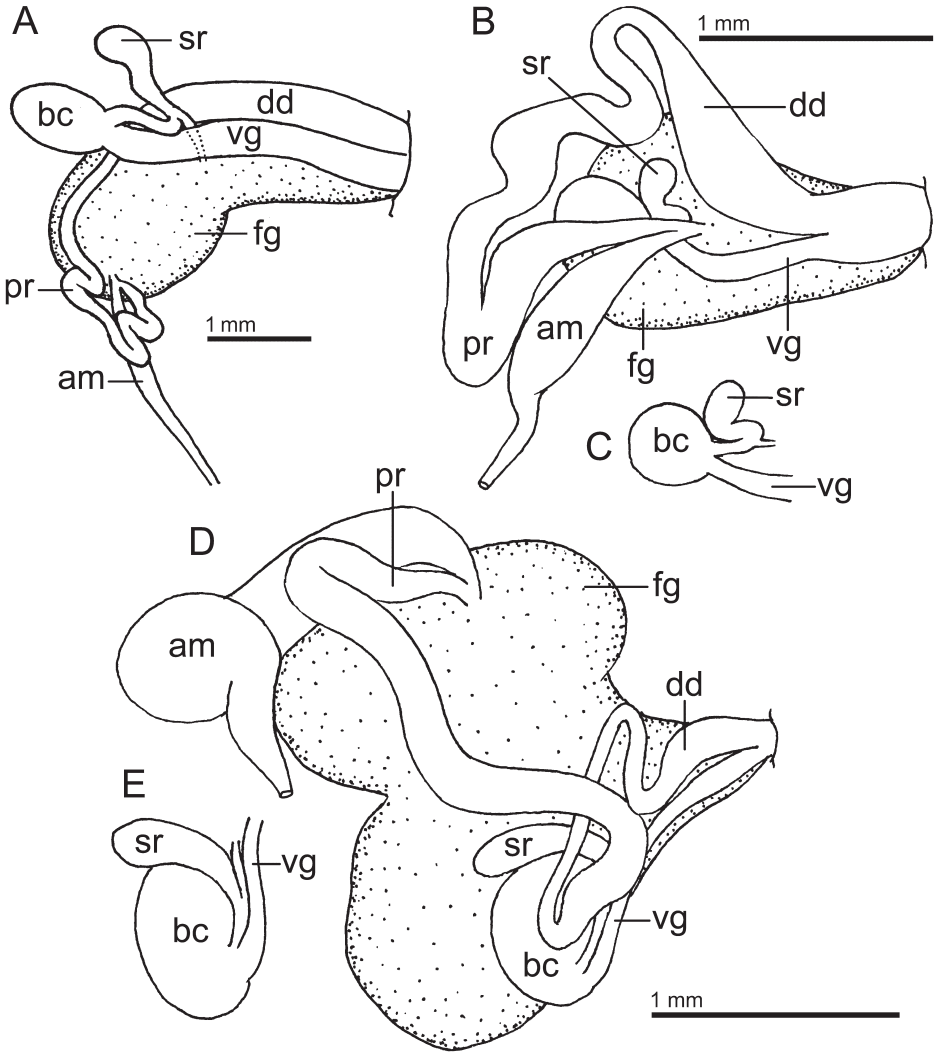

Figure 3. Drawings of the reproductive systems of specimens of the genus *Atagema* Gray, 1850 **A** *Atagema spongiosa* (Kelaart, 1858), MNHN IM-2013-86190 **B, C** *Atagema kimberlyae* sp. nov., MNHN IM-2013-86191, general view (**B**), detail of the bursa copulatrix and seminal receptable (**C**) **D, E** *Atagema papillosa* (Risbec, 1928), MNHN IM-2013-86192, general view (**D**), detail of the bursa copulatrix and seminal receptable (**E**). Abbreviations: am, ampulla; bc, bursa copulatrix; dd, deferent duct; fg, female gland complex; pr, prostate; sr, seminal receptacle; vg, vagina.

receptacle also connects to the bursa copulatrix near the vaginal connection and the short uterine duct that enters the female gland complex. The bursa copulatrix is several times larger than the seminal receptacle (Fig. 3C).

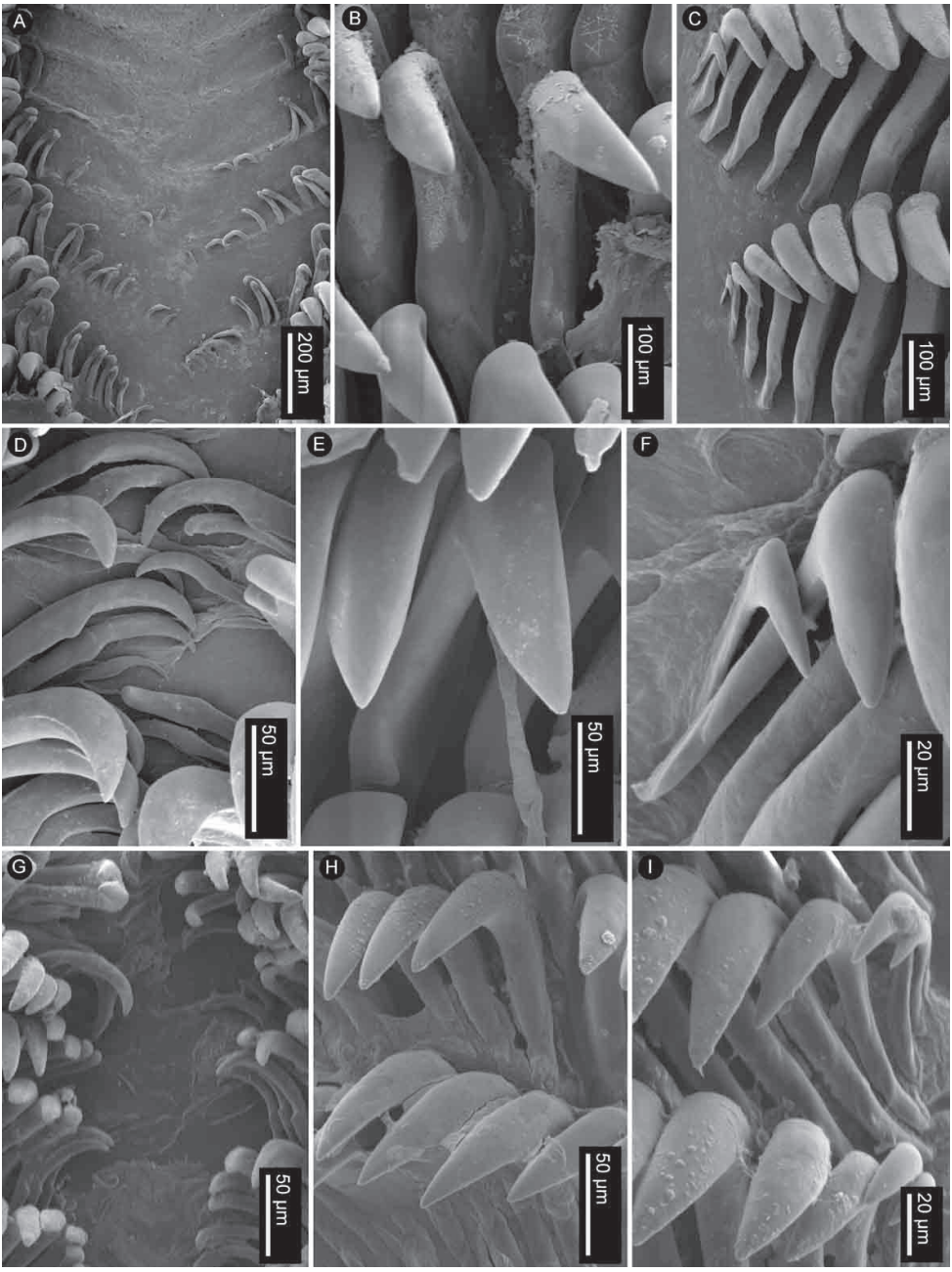

Figure 4. SEM of the radula of specimens of the genus *Atagema* Gray, 1850 **A–C** *Atagema spongiosa* (Kelaart, 1858), MNHN IM-2013-86190, innermost teeth (**A**), mid-lateral teeth (**B**), outer lateral teeth (**C**) **D–F** *Atagema kimberlyae* sp. nov., MNHN IM-2013-86191, innermost teeth (**D**), mid-lateral teeth (**E**), outer lateral teeth (**F**) **G–I** *Atagema papillosa* (Risbec, 1928), MNHN IM-2013-86192, innermost teeth (**G**), mid-lateral teeth (**H**), outer lateral teeth (**I**).

Radular formula 15 × 20.0.20 in a 20-mm long specimen (MNHN IM-2013-86191). Rachidian teeth absent. Inner and mid-lateral teeth hamate, having a small cusp and lacking denticles (Fig. 4D–F). Innermost teeth very small in comparison to mid-laterals (Fig. 4D), elongate, with an inconspicuous secondary cusp mid-length. The teeth increase in size suddenly towards the medial portion of the half-row (Fig. 4E). Outermost teeth small, decreasing in size gradually, and hamate (Fig. 4F). No jaw was observed, labial cuticle smooth.

Biology. Possibly a New Caledonia endemic, rare, 5 m depth. The single specimen was obtained while SCUBA diving by direct collection on an unidentified sponge on which it was highly cryptic.

Etymology. This species is named after Kimberly García Mendez, who participated in two of the Koumac expeditions, collecting a number of specimens and helping enormously with the processing and photographing of samples.

Remarks. *Atagema kimberlyae* sp. nov. is assigned to the genus *Atagema* for two reasons, 1) the molecular phylogenetic analysis places the specimens sequenced in a clade containing *A. spongiosa*, a well stablished member of this genus (see above); 2) the morphological characteristics of this new species are consistent with the diagnosis of the genus provided by Valdés and Gosliner (2001), including a flexible body with series of tubercles all covered with caryophyllidia and depressions, the anterior border of the branchial sheath composed of three lobes and the gill leaves arranged horizontally; furthermore the prostate is tubular, with a single portion, the penis and vagina are unarmed, the labial cuticle smooth, and all radular teeth are hamate and smooth.

Atagema kimberlyae sp. nov. is morphologically similar to *Atagema spongiosa* (described above), particularly to the juvenile specimens, but is genetically distinct. Also, it lacks the distinctive dorsal ridge of *A. spongiosa* and presents a number of anatomical differences, including a comparatively much shorter and wider ampulla, a wider prostate, a rounded bursa copulatrix instead of oval, and comparatively larger innermost lateral teeth. A review of the literature reveals that no other described Indo-Pacific species of *Atagema* are morphologically similar to *A. kimberlyae* sp. nov., hence it is described as new.

The geographic range of *Atagema kimberlyae* sp. nov. is close to that of *Atagema molesta* (Miller, 1989 as *Trippa molesta*), introduced based on a single specimen collected from Te Hāwere-a-Maki (Goat Island), New Zealand. Miller (1989) described and illustrated the holotype, which differs from *A. kimberlyae* sp. nov. in several regards, including the more complex dorsal pattern of tubercles and ridges present in *A. molesta*, giving the animal a spikier appearance, and the reproductive system, which has a much larger deferent duct and a shorter prostate in *A. kimberlyae* sp. nov. While the radular morphology of the two species is similar, the radular formula is not, 23 × 32.0.32 in a 12-mm specimen of *A. molesta* versus 15 × 20.0.20 in a 20-mm long specimen of *A. kimberlyae* sp. nov.

Based on the species delimitation analysis presented here, *A. kimberlyae* sp. nov. is closely related but genetically distinct from specimens identified as *Atagema* cf. *osseosa* and *Atagema notacristata* whose sequences are deposited in GenBank.

***Atagema sobanovae* sp. nov.**
https://zoobank.org/C296974E-92C6-4F7C-8E4A-ABF61D48F896
Figs 5–7

?*Atagema* sp. 9: Gosliner et al. 2018: 116.

Type material. *Holotype*: Koumac, New Caledonia (20°35.6'S, 164°16.3'E), 3 m depth [Koumac 2.1 stn. KR230], 28 Sep 2018, 22 mm long (MNHN IM-2013-86211, isolate JI16).

Other material examined. Cap Deverd, Koumac, New Caledonia (20°46.2'S, 164°22.6'E), 5 m [Koumac 2.1 stn. KR213], 12 Sep 2018, 1 specimen 13 mm long (MNHN IM-2013-86178, isolate JI06). Koumac, New Caledonia (20°39.6'S, 164°16.2'E), 6 m depth [Koumac 2.1 stn. KR229], 27 Sep 2018, 1 specimen 8 mm long (MNHN IM-2013-86175, isolate JI28). Koumac, New Caledonia (20°35.6'S, 164°16.3'E), 3 m depth [Koumac 2.1 stn. KR230], 28 Sep 2018, 1 specimen 17 mm long, dissected (MNHN IM-2013-86180, isolate JI23); 1 specimen 18 mm long, dissected (MNHN IM-2013-86179, isolate JI21). Koumac, New Caledonia (20°35.1'S, 164°16.3'E), 7 m depth [Koumac 2.1 stn. KR409, muddy bottom with solitary soft and hard corals and hydroids], 28 Sep 2018, 1 specimen 8 mm long (MNHN IM-2013-86229). Koumac, New Caledonia (20°35.1'S, 164°16.3'E), 3 m [Koumac 2.2 stn. KR231], 1 Mar 2019, 1 specimen 9 mm long (MNHN IM-2013-86176, isolate JI44). Koumac, New Caledonia (20°37.3'S, 164°18'E), 6 m depth [Koumac 2.3 stn. KD522, grey sand with *Caulerpa* and *Halimeda*], 2 Nov 2019, 1 specimen 10 mm long (MNHN IM-2013-86174, isolate JI19). Koumac, New Caledonia (20°34.3'S, 164°13.5'E), 1–10 m depth [Koumac 2.3 stn. KR907, sanded slab with gorgonians, scattered seagrass, and *Caulerpa*; channel drop-off with gorgonians], 7 Nov 2019, 1 specimen 7 mm long (MNHN IM-2013-86173, isolate JI41). Koumac, New Caledonia (20°34.4'S, 164°13.8'E), 8 m depth [Koumac 2.3 stn. KR913], 14 Nov 2019, 1 specimen 11 mm long (MNHN IM-2013-86171, isolate JI29); 1 specimen 10 mm long (MNHN IM-2013-86172, isolate JI46). Koumac, New Caledonia (20°35.1'S, 164°16.3'E), 7 m depth [Koumac 2.3 stn. KR1019, "fond de vase" with *Caulerpa* and sponges], 4 Nov 2019, 1 specimen 28 mm long (MNHN IM-2013-86181, isolate JI05); 1 specimen 22 mm long, dissected (MNHN IM-2013-86187, isolate JI08); 1 specimen 9 mm long (MNHN IM-2013-86177, isolate JI45).

Description. Body oval, elevated, completely covered with a dense, complex network of delicate ridges (Fig. 5). Large caryophyllidia present at the points where ridges meet. A series of small depressions free of ridges and caryophyllidia present on each side of the mantle. A single, elevate dorsal hump present on the center of the dorsum, not visible in juvenile specimens (Fig. 5E). Branchial sheath composed of three lobes; gill composed of five tripinnate branchial leaves, arranged horizontally in the living animal. Rhinophoral sheaths elevated; rhinophores long, lamellated, with 8–10 lamellae. Body color opaque creamy grey, depressions a bit darker. Rhinophores and branchial leaves are the same color as the dorsum.

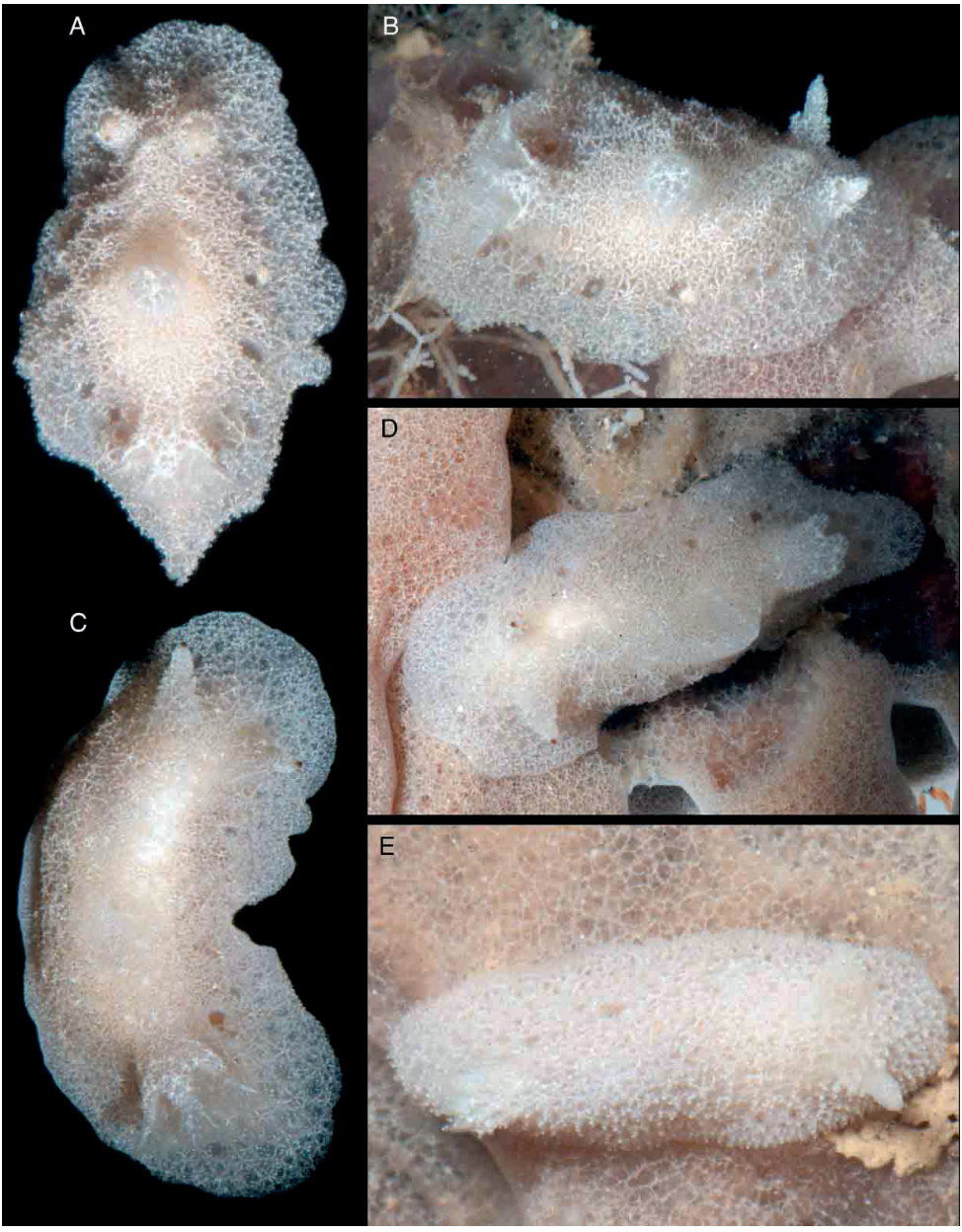

Figure 5. Photographs of live animals of *Atagema sobanovae* sp. nov. **A, B** MNHN IM-2013-86180, on black background (**A**), in situ (**B**) **C, D** holotype (MNHN IM-2013-86211), on black background (**A**), in situ (**B**) **E** MNHN IM-2013-86229 juvenile specimen on black background.

Reproductive system (Fig. 6) with a short, convoluted ampulla that connects with the female gland complex and an elongated prostate. The prostate is as long as the ampulla and it narrows slightly into an elongate duct before expanding into the short,

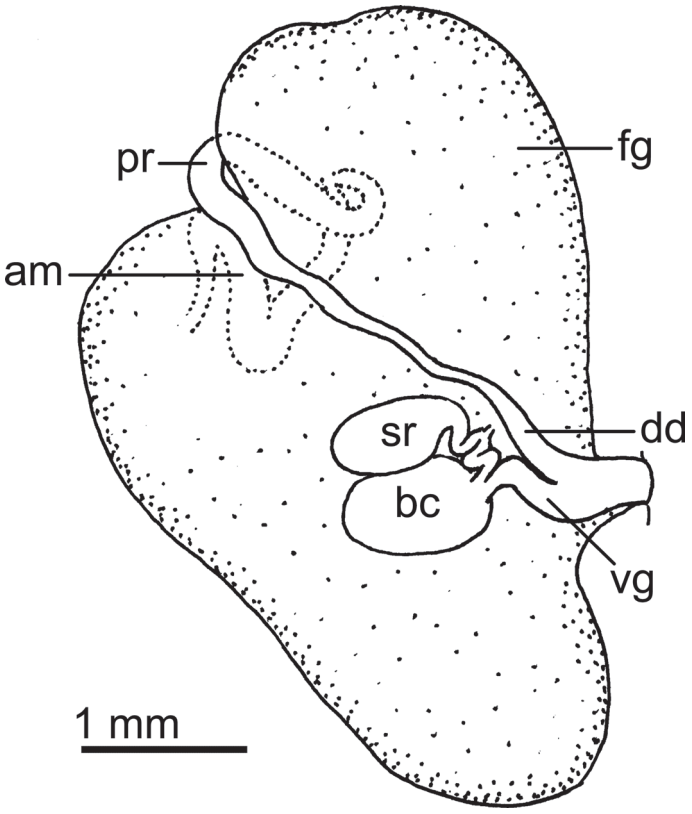

Figure 6. Drawing of the reproductive system of *Atagema sobanovae* sp. nov., MNHN IM-2013-86180. Abbreviations: am, ampulla; bc, bursa copulatrix; dd, deferent duct; fg, female gland complex; pr, prostate; sr, seminal receptacle; vg, vagina.

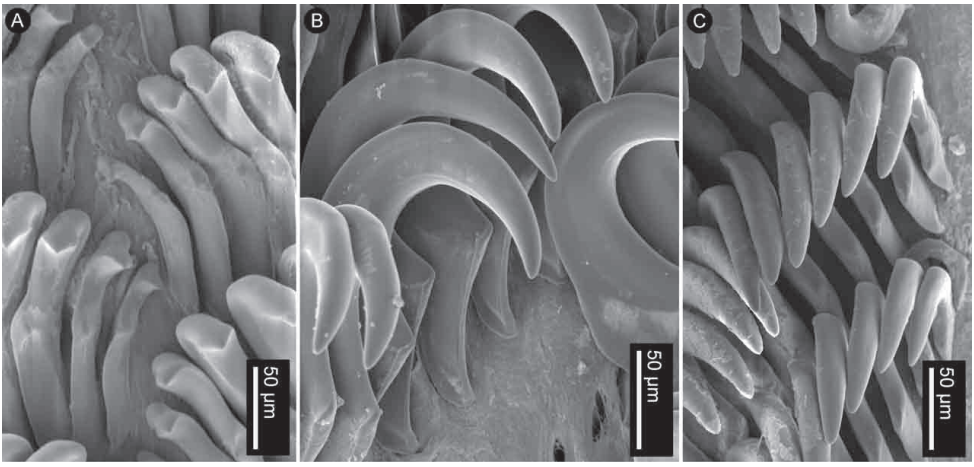

Figure 7. SEM of the radula of specimens of *Atagema sobanovae* sp. nov., MNHN IM-2013-86179, innermost teeth (**A**), mid-lateral teeth (**B**), outer lateral teeth (**C**).

simple, deferent duct. The penis is unarmed. The vagina is short and wide, approximately as wide as the deferent duct, and connects directly to the oval bursa copulatrix. The oval seminal receptacle also connects to the bursa copulatrix next to the vaginal opening and the short uterine duct that enters the female gland complex. The bursa copulatrix is slightly larger than the seminal receptable.

Radular formula 22 × 35.0.35 in an 18-mm long specimen (MNHN IM-2013-86179) and 17 × 34.0.34 in a 22-mm long specimen (MNHN IM-2013-86187). Rachidian teeth absent. Inner and mid-lateral teeth hamate, having a small cusp and lacking denticles (Fig. 7A, B). Innermost teeth very small in comparison to mid-laterals (Fig. 7A). The teeth increase in size gradually towards the medial portion of the half-row (Fig. 7A). Outermost teeth small, decreasing in size gradually, and hamate (Fig. 7C). No jaw was observed, labial cuticle smooth.

Biology. This species could be widespread in the Western Pacific (see remarks). Found in shallow water (1–10 m depth). The specimens were exclusively collected on an unidentified species of grey sponge inhabiting the surface of scallops; the nudibranchs were highly cryptic on the sponge and often found buried in the sponge tissue. Few specimens were obtained by direct collection while SCUBA diving but more of them were found in the lab while searching for crustaceans associated with the sponges.

Etymology. This species is named after Anna Šobáňová, crustacean expert who originally discovered this species in the field while looking for crustaceans living in sponges.

Remarks. *Atagema sobanovae* sp. nov. is assigned to the genus because of its position in the molecular phylogenetic trees, in a clade containing other species of *Atagema* such as *A. spongiosa* and *A.* cf. *osseosa*. Also, the morphological characteristics of this new species are consistent with the diagnosis of the genus by Valdés and Gosliner (2001). *Atagema sobanovae* sp. nov. has a flexible body with series of dorsal ridges and a central conspicuous tubercle, all covered with caryophyllidia, the anterior border of the branchial sheath is composed of three lobes and the gill is arranged horizontally; the prostate is tubular, with a single portion, the penis and vagina are unarmed; the labial cuticle smooth and all radular teeth are hamate and smooth.

A review of the literature shows that no other described species of *Atagema* possesses the external characteristics of *A. sobanovae* sp. nov. The only other tropical Indo-Pacific species with a uniform color is *Atagema carinata* (Quoy & Gaimard, 1832), which was described from the coast of Thames, New Zealand, as yellowish white with a dorsal longitudinal ridge between the rhinophores and the gill. The illustration provided by Quoy and Gaimard (1832–1833: pl. 16, figs 10–14) represents an animal with a distinct dorsal ridge very different from the complex dorsal pattern of *A. sobanovae* sp. nov. with depressions, ridges, and a central tubercle. The specimens of *A. carinata* described and illustrated by Rudman (2005) are consistent with the original description.

A specimen from the Philippines illustrated by Gosliner et al. (2018) as *Atagema* sp. 9 could belong to *A. sobanovae* sp. nov. but this needs anatomical and molecular confirmation.

Genus *Jorunna* Bergh, 1876

Kentrodoris Bergh, 1876: 413. Type species: *Kentrodoris rubescens* Bergh, 1876 [= *Jorunna rubescens* Bergh, 1876], by subsequent designation by Ev. Marcus (1976).
Jorunna Bergh, 1876: 414. Type species: *Doris johnstoni* Alder & Hancock, 1845 [= *Jorunna tomentosa* (Cuvier, 1804)], by monotypy.
Audura Bergh, 1878: 567–568. Type species: *Audura maima* Bergh, 1878 [= *Jorunna maima* (Bergh, 1878)], by monotypy.
Centrodoris P. Fischer 1880–1887 [1883]: 522 (unjustified emendation for *Kentrodoris* Bergh, 1876).
Awuka Er. Marcus, 1955: 155–156. Type species *Awuka spazzola* Er. Marcus, 1955 [= *Jorunna spazzola* (Er. Marcus, 1955)], by original designation.

Remarks. For an in-depth discussion of the characteristics of the genus *Jorunna* and its synonyms see Camacho-García and Gosliner (2008).

***Jorunna daoulasi* sp. nov.**
https://zoobank.org/0D41E0FA-826A-4761-BB7B-B71CE0B2E97E
Figs 8A–C, 9A, 10A, B

?*Jorunna* sp. 10: Gosliner et al. 2018: 122.
?*Rostanga* sp. 4: Nakano 2018: 263.

Type material. *Holotype*: In front of the harbor, Koumac, New Caledonia (20°35.3'S, 164°16.4'E), 6 m depth [Koumac 2.1 stn. KR220], 17 Nov 2018, 12 mm long, (MNHN IM-2013-86230).

Other material examined. In front of the harbor, Koumac, New Caledonia (20°35.3'S, 164°16.4'E), 6 m depth [Koumac 2.1 stn. KR220], 17 Nov 2018, 1 specimen 24 mm long, dissected (MNHN IM-2013-86220). Koumac, New Caledonia (20°35.2'S, 164°16.3'E), 6 m depth [Koumac 2.3 stn. KR886], 21 Nov 2019, 1 specimen 27 mm long, dissected (MNHN IM-2013-86219, isolate JI22).

Description. Body oval, narrow, elongate, completely covered with numerous caryophyllidia (Fig. 8A–C). Branchial and rhinophoral sheaths low, simple, circular; gill composed of nine short, tripinnate branchial leaves, imbricated, arranged upright, with the apices close to each other in the living animal. Rhinophores short, lamellated, with eight or nine lamellae. Body color grey, with a complex network of white lines of different thicknesses; in some specimens some of the lines are very thick and contain darker areas (Fig. 8A), whereas in others thicker lines form the main network and thinner lines form a secondary network (Fig. 8) and in others all lines are approximately the same thickness (Fig. 8B). Rhinophores and branchial leaves are the same color as the dorsum but the rhinophoral lamellae and in some cases the gill lamellae are white.

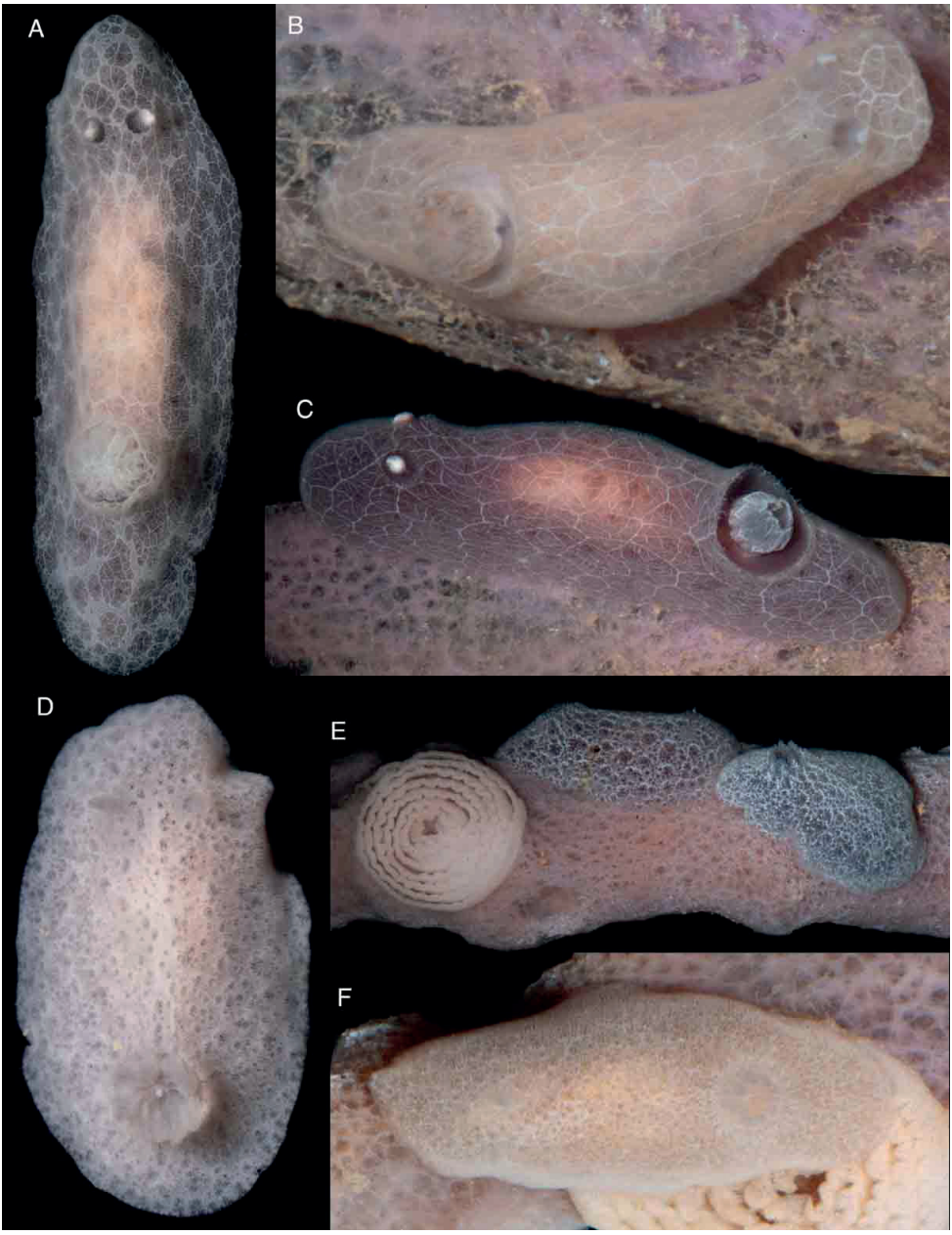

Figure 8. Photographs of live animals of the genus *Jorunna* Bergh, 1876 **A–C** *Jorunna daoulasi* sp. nov., MNHN IM-2013-86219 on black background (**A**), MNHN IM-2013-86220 in situ (**B**), Holotype (MNHN IM-2013-86230) in situ (**C**) **D–F** *Jorunna hervei* sp. nov., MNHN IM-2013-86228 on black background (**D**), MNHN IM-2013-86224 and Holotype MNHN IM-2013-86225 in situ with egg mass (**E**), MNHN IM-2013-86226 in situ with egg mass (**F**).

Reproductive system (Fig. 9A) with a long, narrow, curved ampulla that connects with the female gland complex and an elongate prostate. The prostate is as wide as the ampulla but narrows substantially before expanding into the short, curved, narrow deferent duct. The deferent duct is much narrower than the prostate. The penis is unarmed. The vagina is very elongate and wide distally, several times wider than the deferent duct, narrowing considerably proximally and connecting directly to the irregular bursa copulatrix. The oval seminal receptacle also connects to the bursa copulatrix next to the vaginal connection, and the short uterine duct that enters the female gland complex. The bursa copulatrix is ~ 3× as large as the seminal receptable. A large accessory gland connects to a narrow and convoluted duct that opens into the genital atrium, where a curved, sharp stylet is located.

Radular formula 24 × n.0.n in a 26-mm long specimen (MNHN IM-2013-86220) and 25 × n.0.n in a 27-mm long specimen (MNHN IM-2013-86219). Rachidian teeth absent. Innermost lateral teeth wide, having a short cusp with four or five irregular denticles (Fig. 10A). Mid-lateral teeth hamate, lacking denticles (Fig. 10A). The teeth increase in size gradually towards the distal portion of the half-row (Fig. 10B). Outermost teeth very elongate, longer than mid-lateral teeth, with several elongate apical denticles (Fig. 10B). No jaws ware observed.

Biology. Range includes New Caledonia and possibly Papua New Guinea and Japan (see Remarks section below); uncommon, found at ~ 6 m depth on an unidentified grey sponge on which it is highly cryptic. All the specimens were found directly on the sponges while SCUBA diving.

Etymology. This species is named after Alain Daoulas, outstanding collector and naturalist, who participated in two of the Koumac expeditions, collecting a number of important specimens.

Remarks. *Jorunna daoulasi* sp. nov. is placed in the genus *Jorunna* because it fits morphologically within the diagnoses of the genus provided by Valdés and Gosliner (2001) and Camacho-García and Gosliner (2008). Specifically, *J. daoulasi* sp. nov. has a soft mantle covered with long caryophyllidia, the radular teeth are hamate, and the reproductive system has an accessory gland and a copulatory stylet. Finally, in the molecular phylogenetic analyses, *J. daoulasi* sp. nov. is a member of a well-supported clade containing other members of *Jorunna*.

Camacho-García and Gosliner (2008) provided a comprehensive revision and illustrations of the valid species of the genus *Jorunna*, including all the Indo-Pacific taxa described to date. None of the species included in Camacho-García and Gosliner's (2008) monograph have a similar color pattern and morphology to *J. daoulasi* sp. nov. Since then, several additional new species have been described from the Atlantic Ocean (Edmunds 2011; Alvim and Pimenta 2013; Ortea et al. 2014; Ortea and Moro 2016; Neuhaus et al. 2021) and the Indian Ocean (Tibiriçá et al. 2023), but they are also morphologically and/or genetically different from *J. daoulasi* sp. nov. The most similar species to *J. daoulasi* sp. nov. in external morphology are *Jorunna* sp. 10 from Papua

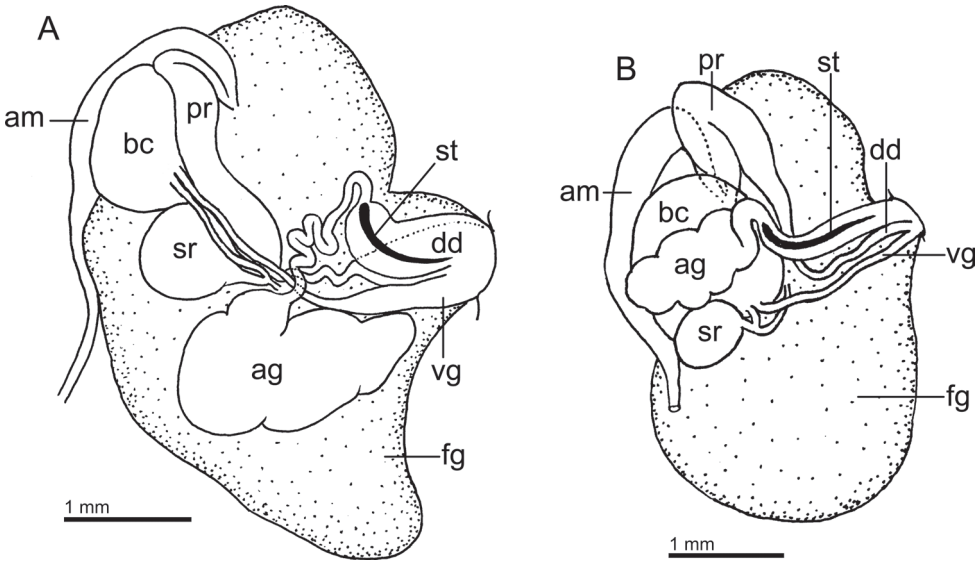

Figure 9. Drawings of the reproductive systems of specimens of the genus *Jorunna* Bergh, 1876 **A** *Jorunna daoulasi* sp. nov., MNHN IM-2013-86219 **B** *Jorunna hervei* sp. nov., MNHN IM-2013-86226. Abbreviations: ag, accessory gland; am, ampulla; bc, bursa copulatrix; dd, deferent duct; fg, female gland complex; pr, prostate; sr, seminal receptacle; st, stylet; vg, vagina.

New Guinea illustrated by Gosliner et al. (2018) and *Rostanga* sp. 4 from Japan illustrated by Nakano (2018), which have a very similar body shape and color and could represent the same species.

***Jorunna hervei* sp. nov.**

https://zoobank.org/DAD18B3C-3AFA-428E-909E-71309CE1ACB3

Figs 8D–F, 9B, 10C–E

Type material. *Holotype*: Pandop, Koumac, New Caledonia (20°34.9'S, 164°16.5'E), 7 m depth [Koumac 2.1 stn. KR868, rock, sponges, algae including *Halimeda*], 26 Sep 2018, 1 specimen 24 mm long (MNHN IM-2013-86225, isolate JI47)

Other material examined. Koumac, New Caledonia (20°35.6'S, 164°16.3'E), 3 m depth [Koumac 2.1 stn. KR230], 28 Sep 2018, 1 specimen 11 mm long (MNHN IM-2013-86221). Koumac, New Caledonia (20°35.1'S, 164°16.3'E), 3 m depth [Koumac 2.1 stn. KR231], 29 Sep 2018, 1 specimen 21 mm long, dissected (MNHN IM-2013-86222). Koumac, New Caledonia (20°35.1'S, 164°16.2'E), 8 m depth [Koumac 2.1 stn. KR410, sponge bottom], 29 Sep 2018, 1 specimen 14 mm long (MNHN IM-2013-86223). Pandop Point Reef, Koumac, New Caledonia (20°35.2'S, 164°16.3'E), 6 m depth [Koumac 2.1 stn. KR859, sandy-muddy bottom with sponges, *Caulerpa*], 17 Sep 2018, 1 specimen 25 mm long, dissected (MNHN IM-2013-86226, isolate JI48); 1 specimen 14 mm long (MNHN IM-2013-86227). Pointe

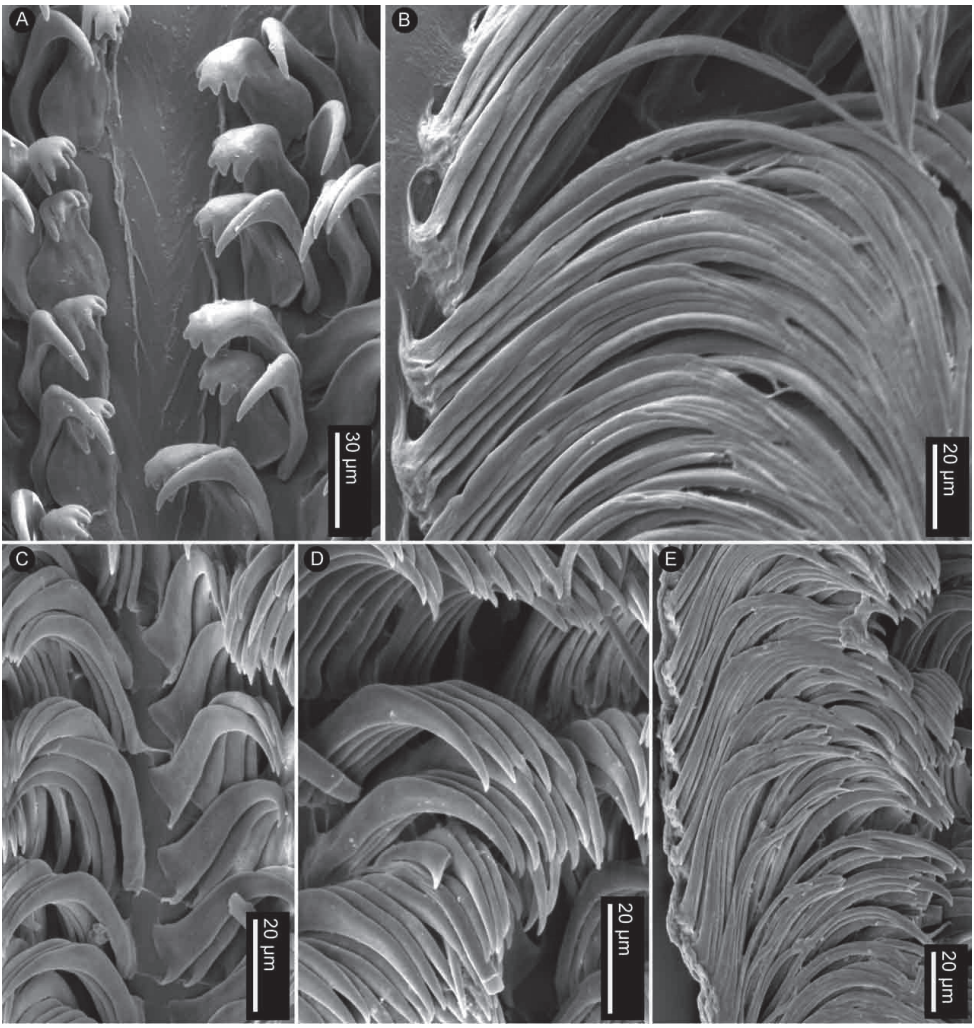

Figure 10. SEM of the radula of specimens of the genus *Jorunna* Bergh, 1876 **A, B** *Jorunna daoulasi* sp. nov., MNHN IM-2013-86220, innermost teeth (**A**), outer lateral teeth (**B**) **C–E** *Jorunna hervei* sp. nov., MNHN IM-2013-86224, innermost teeth (**C**), mid-lateral teeth (**D**), outer lateral teeth (**E**).

de Pandop, Koumac, New Caledonia (20°34.9'S, 164°16.5'E), 7 m depth [Koumac 2.1 stn. KR868, rock, sponges, algae including *Halimeda*], 26 Sep 2018, 1 specimen 22 mm long (MNHN IM-2013-86224). Koumac, New Caledonia (20°32.9'S, 164°16.8'E), 5 m depth [Koumac 2.3 stn. KR917], 19 Nov 2019, 1 specimen 16 mm long (MNHN IM-2013-86228).

Description. Body oval, flattened, completely covered with numerous caryophyllidia (Fig. 8D–F). Branchial and rhinophoral sheaths low, simple, circular; gill composed of nine short, tripinnate branchial leaves, slightly imbricated, arranged fully upright in the living animal. Rhinophores short, lamellated with elongate apices, seven or eight lamellae. Body color variable from pale brown to grey, with numerous irregular

dark patches, surrounded by white pigment (Fig. 8E). Rhinophores and branchial leaves are the same color as the dorsum.

Reproductive system (Fig. 9B) with an elongate, curved ampulla that connects with the female gland complex and an elongate prostate with a single fold. The prostate is as wide as the ampulla but narrows substantially into a long tube before expanding slightly into the short, curved, narrow deferent duct. The penis is unarmed. The vagina is narrow, as wide as the deferent duct, and very elongate, connecting directly to the oval bursa copulatrix. The oval seminal receptacle also connects to the bursa copulatrix next to the vaginal connection, and the long uterine duct that enters the female gland complex. The bursa copulatrix is many times larger than the seminal receptacle. A large accessory gland connects to a wide duct that opens into the genital atrium, where a sharp, curved stylet is located.

Radular formula 24 × n.0.n, in a 21-mm long specimen (MNHN IM-2013-86222), 28 × n.0.n in a 22-mm long specimen (MNHN IM-2013-86224), and 30 × n.0.n in a 25-mm long specimen (MNHN IM-2013-86226). Rachidian teeth absent. Inner and mid-lateral teeth hamate, having a long cusp and lacking denticles (Fig. 10C–E). Innermost teeth smaller than mid-laterals (Fig. 10C). The teeth increase in size gradually towards the medial portion of the half-row (Fig. 10D). Outermost teeth very elongate, longer than mid-lateral teeth, increasing in size gradually, and hamate (Fig. 10E). No jaws were observed.

Biology. The pale brown egg mass is a highly coiled ribbon with ca. seven tightly packed whorls with a wavy upper edge (Fig. 8E). Eggs are ~ 105 μm in diameter. The geographic range includes New Caledonia and could be an endemic species; uncommon, found at 3–8 m depth on an unidentified brownish grey sponge on which is highly cryptic. All the specimens were collected directly from the sponges while SCUBA diving.

Etymology. This species is named after Jean-François Hervé, pioneer in the study of the sea slugs of New Caledonia and excellent collector; he participated in two of the Koumac expeditions, finding numerous specimens.

Remarks. As in the case of *Jorunna daoulasi* sp. nov., *Jorunna hervei* sp. nov. is placed in the genus *Jorunna* because it fits morphologically within the diagnoses of the genus provided by Valdés and Gosliner (2001) and Camacho-García and Gosliner (2008). *Jorunna hervei* sp. nov. has a soft mantle covered with long caryophyllidia, the radular teeth are hamate, and the reproductive system has an accessory gland and a copulatory stylet, all of which are characteristics of *Jorunna*. Furthermore, in the molecular phylogenetic analyses, *Jorunna hervei* sp. nov. is sister to *J. daoulasi* sp. nov. as well as a member of a well-supported clade containing other members of *Jorunna*.

Jorunna hervei sp. nov. differs from *Jorunna daoulasi* sp. nov. in several regards. Externally, *J. hervei* sp. nov. is less elongate than *J. daoulasi* sp. nov. and lacks the network of white pigment; instead it has numerous irregular dark patches, in some specimens surrounded by white pigment. The reproductive system of *J. hervei* sp. nov. is similar to that of *J. daoulasi* sp. nov., but the accessory gland is comparatively smaller, the bursa copulatrix is much larger in comparison to the seminal receptable, and the deferent duct is shorter in comparison to the vagina. The main anatomical difference between these two species is the radular morphology, while *Jorunna hervei* sp. nov. has inner and mid-lateral

teeth hamate, having a long cusp and lacking denticles, in *J. daoulasi* sp. nov. the innermost lateral teeth are wide, having a short cusp with four or five irregular denticles. Finally, the ABGD analysis recovered *J. hervei* sp. nov. and *J. daoulasi* sp. nov. as distinct species.

Jorunna liviae Tibiriçá, Strömvoll & Cervera, 2023 recently described from Mozambique (Tibiriçá et al. 2023) is sister to *J. hervei* sp. nov. and is morphologically similar but differs in several important respects. First of all, the species delimitation analysis recovered *J. hervei* sp. nov. and *Jorunna liviae* as different species. Additionally, the body of *J. liviae* appears to be narrower and more elongate than that of *J. hervei* sp. nov. More importantly, the outermost radular teeth of *J. liviae* contain multiple elongate denticles, which are absent in all specimens examined of *J. hervei* sp. nov. Also, the prostate of *J. liviae* is flattened, whereas the prostate of *J. hervei* sp. nov. is tubular an elongate, and the accessory gland appears to be comparatively much larger in *J. liviae* than in *J. hervei* sp. nov. although is it variable in size (Tibiriçá et al. 2023). Finally, the eggs of *J. liviae* are white, whereas they are pale brown in *J. hervei* sp. nov. It is clear that these two species are similar but distinct.

A review of the literature does not reveal any other species morphologically similar to *J. hervei* sp. nov. *Rostanga* sp. 7 in Gosliner et al. (2018) has some superficial resemblance but there are some obvious differences, including the background color, grey in *J. hervei*, pink in *Rostanga* sp. 7, and the egg mass, having one or two loosely packed whorls with ochre, large eggs in *Rostanga* sp. 7, versus seven tightly packed whorls with pale brown eggs in *J. hervei*.

Genus *Rostanga* Bergh, 1879

Rostanga Bergh, 1879: 353–354. Type species: *Doris coccinea* Forbes in Alder & Hancock, 1848 [= *Rostanga rubra* (Risso, 1818)], by original designation.

Boreodoris Odhner, 1939: 31–33. Type species: *Boreodoris setidens* Odhner, 1939 [= *Rostanga setidens* (Odhner, 1939)], by monotypy.

Rhabdochila P. Fischer, 1880–1887 [1883]: 521. Type species *Doris coccinea* Forbes in Alder & Hancock, 1848 [= *Rostanga rubra* (Risso, 1818)], by subsequent designation by Iredale and O'Donoghue (1923).

Remarks. For an in-depth discussion of the characteristics of the genus *Rostanga* and its synonyms see Rudman and Avern (1989) and Valdés and Gosliner (2001).

Rostanga poddubetskaiae sp. nov.

https://zoobank.org/EF949405-58D8-4D48-AD09-1CB3CE3993F5
Figs 11–13

Type material. ***Holotype*:** Anse de Koumac, Koumac, New Caledonia (20°34'S, 164°16'E), 4 m depth [Koumac 2.1 stn. KR206], 5 Sep 2018, 1 specimen 23 mm long (MNHN IM-2013-86199, isolate JI01).

Other material examined. Anse de Koumac, Koumac, New Caledonia (20°34'S, 164°16'E), 4 m depth [Koumac 2.1 stn. KR206], 5 Sep 2018, 1 specimen 25 mm long (MNHN IM-2013-86200, isolate JI17); 1 specimen 12 mm long (MNHN IM-2013-86201, isolate JI32); 1 specimen 26 mm long, dissected (MNHN IM-2013-86202, isolate JI03); 1 specimen 19 mm long, dissected (MNHN IM-2013-86203, isolate JI12); 1 specimen 16 mm long, dissected (MNHN IM-2013-86204, isolate JI20). Cap Deverd, Koumac, New Caledonia (20°46.2'S, 164°22.6'E), 5 m depth [Koumac 2.1 stn. KR213], 29 Sep 2018, 1 specimen 26 mm long, dissected (MNHN IM-2013-86205, isolate JI27); 1 specimen 28 mm long, dissected (MNHN IM-2013-86206, isolate JI13). Anse de Koumac, Koumac, New Caledonia (20°34.6'S, 164°16.1'E), 5 m depth [Koumac 2.1 stn. KR219], 17 Sep 2018, 1 specimen 12 mm long (MNHN IM-2013-86207, isolate JI39); 1 specimen 23 mm long, dissected (MNHN IM-2013-86208, isolate JI25); 1 specimen 26 mm long (MNHN IM-2013-86209, isolate JI18); 1 specimen 17 mm long (MNHN IM-2013-86210, isolate JI40). Koumac, New Caledonia (20°35.6'S, 164°16.3'E), 3 m depth [Koumac 2.2 stn. KR230], 2 Mar 2019, 1 specimen 20 mm long (MNHN IM-2013-86213, isolate JI36); 2 Mar 2019, 1 specimen 21 mm long (MNHN IM-2013-86214, isolate JI37); 3 Mar 2019, 1 specimen 20 mm long (MNHN IM-2013-86212, isolate JI31). Pointe de Pandop, Koumac, New Caledonia (20°34.9'S, 164°16.5'E), 7 m depth [Koumac 2.1 stn. KR868], 26 Sep 2018, 1 specimen 26 mm long (MNHN IM-2013-86215, isolate JI15); 1 specimen 24 mm long (MNHN IM-2013-86216, isolate JI24); 1 specimen 14 mm long (MNHN IM-2013-86217, isolate JI38). Koumac, New Caledonia (20°33.7'S, 164°13.1'E), 12 m depth [Koumac 2.3 stn. KR206], 3 Nov 2019, 1 specimen 19 mm long (MNHN IM-2013-86218, isolate JI07).

Description. Body oval, elongate, completely covered with numerous caryophyllidia (Fig. 11). Branchial and rhinophoral sheaths low, simple, circular; gill composed of seven wide, tripinnate branchial leaves, extended laterally, lying on the dorsum in the living animal. A low, irregular, inconspicuous ridge runs between the rhinophores and the gill, not clearly visible in all specimens. Rhinophores very elongate, almost conical, lamellated, with 15 or 16 lamellae. Body color pinkish to orange, with irregular darker patches all over the dorsum. Rhinophores reddish; branchial leaves the same color as the dorsum.

Reproductive system (Fig. 12) with a long, narrow, curved ampulla that connects with the female gland complex and an irregular, elongate prostate. The prostate is wider than the ampulla, but it narrows substantially into a long, folded tube, before expanding into the short, wide deferent duct. The penis is unarmed. The vagina is elongate, several times narrower than the deferent duct, connecting directly to the large, oval bursa copulatrix. The smaller, elongate seminal receptacle also connects to the bursa copulatrix next to the vaginal connection, and the short uterine duct that enters the female gland complex. The bursa copulatrix is several times larger than the seminal receptacle.

Radular formula 28 × 73.0.73 in a 23-mm long specimen (MNHN IM-2013-86208), 36 × 80.0.80 in a 26-mm long specimen (MNHN IM-2013-86205), and 37 × 81.0.81 in a 26-mm long (MNHN IM-2013-86209). Rachidian teeth absent. Inner

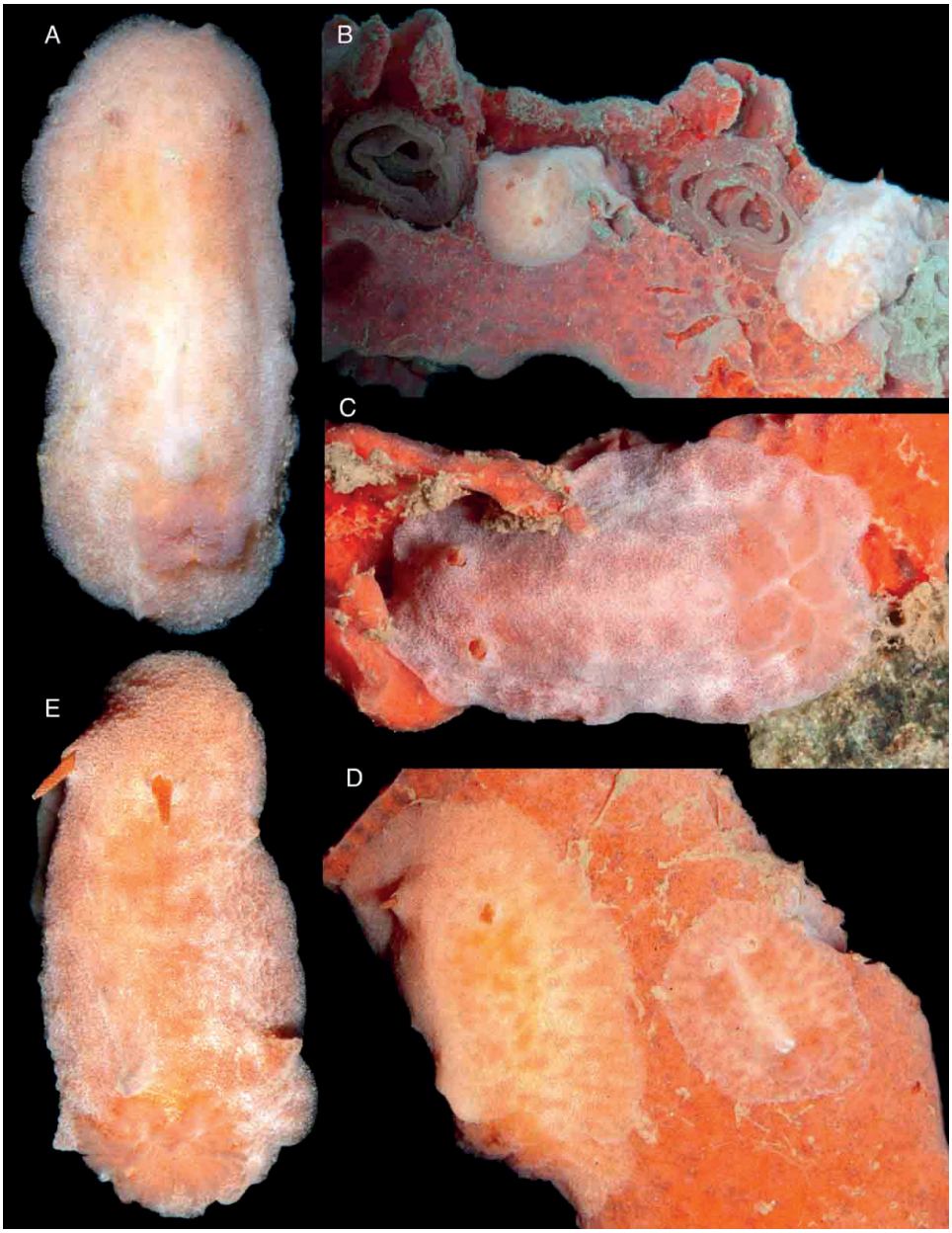

Figure 11. Photographs of live animals of *Rostanga poddubetskaiae* sp. nov. **A** holotype MNHN IM-2013-86199 on black background **B** holotype (MNHN IM-2013-86199) and MNHN IM-2013-86217 in situ with egg masses **C** MNHN IM-2013-86205 in situ **D** MNHN IM-2013-86216 and MNHN IM-2013-86217 in situ **E** MNHN IM-2013-86209 on black background.

and mid-lateral teeth hamate, having a small cusp and lacking denticles (Fig. 13A, B). Innermost teeth very small in comparison to mid-laterals (Fig. 13A). The teeth increase in size gradually towards the medial portion of the half-row (Fig. 13B). Outermost

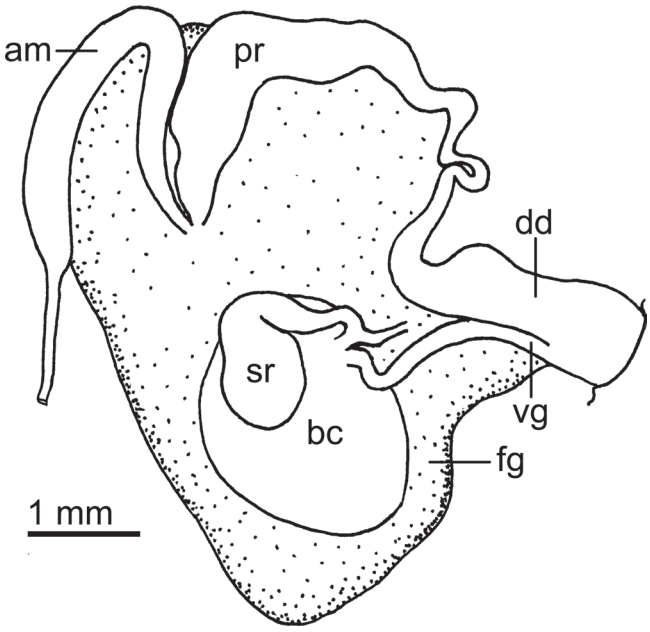

Figure 12. Drawing of the reproductive system of *Rostanga poddubetskaiae* sp. nov., MNHN IM-2013-86202. Abbreviations: am, ampulla; bc, bursa copulatrix; dd, deferent duct; fg, female gland complex; pr, prostate; sr, seminal receptacle; vg, vagina.

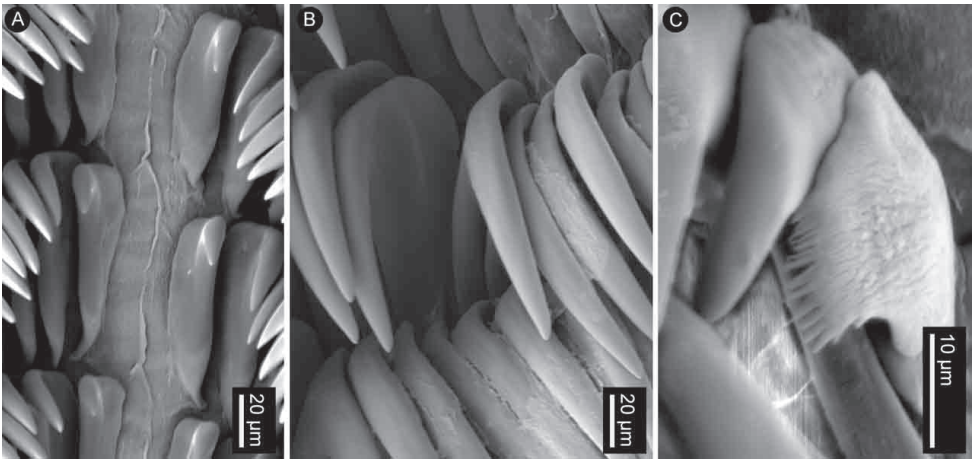

Figure 13. SEM of the radula of specimens of *Rostanga poddubetskaiae* sp. nov., MNHN IM-2013-86205 **A** innermost teeth **B** mid-lateral teeth **C** outer lateral teeth.

teeth small, decreasing in size gradually, and hamate (Fig. 13C), outermost one with 13–20 irregular denticles. No jaw was observed, labial cuticle smooth.

Biology. All the specimens were found on an unidentified species of sponge while SCUBA diving. The presence of these highly cryptic nudibranchs was initially

determined in the field by observing the egg masses on the sponges. In most cases, to separate the nudibranchs, the sponges were brought to the lab and examined under a microscope.

Etymology. This species is named after Marina Poddubetskaia, indefatigable collector and diver, who first discovered the animals here described during the two of the Koumac expeditions.

Remarks. *Rostanga poddubetskaiae* sp. nov. is provisionally assigned to the genus *Rostanga* based on the results of the molecular phylogenetic analyses, which place this species solidly nested within a clade containing other species identified as members of *Rostanga*. However, there are some notable differences between *Rostanga poddubetskaiae* sp. nov. and the diagnoses of the genus *Rostanga* provided by Rudman and Avern (1989) and Valdés and Gosliner (2001), such as the absence of jaws and elongate outermost radular teeth, and the presence of short caryophyllidia; moreover, the arrangement of the branchial leaves flattened against the dorsum and the presence of a dorsal ridge are unusual for a species of *Rostanga*. Additional resolution in the phylogeny of dorid nudibranchs and a larger sample are needed before this species can be placed in a genus with confidence.

Rostanga poddubetskaiae sp. nov. appears to be sister to *Rostanga elandsia* Garovoy, Valdés & Gosliner, 2001 from South Africa, but additional species need to be included in the analysis to confirm those relationships. Morphologically, *R. poddubetskaiae* sp. nov. exhibits a number of differences from other members of this genus, including the presence of a dorsal ridge, elongate rhinophores, a gill flattened against the body, and smooth, hamate inner and mid radular teeth, and short, pectinate outermost lateral teeth. The Indo-Pacific species of *Rostanga* have been reviewed in papers by Rudman and Avern (1989), Baba (1991), and Garovoy et al. (2001), and none of them have external and internal characteristics present in *R. poddubetskaiae* sp. nov. The only exception is *Rostanga crawfordi* (Burn, 1969), described as *Rostanga australis* Rudman & Avern, 1989, which appears to have a dorsal ridge in some specimens (see Rudman and Avern 1989; Coleman 2008) and a similar external coloration to *R. poddubetskaiae* sp. nov., but the radular teeth are very different: specifically, the outer teeth are elongate with numerous denticles on the tip.

Genus *Sclerodoris* Eliot, 1904

Sclerodoris Eliot, 1904: 361. Type species: *Sclerodoris tuberculata* Eliot, 1904, by subsequent designation by Valdés and Gosliner (2001).

?*Gravieria* Vayssière, 1912: 29–30. Type species: *Gravieria rugosa* Vayssière, 1912, by monotypy.

Tumbia Burn, 1962b: 161–163. Type species: *Asteronotus* (*Tumbia*) *trenberthi* Burn, 1962b [= *Sclerodoris trenberthi* (Burn, 1962b)], by monotypy.

Remarks. For an in-depth discussion of the characteristics of the genus *Sclerodoris* and its synonyms see Valdés and Gosliner (2001).

***Sclerodoris tuberculata* Eliot, 1904**
Figs 14A, 15A–C, 16A–C

?*Doris castanea* Kelaart, 1858: 110. Type locality: Sober Island, Tricomalie [= Trincomalee] harbor, Ceylon [= Sri Lanka].
Sclerodoris tuberculata Eliot, 1904: 381–382. Type locality: Prison Island [= Changuu], Zanzibar harbor, Tanzania.
Sclerodoris minor Eliot, 1904: 381. Type locality: Chuaka [= Chwaka], Zanzibar, Tanzania.
Sclerodoris rubra Eliot, 1904: 382–383. Type locality: reef off the east coast of Zanzibar, Tanzania.
Halgerda rubra Bergh, 1905: 126–127, pl. 4 fig. 2, pl. 15 figs 34–36. Type locality: Bandas [= Banda Islands], Indonesia, 36 m depth.

Material examined. Pointe de Pandop, Koumac, New Caledonia (20°34.9'S, 164°16.5'E), 7 m depth [Koumac 2.1 stn. KR868], 26 Sep 2018, 1 specimen 44 mm long, dissected (MNHN IM-2013-86197, isolate JI10).

Description. Body oval, flattened, with an irregular, coriaceous texture (Fig. 14A). Branchial and rhinophoral sheaths somewhat elevated, simple, circular. Gill composed of eight short, tripinnate branchial leaves, arranged upright. Rhinophores short, lamellated, with 18 lamellae. Visceral hump clearly elevated over the rest of the mantle, with several lateral protuberances and a conspicuous depression mid-length. Dorsum completely covered with small caryophyllidia. Body color red, with several large, irregularly opaque white patches, mainly on the mantle margin and some white pigment irregularly scattered all over. Rhinophores and branchial leaves are the same color as the dorsum.

Reproductive system (Fig. 15A, B) with a long, wide, convoluted ampulla with several folds, which connects with the female gland complex and the oval, flattened prostate. The prostate narrows substantially into a long, straight duct, before expanding into the short, wide deferent duct. The penis is armed with triangular spines, varying in size (Fig. 15C) with thickened bases and sharp cusps. The vagina is elongate, narrow, as wide as the deferent duct, connecting directly to the large, oval bursa copulatrix. The elongate seminal receptacle also connects to the bursa copulatrix next to the vaginal connection, and the short uterine duct that enters the female gland complex (Fig. 15B). The bursa copulatrix is ~ 4× as large as the seminal receptable. An accessory gland connects to the genial atrium where the deferent duct and the vagina meet. The accessory gland is granular in texture and approximately as large as the seminal receptable.

Radular formula 38 × 49.0.49 in a 44-mm long specimen (MNHN IM-2013-86197). Rachidian teeth absent. Inner and mid-lateral teeth hamate, having an elongate cusp and lacking denticles (Fig. 16A, B). Innermost teeth very small in comparison to mid-laterals (Fig. 16A). The teeth increase in size gradually towards the medial portion of the half-row. Outermost teeth small, decreasing in size gradually, composed of a short, blunt cusp with numerous small denticles (Fig. 13C). No jaw was observed, labial cuticle smooth.

Biology. Rare, found under rocks at 7 m depth. Widespread in the Indo-Pacific region. The single specimen was found under a rock while SCUBA diving where it was highly cryptic.

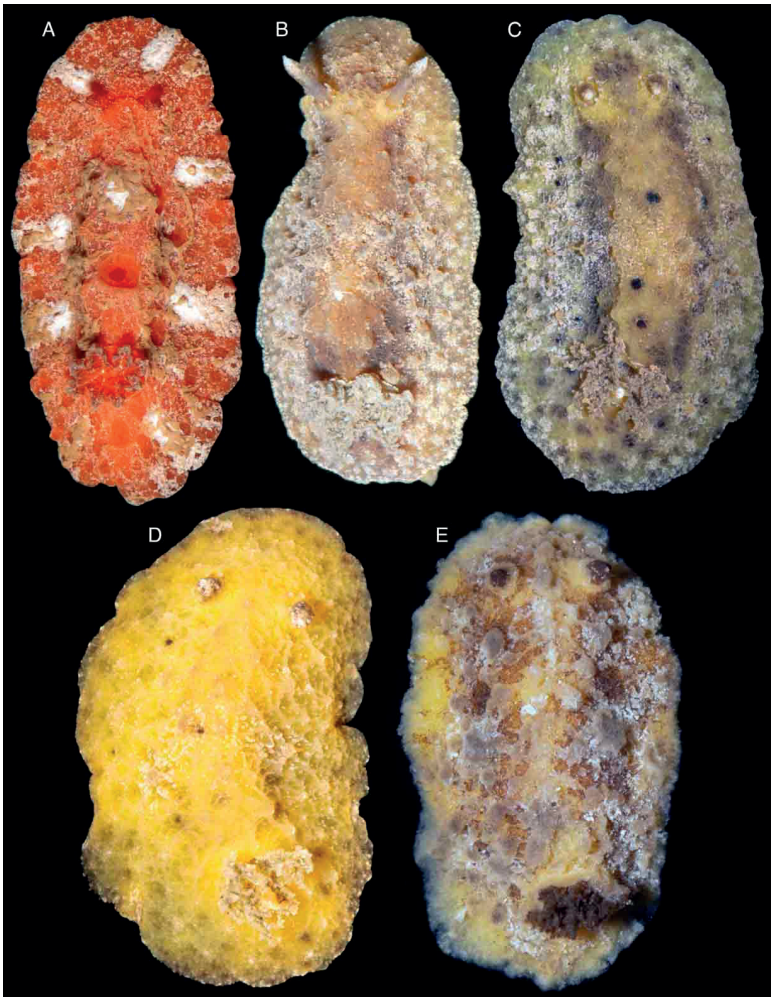

Figure 14. Photographs of live animals of the genus *Sclerodoris* Eliot, 1904 **A** *Sclerodoris tuberculata* Eliot, 1904, MNHN IM-2013-86197 on black background **B–D** "*Sclerodoris*" *dutertrei* sp. nov., Holotype (MNHN IM-2013-86193) on black background (**B**), MNHN IM-2013-86195 on black background (**C**), MNHN IM-2013-86194 on black background (**D**) **E** *Sclerodoris faninozi* sp. nov., Holotype (MNHN IM-2013-86198) on black background.

Remarks. Eliot (1904) described *Sclerodoris tuberculata* based on one specimen collected in Zanzibar as follows: "Dark brown with sandy spots, exactly like a sponge splashed with sand. Underside clear bright brownish red. Branchial pocket crenulate. The middle part of back covered with conical warts, which form an irregular keel; smaller warts on mantle-edge. Rhinophores red; branchiae eight, voluminous; axes red, tips white. Animal alters shape, sometimes rather high, sometimes quite flat like *Platydoris*. Consistency quite hard and rather rough. Two depressions with deep black markings as in some species of *Trippa*." In the same paper Eliot (1904) introduced two additional species also resembling sponges, *Sclerodoris minor* Eliot, 1904, and *Sclerodoris rubra*

Eliot, 1904, both synonyms of *S. tuberculata*. *Sclerodoris tuberculata* is considered a widespread species in the Indo-Pacific region and is well documented in the literature (Valdés and Gosliner 2001; Yonow 2008; Gosliner et al. 2018; Nakano 2018). The material here examined is consistent with the original description of *S. tuberculata* and subsequent records; however, a record of this species from New Caledonia (Hervé 2010) is probably the closely related species *Sclerodoris rubicunda* (Baba, 1949).

Eliot (1906) suggested that *Doris castanea* Kelaart, 1858 was possibly the same species as *Sclerodoris tuberculata* Eliot, 1904, but indicated the identity of the latter could not be established with certainty based on the type material. Eliot (1906: pl. 42, figs 6, 7) reproduced the original drawing by Kelaart, which clearly resembles a dark specimen of *S. tuberculata*. Later, Eliot (1908) regarded *Sclerodoris rubra* Eliot, 1904 as a senior synonym of *Halgerda rubra* Bergh, 1905.

Allan (1947) reported *S. tuberculata* from New South Wales, Australia, under the genus name *Peronodoris* Bergh, 1904 and commented on Eliot's (1906) proposed synonymy between this species and *D. castanea*. Allan (1947) indicated that "although the colour sketch of the upper surface of Kelaart's specimen resembles that of our specimen to a very slight degree," the undersurface is exactly like the color sketch of the New South Wales material of *S. tuberculata*. Allan (1947) concluded that whether *S. tuberculata* was eventually to become a synonym of *D. castanea* remained to be seen, as fresh material from the two type localities needs to be examined before this can be determined.

Rudman (1978) endorsed Eliot's (1908) decision to synonymize *Halgerda rubra* Bergh, 1905 with *Sclerodoris rubra* Eliot, 1904. At the same time Rudman (1978) regarded *Sclerodoris rubra* Eliot, 1904 and *Sclerodoris minor* Eliot, 1904 as synonyms of *Sclerodoris tuberculata* Eliot, 1904, and based on the Principle of First Reviser (ICZN 1999: Article 24), Rudman (1978) established *S. tuberculata* as the valid name for this species. Rudman (1978) also commented that the original description of *D. castanea* by Kelaart (1858) was most inadequate and therefore best to ignore it. In this paper we follow Rudman's (1978) conclusion and regard *Sclerodoris tuberculata* Eliot, 1904 as the valid name for this species with the synonymies established above. We also leave the question of the identity of *D. castanea* as unresolved.

Hervé (2010) reported *Sclerodoris tuberculata* from New Caledonia but based on the photographs published (Hervé 2010: 214), it seems that these records correspond to *Sclerodoris rubicunda* (Baba, 1949). The present study is the first confirmed record of *Sclerodoris tuberculata* from New Caledonia.

***Sclerodoris faninozi* sp. nov.**

https://zoobank.org/619B72BC-611E-4E53-ABAA-0D8D67284448

Figs 14E, 15D–F, 16G–I

Type material. *Holotype*: Koumac, New Caledonia (20°33.7'S, 164°11.2'E), 0 m depth [Koumac 2.3 stn. KB518, blocks of dead coral on the margin of the fringing reef flat of the lagoon island], 20 Nov 2019, 25 mm long, dissected (MNHN IM-2013-86198, isolate JI11).

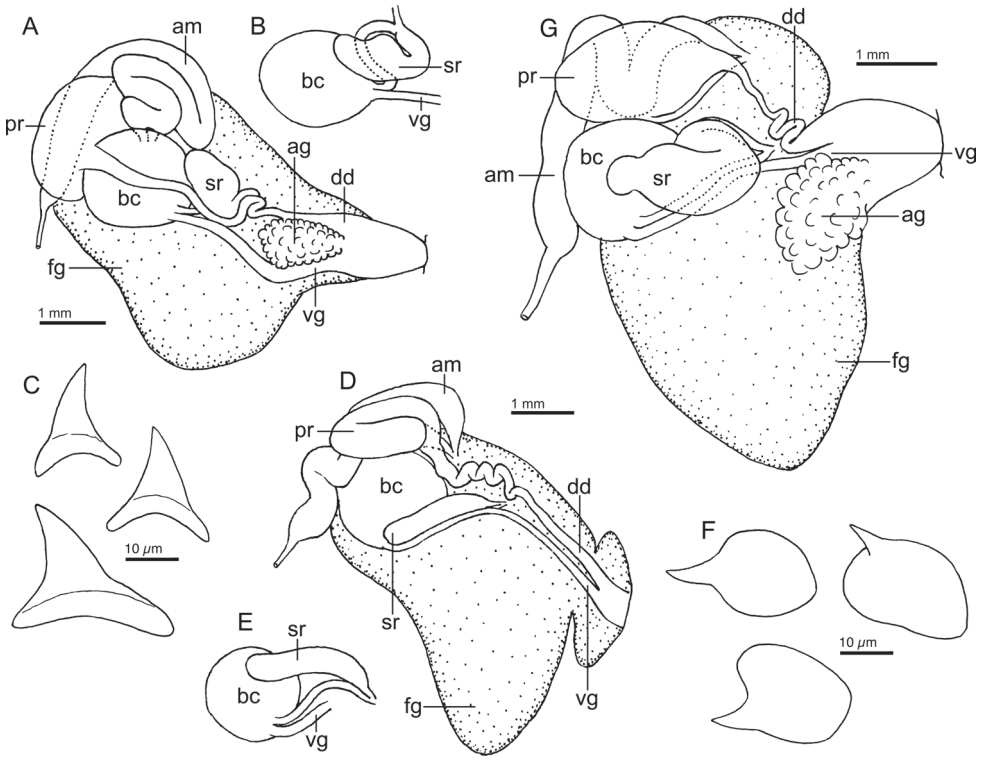

Figure 15. Drawing of the reproductive system of specimens of the genus *Sclerodoris* Eliot, 1904 **A–C** *Sclerodoris tuberculata* Eliot, 1904, MNHN IM-2013-86197, general view (**A**), detail of the bursa copulatrix and seminal receptable (**B**), penial spines (**C**) **D–F** *Sclerodoris faninozi* sp. nov., Holotype (MNHN IM-2013-86198), general view (**D**), detail of the bursa copulatrix and seminal receptable (**E**), penial spines (**F**) **G** "*Sclerodoris*" *dutertrei* sp. nov., MNHN IM-2013-86193. Abbreviations: ag, accessory gland; am, ampulla; bc, bursa copulatrix; dd, deferent duct; fg, female gland complex; pr, prostate; sr, seminal receptacle; vg, vagina.

Description. Body oval, flattened, with an irregular, coriaceous texture (Fig. 14E). Branchial and rhinophoral sheaths somewhat elevated, simple, irregular. Gill composed of five short, tripinnate branchial leaves, arranged upright. Rhinophores short, lamellated, with 15 lamellae. Visceral hump elevated over the rest of the mantle. Dorsum completely covered with small caryophyllidia, a longitudinal ridge, and several large, rounded tubercles. Body color yellowish brown, with scattered opaque white pigment, and areas or dark brown and dark gray. Branchial leaves and rhinophores dark brown.

Reproductive system (Fig. 15D, E) with a long, wide, convoluted ampulla with several folds, which connects with the female gland complex and the elongate, convoluted prostate. The prostate is as wide as the ampulla, but narrows substantially into a very long duct, before expanding into the long, narrow deferent duct. The penis is armed with rounded spines having a short, sharp cusp (Fig. 15F). The vagina is elongate, narrow, as wide as the deferent duct, connecting directly to the large, spherical bursa copulatrix. The elongate seminal receptacle also connects to the bursa copulatrix

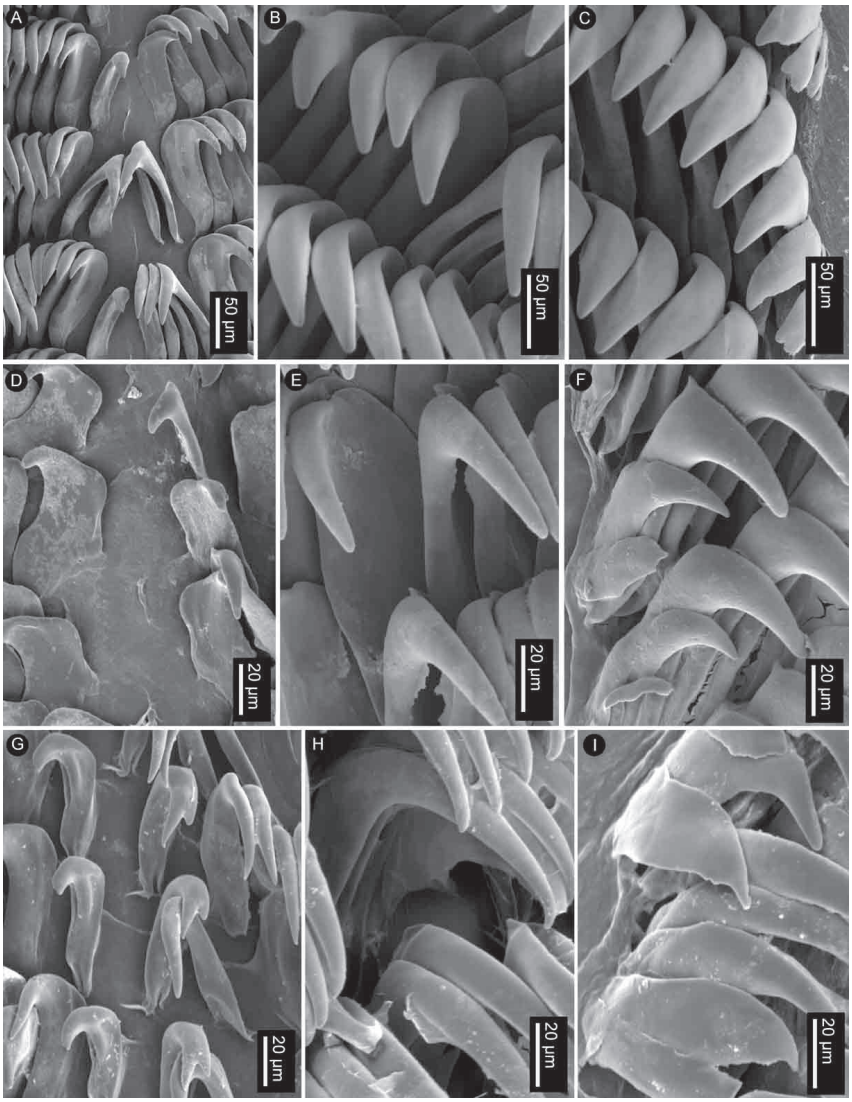

Figure 16. SEM of the radula of specimens of the genus *Sclerodoris* Eliot, 1904 **A–C** *Sclerodoris tuberculata* Eliot, 1904, MNHN IM-2013-86197, innermost teeth (**A**), mid-lateral teeth (**B**), outer lateral teeth (**C**) **D–F** "*Sclerodoris*" *dutertrei* sp. nov., MNHN IM-2013-86195, innermost teeth (**D**), mid-lateral teeth (**E**), outer lateral teeth (**F**) **G–I** *Sclerodoris faninozi* sp. nov., Holotype (MNHN IM-2013-86198), innermost teeth (**G**), mid-lateral teeth (**H**), outer lateral teeth (**I**).

and the uterine duct that enters the female gland complex. The bursa copulatrix is ~ 3× wider than the seminar receptable, but similar in volume (Fig. 15D). No accessory gland was observed.

Radular formula 32 × 68.0.68 in a 25-mm long specimen (MNHN IM-2013-86198). Rachidian teeth absent. Inner and mid-lateral teeth hamate, having an elongate

cusp (sometimes bifurcate) and lacking denticles (Fig. 16G–I). Innermost teeth very small in comparison to mid-laterals (Fig. 16G). The teeth increase in size gradually towards the medial portion of the half-row. Outermost teeth small, decreasing in size gradually, elongate, with a short cusp and numerous denticles (Fig. 13I). No jaw was observed, labial cuticle smooth.

Biology. Rare, found intertidally under rocks, possibly a New Caledonia endemic. The single specimen was obtained by brushing blocks of dead coral on the margin of a fringing reef flat.

Etymology. This species is named after Sébastien Faninoz whose efforts were critical for the organization of the Koumac expeditions.

Remarks. In the phylogenetic analyses conducted herein, *Sclerodoris faninozi* sp. nov. is sister to *Sclerodoris tuberculata*, the type species of *Sclerodoris*, forming a well-supported clade; for this reason, *S. faninozi* sp. nov. is placed in the genus *Sclerodoris*. Moreover, most of the anatomical characteristics of *S. faninozi* sp. nov. match the diagnosis of the genus *Sclerodoris* provided by Valdés and Gosliner (2001). Specifically, *S. faninozi* sp. nov. has a flattened, coriaceous dorsum covered with caryophyllidia, the rhinophoral sheaths are somewhat elevated; the penis is armed with hooks and the vagina is unarmed; the labial cuticle and radular teeth are smooth, hamate with the outermost lateral teeth multi-denticulate. The only exception is the accessory gland, which is a diagnostic trait for *Sclerodoris*, but was not observed in *S. faninozi* sp. nov. Although the absence of an accessory gland in *S. faninozi* sp. nov. could have been result of damage to the specimen, it appears that the presence of this organ is variable in *Sclerodoris*.

Sclerodoris faninozi sp. nov. is externally similar to *Sclerodoris coriacea* Eliot, 1904 introduced based on a specimen collected near Chwaka (as Chuaka), on the east coast of Zanzibar, Tanzania. Eliot (1904) described *S. coriacea* as yellowish brown in color with the dorsal surface covered with a "distinctly raised but somewhat irregular reticulate pattern." Rudman (1978) redescribed *S. coriacea* also based on specimens from Zanzibar, and a color photograph of a live animal was illustrated by Gosliner et al. (2018). The specimen of *S. faninozi* sp. nov. here examined is similar to all these descriptions with the exception of the presence of a dorsal ridge, absent in *S. coriacea*. The radular morphology of *S. faninozi* sp. nov. is also similar to that of *S. coriacea* as described by Rudman (1978) but the innermost teeth of *S. faninozi* sp. nov. have a bifurcated cusp, whereas they are simple in *S. coriacea* (Rudman 1978: fig. 13).

"*Sclerodoris*" *dutertrei* sp. nov.

https://zoobank.org/504AD504-89AE-48D4-9840-4800830CC0AC

Figs 14B–D, 15G, 16D–F

Type material. *Holotype*: Anse de Koumac, New Caledonia (20°34.2'S, 164°16.5'E), 0 m depth [Koumac 2.1 stn. KR213], 11 Sep 2018, 31 mm long (MNHN IM-2013-86193, isolate JI04).

Material examined. Récif Sud de Pandop, Koumac, New Caledonia (20°35.4'S, 164°16.5'E), 0 m depth [Koumac 2.1 stn. KR322, reef flat with rocks, living and dead corals], 27 Sep 2018, 1 specimen 23 mm long (MNHN IM-2013-86196, isolate JI14). Koumac, New Caledonia (20°35.6'S, 164°16.3'E), 3 m depth [Koumac 2.2 stn. KR230], 2 Mar 2019, 1 specimen 12 mm long (MNHN IM-2013-86194, isolate JI35); 1 specimen 20 mm long, dissected (MNHN IM-2013-86195, isolate JI34).

Description. Body oval, flattened, with an irregular, coriaceous texture (Fig. 14B–D). Branchial and rhinophoral sheaths somewhat elevated, simple, irregular. Gill composed of five short, tripinnate branchial leaves, arranged upright. Rhinophores short, lamellated, with 12–14 lamellae. Visceral hump elevated over the rest of the mantle. Dorsum completely covered with small caryophyllidia and a complex network of ridges and scattered large, rounded tubercles. Body color variable, yellow to pale brown with scattered opaque white pigment and some specimens with rounded black spots. Branchial leaves are the same color as the dorsum; rhinophores brown proximally, with white apices.

Reproductive system (Fig. 15G) with a long, wide, convoluted ampulla with several folds, which connects with the female gland complex and the oval, flattened prostate. The prostate narrows substantially into a long, convoluted duct, before expanding into the short, wide deferent duct. The penis is unarmed. The vagina is elongate, much narrower than the deferent duct, connecting directly to the large, oval bursa copulatrix. The elongate seminal receptacle also connects to the bursa copulatrix next to the vaginal connection, and the short uterine duct that enters the female gland complex. The seminal receptable possesses a spherical tip and it is similar in volume to the bursa copulatrix. An accessory gland connects to the genial atrium where the deferent duct and the vagina meet. The accessory gland is granular in texture and approximately as large as the bursa copulatrix.

Radular formula 37 × 54.0.54 in a 20-mm long specimen (MNHN IM-2013-86195). Rachidian teeth absent. Inner and mid-lateral teeth hamate, having a short cusp and lacking denticles (Fig. 16D, E). Innermost teeth very small in comparison to mid-laterals (Fig. 16D). The teeth increase in size gradually towards the medial portion of the half-row. Outermost teeth small, decreasing in size gradually, elongate, with a short cusp and lacking differentiated denticles (Fig. 16F). No jaw was observed, labial cuticle smooth.

Biology. Found under rocks at 0–3 m depth. All the specimens were obtained by direct collection while SCUBA diving. The specimens were very cryptic on rocks with sponges and other encrusting organisms.

Etymology. This species is named after Valentine Dutertre whose hard work, dedication, and skill were critical for the collection of numerous important sea slug species during the Koumac expeditions.

Remarks. The phylogenetic analysis places "*Sclerodoris*" *dutertrei* sp. nov. in a well-supported clade containing two other species identified as members of *Sclerodoris*. These two species were sequenced and submitted to GenBank but never formally studied, thus their morphological characteristics remain undescribed. This clade is not closely related to the clade containing the rest of the species of *Sclerodoris*, including

the type species, *Sclerodoris tuberculata*. Therefore, "*S.*" *dutertrei* sp. nov. cannot be definitely included in the genus *Sclerodoris* and the generic placement of this species is regarded as tentative until a well resolved phylogeny of the Discodorididae permits a more accurate taxonomic placement. "*Sclerodoris*" *dutertrei* sp. nov. is tentatively placed in *Sclerodoris* (as indicated by the quotation marks) because anatomically this species is for the most part consistent with the diagnosis for *Sclerodoris* provided by Valdés and Gosliner (2001), including a flattened, coriaceous dorsum covered with caryophyllidia, rhinophoral sheaths somewhat elevated; a lobate accessory gland, without stylet; labial cuticle and radular teeth smooth, hamate with the outermost lateral teeth multidenticulate. The only exception is the penis, which appears to be unarmed in "*S.*" *dutertrei* sp. nov., but the presence of penial spines is a characteristic of *Sclerodoris* sensu stricto (see Valdés and Gosliner 2001).

"*Sclerodoris*" *dutertrei* sp. nov. is distinct from other species previously assigned to *Sclerodoris*: no other species described to date possesses a yellow to pale brown dorsum with scattered opaque white pigment (sometimes with rounded black spots), completely covered with small caryophyllidia and a complex network of ridges and scattered large, rounded tubercles. As mentioned above, *Sclerodoris tuberculata* is red with several large, irregularly shaped, opaque white patches and a conspicuous depression mid-length on the dorsum, not present in "*Sclerodoris*" *dutertrei* sp. nov.; *Sclerodoris faninozi* sp. nov. is yellowish brown, with scattered opaque white pigment, and areas of dark brown and dark gray but also has a longitudinal ridge, and several large, rounded tubercles, also absent in "*Sclerodoris*" *dutertrei* sp. nov. Other Indo-Pacific species described also present external characteristics that distinguish them from "*Sclerodoris*" *dutertrei* sp. nov. For example, *Sclerodoris apiculata* (Alder & Hancock, 1864) is characterized by having a network of ridges radiating from elevated conical centers, each with an elongated filament (see Alder and Hancock 1864; Hervé 2010; Gosliner et al. 2018; Nakano 2018). *Sclerodoris coriacea* has the dorsum completely covered with large, elongate tubercles joined by conspicuous ridges (see Rudman 1978; Gosliner et al. 2018), very different from those in "*Sclerodoris*" *dutertrei* sp. nov. *Sclerodoris japonica* (Eliot, 1913), originally described as a member of the genus *Halgerda* (see Eliot 1913) is characterized by having a yellowish grey dorsum covered with small ridges, and numerous, large roundish areas of a darker grey, varying in intensity, which correspond to dorsal depressions or pits. *Sclerodoris rubicunda* is a red species with two large patches of white and purple pigment and a series of conspicuous dorsal ridges (Baba 1949; Gosliner et al. 2018; Nakano 2018). *Sclerodoris trenberthi* (Burn, 1962b) and *Sclerodoris tarka* Burn, 1969 both described from Victoria, Australia are also distinct from "*Sclerodoris*" *dutertrei* sp. nov. *Sclerodoris trenberthi* has a characteristic longitudinal dorsal structure composed of "irregularly sized and spaced low hard pustules surmounting a low ridge" running from the rhinophores to the gill (Burn 1962b), which is absent from "*Sclerodoris*" *dutertrei* sp. nov. *Sclerodoris tarka* is a dusky yellow to yellowish orange species with a pattern of conspicuous dorsal ridges (Burn, 1969) and an indistinct medial ridge, also absent in "*Sclerodoris*" *dutertrei* sp. nov. Finally, *Sclerodoris virgulata* Valdés, 2001 is the only species of *Sclerodoris* with a white dorsum lacking dorsal ridges or depressions (Valdés 2001), also very different from "*Sclerodoris*" *dutertrei* sp. nov.

Discussion

The phylogeny presented here is largely consistent with previous morphological studies and the classification of the Discodorididae proposed by Valdés and Gosliner (2001) and Valdés (2002) with some exceptions. For example, the genus *Atagema* is sister to the rest of Discodorididae + Cadlinidae, but due to the poor representation of Cadlinidae in this study, these results should be taken cautiously. There is also a discrepancy with the molecular analysis by Hallas et al. (2017), who found *Atagema* + *Aphelodoris* as sister to remaining members of Discodorididae, but *Aldisa* + *Cadlina* forming a distinct clade, as also recovered by Johnson (2010) and Johnson and Gosliner (2012). On the contrary, in the present analyses *Aldisa* is nested within the Discodorididae. The more limited taxon sampling in the present study could explain this discrepancy, but the goal of the present analysis is only to place the new species here described in a phylogenetic context, not to provide a reliable reconstruction of the phylogeny of Discodorididae, which may only be achieved with next generation sequence data. There are some other differences between the present analyses and previous classification attempts of species included herein. For example, *Discodoris coerulescens* was regarded by Dayrat (2010) as a member of a metaphyletic group branching from near the basal node of Discodorididae he named "*Montereina*," but the present analyses appear to suggest a close relationship with the genus *Tayuva* Er. Marcus and Ev. Marcus, 1967. *Tayuva* was considered a synonym of *Discodoris* by Valdés (2002) and *T. lilacina*, originally described as *Doris lilacina* Gould, 1852, is regarded as a member *Discodoris* by some authors (e.g., Gosliner et al. 2018); however, other authors following Dayrat (2010) placed this species in *Tayuva*, a distinct genus with a single pantropical species (e.g., Ballesteros et al. 2016; Yonow 2017). The results of the present analysis appear to confirm that *Tayuva* is distinct from *Discodoris* as suggested by Dayrat (2010), but it is unclear how many species are present in this pantropical complex. Finally, the genus *Montereina* MacFarland, 1905 was synonymized with *Peltodoris* by Valdés (2002), but the results of the present analyses suggest that these two groups are distinct as suggested by Dayrat (2010).

Based on the phylogenetic analyses here presented, it appears that the genus *Sclerodoris* is paraphyletic. The new species "*Sclerodoris*" *dutertrei* sp. nov. was recovered in a well-supported clade containing two other species identified as members of *Sclerodoris*, but not in the clade including *Sclerodoris tuberculata* Eliot, 1904, which is the type species of *Sclerodoris*. Thus, the description of a new genus name for the clade including "*Sclerodoris*" *dutertrei* sp. nov. is an option. However, due to the limited sample size in our molecular phylogenies and the lack of support for several clades, we prefer to postpone any decisions regarding this group until a more reliable phylogeny of the Discodorididae is available, as there could be available genus-level names for this group. Therefore, the generic placement of "*Sclerodoris*" *dutertrei* sp. nov. is regarded as tentative, indicated by the quotation marks.

Bouchet et al. (2007) argued that "it can safely be affirmed that, as a result of the recent sampling programs, both in shallow and in deep-water, no other South Pacific

island group has been so intensively surveyed as New Caledonia." However, recent field work during the Koumac expeditions seems to have revealed additional diversity missed during early work, suggesting that documenting the New Caledonia molluscan diversity is still a work in progress. As Bouchet et al. (2007) indicated, the question of how many mollusk species are present in New Caledonia remains unanswered and this is particularly true for sea slugs. This paper is a small contribution towards the goal of describing the sea slug diversity of New Caledonia as field work continues to produce previously unseen taxa.

It is unclear how many of the species here described are endemic to New Caledonia. Payri et al. (2019) suggested that probably < 15% of the New Caledonia marine mollusks are endemic, although they also indicated that "several scientists have already demonstrated connections between the marine life of New Caledonia, the Great Barrier reef, and the center of maximum diversity of the Coral Triangle." Based on photographs published in field guides or other publications, it is likely that *Atagema papillosa* (Risbec, 1928), *Atagema sobanovae* sp. nov., and *Jorunna daoulasi* sp. nov. are widespread in the Western Pacific, but we have been unable to find photographs of *Atagema kimberlyae* sp. nov., *Jorunna hervei* sp. nov., *Rostanga poddubetskaiae* sp. nov., *Sclerodoris faninozi* sp. nov., and "*Sclerodoris*" *dutertrei* sp. nov. in other publications outside New Caledonia. But due to the very cryptic nature of these species, it could very well be that they have been overlooked. While the small size of the eggs of *J. hervei* sp. nov. suggests planktotrophic development and therefore a potentially large geographic range, the recent description of a very similar species from the Indian Ocean, *J. liviae*, may indicate there is a species complex of species with similar external morphologies present in different ocean basins. Much more work on these neglected dorid nudibranchs is needed to have a better understanding of their taxonomy, diversity, and evolution.

The specimens here examined where collected using different techniques, including dredging, direct collecting (intertidally and SCUBA diving), and substrate collecting. Due to the highly cryptic coloration and morphology of some of the species, their presence was detected initially by the observation of egg masses on the sponges. In the particular case of *A. sobanovae* sp. nov., most of the specimens were collected by dissecting the sponges in the laboratory as the nudibranchs were buried in the tissue, and almost invisible. The diversity of collecting techniques and specialized methods used during the Koumac expeditions were critical in the discovery of the species here examined. This paper provides a rare example of the description and re-description of ecologically cryptic sea slug species using contemporary taxonomic techniques and focusing on a narrow geographic region that, despite substantial collecting efforts (Bouchet et al. 2007), appears to remain under-sampled.

Acknowledgements

The material examined was collected during the "Our Planet Reviewed" – New Caledonia expeditions (2016–2019), a joint project of MNHN and Conservatoire d'Espaces

Naturels (CEN) de Nouvelle-Calédonie, funded mainly by the Gouvernement de la Nouvelle-Calédonie, Province Nord, Agence Française de la Biodiversité (AFB), the Lounsbery Foundation, and Office des Postes et Télécommunications (OPT). The expedition operated under a permit issued by Direction du Développement Economique et de l'Environnement (DDEE) of Province Nord. We are especially grateful to Philippe Bouchet for the invitation to participate in the expedition and to Sébastien Faninoz, Virginie Héros, Philippe Maestrati, Pierre Lozuet, Alain Daoulas, Jean-François Hervé, Yves Thévenet, and many others for their help and support. We also thank Jenelle Innabi, Tatiana Vargas, and Jade de Souza for their assistance with the molecular work.

References

Alder J, Hancock A (1864) Notice of a collection of nudibranchiate Mollusca made in India by Walter Elliot Esq. with descriptions of several new genera and species. Transactions of the Zoological Society of London 5: 113–147. [pls. 28–33] https://doi.org/10.1111/j.1096-3642.1864.tb00643.x

Allan JK (1947) Nudibranchia from the Clarence River Heads, north coast, New South Wales. Records of the Australian Museum 21: 433–463. [pls. 41–43] https://doi.org/10.3853/j.0067-1975.21.1947.561

Alvim J, Pimenta AD (2013) Taxonomic review of the family Discodorididae (Mollusca: Gastropoda: Nudibranchia) from Brazil, with descriptions of two new species. Zootaxa 3745(2): 152–198. https://doi.org/10.11646/zootaxa.3745.2.2

Baba K (1949) Opisthobranchia of Sagami Bay Collected by His Majesty the Emperor of Japan. Iwanami Shoten, Tokyo, 194 pp. [50 pls.]

Baba K (1991) Review of the genus *Rostanga* of Japan with the description of a new species (Nudibranchia: Doridídae). Venus 50: 43–53. https://doi.org/10.18941/venusjjm.50.1_43

Ballesteros M, Madrenas E, Pontes M (2016) Actualización del catálogo de los moluscos opistobranquios (Gastropoda: Heterobranchia) de las costas catalanas. Spira 6: 1–28.

Bergh LSR (1876) Malacologische Untersuchungen. In: Semper C (Ed.) Reisen im Archipel der Philippinen, Theil 2, Heft 10. Kreidel, Wiesbaden, 377–428. [pls. 50–53]

Bergh LSR (1877) Kritische Untersuchung der Ehrenberg'schen Doriden. Jahrbücher der Deutschen Malakozoologischen Gesellschaft 4: 45–76.

Bergh LSR (1878) Malacologische Untersuchungen. In: Semper C (Ed.) Reisen im Archipel der Philippinen, Theil 2, Wissenschaftliche Resultate, Band 2, Theil 2, Heft 13. Kreidel, Wiesbaden, 547–601. [pls. 62–65; Heft 14, pp. 603–645, i–l, pls. 66–68.]

Bergh LSR (1879) Gattungen nordischer Doriden. Archiv für Naturgeschichte 45: 340–369. [pl. 19]

Bergh LSR (1881) Beiträge zur Kenntniss der japanischen Nudibranchien. II. Verhandlungen der königlich-kaiserlich Zoologisch-botanischen Gesellschaft in Wien 31: 219–254. [pls. 6–10]

Bergh LSR (1905) Die Opisthobranchiata der Siboga-expedition. Siboga-Expeditie 50: 1–248. [pls 1–20. Brill, Leiden.]

Bouchet P, Héros V, Maestrati P, Lozouet P, von Cosel R, Brabant D (2007) Mollusca of New Caledonia. In: Payri CE, Richer de Forges B (Eds) Compendium of Marine Species from New Caledonia. IRD Documents Scientifiques et Techniques 117 (2nd Ed.). IRD, Nouméa, New Caledonia, 197–217.

Burn RF (1962a) Descriptions of Victorian nudibranchiate Mollusca, with a comprehensive review of the Eolidacea. Memoirs of the National Museum of Victoria, Melbourne 25: 95–128. https://doi.org/10.24199/j.mmv.1962.25.05

Burn RF (1962b) Notes on a collection of Nudibranchia (Gastropoda: Dorididae and Dendrodorididae) from South Australia with remarks on the species of Basedow and Hedley, 1905. Memoirs of the National Museum of Victoria 25: 149–171. [pl. 1] https://doi.org/10.24199/j.mmv.1962.25.07

Burn RF (1969) A memorial report on the Tom Crawford collection of Victorian Opisthobranchia. Journal of the Malacological Society of Australia 1: 64–106. [pl. 4] https://doi.org/10.1080/00852988.1969.10673833

Camacho-García YE, Gosliner TM (2008) Systematic revision of *Jorunna* Bergh, 1876 (Nudibranchia: Discodorididae) with a morphological phylogenetic analysis. The Journal of Molluscan Studies 74(2): 143–181. https://doi.org/10.1093/mollus/eyn002

Cheney KL, Cortesi F, How MJ, Wilson NG, Blomberg SP, Winters AE, Umanzör S, Marshall NJ (2014) Conspicuous visual signals do not coevolve with increased body size in marine sea slugs. Journal of Evolutionary Biology 27(4): 676–687. https://doi.org/10.1111/jeb.12348

Churchill CK, Valdés A, Foighil DÓ (2014) Molecular and morphological systematics of neustonic nudibranchs (Mollusca: Gastropoda: Glaucidae: *Glaucus*), with descriptions of three new cryptic species. Invertebrate Systematics 28(2): 174–195. https://doi.org/10.1071/IS13038

Coleman N (2008) Nudibranchs Encyclopedia: Catalogue of Asia/Indo-Pacific Sea Slugs. Neville Coleman's Underwater Geographic, 416 pp.

Colgan DJ, McLauchlan A, Wilson GDF, Livingston SP, Edgecombe GD, Macaranas J, Cassis G, Gray MR (1998) Histone H3 and U2 snRNA DNA sequences and arthropod molecular evolution. Australian Journal of Zoology 46(5): 419–437. https://doi.org/10.1071/ZO98048

Dalton SJ, Godwin S (2006) Progressive coral tissue mortality following predation by a corallivorous nudibranch (*Phestilla* sp.). Coral Reefs 25(4): 529–529. https://doi.org/10.1007/s00338-006-0139-0

Dayrat B (2010) A monographic revision of basal discodorid sea slugs (Mollusca: Gastropoda: Nudibranchia: Doridina). Proceedings of the California Academy of Sciences 61(4, supplement 1): 1–403.

Donohoo SA, Gosliner TM (2020) A tale of two genera: The revival of *Hoplodoris* (Nudibranchia: Discodorididae) with the description of new species of *Hoplodoris* and *Asteronotus*. Zootaxa 4890(1): 1–37. https://doi.org/10.11646/zootaxa.4890.1.1

Edgar RC (2004) MUSCLE: Multiple sequence alignment with high accuracy and high throughput. Nucleic Acids Research 32(5): 1792–1797. https://doi.org/10.1093/nar/gkh340

Edmunds M (2011) Opisthobranchiate Mollusca from Ghana: Discodorididae. Journal of Conchology 40: 617–649.

Ekimova I, Korshunova T, Schepetov D, Neretina T, Sanamyan N, Martynov A (2015) Integrative systematics of northern and Arctic nudibranchs of the genus *Dendronotus* (Mollusca,

Gastropoda), with descriptions of three new species. Zoological Journal of the Linnean Society 173(4): 841–886. https://doi.org/10.1111/zoj.12214

Eliot CNE (1904) On some nudibranchs from East Africa and Zanzibar part. III. Proceedings of the Zoological Society of London 1903: 354–385.

Eliot CNE (1906) On the nudibranchs of Southern India and Ceylon, with special reference to the drawings by Kelaart and the collections belonging to Alder and Hancock preserved in the Hancock Museum at Newcastle-on-Tyne. Proceedings of the Zoological Society of London 1906: 636–691. [pls. 42–47]

Eliot CNE (1908) Reports on the Marine Biology of the Sudanese Red Sea.–XI. Notes of a Collection of Nudibranchs from the Red Sea. Zoological Journal of the Linnean Society 31(204): 86–122. https://doi.org/10.1111/j.1096-3642.1908.tb00457.x

Eliot CNE (1913) Japanese nudibranchs. Journal of the College of Science. Imperial University Tokyo 35: 1–47.

Epstein HE, Hallas JM, Johnson RF, Lopez A, Gosliner TM (2019) Reading between the lines: Revealing cryptic species diversity and colour patterns in *Hypselodoris* nudibranchs (Mollusca: Heterobranchia: Chromodorididae). Zoological Journal of the Linnean Society 186(1): 116–189. https://doi.org/10.1093/zoolinnean/zly048

Er M (1955) Opisthobranchia from Brazil. Boletim da Faculdade de Filosofia. Ciências e Letras da Universidade de São Paulo (Zoologia) 20: 89–261. https://doi.org/10.11606/issn.2526-3382.bffclzoologia.1955.120213

Faulkner DJ, Ghiselin MT (1983) Chemical defense and evolutionary ecology of dorid nudibranchs and some other opisthobranch gastropods. Marine Ecology Progress Series 13: 295–301. https://doi.org/10.3354/meps013295

Fischer P (1880–1887) Manuel de Conchyliologie et de Paléontologie Conchyliologique, ou Histoire Naturelle des Mollusques Vivants et Fossiles Suivi d'un Appendice sur les Brachiopodes par D. P. Oehlert. Avec 23 Planches Contenant 600 Figures Dessinées par S. P. Woodward. Savy, Paris, xxiv + 1369 pp. [23 pls. Dates of publication: 1–112 [1880], 113–304 [1881]; 305–416 [1882]; 417–608 [1883]; 609–688 [1884]; 689–896 [1885]; 897–1008 [1886]; 1009–1369 [1887]]

Folmer O, Black M, Hoeh W, Lutz R, Vrijenhoek R (1994) DNA primers for amplification of mitochondrial cytochrome c oxidase subunit I from diverse metazoan invertebrates. Molecular Marine Biology and Biotechnology 3: 294–299.

Garovoy JB, Valdés A, Gosliner TM (2001) Phylogeny of the genus *Rostanga* (Nudibranchia), with descriptions of three new species from South Africa. The Journal of Molluscan Studies 67(2): 131–144. https://doi.org/10.1093/mollus/67.2.131

Gosliner TM, Valdés A, Behrens DW (2018) Nudibranch and Sea Slug Identification: Indo-Pacific (2nd Ed.). New World Publications, Jacksonville, Florida, 451 pp.

Gould AA (1852) Mollusca and shells. United States Exploring Expedition During the Years 1838, 1839, 1840, 1841, 1842 Under the Command of Charles Wilkes (Vol. 12). Gould and Lincoln, Boston, 510 pp. [Atlas [1856]: pls. 1–16]

Gray ME (1842–1850) Figures of Molluscous Animals, Selected from Various Authors. Etched for the Use of Students. Longman, Brown, Green, and Longmans, London. [Dates of publication: vol. 1, pls. 1–78 [1842], vol. 2, pls. 79–199 [1850]; vol. 3, pls. 200–312 [1850]; vol. 4, pp. 1–124 [1850]]

Hallas JM, Chichvarkhin A, Gosliner TM (2017) Aligning evidence: Concerns regarding multiple sequence alignments in estimating the phylogeny of the Nudibranchia suborder Doridina. Royal Society Open Science 4(10): e171095. https://doi.org/10.1098/rsos.171095

Hervé J-F (2010) Guide des Nudibranchs de Nouvelle-Calédonie et Autres Opisthobranches. Catherine Ledru, Nouméa, New Caledonia, 401 pp.

ICZN (1999) International Code of Zoological Nomenclature (4th edn.). International Trust for Zoological Nomenclature, London, 306 pp.

Iredale T, O'Donoghue CH (1923) List of British nudibranchiate Mollusca. Proceedings of the Malacological Society of London 15: 195–233. https://doi.org/10.1093/oxfordjournals.mollus.a063805

Johnson RF (2010) Breaking family ties: Taxon sampling and molecular phylogeny of chromodorid nudibranchs (Mollusca, Gastropoda). Zoologica Scripta 40(2): 137–157. https://doi.org/10.1111/j.1463-6409.2010.00457.x

Johnson RF, Gosliner TM (2012) Traditional taxonomic groupings mask evolutionary history: A molecular phylogeny and new classification of the chromodorid nudibranchs. PLoS ONE 7(4): e33479. https://doi.org/10.1371/journal.pone.0033479

Jörger KM, Schrödl M (2013) How to describe a cryptic species? Practical challenges of molecular taxonomy. Frontiers in Zoology 10(1): 1–27. https://doi.org/10.1186/1742-9994-10-59

Jörger KM, Norenburg JL, Wilson NG, Schrödl M (2012) Barcoding against a paradox? Combined molecular species delineations reveal multiple cryptic lineages in elusive meiofaunal sea slugs. BMC Evolutionary Biology 12(1): 1–18. https://doi.org/10.1186/1471-2148-12-245

Kearse M, Moir R, Wilson A, Stones-Havas S, Cheung M, Sturrock S, Buxton S, Cooper A, Markowitz S, Duran C, Thierer T, Ashton B, Meintjes P, Drummond A (2012) Geneious Basic: An integrated and extendable desktop software platform for the organization and analysis of sequence data. Bioinformatics 28(12): 1647–1649. https://doi.org/10.1093/bioinformatics/bts199

Kelaart EF (1858) New and little known species of Ceylon nudibranchiate molluscs, and zoophytes. Journal of the Ceylon Branch of the Royal Asiatic Society 3: 76–124.

Kimura M (1980) A simple method for estimating evolutionary rates of base substitutions through comparative studies of nucleotide sequences. Journal of Molecular Evolution 16(2): 111–120. https://doi.org/10.1007/BF01731581

Knutson VL, Gosliner TM (2022) The first phylogenetic and species delimitation study of the nudibranch genus *Gymnodoris* reveals high species diversity (Gastropoda: Nudibranchia). Molecular Phylogenetics and Evolution 171: e107470. https://doi.org/10.1016/j.ympev.2022.107470

Krug PJ, Vendetti JE, Valdés A (2016) Molecular and morphological systematics of *Elysia* Risso, 1818 (Heterobranchia: Sacoglossa) from the Caribbean region. Zootaxa 4148(1): 1–137. https://doi.org/10.11646/zootaxa.4148.1.1

Krug PJ, Wong NL, Medina MR, Gosliner TM, Valdés A (2018) Cryptic speciation yields remarkable mimics: A new genus of sea slugs that masquerade as toxic algae (*Caulerpa* spp.). Zoologica Scripta 47(6): 699–713. https://doi.org/10.1111/zsc.12310

Kumar S, Stecher G, Li M, Knyaz C, Tamura K (2018) MEGA X: Molecular evolutionary genetics analysis across computing platforms. Molecular Biology and Evolution 35(6): 1547–1549. https://doi.org/10.1093/molbev/msy096

Mahguib J, Valdés A (2015) Molecular investigation of the phylogenetic position of the polar nudibranch *Doridoxa* (Mollusca, Gastropoda, Heterobranchia). Polar Biology 38(9): 1369–1377. https://doi.org/10.1007/s00300-015-1700-5

Marcus Ev (1976) On *Kentrodoris* and *Jorunna* (Gastropoda, Opisthobranchia). Boletim de Zoologia. Universidade de São Paulo 1: 11–68. https://doi.org/10.11606/issn.2526-3358.bolzoo.1976.121551

Martín-Hervás MDR, Carmona L, Malaquias MAE, Krug PJ, Gosliner TM, Cervera JL (2021) A molecular phylogeny of *Thuridilla* Bergh, 1872 sea slugs (Gastropoda, Sacoglossa) reveals a case of flamboyant and cryptic radiation in the marine realm. Cladistics 37(6): 647–676. https://doi.org/10.1111/cla.12465

Miller MC (1989) *Trippa molesta*, a new dorid nudibranch (Gastropoda: Opisthobranchia) from New Zealand. New Zealand Journal of Zoology 16(2): 243–250. https://doi.org/10.1080/03014223.1989.10422574

Nakano R (2018) Field Guide to Sea Slugs and Nudibranchs of Japan. Bun-ichi Sogo, Shizuoka, Japan, 543 pp.

Neuhaus J, Rauch C, Bakken T, Picton B, Pola M, Malaquias MAE (2021) The genus *Jorunna* (Nudibranchia: Discodorididae) in Europe: A new species and a possible case of incipient speciation. Journal of Molluscan Studies 87: eyab028. https://doi.org/10.1093/mollus/eyab028

O'Donoghue CH (1927) Notes on a collection of nudibranchs from Laguna Beach, California. Journal of Entomology and Zoology of Pomona College 19: 77–119. [pls. 1–3]

Odhner NH (1939) Opisthobranchiate Mollusca from the western and northern coasts of Norway. Det Kongelige Norske Videnskabers Selskabs Skrifter 1: 1–93.

Ortea J, Moro L (2016) Nuevos datos sobre el género *Jorunna* Bergh, 1876 (Mollusca: Heterobranchia: Discodorididae) en la Macaronesia y el mar Caribe. Vieraea 44: 25–52.

Ortea J, Moro L, Bacallado JJ, Caballer M (2014) Nuevas especies y primeras citas de babosas marinas (Mollusca: Opisthobranchia) en las islas Canarias y en otros archipiélagos de la Macaronesia. Vieraea 42(Vieraea 42): 47–77. https://doi.org/10.31939/vieraea.2014.42.04

Palumbi SR (1996) Nucleic Acids II: The polymerase chain reaction. In: Hillis DM, Moritz C, Mable BK (Eds) Molecular Systematics. Sinauer, Sunderland, 205–247.

Payri CE, Allain V, Aucan J, David C, David V, Dutheil C, Loubersac L, Menkes C, Pelletier B, Pestana G, Samadi S (2019) New Caledonia. In: Sheppard C (Ed.) World Seas: An Environmental Evaluation (2nd edn.). Academic Press, London, 593–618. https://doi.org/10.1016/B978-0-08-100853-9.00035-X

Pola M, Camacho-Garcia YE, Gosliner TM (2012) Molecular data illuminate cryptic nudibranch species: The evolution of the Scyllaeidae (Nudibranchia: Dendronotina) with a revision of *Notobryon*. Zoological Journal of the Linnean Society 165(2): 311–336. https://doi.org/10.1111/j.1096-3642.2012.00816.x

Puillandre N, Lambert A, Brouillet S, Achaz G (2012) ABGD, Automatic Barcode Gap Discovery for primary species delimitation. Molecular Ecology 21(8): 1864–1877. https://doi.org/10.1111/j.1365-294X.2011.05239.x

Quoy J, Gaimard J (1832–1833) Zoologie. In: Dumont d'Urville JSC (Ed.) Voyage de Découvertes de "l'Astrolabe" Exécuté par Ordre du Roi, Pendant les Années 1826–1827–1828–1829, Sous le Commandement de M. J. Dumont d'Urville (Vol. 2 and Atlas). Tastu, Paris,

686 pp. [pls. 1–26. Dates of publication: pp. 1–320 [1832], pp. 321–686 [1833], pls. 1–26 [1833]]

Risbec J (1928) Contribution à l'étude des Nudibranches néo-calédoniens. Faune des Colonies Françaises 2: 1–328. [pls. 1–12]

Risbec J (1930) Nouvelle contribution à l'étude des nudibranches néo-calédoniens. Annales de l'Institut Océanographique 7: 263–298. [pl. 1]

Risbec J (1953) Mollusques nudibranches de la Nouvelle Calédonie. Faune de l'Union Française 15: 1–189.

Ronquist F, Teslenko M, van der Mark P, Ayres DL, Darling A, Höhna S, Larget B, Liu L, Suchard MA, Huelsenbeck JP (2012) MrBayes 3.2: Efficient Bayesian phylogenetic inference and model choice across a large model space. Systematic Biology 61(3): 539–542. https://doi.org/10.1093/sysbio/sys029

Rudman WB (1978) The dorid opisthobranch genera *Halgerda* Bergh and *Sclerodoris* Eliot from the Indo-West Pacific. Zoological Journal of the Linnean Society 62(1): 59–88. https://doi.org/10.1111/j.1096-3642.1978.tb00523.x

Rudman WB (2002) *Atagema spongiosa* (Kelaart, 1858). Sea Slug Forum. Australian Museum, Sydney. http://www.seaslugforum.net/find/tripspon

Rudman WB (2005) *Atagema carinata* (Quoy and Gaimard, 1832). Sea Slug Forum. Australian Museum, Sydney. http://www.seaslugforum.net/find/atagcari

Rudman WB, Avern GJ (1989) The genus *Rostanga* Bergh, 1879 (Nudibranchia: Doridiidae) in the Indo-West Pacific. Zoological Journal of the Linnean Society 96(3): 281–338. https://doi.org/10.1111/j.1096-3642.1989.tb01832.x

Silvestro D, Michalak I (2012) RaxmlGUI: A graphical front-end for RAxML. Organisms, Diversity & Evolution 12(4): 335–337. https://doi.org/10.1007/s13127-011-0056-0

Tibiriçá Y, Pola M, Cervera JL (2017) Astonishing diversity revealed: An annotated and illustrated inventory of Nudipleura (Gastropoda: Heterobranchia) from Mozambique. Zootaxa 4359(1): 1–133. https://doi.org/10.11646/zootaxa.4359.1.1

Tibiriçá Y, Strömvoll J, Cervera JL (2023) Can you find me? A new sponge-like nudibranch from the genus *Jorunna* Bergh, 1876 (Mollusca, Gastropoda, Discodorididae). Zoosystematics and Evolution 99(1): 63–75. https://doi.org/10.3897/zse.99.95222

Valdés A (2001) Deep-sea cryptobranch dorid nudibranchs (Mollusca, Opisthobranchia) from the tropical West Pacific, with descriptions of two new genera and eighteen new species. Malacologia 43: 237–311.

Valdés A (2002) A phylogenetic analysis and systematic revision of the cryptobranch dorids (Mollusca, Nudibranchia, Anthobranchia). Zoological Journal of the Linnean Society 136(4): 535–636. https://doi.org/10.1046/j.1096-3642.2002.00039.x

Valdés A, Gosliner TM (2001) Systematics and phylogeny of the caryophyllidia-bearing dorids (Mollusca, Nudibranchia), with the description of a new genus and four new species from Indo-Pacific deep waters. Zoological Journal of the Linnean Society 133(2): 103–198. https://doi.org/10.1111/j.1096-3642.2001.tb00689.x

Vayssière A (1912) Recherches zoologiques et anatomiques sur les Opisthobranches de la Mer Rouge et du Golfe d'Aden. Deuxième Partie. Annales de la Faculté des Sciences de l'Université de Marseille 20: 5–157.

Wells FE, Bryce CW (1993) Sea Slugs and their Relatives of Western Australia. Western Australian Museum, Perth, 184 pp.
Willan RC, Coleman N (1984) Nudibranchs of Australasia. Australasian Marine Photographic Index, Sydney, 56 pp.
Yonow N (2008) Sea Slugs of the Red Sea. Pensoft, Sofia, 303 pp.
Yonow N (2017) Results of the Rumphius Biohistorical Expedition to Ambon (1990). Part 16. The Nudibranchia–Dendronotina, Arminina, Aeolidina, and Doridina (Mollusca: Gastropoda: Heterobranchia). Archiv für Molluskenkunde 146(1): 135–172. https://doi.org/10.1127/arch.moll/146/135-172

Supplementary material 1

Individual analysis of COI gene fragments
Authors: Julie Innabi, Carla C. Stout, Ángel Valdés
Data type: figure (jpg file)
Explanation note: Posterior probabilities are shown above the branches and bootstrap values from the maximum-likelihood analysis values shown below branches.

Link: https://doi.org/10.3897/zookeys.1152.98258.suppl1

Supplementary material 2

Individual analysis of 16S gene fragments
Authors: Julie Innabi, Carla C. Stout, Ángel Valdés
Data type: figure (jpg file)
Explanation note: Posterior probabilities are shown above the branches and bootstrap values from the maximum-likelihood analysis values shown below branches.

Link: https://doi.org/10.3897/zookeys.1152.98258.suppl2

Supplementary material 3

Individual analysis of Histone H3 gene fragments

Authors: Julie Innabi, Carla C. Stout, Ángel Valdés

Data type: figure (jpg file)

Explanation note: Posterior probabilities are shown above the branches and bootstrap values from the maximum-likelihood analysis values shown below branches.

Link: https://doi.org/10.3897/zookeys.1152.98258.suppl3

ZooKeys 1152: 97–118 (2023)
doi: 10.3897/zookeys.1152.99161
https://zookeys.pensoft.net

RESEARCH ARTICLE

A peer-reviewed open-access journal
ZooKeys
Launched to accelerate biodiversity research

Systematics of *Lepidocyrtinus boneti* Denis, 1948 (Collembola, Seirinae) reveals a new position for the species within Seirinae

Nerivania Nunes Godeiro[1], Yun Bu[1], Areeruk Nilsai[2], Louis Deharveng[3], Nikolas Gioia Cipola[4]

1 *Shanghai Natural History Museum, Shanghai Science & Technology Museum, Shanghai 200041, China* **2** *Division of Biological Science, Faculty of Science, Prince of Songkla University, Hat Yai, Songkhla, 90110, Thailand* **3** *Institut de Systématique, Evolution, Biodiversité (ISYEB) – UMR 7205 CNRS, MNHN, UPMC, EPHE, Museum national d'Histoire naturelle, Sorbonne Universités, 45 rue Buffon, CP50, F-75005 Paris, France* **4** *Laboratório de Sistemática e Ecologia de Invertebrados do Solo, Instituto Nacional de Pesquisas da Amazônia—INPA, CPEN, Manaus, AM, Brazil*

Corresponding author: Nikolas Gioia Cipola (nikolasgc@gmail.com)

Academic editor: W. M. Weiner | Received 22 December 2022 | Accepted 14 February 2023 | Published 7 March 2023

https://zoobank.org/2C7256CF-B4C7-48D2-A6B0-CDA40C2F69F2

Citation: Godeiro NN, Bu Y, Nilsai A, Deharveng L, Cipola NG (2023) Systematics of *Lepidocyrtinus boneti* Denis, 1948 (Collembola, Seirinae) reveals a new position for the species within Seirinae. ZooKeys 1152: 97–118. https://doi.org/10.3897/zookeys.1152.99161

Abstract

Seira boneti Denis, 1948, **comb. nov.** is examined and redescribed based on syntypes and by a newly discovered Chinese population. Lectotype and paralectotypes were designated, and the type locality of the species has been fixed to Câuda, near Nhatrang, Vietnam. The species was first described in the genus *Lepidocyrtinus*, but based on morphological and molecular evidence it is here transferred to *Seira*. For the phylogenetic placement of *Seira boneti* **comb. nov.**, its mitogenome was included in a dataset comprising 19 species of Seirinae. Maximum Likelihood and Bayesian inferences clustered the species next to *Seira sanloemensis* Godeiro & Cipola, 2020 from Cambodia, forming a distinct *Seira* clade from the Old World, confirming the hypothesis of the existence of a different basal lineage of Seirinae in Southern Asia.

Keywords

Asian springtails, Entomobryidae, mitogenome, paraphyletic genus, phylogeny, review, taxonomy

Introduction

Understanding the patterns of species diversity is a major goal for most of the researchers studying evolutionary biology. With this aim, an extensive comparison of phenotypic attributes across taxa and well-corroborated phylogenies are necessary (Simon et al. 2019). Seirinae Yosii, 1961 (sensu Zhang and Deharveng 2015) is an Entomobryidae subfamily with currently ca. 230 species in three genera (Bellinger et al. 1996–2023). The first published molecular phylogeny regarding the Seirinae was based on three genes: two mitochondrial and one nuclear, and only three species of *Seira* Lubbock, 1870 and one of *Lepidocyrtinus* Börner, 1903 were sampled (Zhang et al. 2014). This study supported the Seirinae monophyly and a closer relationship of the subfamily with Lepidocyrtinae. Recently, these results were corroborated by a phylogeny based on morphological and barcode data (Zhang et al. 2019), as well as two studies with complete mitogenomes including 26 terminal taxa of the Entomobryidae (Godeiro et al. 2020a, 2021). Robust phylogenetic studies including the Seirinae are still scarce. Despite including representatives of the three current genera of Seirinae, these studies were focused only on species from the Neotropical region (Godeiro et al. 2020a, 2021), not sufficient to define infrageneric relationships. Only with the inclusion of species from several biogeographic regions we can have a clearer overview of the internal organization of the subfamily. In a study including data from an Asian Seirinae species in a phylogeny based only on mitogenomes from New World species, the Asian species appeared as a basal taxon to the entire New World group of Seirinae (Godeiro et al. 2020b).

The Asian continent has a great diversity of Seirinae species, whose species have been described during the last 80 years, but the morphological data originally described are mostly not sufficient for their comparison with other species (Denis 1948; Yosii 1959, 1961b; Yoshii and Suhardjono 1992; Bellinger et al. 1996–2023). Among the Asian taxa, *Lepidocyrtinus boneti* Denis, 1948 was described from Vietnam and Cambodia based on a few morphological characteristics such as the body color pattern, measurements of the body and appendices, bothriotricha pattern of the second to fourth abdominal segment, and morphology of the eyes and scales (Denis 1948). This species was never taxonomically revised, and it is only possible to know from the original description that it belongs to Seirinae due to the presence of heavily ciliated scales on body, the fourth abdominal segment with three bothriotricha, and the mucro falcate without a basal spine (Yoshii and Suhardjono 1992; Soto-Adames 2008; Cipola et al. 2018a, 2020; Zhang et al. 2019; Godeiro et al. 2020a). A systematic study is necessary to reveal its position among the current Seirinae genera, as well as to provide a revision of its diagnostic characters for future interspecific comparisons.

Here we present a systematic study of *Lepidocyrtinus boneti* Denis, 1948 based on the lectotype and paralectotypes designated from syntypes, the species redescription, and a new record from China. We also transfer the species to *Seira* after a phylogenetic study using 19 other mitogenomes of Seirinae.

Materials and methods

Taxa sampling, sequencing, and mitogenome assembly

The sequenced specimen belongs to the Chinese population of *S. boneti* comb. nov. and it was collected by NNG in October 2021 using an entomological aspirator. One specimen preserved in absolute alcohol was sent to Shanghai Yaoen Biotechnology Co., Ltd, China, where the DNA was extracted using TIANamp Micro-DNA extraction kit (Tiangen Co., Ltd, China). Libraries were constructed using KAPA Hyper Prep Kit (Roche) following custom procedures. Illumina NovaSeq platform was used to produce paired-end reads with 150 bp length. Approximately 10 Gb of data was delivered. NOVOPLASTY v. 3.8.3 (Dierckxsens et al. 2016) was used to assemble the mitogenome with kmer value = 33. MITOZ v. 2.4-alpha (Meng et al. 2019) was used to annotate and visualize the mitogenome. The final mitogenome sequence was submitted to the NCBI database, and the accession number is listed in Table 1.

To complete our dataset, following the relationship hypothesis of Seirinae + Lepidocyrtinae (Zhang et al. 2014, 2019; Godeiro et al. 2020a, 2021), we downloaded from NCBI the 13 mitochondrial protein coding genes (PCG's) sequences from 19 Seirinae species and seven Lepidocyrtinae to be used as outgroups. The detailed classification information and accession numbers of the 27 species analyzed in this study are listed in Table 1.

Table 1. Taxonomical information and GenBank accession numbers of the species used in the phylogenetic analyses. Newly sequenced in the present study in bold.

	Species	Country	Subfamily	GenBank number
1	*Acrocyrtus* sp.	Thailand	Lepidocyrtinae	MT914190
2	*Ascocyrtus cinctus* Schäffer, 1898	Indonesia	Lepidocyrtinae	OP094720
3	*Lepidocyrtus* sp.	Brazil	Lepidocyrtinae	MF716621
4	*Lepidocyrtus fimetarius* Gisin, 1964	China	Lepidocyrtinae	MK431900
5	*Lepidocyrtus nigrosetosus* Folsom, 1927	Brazil	Lepidocyrtinae	MW033192
6	*Lepidocyrtus sotoi* Bellini & Godeiro, 2015	Brazil	Lepidocyrtinae	MT928545
7	*Pseudosinella tumula* Wang, Chen & Christiansen, 2002	China	Lepidocyrtinae	MT611221
8	*Lepidocyrtinus dapeste* Santos & Bellini, 2018	Brazil	Seirinae	MF716609
9	*Lepidocyrtinus diamantinae* (Godeiro & Bellini, 2015)	Brazil	Seirinae	MF716594
10	*Lepidocyrtinus harenus* (Godeiro & Bellini, 2014)	Brazil	Seirinae	MF716617
11	*Lepidocyrtinus paraibensis* (Bellini & Zeppelini, 2009)	Brazil	Seirinae	MF716600
12	*Lepidocyrtinus* ca. *prodiga* (Arlé, 1959)	Brazil	Seirinae	MF716595
13	*Seira atrolutea* (Arlé, 1939)	Brazil	Seirinae	MF716602
14	***Seira boneti* comb. nov.**	**China**	**Seirinae**	**OP181099**
15	*Seira brasiliana* Arlé, 1939	Brazil	Seirinae	MF716619
16	*Seira paulae* Cipola & Bellini, 2014 (*in*: Cipola et al. 2014b)	Brazil	Seirinae	MF716601
17	*Seira coroatensis* Godeiro & Bellini, 2015	Brazil	Seirinae	MF716614
18	*Seira dowlingi* (Wray, 1953)	Brazil	Seirinae	MF716615
19	*Seira dowlingi*	China	Seirinae	MW419950
20	*Seira mendoncae* Bellini & Zeppelini, 2008	Brazil	Seirinae	MF716597
21	*Seira potiguara* Bellini, Fernandes & Zeppelini, 2010	Brazil	Seirinae	MF716613
22	*Seira ritae* Bellini & Zeppelini, 2011	Brazil	Seirinae	MF716605
23	*Seira sanloemensis* Godeiro & Cipola, 2020	Cambodia	Seirinae	MT997754
24	*Seira tinguira* Cipola & Bellini, 2014 (*in*: Cipola et al. 2014b)	Brazil	Seirinae	MF716620
25	*Tyrannoseira bicolorcornuta* (Bellini, Pais & Zeppelini, 2009)	Brazil	Seirinae	MF716599
26	*Tyrannoseira gladiata* Zeppelini & Lima, 2012	Brazil	Seirinae	MT914185
27	*Tyrannoseira raptora* (Zeppelini & Bellini, 2006)	Brazil	Seirinae	MF716610

Phylogenetic inference

Protein coding genes (PCG's) sequences from the 27 species were translated into amino acids using TRANSDECODER v. 5.5.0 (Haas et al. 2013) and aligned separately with MAFFT (Katoh and Standley 2013), "linsi" strategy. BMGE v. 1.12 (Criscuolo and Gribaldo 2010) performed the trimming with default strategy. PHYKIT v. 1.9.0 (Steenwyk et al. 2021) was used to generate the matrices and partition schemes. Maximum Likelihood (ML) analyses were performed with IQTREE v. 2.0.7 (Minh et al. 2020), ultrafast bootstrap 1000 replicates (Hoang et al. 2018) and SH-aLRT support. Bayesian inference was performed using PHYLOBAYES-MPI v1.8 (Lartillot et al. 2013), default model CAT+GTR with four rate categories, discretized gamma distribution of rates across sites. Phylogenetic trees were visualized in FIGTREE v. 1.3.1 (Rambaut 2010).

Morphological analysis

The type material of *Lepidocyrtinus boneti* deposited at the Muséum National d'Histoire Naturelle, France, and specimens recently collected from China (Hainan island) were analyzed. Under a stereomicroscope Teelen XTL- 207, Chinese specimens were bleached and diaphanized, first in 5% KOH and after in 10% lactophenol for 3 min/each. Hoyer's liquid was used to mount the specimens between a slide and a glass coverslip (Christiansen and Bellinger 1980, 1998). Mounted specimens were examined using a Leica DM2500 microscope. Illustrations were made with the help of an attached drawing tube and based on photographs taken with DMC4500 camera and LEICA APPLICATION SUITE v. 4.9. Specimens in ethanol gel were photographed using a Leica stereomicroscope S8AP0 attached to a Leica DMC4500 digital sight camera. Maps of species localities were made after Shorthouse (2010). The examined material is deposited at the collections of the Shanghai Natural History Museum (**SNHM**), Shanghai, China; Invertebrate collection of the Instituto Nacional de Pesquisas da Amazônia (**INPA**); and Muséum National d'Histoire Naturelle (**MNHN**), Paris, France.

The terminology used in descriptions follows: clypeal chaetotaxy after Yoshii and Suhardjono (1992); labral chaetotaxy after Cipola et al. (2014a); labial papillae, maxillary palp and basolateral and basomedian labial fields after Fjellberg (1999), but using the Gisin's system (1964) for naming the chaetae rows; postlabial chaetotaxy after Chen and Christiansen (1993) and Cipola et al. (2018a); subcoxae outer chaetotaxy after Yosii (1959); trochanteral organ after Christiansen (1958b) and South (1961); unguiculus lamellae after Hüther (1986); male genital plate after Christiansen (1958a); and manubrial ventral formula after Christiansen and Bellinger (2000). The head dorsal chaetotaxy was described based on Mari-Mutt (1979) and that of the body based on Szeptycki (1979), both with additions of Soto-Adames (2008), Cipola et al. (2018a), and Zhang et al. (2019); and specialized chaetae (S-chaetae) after Zhang and Deharveng (2015). Symbols used to depict the chaetotaxy are presented in Fig. 3. Chaetotaxy data are all given by one side of body only, except for the head plate.

Abbreviations used in the description

Abd abdominal segment(s);
ae antero-external lamella;
ai antero-internal lamella;
Ant antennal segment(s);
a.t. unpaired apical tooth;
b.c. basal chaeta of maxillary palp;
b.t. paired basal teeth;
f frontal chaetae of clypeus;
l lateral chaetae of clypeus;
l.p. lateral process of papilla E;
mac macrochaeta(e);
m.t. unpaired median tooth;
ms specialized microchaeta(e);
pf prefrontal chaetae of clypeus;
psp pseudopore(s);
pe postero-external lamella;
pi postero-internal lamella;
sens specialised ordinary chaeta(e);
t.a. terminal appendage of maxillary palp;
Th. thoracic segment(s).

Results

Mitogenome features and phylogenetic placement

The assembled mitogenome of *Seira boneti* comb. nov. is a circular molecule of 14,605 bp (Fig. 1). All 13 protein coding genes, 22 tRNA, and two rRNA were successfully recovered. The most frequent gene order observed in springtails, the same as the Pancrustacea gene order, was observed in the mitogenome of *S. boneti* comb. nov. The genome base composition was as follows: A (38%, 5587), T (35%, 4939), G (10%, 1512), C (17%, 2567).

The final matrix containing the 13 PCG's concatenated of the 27 species had a length of 3,391 amino acid sites. Maximum likelihood and Bayesian inference analyses placed *Seira boneti* comb. nov. in the same branch as *Seira sanloemensis* from Cambodia with moderate support values (86.4/84/1 - SH-aLRT support, bootstrap, and posterior probability, respectively). Also, the monophyly of Seirinae was recovered with high support values (100/100/1) (Fig. 2). Regarding the Neotropical species, the phylogeny remained the same as previous results (Godeiro et al. 2020a, b, 2021; Godeiro and Zhang 2021). This result corroborates our previous finding that the Asian population is likely to belong to a different lineage of Seirinae.

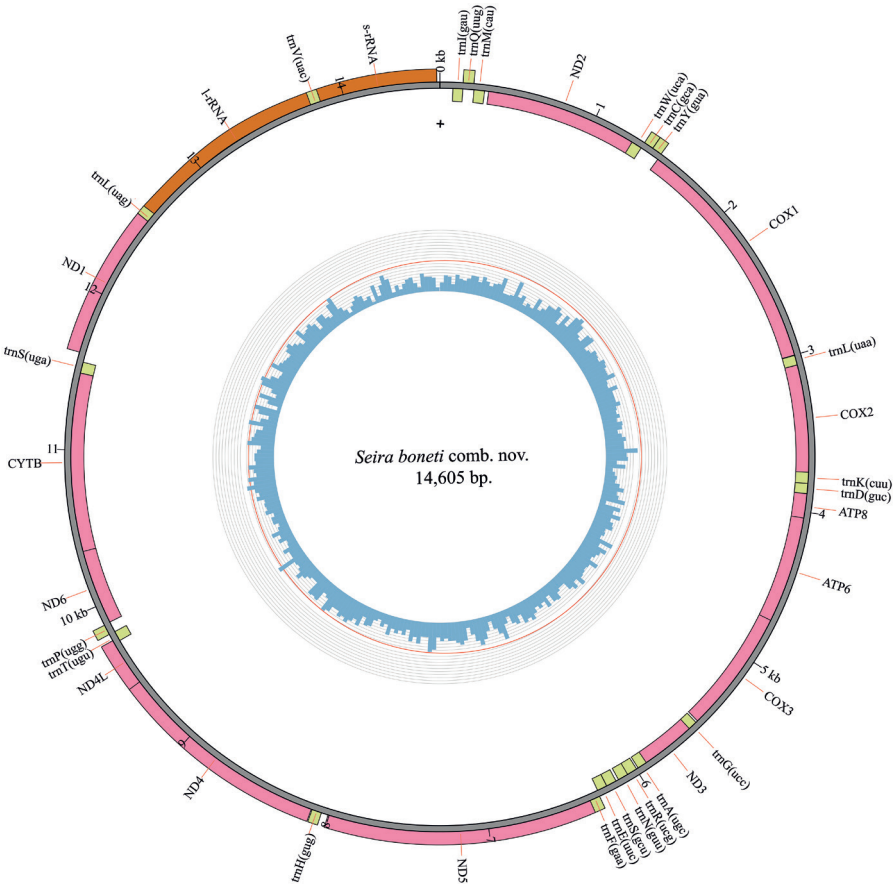

Figure 1. Circular representation of the mitogenome of *Seira boneti* comb. nov. The innermost circle shows the GC content and the outermost circle shows the gene features, rRNAs (orange), tRNAs (green), and PCGs (pink), (+) indicates the side of the major J-strand.

Taxonomy

Class Collembola Lubbock, 1873
Order Entomobryomorpha Börner, 1913
Family Entomobryidae Tömösváry, 1882
Subfamily Seirinae Yosii, 1961 (in 1961b) sensu Zhang et al., 2019
Genus *Seira* Lubbock, 1870

***Seira boneti* (Denis, 1948), comb. nov.**
Figs 3–9

Lepidocyrtinus boneti Denis, 1948: 261, fig. 26, Vietnam and Cambodia.

Typological note. *Seira boneti* comb. nov. was described based on 18 specimens from five localities of Vietnam and Cambodia (Figs 4, 5), which are deposited in

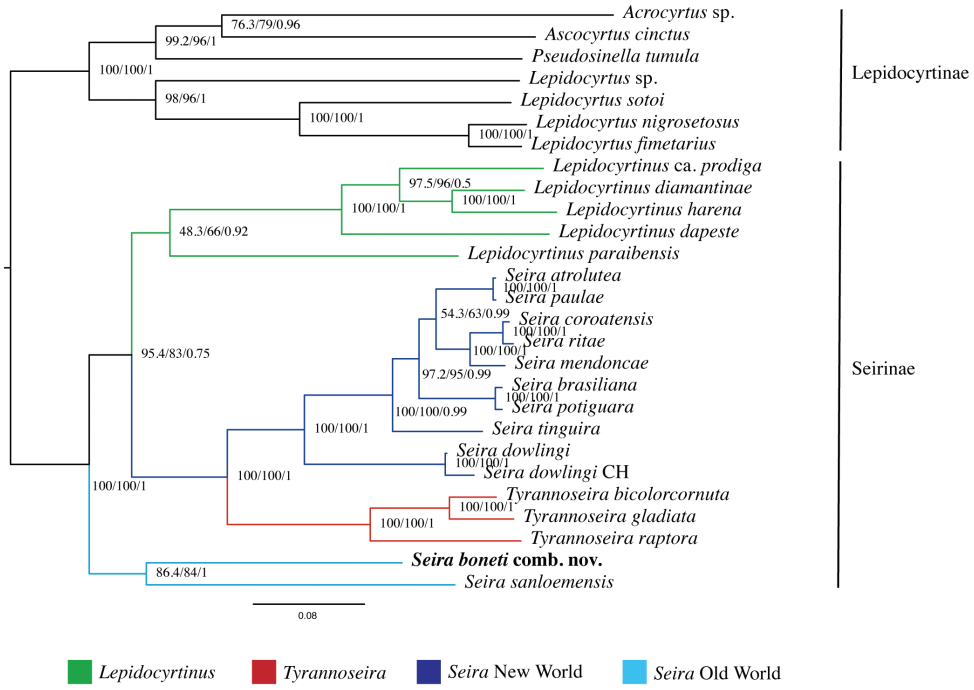

Figure 2. Phylogenetic placement of *Seira boneti* comb. nov. (in bold) based on Bayesian Inference and Maximum Likelihood analyses. Numbers in the nodes represent the SH-aLRT support, bootstrap values (both for Maximum Likelihood), and the posterior probability (Bayesian Inference support), respectively.

the MNHN, Paris. The description of *S. boneti* comb. nov. was based on a series of 13 syntypes (ICZN 2000, chapter 16, Article 73.2), without a designated holotype. Hence, we designate a lectotype, as well as paralectotypes for the other specimens from the same locality, Câuda [Cầu Đá, Nha Trang], Vietnam (ICZN 2000, chapter 16, Articles 73.2.2 and 74). From now, this becomes the type locality of *S. boneti* comb. nov. (ICZN 2000, chapter 16, Articles 73.2.3 and 76.2).

Type material. ***Lectotype*** (sex unclear, not possible to see) designated on slide (MNHN): Vietnam, Câuda [Cầu Đá, Nha Trang], viii–i (Figs 4A, 5). ***Paralectotypes*** designated on slides (MNHN): three specimens with the same data as the lectotype, two specimens collected ix.1929, one collected xii.1929, four collected x.1930, one collected x.1933, and one collected x-xi.1933 (Fig. 4B–G).

Other examined material. One specimen in slide (MNHN): Vietnam, Pic Lang Biang [Lang Biang Peak, Dalat], 2,100 m., 1.ii.1931. One specimen on slide (MNHN): Vietnam, Cua-Be [Cầa Bé, Nha Trang], x.1930. Two specimens pn slides (MNHN): Cambodia, Réam [Ream]. One specimen in slide (MNHN): Cambodia, Kampot (Figs 4H–L, 5). One male and four females on slides (SAN4 1–5): China, Hainan Island, Sanya Beach, Dadonghai forest in litter samples collected near ancient tombs, 18°13'06.8"N, 109°30'14.6"E (Fig. 5), rain forest, 20 meters of altitude, entomological aspirator, 05.x.2021, NN Godeiro leg.

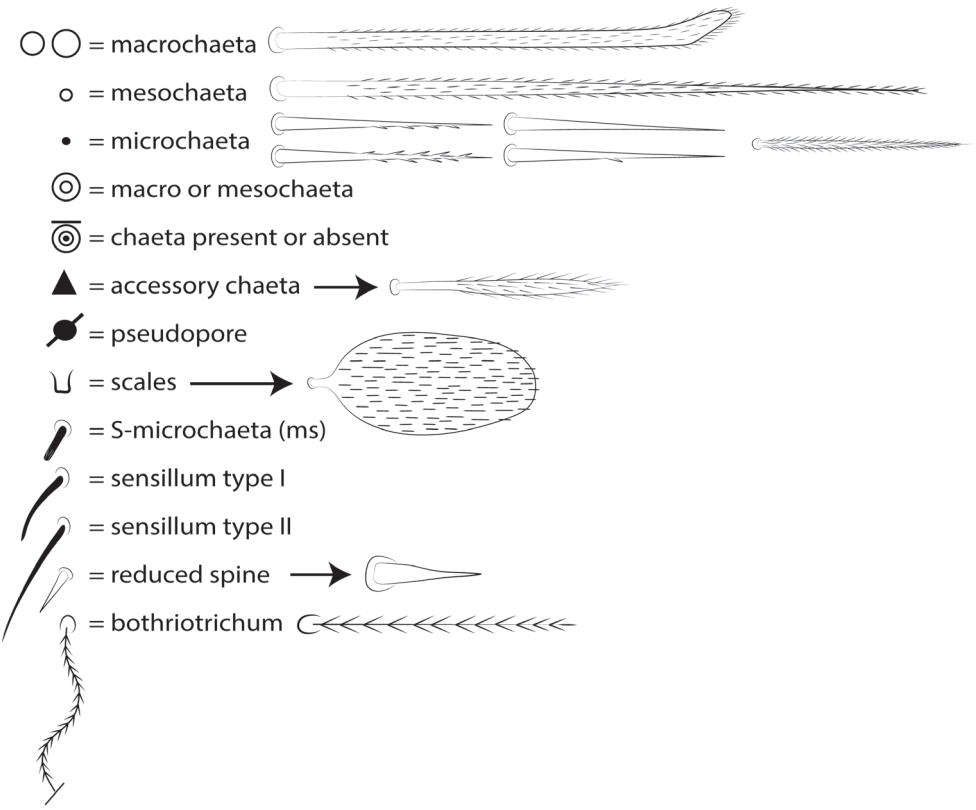

Figure 3. Symbols used in the chaetotaxy redescription of *Seira boneti* comb. nov.

Diagnosis. Body with dark lateral spots on Th III–Abd I (rarely absent) and 1+1 smaller one on Abd IV posteriorly. Ant IV not annulated with an apical bulb bilobed; labral papillae conical, outer slightly smaller; labial papilla E l.p. apically thinner and exceeding the apex of the papilla; head macrochaetotaxy with 8 'An', 4 'A', 3 'M', 8 'S', 5 'Pa', 2 'Pm', 4 'Pp' and 2 'Pe' mac; Th II with 11–12 anterior, 9 median and 17 posterior mac (p5 mac absent); Th III–Abd III with 14, 6–7, 4 and 1 inner mac, respectively; Abd IV with 12 or 13 inner and 19–23 lateral mac; trochanteral organ with about 16–18 spine-like chaetae; unguis a.t. present and unguiculus pe lamella serrated; collophore anteriorly with 2 distal mac, posteriorly with 3 spines on each side, lateral flap with 4 smooth and 9 ciliated chaetae; manubrium ventrally with 4 subapical chaetae, outer chaeta smaller than the inner chaeta; manubrial plate with 4 chaetae.

Note. On the basis of color pattern and morphological information extracted from the lectotype and type material (despite the poor state of conservation), we consider that both populations are conspecific.

Redescription. ***Body.*** Total length (head + trunk) of specimens 2.28–2.51 mm ($n = 2$ paralectotypes), lectotype 1.68 mm. Specimens whitish with brownish pigment on Ant I–IV; dark blue pigment forming a spot on Th III–Abd I laterally (rarely

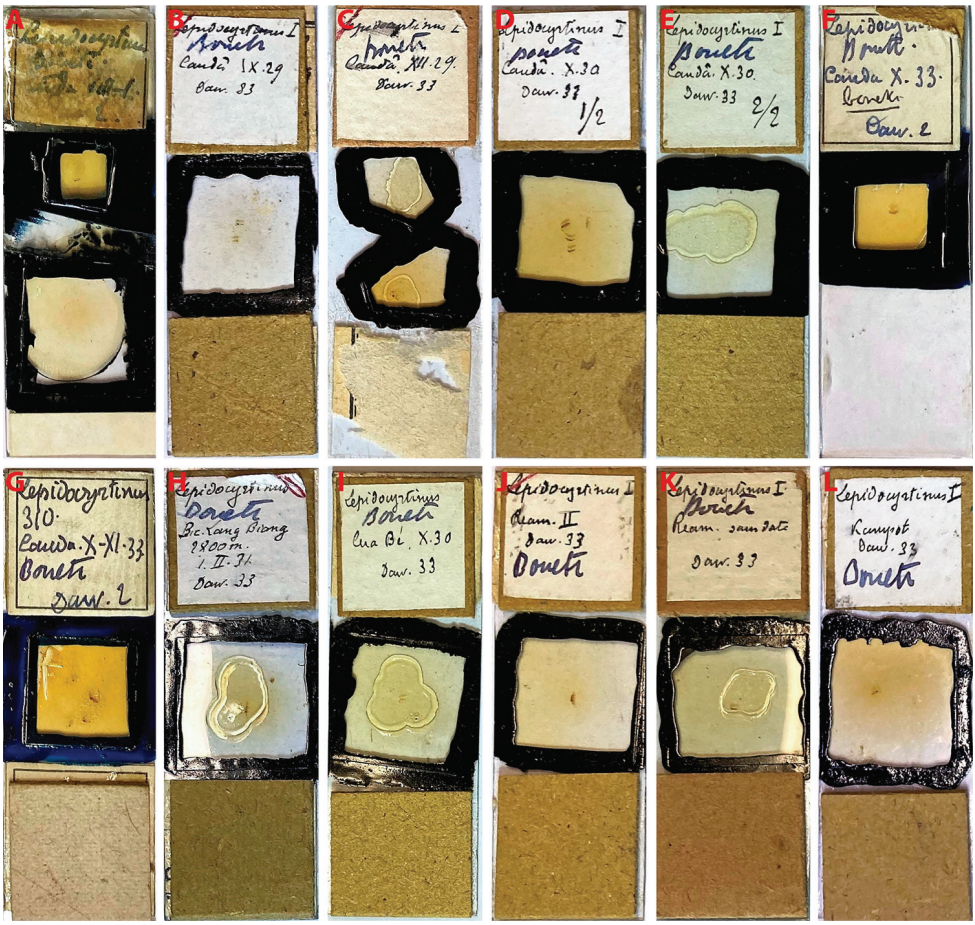

Figure 4. Syntypes slides of *S. boneti* comb. nov. deposited in MNHN (Paris, France) **A–H** specimens from the type locality herein designated, Câuda [Cầu Đá, Nha Trang], Vietnam **A** lectotype designed **B–H** paralectotypes herein designated **I** specimens from Pic Lang Biang [Lang Biang Peak, Dalat], Vietnam **J** specimen from Cua-Be [Cầa Bé, Nha Trang], Vietnam **K** specimens from Réam [Ream], Cambodia **L** specimen from Kampot, Cambodia.

absent) and a smaller spot postero-laterally on Abd IV, coxae I, and femur III distally pigmented in dark-blue; eyepatches black (Fig. 6). Scales heavily ciliated, oval or elongated and apically rounded (rarely truncate, pointed or irregular) present on Ant I to proximal 1/4 of Ant III, dorsal and ventral head, thorax, and abdomen, legs (except empodia), collophore anteriorly, both sides of the manubrium and dens ventrally; mac heavily ciliated apically, slightly foot shaped, rounded or acuminate; smooth microchaetae apically ramified or simple (Fig. 3).

Head. Antennae shorter than the trunk (Fig. 6); ratio antennae: trunk = 1: 1.46–1.68 (n=3), lectotype 1: 1.46; antennal segments ratio as I: II: III: IV = 1: 1.24–1.55: 1.33–1.75: 2.20–3.11, lectotype 1: 1.55: 1.55: 2.75. Ant IV not annulated, with an

Figure 5. Records map of *S. boneti* comb. nov. in Southeast Asia; star represents the type locality herein designated, Cầu Đá (Vietnam); circles in Cambodia and Vietnam are additional localities reported in the original description (Denis, 1948), and circle in Hainan Island is a new record for China.

apical bulb bilobed. Ant III distally with 2 finger-shaped sens (apical organ), some sens of different sizes and ciliated chaetae (Fig. 7A). Ant I dorsally with 1 outer mac, 2 median sens, and 3 proximal sens-like smooth chaetae. Clypeal formula with 4 (l1–2), 6 (f), 3 (pf0–1) ciliated chaetae, l1–2 larger than the others and apically acuminate, two f smaller, others subequal (Fig. 7B). Four prelabral ciliated chaetae; labral formula with 4 (a1–2), 5 (m0–2), 5 (p0–2) smooth chaetae; a1 regular (not thick), p0–1 larger than others. Four labral papillae conical, outer papillae slightly smaller than the inner papillae (Fig. 7C). Labial palp with five main papillae (A–E) plus one hypostomal papilla (H) with 0, 5, 0, 4, 4, 2 guard appendages, respectively; labial papilla E with l.p. apically thinner and exceeding the apex of the papilla (Fig. 7D). Eyes 8+8, A and B larger than the others, G and H smaller, with 5 interocular chaetae (q, s, p, r, t); head dorsal chaetotaxy (Fig. 7E) with 8 'An' (An1a–1, An2–3), 4 'A' (A0, A2–3, A5), 3 'M' (M1–2, M4), 6 'S' (S0–7), 5 'Pa' (Pa1–5), 2 'Pm' (Pm1, Pm3), 4 'Pp' (Pp1–4, Pp5) and 2 'Pe' (Pe3–3p) mac; 2 pairs of bothriotricha (1 subantennal and 1 post-ocellar) present. Basolateral and basomedian labial fields with chaetae a1–5 smooth (a2 largest), M1–2, E, L1–2 ciliated, r in a small smooth spine; labium with 5 subequal smooth chaetae (Fig. 7F). Maxillary palp with t.a. smooth and b.c. rough, thicker and 1.15 larger than the t.a.; sublobal plate internally with 3 smooth main appendages (1 proximal slightly thinner and shorter) plus a minute smooth appendage distally. Ventral chaetotaxy with 15 ciliated chaetae; postlabial chaetotaxy with 4 (G1–4), 3 (H2–4), 4 (J1–4) chaetae, b.c. and J2 thin, acuminate and elongated (J2 smaller that b.c.), others subequal (Fig. 7F).

Thorax chaetotaxy (Fig. 8A). Th II 'a', 'm' and 'p' series with 11–12 (group a5, excluding the anterior collar), 9 (m1–1ip, m2–2i2, m4i–4p) and 17 (p1ip2–p1p3, p2a–2p, p2e–2ep, p3p–3i2) mac, respectively. Th III 'a', 'm' and 'p' series with 5 (a1–5), 2 (m1i, m6) and 8 (p1i–1p, p2a–2ea, p3) mac, respectively. Th II–Abd V with ms and

Figure 6. *Seira boneti* comb. nov.: habitus of specimen fixed in alcohol from Hainan Island, China (lateral view). Scale bar: 0.5 mm.

sens formula 1, 0| 1, 0, 1, 0, 0 and 1, 1| 0, 2, 2, 8, 3, respectively (Fig. 8). Ratio Th II: III = 1.67–1.45: 1 (*n* = 3), lectotype 1.67: 1.

Abdomen chaetotaxy (Fig. 8B, C). Abd I 'a', 'm' and 'p' series with 1–2 (a2–3), 5 (m2i–2, m3, m4–4i) and 0 mac, respectively. Abd II 'a', 'm' and 'p' series with 1 (a2), 4 (m2–3e, m5), 0 mac, respectively; a5 and m2 as bothriotricha with 7 and 5 accessory chaetae, respectively. Abd III 'a', 'm' and 'p' series with 0, 3 (m3, am6, pm6) and 1 (p6) mac, respectively; m2 bothriotrichum with 3 accessory chaetae (a1–2 and 1 unnamed), and bothriotricha a5 and m5 with 11 accessory chaetae between them. Abd IV with 12 or 13 inner mac on A–T series (A3–3p, A5a–6, Ae6–7, B3–6, si, sm) and 19–23 lateral mac on D–Fe series (De3, E2–4p2, Ee7, Ee10, Ee12, F1–3p, one of unknown homology, Fe1a?–5); at least 8 sens (ps type I, others type II) and 10 posterior mesochaetae. Abd V 'a', 'm' and 'p' series with 2 (a5–6), 3 (m2–3, m5) and 4 (p1, p3–5) mac, respectively. Ratio Abd III: IV = 1: 3.33–4.10 (n=3), lectotype 1: 4.10. Abd II–IV bothriotrichal formula 2 (a5, m2), 3 (a5, m2, m5), 3 (T2, T4, D3) (Fig. 8B, C).

Legs. Subcoxa I with one row of 3 chaetae and 2 psp; subcoxa II with an 'a' row of 8 chaetae, 'p' row of 4 chaetae and 3 psp; subcoxa III with one row of 8–10 chaetae, 1 anterior chaeta and 2 posterior psp (Fig. 9A–C). Trochanteral organ with 16–18 spine-like chaetae, at least 2 anterior, 4 posterior, 5 internal, 1 apical and 4 distal arms (Fig. 9D). Anterior side of femurs II and III with 1 small proximal spine-like chaeta. Tibiotarsus outer

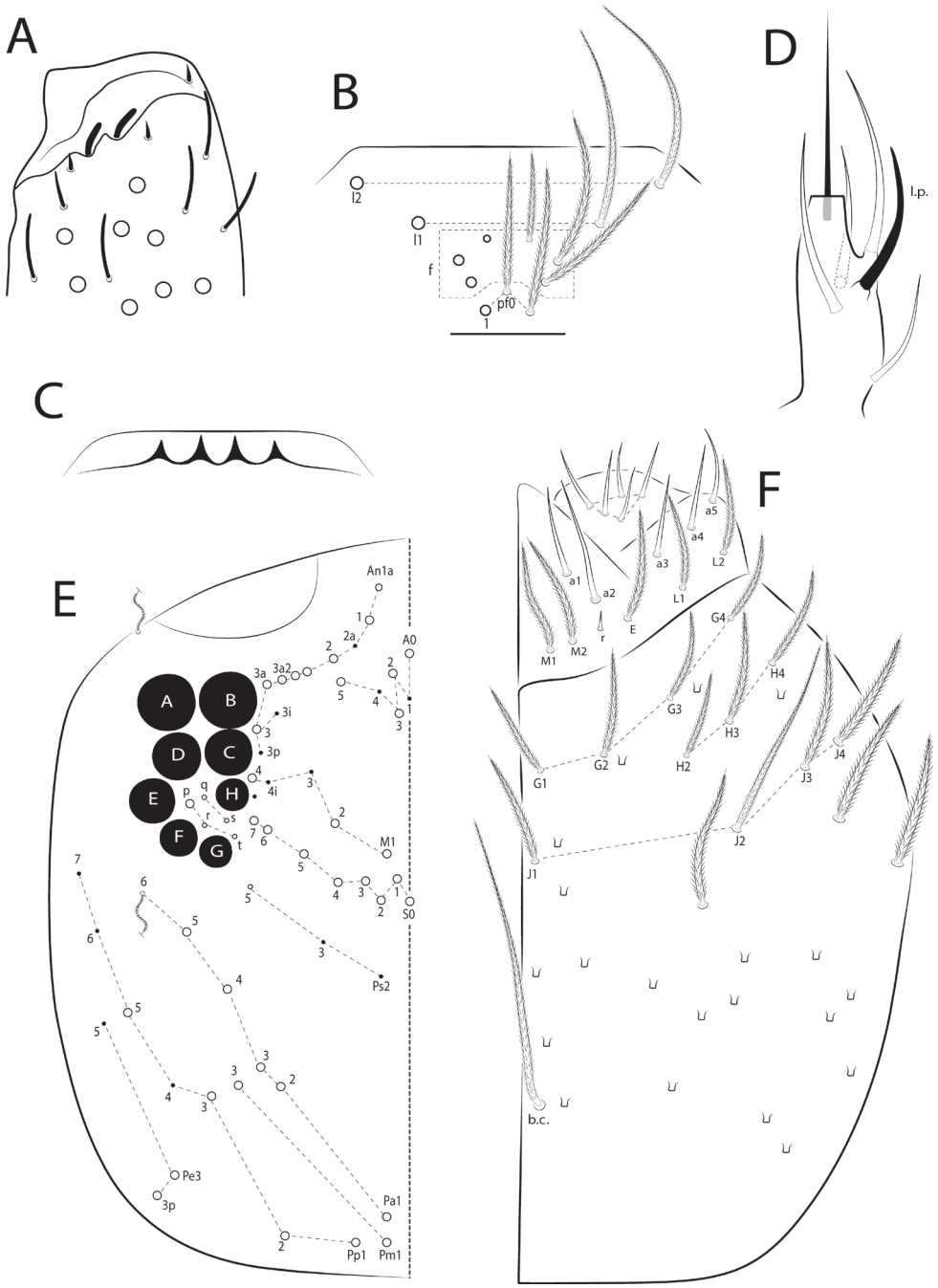

Figure 7. *Seira boneti* comb. nov.: head **A** Ant III distal chaetotaxy (lateral view) **B** clypeal chaetotaxy **C** labral papillae **D** labial papilla E (right side) **E** head dorsal chaetotaxy (left side) **F** labial proximal chaetae, basomedian and basolateral labial fields, and complete postlabial chaetotaxy (right side).

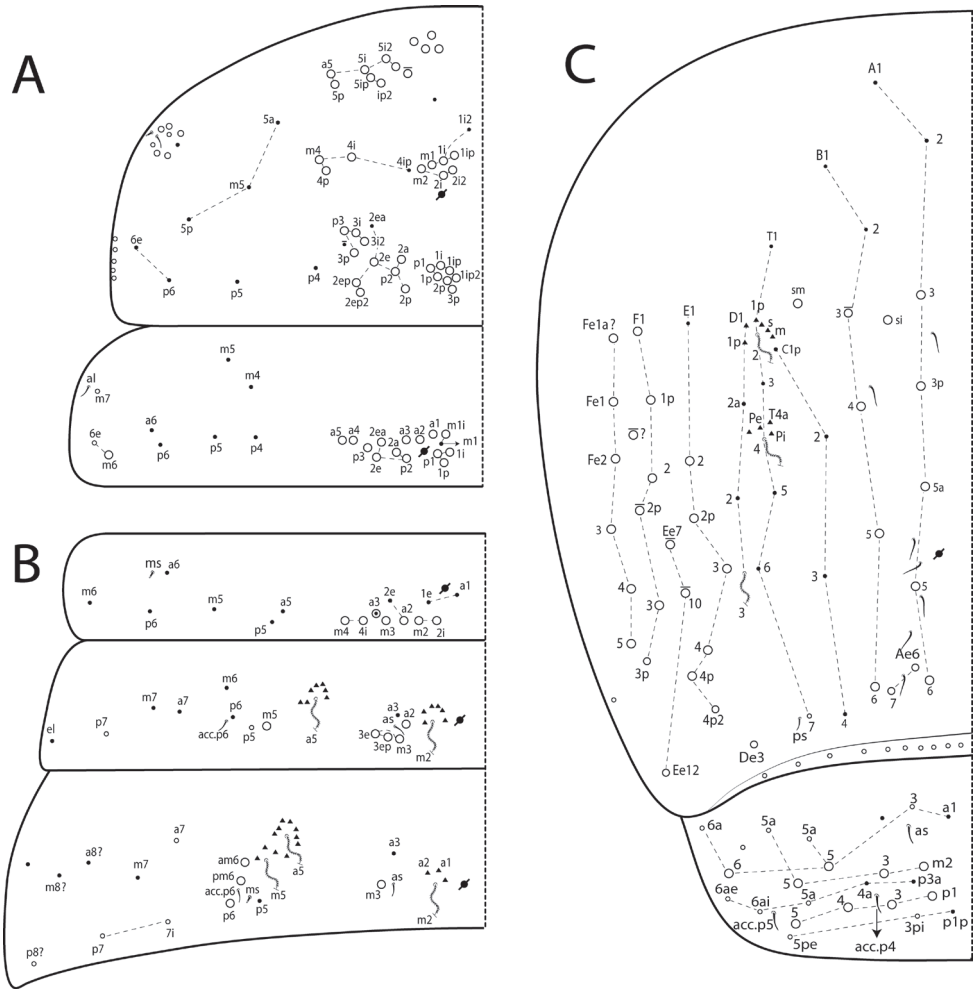

Figure 8. *Seira boneti* comb. nov.: dorsal chaetotaxy (left side) **A** Th II–III **B** Abd I–III **C** Abd IV–V.

side distally with 1 tenent hair ciliated, apically capitate, and subequal to unguis outer length; inner side of tibiotarsus III with 1 smooth chaeta slightly longer than the unguiculus. Pretarsus with 1 minute anterior and 1minute posterior smooth chaetae (Fig. 9E). Unguis outer side with a pair of lateral teeth and 1 unpaired median tooth; inner side with 4 teeth, b.t. on proximal half, m.t. on distal one fourth and slightly longer than b.t., a.t. on distal one eighth and subequal to b.t. Unguiculus with all lamellae acuminate and smooth (ai, ae, pi, pe), except pe serrate and with a minute tooth on distal half (Fig. 9E).

Collophore (Fig. 9F). Anterior side with ~ 10–13 chaetae, 3 proximal smooth spine-like chaetae, 3 median ciliated mac thin and apically acuminate, 1 thin and 1–4 regular ciliated chaetae, and distally 2 ciliated mac; posterior side with 3 subapical spines and 1 apical ciliated chaeta; lateral flap with about 13–14 chaetae, 4 smooth (2 larger than the others) and 9 ciliate.

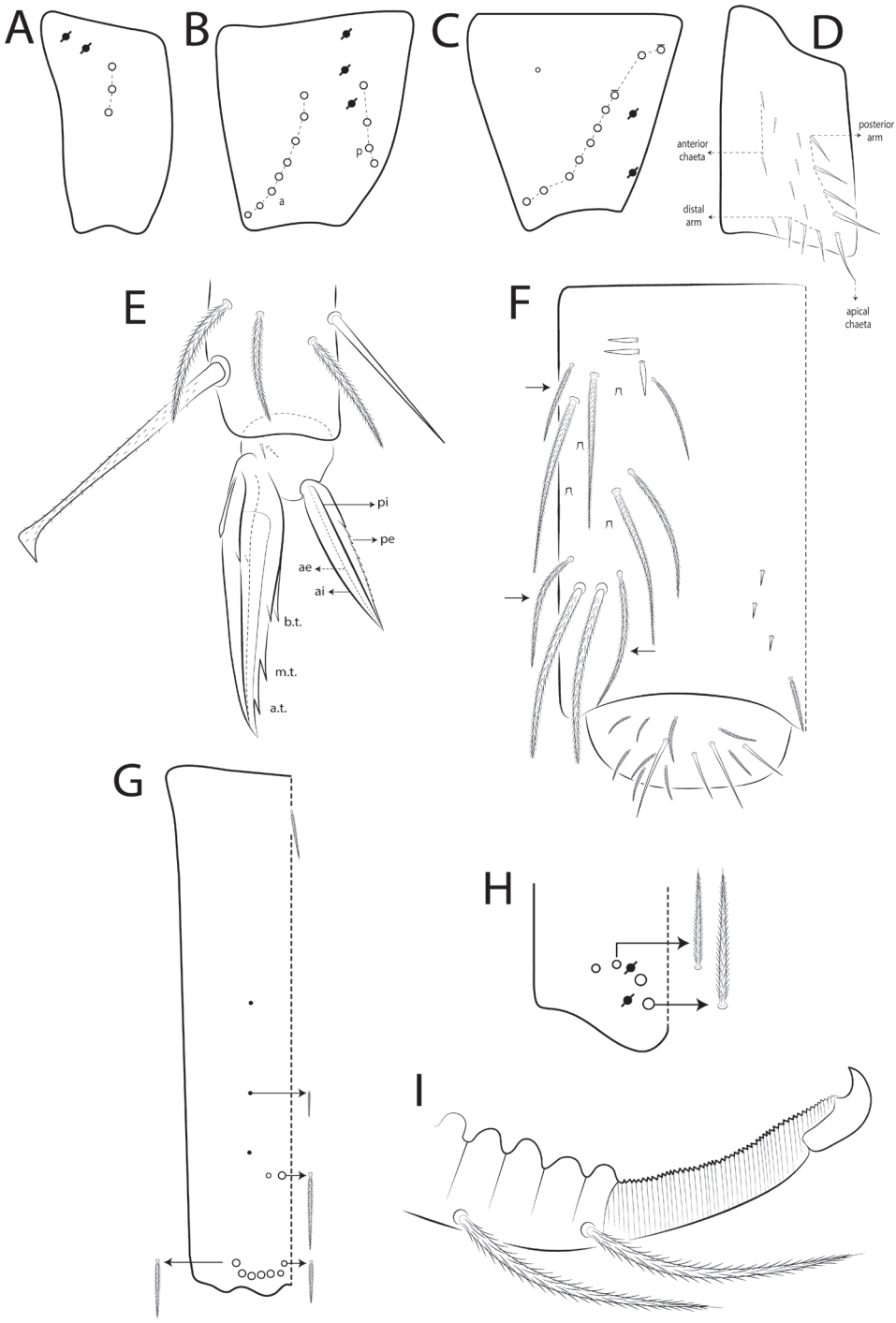

Figure 9. *Seira boneti* comb. nov.: trunk appendages **A–C** chaetotaxy of subcoxa I–III, respectively (outer side) **D** trochanteral organ (posterior side) **E** distal tibiotarsus and empodial complex III (posterior view) **F** collophore (lateral view), arrows in the anterior side indicate chaetae present or absent **G** manubrium ventral chaetotaxy **H** manubrial plate (dorsal view) **I** distal dens and mucro (outer view).

Furcula. Manubrium ventral chaetotaxy with 1, 2, 2, 2/4 (subapical), 14 (apical) ciliated chaetae, outer subapical chaetae smaller than the inner chaetae (Fig. 9G). Manubrial plate with 2 psp and 4 ciliated chaetae, the 2 inner chaetae larger than the lateral ones (Fig. 9H). Mucro falcate (only the distal tooth apparent) and without basal spine; proximal tooth reduced and enveloped by the dens cuticle (Fig. 9I).

Remarks. The present study increased substantially the morphological detailing of *Seira boneti* comb. nov. compared to the original description. Considering that most species of *Seira* from Asia are also poorly described (Denis 1948; Yoshii and Suhardjono 1992; Nguyen 2001; Cipola et al. 2018a), we compared *S. boneti* comb. nov. with other Asian species with 7 mac on Abd I (*S. cinerea* Yosii, 1966, *S. nidarensis* Baquero & Jordana, 2014, *S. simbalwaraii* Baquero & Jordana, 2015 from India, and *S. urbana* Nguyen, 2001 from Vietnam) or 6 mac (*S. hazrai* Baquero & Jordana, 2014 and *S. prabhooi* Baquero & Jordana, 2015 from India) (Table 2). These species also resemble each other in dense head macrochaetotaxy (except for *S. cinerea* and *S. urbana*, which their head chaetotaxy are unknown), although *S. nidarensis* and *S. hazrai* differ from the others by the presence of Ps2 mac. They also resemble each other in Th II by PmA–B groups respectively with 6 or 7 and 3 mac (but differ from each other in PmC group), Th III with 13–14 inner mac apparently with the same homology (a1–5, m1i, p1i–1p, p2a–p2ea, p3), and Abd II–III respectively with 4 (a2, m3–3e, 3ep) and 1 (m3) inner mac, although this last segment was not described in *S. cinerea*. *Seira boneti* comb. nov. is more similar to *S. urbana* in body color pattern with a lateral spot on Th II–Abd II and another on And IV posteriorly, Th II anteriorly with some extra mac, and prelabral and labral chaetotaxy (see Nguyen 2001). Due to the similarities between these two species which coexist in the same region (Indochina), there is a risk they are synonyms. For this reason, we tried to consult the type material of *S. urbana* deposited at Vietnam Academy of Science and Technology, Vietnam, but the loan was not provided by the responsible (Dr. Anh T. T. Nguyen). Although the material was not obtained for a more rigorous comparison, based on the literature *S. boneti* comb. nov. differs from *S. urbana* in Th II anteriorly with 11–12 mac (8 in *S. urbana*), Abd IV with 12–13 inner mac (11 in *S. urbana*), unguiculus pe lamella serrated (apparently smooth in *S. urbana*), and collophore anteriorly with 3 proximal spine-like chaetae (4 in *S. urbana*).

Discussion

Whereas the Asian continent currently has almost 25% (~ 50 spp.) of the known richness of Seirinae (Bellinger et al. 1996–2023), the moderate support values clustering *S. boneti* comb. nov. and *S. sanloemensis* are possibly related to the absence of other Asian taxa in the present phylogenetic analysis, mainly species morphologically similar to them, such as the six compared above with *S. boneti* comb. nov. (Yosii 1966; Nguyen 2001; Baquero et al. 2014, 2015). This makes sense considering that phylogenetically related the Neotropical *Seira* species (e.g. *S. atrolutea* Arlé, 1939, *S. paulae* Cipola & Bellini, 2014 (*in*: Cipola et al. 2014b), *S. coroatensis* Godeiro & Bellini,

Table 2. Comparison between *Seira* species from Asia with 6–7 and 4 central macrochaetae on Abd I–II, respectively.

		Species						
		***S. boneti* comb. nov.**	***S. cinerea***	***S. nidarensis***	***S. simbalwaraii***	***S. urbana***	***S. hazrai***	***S. prabhooi***
	References:	(1–2)	(3)	(4)	(5)	(6)	(4)	(5)
	Type locality:	Vietnam and Cambodia	Bombay, Afghanistan	Himalayas, India	H. Pradesh, India	Hanoi, Vietnam	Himalayas, India	H. Pradesh, India
Characteristics								
Head pigments		–	laterally	dorsally	anteriorly	–	posteriorly (+/–)	except dorsal part
Trunk stains pattern		lateral spot on Th II–Abd I	transversal band on Th II–Abd III	all Th II–Abd III	transversal band on Th II–Abd III	lateral spot on Th III–Abd II	All Th II–Abd III or only Abd II–III	–
Abd IV pigments		spots latero-posterior	band laterally	irregular spots	1/3 posteriorly	spots latero-posterior	central spot (+/–)	spot anteriorly (+/–)
Ant IV apical bulb		2	?	1	1	?	1	1–2
Ant IV annulated		–	–	+	–	+	–	–
Head mac	**Sutural**	8	?	7	5	?	7	5
	Ps2	–	?	+	–	?	+	–
	Pa4	+	?	+	+	?	+	+
Th II mac	**m1–2** complex	6	?	4	6	6	4	5
	PmA group	7	7	6	7	7	6	7
	PmC group	7	7	5	9	9	5	7
	p5 mac	–	–	+	–	–	+	–
Th III central mac		14	13	14	14	14	14	13
Abd I mac		6–7	7	7	7	7	6	6
Abd IV central mac		12–13	?	11	14	11	13	11
Trochanteral organ		16–18	25	11–13	25	20–25	7	11
Manubrial plate chaetae		4	?	4–5	5	?	4	?

Abbreviations: (+) present; (–) absent; (?) unknown. References: [(1)]this study; [(2)]Denis 1948; [(3)]Yosii 1966; [(4)]Baquero et al. 2014; [(5)] Baquero et al. 2015; [(6)]Nguyen 2001.

2015, *S. ritae* Bellini & Zeppelini, 2011, and *S. mendoncae* Bellini & Zeppelini, 2008) are morphologically similar in the pattern of dorsal chaetotaxy, such as head with at least 6 central mac (M1–2, S0–3) and 11 posterior mac (Pa1–5, Pm1–3, Pp1–3, Pp5) and Abd I with 5 mac (m2i–4) (Bellini and Zeppelini 2008, 2011; Cipola et al. 2014b; Godeiro and Bellini 2015). Such observation supports that this pattern of chaetotaxy on head and Abd I (Figs 7E, 8B) likely arose at least twice within Seirinae, once within derived Neotropical *Seira* species, and once within *Seira* from the Oriental region (e.g. *S. boneti* comb. nov. and *S. sanloemensis*) and in *Lepidocyrtinus* (Fig. 2). Consequently, if such a hypothesis is confirmed by further phylogenies, it may also indicate that there was a gradual gain of body macrochaetae in the Neotropical species of *Seira*, but the evolution of these characters is still unknown for Old World species.

From the recovered topology it is also possible to infer the evolution of other characters among the Seirinae. In *Lepidocyrtinus*, the developed lateral tooth on the unguis is likely a synapomorphy of the genus among the Seirinae, but it is not exclusive, as it is also present in other genera of Entomobryinae, such *Acanthocyrtus* Handschin, 1925,

Amazhomidia Cipola & Bellini, 2016 (in Cipola et al. 2016), *Epimetrura* Schött, 1925 and *Lepidocyrtoides* Schött, 1917, suggesting the structure emerged more than once within Entomobryidae (Schött 1925; Cipola et al. 2016, 2017, 2018b; Cipola and Greenslade 2022). Still in *Lepidocyrtinus*, modified macrochaetae on dens represent an autapomorphy which appeared in the most derived taxa, as this characteristic is absent in the basal groups, like *L. paraibensis* (Bellini and Zeppelini 2009) (Fig. 2).

Molecular evidence justifies the transfer of *S. boneti* comb. nov. to *Seira* as found in the present study, clustering the species with another congener, *S. sanloemensis*. Such topology was also recovered in Bellini et al. (2023), although in this latter study the authors considered *L. boneti* as a *Seira* species based on preliminary data of the present study. Contrarily, the use of "*Seira boneti*" in the online database of Bellinger et al. (1996–2023) was possibly following the outdated classification of Yosii (1959, 1961a), in which *Lepidocyrtinus* was considered as a subgenus of *Seira*. This classification was updated in Godeiro et al. (2020a) based on species from the Neotropical region, which raised *Lepidocyrtinus* to the genus level again. Although many species in Bellinger et al. (1996–2023) were transferred back to *Lepidocyrtinus* following this new classification, this was not the case of *L. boneti*.

In addition to the molecular evidence, morphologically this transfer can also be explained by the presence of head posterior macrochaetae (usually absent in *Lepidocyrtinus*), mesothorax normal (usually projected anteriorly in *Lepidocyrtinus*), and the absence of developed lateral teeth in the unguis (Fig. 9E), which is exclusive to *Lepidocyrtinus* compared with other Seirinae (see Cipola et al. 2020).

Our results corroborated that *S. boneti* comb. nov. belongs to an Old World *Seira* lineage (Fig. 2), although to reveal the natural groups and possibly to update new classifications, it is necessary to include more species from other continents, mainly European taxa of the *Seira domestica* group (Nicolet, 1842) (e.g., Cipola et al. 2018a), which is the type species of the genus. At this point, looking only to our phylogenetic tree, *Seira* needs to be better evaluated in the future, because the genus is either a non-monophyletic group, or part of its taxa are classified improperly, and consequently it would be necessary to split the genus.

Conclusion

The present study redescribes *Seira boneti* comb. nov. Also, based on analyses including its mitogenome and 26 other sequences of Entomobryidae species, we surveyed its phylogenetic placement. This study is part of an on-going biogeographical and evolutionary study of the route of Seirinae global dispersion. To comprehend the evolutionary history of the subfamily we need comprehensive worldwide sampling and sufficient molecular markers. Available evidence suggests that the subfamily could be reorganized based on molecular data, especially given that our preliminary results grouped the two sampled Asian species into a distinct, ancestral clade relative to all New Word species of Seirinae.

Acknowledgements

We would like to thank Dr. Cyrille A. D'Haese for localizing the type material of *Lepidocyrtinus boneti* in MNHN, Paris. The first author obtained a grant from the Research Foundation of Shanghai Science and Technology Museum and a postdoctoral fund from the Haibo Program of Pudong New District in 2021. We are also grateful to the Graduate School, Prince of Songkla University, for providing the Ph.D. overseas thesis research scholarship 2022 (OTR2565-001) to AN. The last author was funded by CNPq (PCI-DB, Process # 300925/2019-0). This research was partly supported by the National Natural Science Foundation of China (no: 32170471).

References

Arlé R (1939) Collembola. Anexo n. 2 ao relatório da excursão científica do Instituto Oswaldo Cruz realizada na zona da E. F. N. O. B., em outubro de 1938. Boletim Biológico. Nova Série 4(2): 295–300.

Baquero E, Mandal G, Jordana R (2014) Singular Fauna of Entomobryidae (Collembola) from "Land of Passes" in the Himalayas, India. The Florida Entomologist 97(4): 1554–1587. https://doi.org/10.1653/024.097.0430

Baquero E, Mandal G, Jordana R (2015) Entomobryoidea (Collembola) from Himachal Pradesh (India) in the Himalayas. Zootaxa 4027(1): 1–41. https://doi.org/10.11646/zootaxa.4027.1.1

Bellinger PF, Christiansen KA, Janssens F (1996–2023) Checklist of the Collembola of the World. http://www.collembola.org [Accessed 25 January 2023]

Bellini BC, Zeppelini D (2008) A new species of *Seira* (Collembola: Entomobryidae) from northeastern Brazil. Revista Brasileira de Zoologia 25(4): 724–727. https://doi.org/10.1590/S0101-81752008000400018

Bellini BC, Zeppelini D (2011) A new species of *Seira* (Collembola, Entomobryidae, Seirini) from Northeastern Brazilian coastal region. Revista Brasileira de Zoologia 28(3): 403–406. https://doi.org/10.1590/S1984-46702011000300015

Bellini BC, Fernandes LH, Zeppelini D (2010) Two new species of *Seira* (Collembola, Entomobryidae) from Brazilian coast. Zootaxa 2448(1): 53–60. https://doi.org/10.11646/zootaxa.2448.1.4

Bellini BC, Zhang F, Souza PGC, Santos-Costa RC, Medeiros GS, Godeiro NN (2023) The Evolution of Collembola Higher Taxa (Arthropoda, Hexapoda) Based on Mitogenome Data. Diversity (Basel) 15(1): 7. https://doi.org/10.3390/d15010007

Börner C (1903) Neue altweltliche Collembolen nebst Bemerkungen zur systematik der Isotominen und Entomobryinen. Sitzberg. Gesellshaft Naturforschender Freunde Berlin 3: 129–182. https://doi.org/10.5962/bhl.part.29866

Börner C (1913) Die Familien der Collembolen. Zoologischer Anzeiger 41: 315–322.

Chen JX, Christiansen KA (1993) The genus *Sinella* with special reference to *Sinella* s. s. (Collembola: Entomobryidae) of China. Oriental Insects 27(1): 1–54. https://doi.org/10.1080/00305316.1993.10432236

Christiansen K (1958a) The Entomobryiform male Genital Plate. Proceedings of the Iowa Academy of Science 65: 474–476.

Christiansen K (1958b) The Nearctic members of the genus *Entomobrya* (Collembola). Bulletin of the Museum of Comparative Zoology 118(7): 440–545.

Christiansen K, Bellinger P (1980) The Collembola of North America, North of the Rio Grande: A taxonomic analysis. Grinnell College, Iowa, 1518 pp.

Christiansen K, Bellinger P (1998) The Collembola of North America, North of the Rio Grande: A taxonomic analysis. 2nd Edition. Grinnell College, Iowa, 1520 pp.

Christiansen K, Bellinger P (2000) A survey of the genus *Seira* (Collembola: Entomobryidae) in the Americas. Caribbean Journal of Science 36: 39–75.

Cipola NG, Greenslade P (2022) Two new species of *Acanthocyrtus* Handschin, 1925 (Collembola, Entomobryidae, Entomobryinae) from Western Australia. Zootaxa 5124(3): 341–358. https://doi.org/10.11646/zootaxa.5124.3.4

Cipola NG, Morais JW, Bellini BC (2014a) A new species of *Seira* (Collembola: Entomobryidae: Seirini) from Northern Brazil, with the addition of new chaetotaxic characters. Zoologia 31(5): 489–495. https://doi.org/10.1590/S1984-46702014000500009

Cipola NG, Morais JW, Bellini BC (2014b) Two new species of *Seira* Lubbock (Collembola, Entomobryidae, Seirini) from South Brazil. Zootaxa 3793(1): 147–164. https://doi.org/10.11646/zootaxa.3793.1.7

Cipola NG, Morais JW, Bellini BC (2016) A new genus of Entomobryinae (Collembola, Entomobryidae) from Brazilian Amazon with body scales and dental spines. Zootaxa 4105(3): 261–273. https://doi.org/10.11646/zootaxa.4105.3.3

Cipola NG, Morais JW, Bellini BC (2017) The discovery of *Lepidocyrtoides* Schött, 1917 (Collembola, Entomobryidae, Entomobryinae) from the New World, including three new species from Brazil and one from Australia. Zootaxa 4324(2): 201–248. https://doi.org/10.11646/zootaxa.4324.2.2

Cipola NG, Arbea J, Baquero E, Jordana R, Morais JW, Bellini BC (2018a) The survey *Seira* Lubbock, 1870 (Collembola, Entomobryidae, Seirinae) from Iberian Peninsula and Canary Islands, including three new species. Zootaxa 4458(1): 1–66. https://doi.org/10.11646/zootaxa.4458.1.1

Cipola NG, Morais JW, Bellini BC (2018b) New species, redescriptions and a new combination of *Acanthocyrtus* Handschin, 1925 and *Amazhomidia* Cipola & Bellini, 2016 (Collembola, Entomobryidae, Entomobryinae). Zootaxa 4387(3): 401–435. https://doi.org/10.11646/zootaxa.4387.3.1

Cipola NG, Morais JW, Bellini BC (2020) Review of *Lepidocyrtinus* Börner, 1903 (Collembola, Entomobryidae, Seirinae): The African species. Zootaxa 4898(1): 1–110. https://doi.org/10.11646/zootaxa.4898.1.1

Criscuolo A, Gribaldo S (2010) BMGE (Block Mapping and Gathering with Entropy): A new software for selection of phylogenetic informative regions from multiple sequence alignments. BMC Evolutionary Biology 10(210): 2–21. https://doi.org/10.1186/1471-2148-10-210

Denis JR (1948) Collemboles d'Indochine récoltes de M. C. N. Dawydoff. Notes d'Entomologie Chinoise 12: 183–311.

Dierckxsens N, Mardulyn P, Smits G (2016) NOVOPlasty: De novo assembly of organelle genomes from whole genome data. Nucleic Acids Research 45(4): 1–9. https://doi.org/10.1093/nar/gkw955

Fjellberg A (1999) The Labial Palp in Collembola. Zoologischer Anzeiger 237: 309–330.

Gisin H (1964) Collemboles d'Europe VII. Revue Suisse de Zoologie 71(4): 649–678. https://doi.org/10.5962/bhl.part.75615

Godeiro NN, Bellini BC (2015) Two new species and two detailed chaetotaxy descriptions of *Seira* (Collembola: Entomobryidae) from Brazil. Zootaxa 3972(2): 208–230. https://doi.org/10.11646/zootaxa.3972.2.4

Godeiro NN, Zhang F (2021) First record of *Seira dowlingi* (Wray, 1953) (Collembola, Entomobryidae, Seirinae) from China and mitogenome comparison with the New World specimens. Zootaxa 5020(1): 191–196. https://doi.org/10.11646/zootaxa.5020.1.11

Godeiro NN, Pacheco G, Liu SL, Cipola NG, Berbel-Filho WM, Zhang F, Gilbert MTP, Bellini BC (2020a) Phylogeny of Neotropical Seirinae (Collembola, Entomobryidae) based on mitochondrial genomes. Zoologica Scripta 49(3): 329–339. https://doi.org/10.1111/zsc.12408

Godeiro NN, Zhang F, Cipola NG (2020b) First partial mitogenome of a new *Seira* Lubbock species (Collembola, Entomobryidae, Seirinae) from Cambodia reveals a possible separate lineage from the Neotropical Seirinae. Zootaxa 4890(4): 451–472. https://doi.org/10.11646/zootaxa.4890.4.1

Godeiro NN, Bellini BC, Nifeng D, Cong X, Yinhuan D, Zhang F (2021) A mitogenomic phylogeny of the Entomobryoidea (Collembola): A comparative perspective. Zoologica Scripta 50(5): 658–666. https://doi.org/10.1111/zsc.12487

Haas BJ, Papanicolaou A, Yassour M, Grabherr M, Blood PD, Bowden J, Couger MB, Eccles D, Li B, Lieber M, MacManes MD, Ott M, Orvis J, Pochet N, Strozzi F, Weeks N, Westerman R, William T, Dewey CN, Henschel R, LeDuc RD, Friedman N, Regev A (2013) De novo transcript sequence reconstruction from RNA-seq using the Trinity platform for reference generation and analysis. Nature Protocols 8(8): 1494–1512. https://doi.org/10.1038/nprot.2013.084

Handschin E (1925) Beiträge zur Collembolenfauna der Sundainseln. Treubia 6: 225–270. https://doi.org/10.1002/mmnd.48019250305

Hoang DT, Chernomor O, von Haeseler A, Minh BQ, Vinh LE (2018) UFBoot2: Improving the ultrafast bootstrap approximation. Molecular Biology and Evolution 35(2): 518–522. https://doi.org/10.1093/molbev/msx281

Hüther W (1986) New aspects in taxonomy of *Lepidocyrtus* (Collembola). In: Dallai R (Ed.) 2nd International Seminar on Apterygota, 61–65.

ICZN [International Code of Zoological Nomenclature] (2000) International Commission on Zoological Nomenclature, 4 ed. International Trust for Zoological Nomenclature, London, 306 pp. https://www.iczn.org/the-code/the-international-code-of-zoological-nomenclature/ [Accessed 07 Aug. 2022]

Katoh K, Standley DM (2013) MAFFT multiple sequence alignment software version 7: Improvements in performance and usability. Molecular Biology and Evolution 30(4): 772–780. https://doi.org/10.1093/molbev/mst010

Lartillot N, Rodrigue N, Stubbs D, Richer J (2013) PhyloBayes MPI: Phylogenetic reconstruction with infinite mixtures of profiles in a parallel environment. Systematic Biology 62(4): 611–615. https://doi.org/10.1093/sysbio/syt022

Lubbock J (1870) Notes on the Thysanura. Part IV. Transactions of the Linnean Society of London 27(2): 277–297. https://doi.org/10.1111/j.1096-3642.1870.tb00214.x

Lubbock J (1873) Monograph of the Collembola and Thysanura. Ray Society, London, 276 pp. https://doi.org/10.5962/bhl.title.11583

Mari-Mutt JA (1979) A revision of the genus *Dicranocentrus* Schött (Insecta: Collembola: Entomobryidae). Agricultural Experiment Station Bulletin 259: 1–79.

Meng G, Li Y, Yang C, Liu S (2019) MitoZ: A toolkit for animal mitochondrial genome assembly, annotation and visualization. Nucleic Acids Research 47(11): 1–7. https://doi.org/10.1093/nar/gkz173

Minh BQ, Schmidt HA, Chernomor O, Schrempf D, Woodhams MD, von Haeseler A, Lanfear R (2020) IQ-TREE 2: New models and efficient methods for phylogenetic inference in the genomic era. Molecular Biology and Evolution 37(5): 1530–1534. https://doi.org/10.1093/molbev/msaa015

Nguyen TT (2001) Six new species of Collembola (Entomobryidae) from Vietnam. National Centre for Natural Science and Technology of Vietnam 23(1): 21–29.

Nicolet H (1842) Recherches pour Servir l'Histoire des Podurelles. Neuveaux Mémoires de la Société Helvétiques des Sciences Naturelles 6: 1–88.

Rambaut A (2010) FigTree version 1.3.1. Institute of Evolutionary Biology, University of Edinburgh, Edinburgh. http://tree.bio.ed.ac.uk/software/figtree/ [Accessed 30 October 2022]

Schött H (1917) Results of Dr. E. Mjöberg's Swedish Scientific Expeditions to Australia, 1910-1913. No. 15, Collembola. Arkiv för Zoologi 11(8): 1–60. https://doi.org/10.5962/bhl.part.1499

Schött H (1925) Collembola from Mount Murud and Mount Dulit in Northern Sarawak. Sarawak Museum Journal 3: 107–127.

Shorthouse D (2010) Simple Mappr, an online tool to produce publication-quality point maps. https://www.simplemappr.net/ [Accessed 20 September 2022]

Simon S, Letsch H, Bank S, Buckley TR, Donath A, Liu S, Machida R, Meusemann K, Misof B, Podsiadlowski L, Zhou X, Wipfler B, Bradler S (2019) Old World and New World Phasmatodea: Phylogenomics resolve the evolutionary history of stick and leaf insects. Frontiers in Ecology and Evolution 345(7): 1–14. https://doi.org/10.3389/fevo.2019.00345

Soto-Adames FN (2008) Postembryonic development of the dorsal chaetotaxy in *Seira dowlingi* (Collembola, Entomobryidae); with an analysis of the diagnostic and phylogenetic significance of primary chaetotaxy in *Seira*. Zootaxa 1683(1): 1–31. https://doi.org/10.11646/zootaxa.1683.1.1

South A (1961) The taxonomy of the British species of *Entomobrya* (Collembola). Transactions of the Royal Entomological Society of London 113(13): 387–416. https://doi.org/10.1111/j.1365-2311.1961.tb00798.x

Steenwyk JL, Buida III TJ, Labella AL, Li Y, Shen XX, Rokas A (2021) PhyKIT: A broadly applicable UNIX shell toolkit for processing and analyzing phylogenomic data. Bioinformatics (Oxford, England) 37(16): 2325–2331. https://doi.org/10.1093/bioinformatics/btab096

Szeptycki A (1979) Chaetotaxy of the Entomobryidae and its phylogenetical significance. Morpho-systematic studies of Collembola. IV. Polska Akademia Nauk, Zakład Zoologii Systematycznej i Doświadczalnej, Państwowe Wydawnictwo Naukowe, Warszawa, Kraków, 219 pp.

Yoshii R, Suhardjono YR (1992) Collembolan fauna of Indonesia and its affinities III: Collembola of Timor Island. Acta Zoologica Asiae Orientalis 2: 75–96.

Yosii R (1959) Studies on the Collembolan Fauna of Malay and Singapore with special reference to the Genera: *Lobella*, *Lepidocyrtus* and *Callyntrura*. Contributions from the Biological Laboratory Kyoto University 10: 1–65. https://doi.org/10.5134/176436

Yosii R (1961a) On some Collembola from Thailand. Nature and Life in Southeast Asia 1: 171–198.

Yosii R (1961b) Phylogenetische Bedeutung der Chaetotaxie bei den Collembolen. Contributions from the Biological Laboratory Kyoto University 12: 1–37.

Yosii R (1966) On some Collembola of Afghanistan, India and Ceylon, collected by the Kuphe-expedition, 1960. Results of the Kyoto University Scientific Expedition to the Karakoram and Hindukush 8: 333–405.

Zhang F, Deharveng L (2015) Systematic revision of Entomobryidae (Collembola) by integrating molecular and new morphological evidence. Zoologica Scripta 44(3): 298–311. https://doi.org/10.1111/zsc.12100

Zhang F, Chen Z, Dong RR, Deharveng L, Stevens MI, Huang YH, Zhu CD (2014) Molecular phylogeny reveals independent origins of body scales in Entomobryidae (Hexapoda: Collembola). Molecular Phylogenetics and Evolution 70: 231–239. https://doi.org/10.1016/j.ympev.2013.09.024

Zhang F, Bellini BC, Soto-Adames FN (2019) New insights into the systematics of Entomobryoidea (Collembola: Entomobryomorpha): first instar chaetotaxy, homology and classification. Zoological Systematics 44(4): 249–278. https://doi.org/10.11865/zs.201926

ZooKeys 1152: 119–131 (2023)
doi: 10.3897/zookeys.1152.100341
https://zookeys.pensoft.net

RESEARCH ARTICLE

A peer-reviewed open-access journal
ZooKeys
Launched to accelerate biodiversity research

Three new species of the genus *Ischnothyreus* Simon, 1893 and the discovery of the male of *I. linzhiensis* Hu, 2001 from Tibet, China (Araneae, Oonopidae)

Yanfeng Tong[1*], Dongju Bian[2*], Shuqiang Li[3]

1 *Life Science College, Shenyang Normal University, Shenyang 110034, Liaoning, China* **2** *Key Laboratory of Forest Ecology and Management, Institute of Applied Ecology, Chinese Academy of Sciences, Shenyang 110016, China* **3** *Institute of Zoology, Chinese Academy of Sciences, Beijing 100101, China*

Corresponding author: Yanfeng Tong (tyf68@hotmail.com)

Academic editor: Yuri Marusik | Received 10 January 2023 | Accepted 21 February 2023 | Published 9 March 2023

https://zoobank.org/272CD646-9DC9-4605-885B-2862DB1D5E4C

Citation: Tong Y, Bian D, Li S (2023) Three new species of the genus *Ischnothyreus* Simon, 1893 and the discovery of the male of *I. linzhiensis* Hu, 2001 from Tibet, China (Araneae, Oonopidae). ZooKeys 1152: 119–131. https://doi.org/10.3897/zookeys.1152.100341

Abstract

Four species of the genus *Ischnothyreus* Simon, 1893 from Tibet, China are recognised, including three new species, *I. caoqii* **sp. nov.** (female), *I. metok* **sp. nov.** (female), and *I. pome* **sp. nov.** (male and female). Males of *Ischnothyreus linzhiensis* Hu, 2001 are discovered for the first time since its description. Descriptions, diagnoses, and photographs of the four species are provided.

Keywords

Distribution, goblin spiders, morphology, taxonomy

Introduction

Oonopidae is a diverse spider family with 1888 extant described species in 115 genera (WSC 2023). They have a nearly worldwide distribution, occurring mainly in the leaf litter, under bark, and in the tree canopy (Jocqué and Dippenaar-Schoeman 2006; Ubick and Dupérré 2017). The genus *Ischnothyreus* Simon, 1893 is one of the most

* These authors contributed equally to this work.

speciose genera of Oonopidae, with 121 extant species mainly distributed in the Old World (WSC 2023).

The oonopid spiders of Tibet have been poorly studied. Hu (2001) reported two new species from Nyingchi, Tibet, i.e., *Gamasomorpha linzhiensis* Hu, 2001, and *Ischnothyreus linzhiensis* Hu, 2001. Cheng et al. (2021) reported one new genus and two new species from Nyingchi, Tibet, i.e., *Paramolotra pome* Tong & Li, 2021, and *Paramolotra metok* Tong & Li, 2021. In this paper three new species of the genus *Ischnothyreus*, collected from Tibet, are reported and a detailed re-description of *I. linzhiensis* Hu, 2001 is provided including the first male.

Materials and methods

The specimens were examined using a Leica M205C stereomicroscope. Details were studied under an Olympus BX51 compound microscope. Vulvae were cleared in lactic acid. Photomicroscope images were made with a Canon EOS 750D zoom digital camera (18 megapixels) mounted on an Olympus BX51 compound microscope. Photos were stacked with Helicon Focus 6.7.1 and processed in Adobe Photoshop CC 2020. For scanning electron microscopy (**SEM**), specimens were air-dried, sputter-coated using IXRF SYSTEMS, and imaged with a Hitachi TM3030 SEM. All measurements were taken using an Olympus BX51 compound microscope and are in millimeters. All specimens are preserved in 75% ethanol. The type material is deposited in Shenyang Normal University (**SYNU**) in Shenyang, China.

The following abbreviations are used in the text and figures: **a** = apodeme; **ALE** = anterior lateral eye; **ca** = conical apophysis; **css** = chestnut-shaped structure; **dm** = dorsal membrane; **flp** = flag-like process; **llp** = leaf-like projection; **nlm** = needle-like membrane; **PLE** = posterior lateral eye; **PME** = posterior median eye; **rlp** = ridge-like protuberance; **sls** = snout-like structure; **ssd** = semicircle-shaped depression; **sss** = semicircle-shaped structure; **stp** = strong, tooth-like projection; **vp** = ventral projection; **vpr** = ventral protuberance; **wd** = winding duct.

Taxonomy

Family Oonopidae Simon, 1890
Genus *Ischnothyreus* Simon, 1893

***Ischnothyreus caoqii* sp. nov.**
https://zoobank.org/1BFB2DB2-6119-46E4-B55E-BD37638576BC
Fig. 1A–I

Type material. ***Holotype*** ♀ (SYNU-508): China, Tibet, Nyingchi, Pome County, road to Metok County, 80 K; 29°39.897'N, 95°29.963'E; 2140±5 m; 10.VIII.2013; Qi Cao leg.

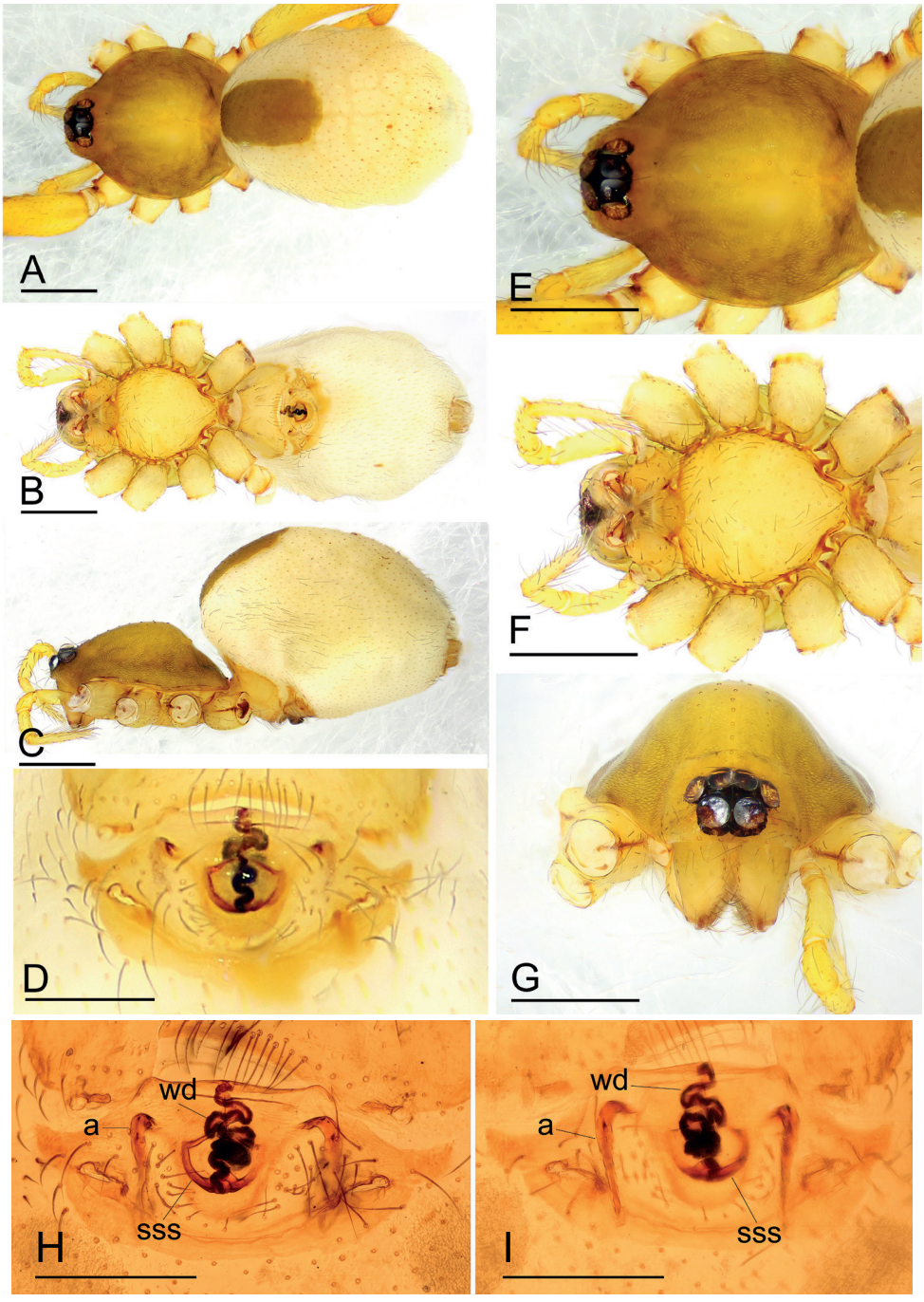

Figure 1. *Ischnothyreus caoqii* sp. nov., female holotype **A–C** habitus in dorsal, ventral and lateral views **D** epigastric region, ventral view **E–G** prosoma, dorsal, ventral and anterior views **H, I** endogyne, ventral and dorsal views (cleared in lactic acid). Abbreviations: a = apodeme; sss = semicircle-shaped structure; wd = winding duct. Scale bars: 0.4 mm (**A–C, E–G**); 0.2 mm (**D, H, I**).

Diagnosis. The new species is similar to *I. jianglangi* Tong & Li, 2020 in the size of the abdominal scuta, but can be distinguished by the large, semicirculared structure of the endogyne and the simple winding duct (Fig. 1H, I) vs. a triangular structure and a complex winding duct (see Tong et al. 2020: fig. 17A, B).

Description. Female (holotype). ***Body*****:** habitus as in Fig. 1A–C; body length 1.96. ***Carapace*****:** 0.94 long, 0.82 wide; brownish, with a yellowish center, broadly oval in dorsal view, pars cephalica strongly elevated in lateral view, surface of elevated portion of pars cephalica smooth, sides finely reticulate, lateral margin straight, smooth (Fig. 1E). ***Clypeus*****:** straight in frontal view, ALE separated from edge of carapace by less than radius (Fig. 1G). ***Eyes*****:** ALE largest, ALE circular, PME squared, PLE oval; posterior eye row recurved from above; ALE touching, ALE-PLE touching (Fig. 1E, G). ***Sternum*****:** longer than wide, pale orange (Fig. 1F). ***Mouthparts*****:** chelicerae, endites, and labium orange; chelicerae and endites unmodified. ***Abdomen*****:** 1.05 long, 0.73 wide; dorsal scutum well sclerotized, pale orange, covering 1/3 of abdomen width and approximately 1/3 of abdomen length; epigastric scutum well sclerotized, pale orange; postgastric scutum hexagonal. ***Legs*****:** pale orange, femur I with two prolateral spines, tibia I with four pairs, metatarsus I with two pairs of long ventral spines. Leg II spination similar to leg I, except femur with only one prolateral spine. Legs III and IV spineless. ***Endogyne*****:** winding duct complex, strongly convoluted, ending in semicircle-shaped structure (Fig. 1H, I).

Male. Unknown.

Etymology. The species is named after Mr. Qi Cao, the collector of the type specimens; noun in genitive case.

Distribution. Known only from the type locality.

Ischnothyreus linzhiensis **Hu, 2001**
Figs 2A–L, 3A–I, 4A–C

Material examined. 7♂, 9♀ (SYNU-509-524): China, Tibet, Nyingchi, Pome County, Yigong Town, Kaduo Village, 30°07.515'N, 95°01.928'E; 2072±3 m; 10.VIII.2013; Qi Cao leg.

Diagnosis. This species is similar to *I. serpentinum* Saaristo, 2001 in the morphology of the winding duct and the size of the abdominal scuta, but can be distinguished by the large, snout-like structure of the endogyne (Fig. 3H, I) vs. a small posterior process (see Richard et al. 2016: fig. 75E), and the conical apophysis of the male cheliceral anterior face and the flag-like sclerotized process of the fang base (Figs 2D–F, 4C) vs. unmodified chelicerae (see Richard et al. 2016: fig. 70E).

Description. Male (SYNU-509). ***Body*****:** habitus as in Fig. 2A–C; body length 1.64. ***Carapace*****:** 0.88 long, 0.65 wide; yellow, oval in dorsal view, pars cephalica strongly elevated in lateral view, surface of elevated portion of pars cephalica smooth, sides finely reticulate, lateral margin straight, smooth (Fig. 2G). ***Clypeus*****:** straight in frontal view, ALE separated from edge of carapace by their diameter (Fig. 2I). ***Eyes*****:** ALE largest, ALE circular, PME squared, PLE oval; posterior eye row recurved from

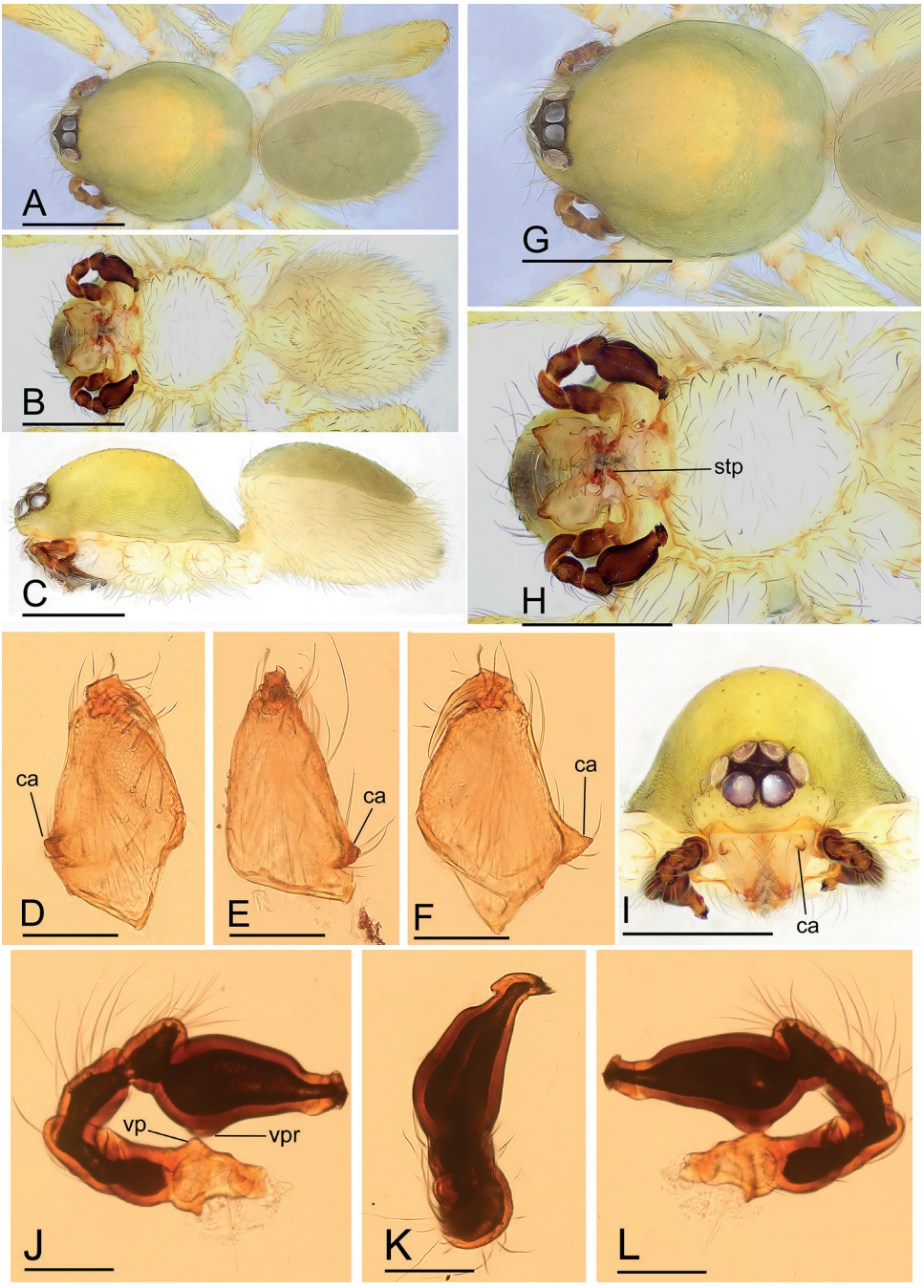

Figure 2. *Ischnothyreus linzhiensis* Hu, 2001, male **A–C** habitus in dorsal, ventral and lateral views **D–F** left chelicera, anterior, lateral and posterior views **G–I** prosoma, dorsal, ventral and anterior views **J–L** left palp, prolateral, dorsal and retrolateral views. Abbreviations: ca = conical apophysis; stp = strong, tooth-like projection; vp = ventral projection; vpr = ventral protuberance. Scale bars: 0.4 mm (**A–C, G–I**); 0.1 mm (**D–F, J–L**).

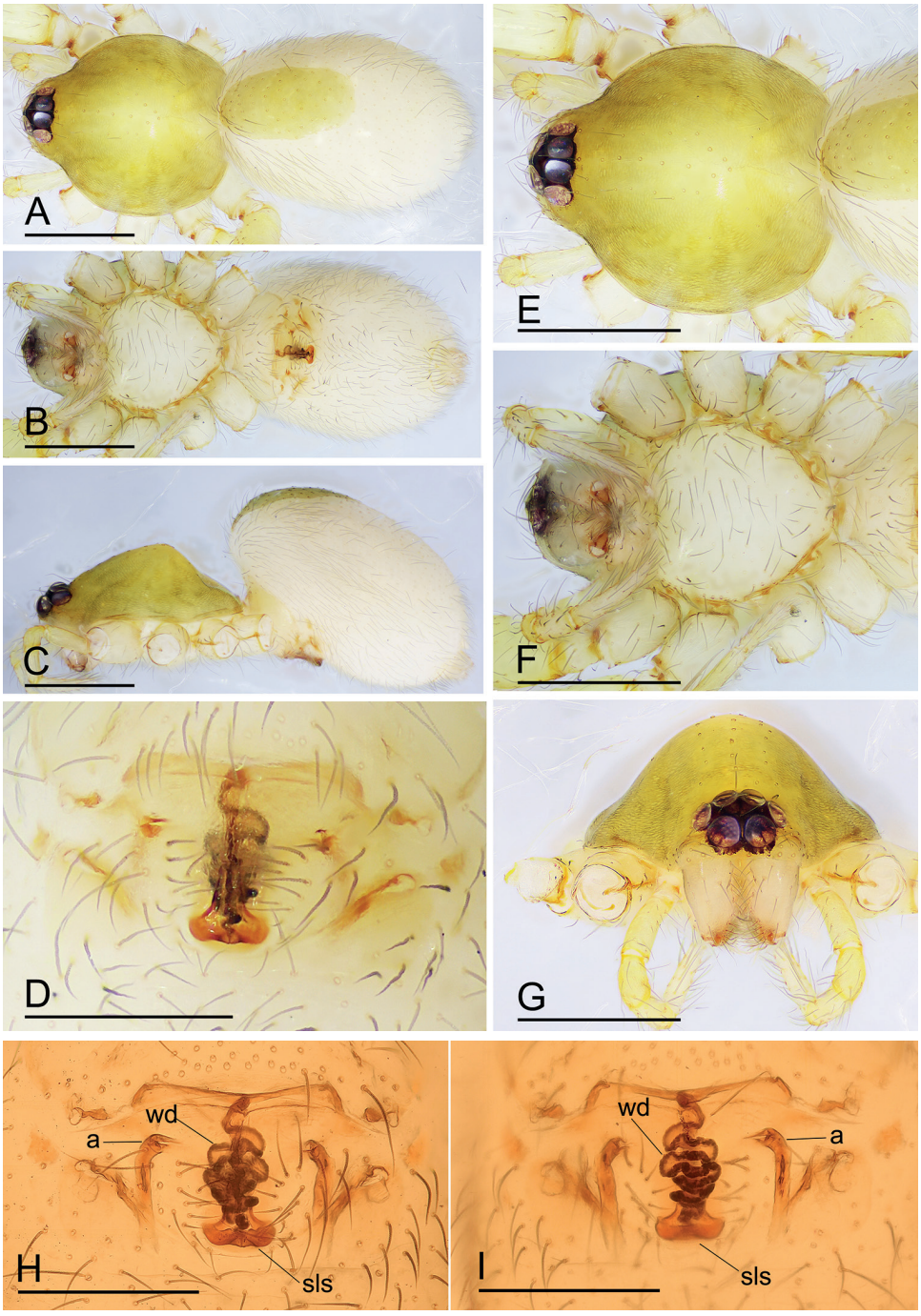

Figure 3. *Ischnothyreus linzhiensis* Hu, 2001, female **A–C** habitus in dorsal, ventral and lateral views **D** epigastric region, ventral view **E–G** prosoma, dorsal, ventral and anterior views **H, I** endogyne, ventral and dorsal views (cleared in lactic acid). Abbreviations: a = apodeme; sls = snout-like structure; wd = winding duct. Scale bars: 0.4 mm (**A–C, E–G**); 0.2 mm (**D, H, I**).

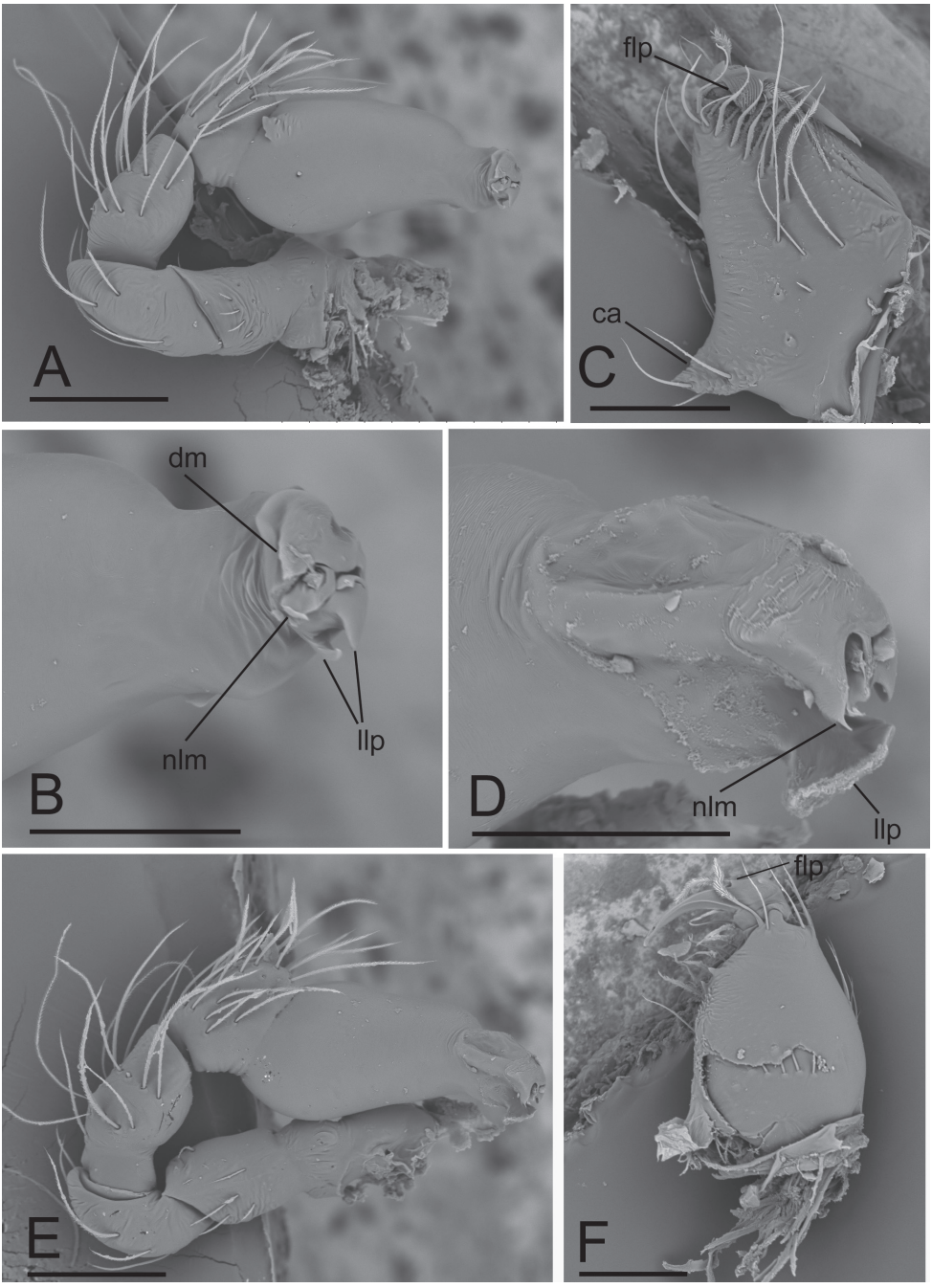

Figure 4. *Ischnothyreus linzhiensis* Hu, 2001, male **A–C** SEM; *Ischnothyreus pome* sp. nov., male holotype **D–F** SEM **A, E** left palp, prolateral view **B, D** distal end of bulb, prolateral view **C, F** left chelicerae, anterior and posterior views. Abbreviations: ca = conical apophysis; dm = dorsal membrane; flp = flag-like process; llp = leaf-like projection; nlm = needle-like membrane. Scale bars: 0.1 mm (**A, C, E, F**); 0.05 mm (**B, D**).

above; ALE touching, ALE-PLE touching (Fig. 2G, I). ***Sternum*:** as long as wide, pale orange (Fig. 2H). ***Mouthparts*:** chelicerae, endites and labium yellow; chelicerae straight, anterior face with conical apophysis, base of fangs with large flag-like sclerotized process, fang groove with a few small and one larger denticles (Figs 2D–F, 3C); anteromedian tip of endites with one strong, tooth-like projection (Fig. 2H). ***Abdomen*:** 0.76 long, 0.44 wide; dorsal scutum dark brown, covering 4/5 of abdomen width and approximately 5/6 of abdomen length, not fused to epigastric scutum; postgastric scutum covering ~ 2/3 of abdomen length. ***Legs*:** pale orange, femur I with two prolateral spines, tibia I with four pairs, metatarsus I with two pairs of long ventral spines. Leg II spination similar to leg I, except femur with only one prolateral spine. Legs III and IV spineless. ***Palp*:** trochanter with ventral projection; bulb with one ventral protuberance, distal end of bulb stout, with dorsal membrane, needle-like membrane and two leaf-like projections (Figs 2J–L, 4A, B).

Female (SYNU-516). Same as male except as noted. ***Body*:** habitus as in Fig. 3A–C; body length 1.76. ***Carapace*:** 0.72 long, 0.67 wide. ***Mouthparts*:** chelicerae and endites unmodified. ***Abdomen*:** 1.05 long, 0.67 wide; dorsal scutum very small; epigastric scutum well sclerotized, orange; postgastric scutum widely hexagonal, only around epigastric furrow. ***Endogyne*:** winding duct complex, strongly convoluted, ending in large, snout-like structure (Fig. 3H, I).

Distribution. China (Tibet: Nyingchi).

***Ischnothyreus metok* sp. nov.**

https://zoobank.org/455D6D15-EE9C-480D-A82B-84813FF407C2

Fig. 5A–I

Type material. ***Holotype*** ♀ (SYNU-525): China, Tibet, Nyingchi, Metok County, Metok Town, Countryside Tour, 29°19.087'N, 95°18.876'E, 1280±5 m, 4.VIII.2013, Qi Cao leg.

Diagnosis. The new species is similar to *I. comicus* Edward & Harvey, 2014 in the size of the abdominal scuta, but can be distinguished by the semicircle-shaped depression of the endogyne (Fig. 5H) vs. a smile-shaped depression (see Edward and Harvey 2014: figs 13I, 14F).

Description. Female (holotype). ***Body*:** habitus as in Fig. 5A–C; body length 1.64. ***Carapace*:** 0.77 long, 0.67 wide; dark brown, broadly oval in dorsal view, pars cephalica strongly elevated in lateral view, surface of elevated portion of pars cephalica finely reticulate, sides strongly reticulate, lateral margin straight, smooth (Fig. 5E). ***Clypeus*:** straight in frontal view, ALE separated from edge of carapace by less than their radius (Fig. 5G). ***Eyes*:** ALE largest, ALE circular, PME squared, PLE oval; posterior eye row procurved from above; ALE separated by less than their radius, ALE-PLE touching (Fig. 5E, G). ***Sternum*:** longer than wide, pale orange (Fig. 5F). ***Mouthparts*:** chelicerae, endites and labium yellow; chelicerae and endites unmodified**.** ***Abdomen*:** 0.88 long, 0.65 wide; dorsal scutum well sclerotized, dark brown, covering 1/3 of

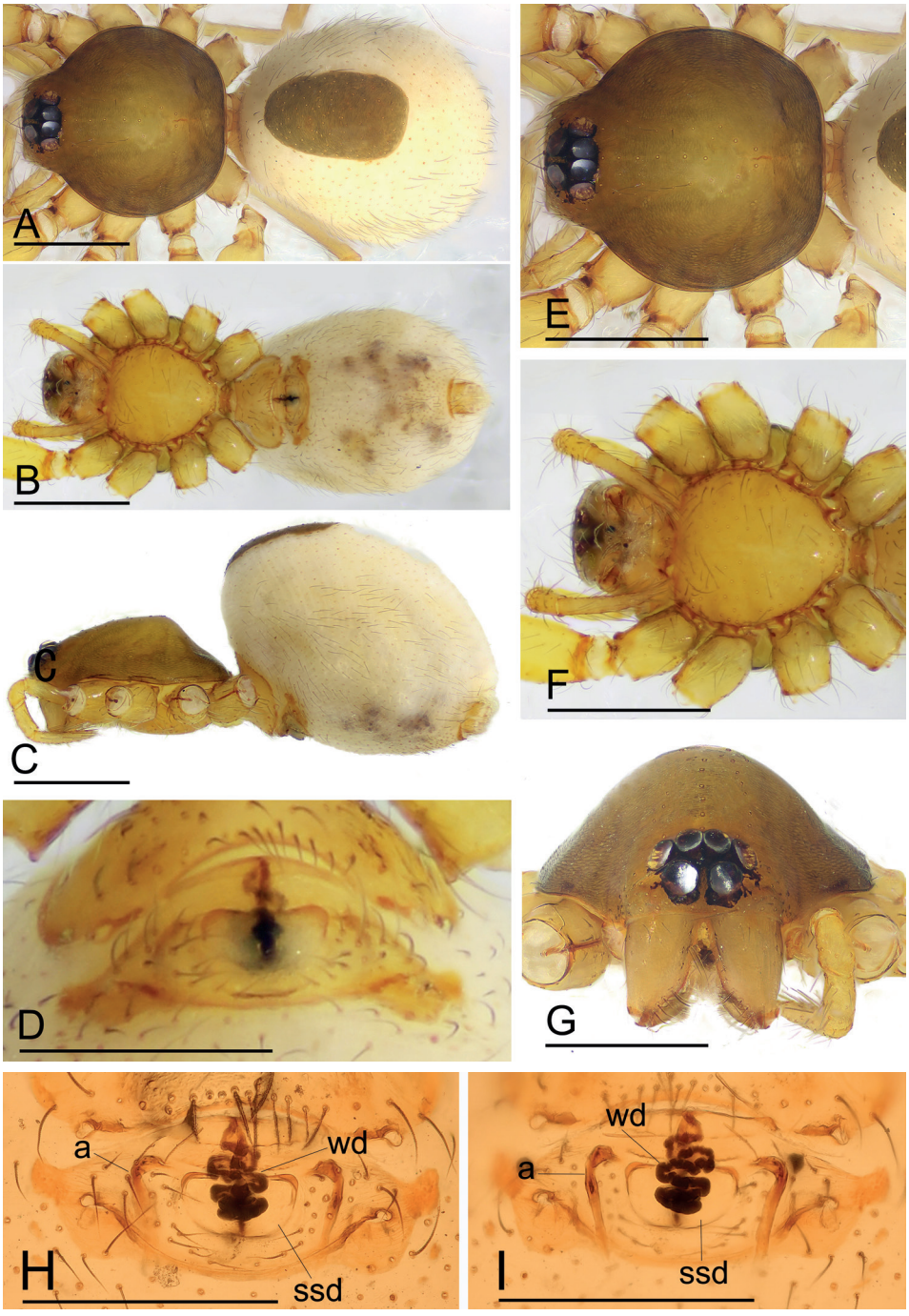

Figure 5. *Ischnothyreus metok* sp. nov., female holotype **A–C** habitus in dorsal, ventral and lateral views **D** epigastric region, ventral view **E–G** prosoma, dorsal, ventral and anterior views **H, I** endogyne, ventral and dorsal views (cleared in lactic acid). Abbreviations: a = apodeme; ssd = semicircle-shaped depression; wd = winding duct. Scale bars: 0.4 mm (**A–C, E–G**); 0.2 mm (**D, H, I**).

abdomen width and approximately 1/3 of abdomen length, not fused to epigastric scutum; epigastric scutum well sclerotized, yellow; postgastric scutum widely hexagonal. ***Legs*****:** femur I with two prolateral spines, tibia I with four pairs, metatarsus I with two pairs of long ventral spines. Leg II spination similar to leg I, except femur with only one prolateral spine. Legs III and IV spineless. ***Endogyne*****:** with large, semicircle-shaped depression; winding duct complex, strongly convoluted (Fig. 5H, I).

Male. Unknown.

Etymology. The specific name is a noun in apposition taken from the type locality.

Distribution. Known only from the type locality.

Ischnothyreus pome **sp. nov.**

https://zoobank.org/89199E5A-66CB-4CA0-8396-6000B96A81EA

Figs 4D–F, 6A–L, 7A–I

Type material. ***Holotype*** ♂ (SYNU-526): China, Tibet, Nyingchi, Pome County, road to Metok County, 80 K; 29°39.897'N, 95°29.963'E; 2140±5 m; 10.VIII.2013; Qi Cao leg. ***Paratypes*** 2♂, 3♀ (SYNU-527-531): same data as for holotype.

Diagnosis. Females of the new species are similar to those of *I. jianglangi* Tong & Li, 2020 in having the large, chestnut-shaped structure of the endogyne, but can be distinguished by the simple winding duct of the endogyne (Fig. 7H, I) vs. the complex winding duct (see Tong et al. 2020: fig. 17B). Males of the new species are similar to those of *I. yunlong* Tong & Li, 2021 in having the large flag-like sclerotized process of the cheliceral fang, but can be distinguished by the fused abdominal dorsal and epigastric scuta (Fig. 6C) vs. unfused (see Huang et al. 2021: fig. 1E), and by lacking the dorsal protuberance on the distal end of the bulb (Fig. 4D, E) vs. with dorsal protuberance (see Huang et al. 2021: fig. 2J).

Description. Male (holotype). ***Body*****:** habitus as in Fig. 6A–C; body length 1.58. ***Carapace*****:** 0.84 long, 0.69 wide; yellow, oval in dorsal view, with brown egg-shaped patches behind eyes, pars cephalica strongly elevated in lateral view, surface of elevated portion of pars cephalica smooth, sides finely reticulate, lateral margin straight, smooth (Fig. 6D). ***Clypeus*****:** straight in frontal view, ALE separated from edge of carapace by 1.4× of their diameter (Fig. 6F). ***Eyes*****:** ALE largest, ALE circular, PME squared, PLE oval; posterior eye row recurved from above; ALE touching, ALE-PLE touching (Fig. 6D, F). ***Sternum*****:** as long as wide, pale orange (Fig. 6E). ***Mouthparts*****:** chelicerae, endites, and labium yellow; chelicerae straight, with ridge-like protuberance at anterior face, base of fangs with large flag-like sclerotized process, fang groove with a few small and two larger denticles (Figs 4F, 6G–I); anteromedian tip of endites with one strong, tooth-like projection (Fig. 6E). ***Abdomen*****:** 0.74 long, 0.46 wide; dorsal scutum well sclerotized, dark brown, covering 3/5 of abdomen width and approximately 2/3 of abdomen length, fused to epigastric scutum (arrow in Fig. 6C); postgastric scutum covering ~ 5/6 of abdomen length. ***Legs*****:** pale orange, femur I with two prolateral spines, tibia I with four pairs, metatarsus I with two pairs of long ventral spines. Leg II spination similar to leg I, except femur with only one prolateral spine. Legs III and IV spineless. ***Palp*****:** trochanter

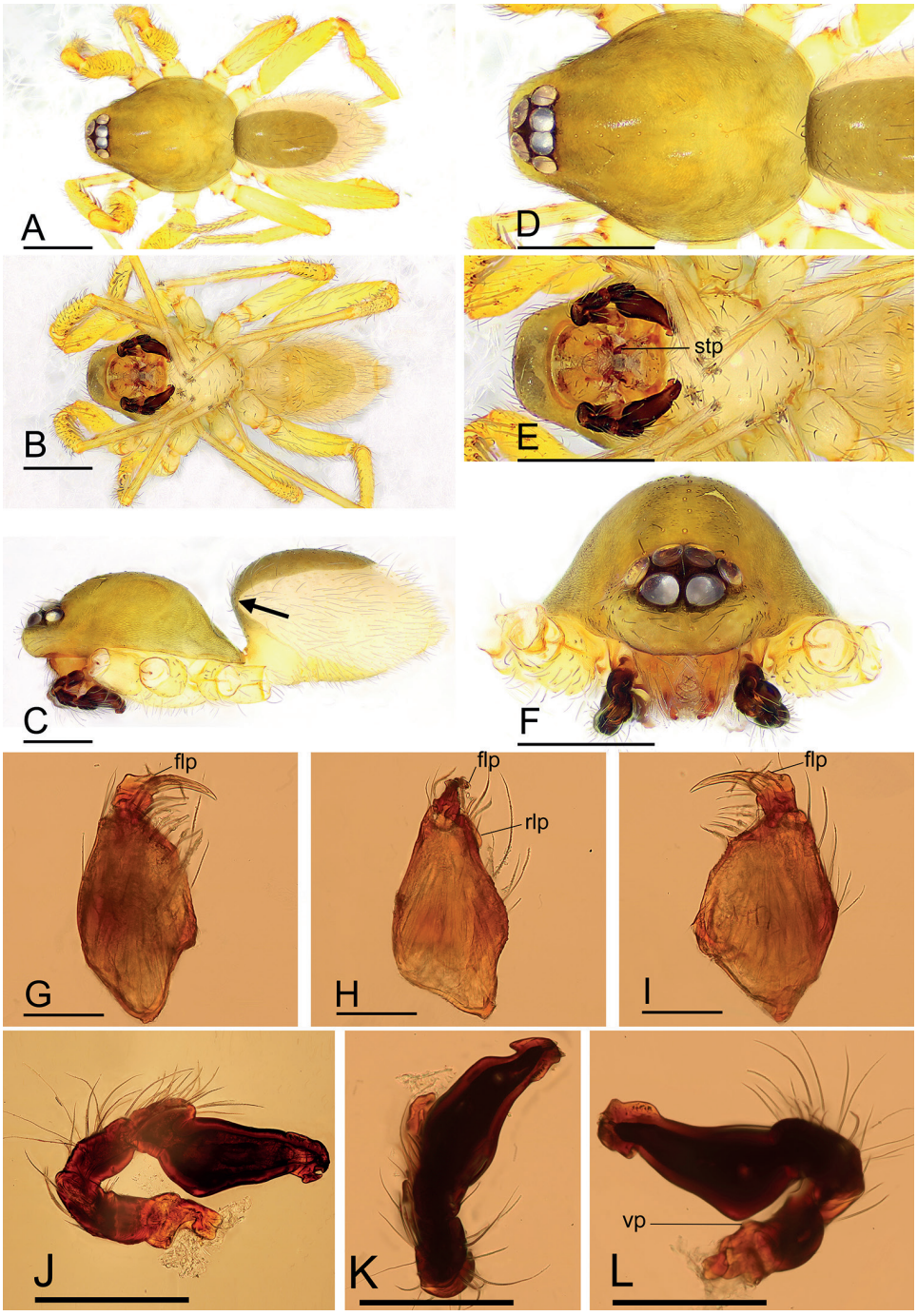

Figure 6. *Ischnothyreus pome* sp. nov., male holotype **A–C** habitus in dorsal, ventral and lateral views (arrow shows the fused scuta) **D–F** prosoma, dorsal, ventral and anterior views **G–I** left chelicera, anterior, lateral and posterior views **J–L** left palp, prolateral, dorsal and retrolateral views. Abbreviations: flp = flag-like process; rlp = ridge-like protuberance; stp = strong, tooth-like projection; vp = ventral projection. Scale bars: 0.4 mm (**A–F**); 0.1 mm (**G–L**).

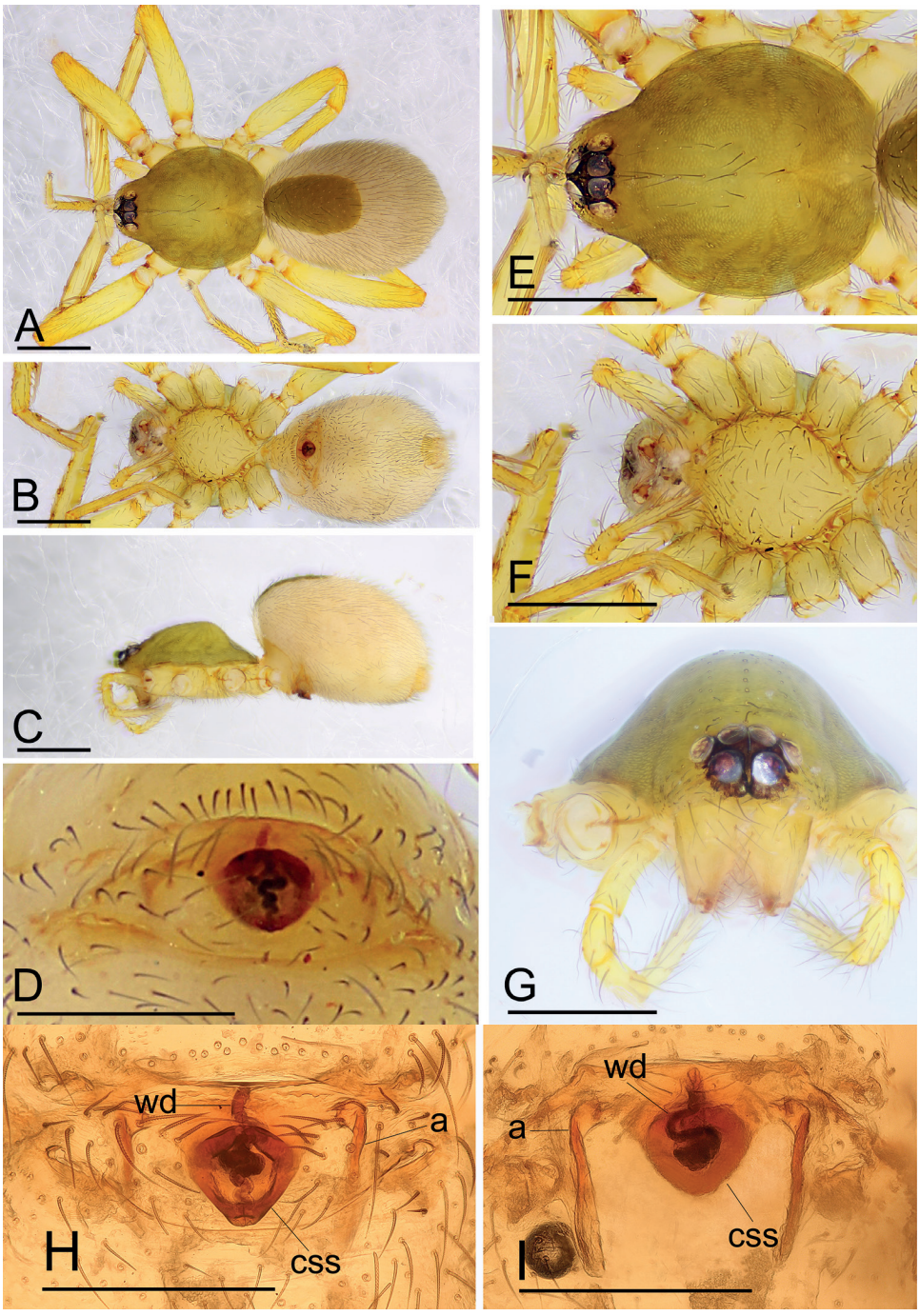

Figure 7. *Ischnothyreus pome* sp. nov., female paratype **A–C** habitus in dorsal, ventral and lateral views **D** epigastric region, ventral view **E–G** prosoma, dorsal, ventral and anterior views **H, I** endogyne, ventral and dorsal views (cleared in lactic acid). Abbreviations: a = apodeme; css = chestnut-shaped structure; wd = winding duct. Scale bars: 0.4 mm (**A–C, E–G**); 0.2 mm (**D, H, I**).

with ventral projection; bulb without small ventral protuberance, distal end of bulb stout, with needle-like membrane and broad leaf-like projection (Figs 4D, E, 6J–L).

Female (paratype, SYNU-529). Same as male except as noted. ***Body*:** habitus as in Fig. 7A–C; body length 1.64. ***Carapace*:** 0.77 long, 0.67 wide. ***Mouthparts*:** chelicerae and endites unmodified. ***Abdomen*:** 0.88 long, 0.65 wide; dorsal scutum very small; epigastric scutum well sclerotized, orange; postgastric scutum widely hexagonal, only around epigastric furrow. ***Endogyne*:** winding duct simple, with anterior portion straight, strongly convoluted only in posterior section, ending in large, chestnut-shaped structure (Fig. 7H, I).

Etymology. The specific name is a noun in apposition taken from the type locality.

Distribution. Known only from the type locality.

Acknowledgements

The manuscript benefitted greatly from comments by Darrell Ubick and Yuri M. Marusik. This study was supported by the National Natural Science Foundation of China (NSFC-31750002, 31972867), and LiaoNing Revitalization Talents Program (XLYC2007044).

References

Cheng W, Bian D, Tong Y, Li S (2021) A new genus and two new species of oonopid spiders from Tibet, China (Araneae, Oonopidae). ZooKeys 1052: 55–69. https://doi.org/10.3897/zookeys.1052.66402

Edward KL, Harvey MS (2014) Australian goblin spiders of the genus *Ischnothyreus* (Araneae, Oonopidae). Bulletin of the American Museum of Natural History 389: 1–144. https://doi.org/10.1206/865.1

Hu J (2001) Spiders in Qinghai-Tibet Plateau of China. Henan Science and Technology Publishing House, Zhengzhou, 658 pp.

Huang Y, Tong Y, Bian D, Li S (2021) One new species of the genus *Ischnothyreus* Simon, 1893 and re-description of *I. yueluensis* Yin & Wang, 1984 from China (Araneae, Oonopidae). Biodiversity Data Journal 9: e66843. [11 pp] https://doi.org/10.3897/BDJ.9.e66843

Jocqué R, Dippenaar-Schoeman AS (2006) Spider Families of the World. Musée Royal del'Afrique Central, Tervuren, 336 pp.

Richard M, Graber W, Kropf C (2016) The goblin spider genus *Ischnothyreus* (Araneae, Oonopidae) in Java and Sumatra. Zootaxa 4151(1): 1–99. https://doi.org/10.11646/zootaxa.4151.1.1

Tong Y, Li S, Bian D (2020) Taxonomic study of the genus *Ischnothyreus* Simon, 1893 from Myanmar (Araneae, Oonopidae). ZooKeys 993: 1–26. https://doi.org/10.3897/zookeys.993.57676

Ubick D, Dupérré N (2017) Oonopidae. In: Ubick D, Paquin P, Cushing P, Roth V (Eds) Spiders of North America: an Identification Manual (2nd edn.). American Arachnological Society, Keene, New Hampshire, 181–182.

WSC (2023) World Spider Catalog. Version 23.5. Natural History Museum Bern. http://wsc.nmbe.ch [Accessed on 6 Jan 2023]

ZooKeys 1152: 133–161 (2023)
doi: 10.3897/zookeys.1152.98234
https://zookeys.pensoft.net

RESEARCH ARTICLE

A peer-reviewed open-access journal
ZooKeys
Launched to accelerate biodiversity research

Taxonomic review of Manocoreini with description of a new species from China (Hemiptera, Heteroptera, Coreidae)

Yanyan Zhou[1], Huaxi Liu[2,3], Wenjun Bu[4], Zhiqiang Li[1]

1 *Guangdong Key Laboratory of Animal Conservation and Resource Utilization, Guangdong Public Laboratory of Wild Animal Conservation and Utilization, Institute of Zoology, Guangdong Academy of Sciences, No.105 Xingangxi Road, Guangzhou, 510260, Guangdong, China* **2** *Department of Life Sciences, Silwood Park Campus, Imperial College London, SL5 7PY, Ascot, UK* **3** *Department of Life Sciences, Natural History Museum, SW7 5BD, London, UK* **4** *Institute of Entomology, College of Life Sciences, Nankai University, Weijin Road 94, 300071, Tianjin, China*

Corresponding authors: Wenjun Bu (wenjunbu@nankai.edu.cn); Zhiqiang Li (lizq@giz.gd.cn)

Academic editor: Jader Oliveira | Received 1 December 2022 | Accepted 17 February 2023 | Published 9 March 2023

https://zoobank.org/50AEF448-C3B7-4817-910C-3D55203F5670

Citation: Zhou Y, Liu H, Bu W, Li Z (2023) Taxonomic review of Manocoreini with description of a new species from China (Hemiptera, Heteroptera, Coreidae). ZooKeys 1152: 133–161. https://doi.org/10.3897/zookeys.1152.98234

Abstract

In the present paper, all seven species of Manocoreini are reviewed, and a new species *Manocoreus hsiaoi* **sp. nov.** is described from Guangxi, China. Photographs of habitus of all species, and detailed structures of the new species and type species of *Manocoreus* Hsiao, 1964 are provided. All species of Manocoreini of the world are keyed. A distribution map of all species is also provided.

Keywords

Coreoidea, *Manocoreus*, Oriental Region, taxonomy

Introduction

The tribe Manocoreini Hsiao, 1964 is a small group of Coreinae Leach, 1815, which only comprises the genus *Manocoreus* Hsiao, 1964, endemic to China (Li 1996). Hsiao (1964) described *Manocoreus* and four species from southern China as belonging to it: the type species *M. vulgaris* from Fujian, Guangdong, Jiangxi, and Zhejiang;

M. marginatus from Yunnan; *M. montanus* from Sichuan; and *M. yunnanensis* from Yunnan. Ren (1983) provided brief notes on all four known species of *Manocoreus* and described *M. astinus* from Yunnan. Ren (1993) described *M. grypidus* from Hubei, while Liu and Ren (1993) described *M. furcatus* from Fujian. Up to now, the genus *Manocoreus* contains seven species, and all of which are only found in southern China.

Tribe Manocoreini was established based on characteristics of head and plica on abdominal sternite VII of female, and was considered as closely related to Dasynini Bergroth, 1913 and Gonocerini Mulsant & Rey, 1870 (Hsiao 1964). Li (1996, 1997) published the comparative morphological and cladistic analysis of Coreidae, his result supported Manocoreini as a taxon of tribal rank. Upon examination of Manocoreini collections from China, *Manocoreus* is reviewed, and a new species *Manocoreus hsiaoi* sp. nov. is described from Guangxi province, China.

Materials and methods

External structures were examined by using a Zeiss Discovery V20 stereomicroscope. Measurements (in mm) were taken using Zeiss ZEN 2.5 pro software.

The male genital capsule and female abdomen were removed in dry condition and soaked in 75 °C, 10% KOH for 30 minutes to one hour to remove muscles. Endosoma was carefully stretched with a pair of forceps under a Zeiss Discovery V20 stereomicroscope. Photographs of habitus and detailed structures were taken by using a Canon EOS 7D Mark II camera equipped with a LAOWA 100 mm F2.8 macro 2× macro lens. Photographs of the genitalic structures were taken using a Canon EOS 7D Mark II camera equipped with a LAOWA 25 mm F2.8 macro 2.5–5× macro lens, or equipped with a tube lens and a Mitutoyo M Plan Apo 10× objective lens. Morphological terminology follows Hsiao (1964), Ren (1993), Brailovsky (2007a, b), Yi and Bu (2015), Zhou and Rédei (2020), and Pluot-Sigwalt and Moulet (2020).

Abbreviations used in the text and figures are as follows:

aed aedeagus;
am ampulla;
bp basal plates;
cd coiled duct;
dpr dorsoposterior rim;
ds duct seminis;
fz flexible zone;
ga gonangulum;
lpc lateroposterior convexes;
lt8, 9 laterotergites VIII, IX;
mdp median projection;
mvp median ventroposterior process;
ph process on head in front of antenniferous tubercles;
phth phallotheca;
ra8, 9 ramus of valvula VIII, IX;
rs ring sclerite;
s6, 7, 10 sternites VI, VII, X;
sd spermathecal duct;
sp8 spiracle VIII;
sr seminal receptacle;
sth spermatheca;
t9, 10 tergites IX, X;
vcs ventral conjunctival sclerites;
va8, 9 valvulae VIII, IX;
vf8, 9 valvifers VIII, IX.

Label data of type specimens were cited verbatim: a slash (/) separates the lines and a double slash (//) different labels from the same specimen; notes about the label data were indicated in square brackets ([]).

Abbreviations for depositories:

IZCAS Institute of Zoology, Chinese Academy of Sciences, Beijing, China;
NKUM Institute of Entomology, Nankai University, Tianjin, China;
SYSBM Museum of Biology, Sun Yat-sen University, Guangzhou, China.

Taxonomy

Tribe Manocoreini Hsiao, 1964

Manocoreini Hsiao, 1964: 90. Hsiao (1977): 217 (in key), 243 (diagnostic characters); Dolling (2006): 87 (catalogue).

Type genus by monotypy. *Manocoreus* Hsiao, 1964.

Genus *Manocoreus* Hsiao, 1964

Figs 1–16

Manocoreus Hsiao, 1964: 90. Hsiao (1977): 217 (in key), 244 (listed); Ren (1983): 321 (diagnostic characters, habitat, hosted plant); Chen and Li (1999): 128 (catalogue, diagnostic characters); Dolling (2006): 87 (catalogue).

Type species by original designation. *Manocoreus vulgaris* Hsiao, 1964.

Diagnosis. *Manocoreus* can be distinguished from other genera of Coreinae by the following combined characters: body elongate (Figs 1–3, 7–8); head wide, extending beyond antenniferous tubercles (Figs 12, 13); anteclypeus slender, slightly longer than mandibular plate (Figs 12, 13); head with small dentate or plate-like process in front of antenniferous tubercles (Figs 4A, B, 9A, B: hp); anterior portion of buccula right angled; eye not reaching anterior margin of pronotum (Figs 12, 13); profemora unarmed; vein Cu of hind wing away from base of hamus; meso- and metasternum with a mid-longitudinal groove; dorsum of tibiae sulcate, base of each tibiae slightly protuberant; metatarsal segment I longer than the sum of segments II and III; spiracles of abdomen situated before middle of sternites, near lateral margin (Figs 14, 15); sternum VII of female with middle longitudinal cleft, plica triangular, or rectangular depressed, covered by sternum VI (Figs 6C, 11B, 15); posterior margin of genital capsule broadly sinuate, with median ventroposterior process (Figs 4E, F, 5D, 9E, F, 10D, 14).

Redescription. Body medium to relatively large (11–17 mm), elongate, nearly parallel-sided, ~ 3.2–4.3× as long as humeral width (Figs 12, 13). ***Body surface and vestiture.*** Body surface rather dull; head, thorax, abdomen, with dense punctures;

antennae, legs with short, semierect to erect setae, and dense small tubercles; abdomen with short and dense setae.

Head porrect, wider than long, shorter than pronotum, nearly pentagonal, dorsally flat, apex distinctly produced and surpassing antenniferous tubercles; anteclypeus slender, slightly surpassing mandibular plate (Figs 12, 13); antenniferous tubercles almost circular, not prominent; genae with small dentate or plate-like process in front of antenniferous tubercles (Figs 4A, B, 9A, B); anterior of buccula nearly right angled; eyes globular, not reaching anterior margin of pronotum (Figs 12, 13); ocelli not close to each other, relatively close to eyes, dorsally situated before connecting line of posterior edge of eyes (Figs 12, 13); preocellar pit deep, transverse; ocellar tubercles barely raised (Figs 12, 13); antenna four-segmented, antennomere I thickest, apex of antennomere I far from apex of head, with a glabrous and narrow base; antennomeres I–III subcylindrical, subequal in length, antennomere IV fusiform, shortest; labium four-segmented, surpassing posterior margin of mesosternum but not surpassing posterior margin of metasternum (Figs 1B, D, 2B, 3B, D, 7B, E, 8B, E); labial segment I not extending beyond base of head (*M. vulgaris*), or reaching anterior margin of prosternum (other species). ***Thorax.*** Pronotum wider than long, hexagonal, gradually declivent, anterior margin with narrow, indistinct, depressed anterior collar (Figs 12, 13); cicatrices distinct, somewhat depressed; anterolateral margin concave to nearly straight, nodulose; humeral angle rectangular or tapering into stout or acute spine pointing outward (Figs 12, 13); posterolateral angle broadly angulate, posterolateral margin sinuate; posterior margin nearly straight or slight concave; pronotal disk with distinct or indistinct longitudinal medial carinae (Figs 12, 13). Scutellum longer than wide, triangular, apically subacute. Prosternum small, area before mesocoxae of mesosternum large, mesosternum and metasternum with longitudinal median groove; metathoracic scent gland ostiole provided with a bilobate peritreme, evaporatorium extending ~ 1/2 of mesopleuron (Figs 4C, D, 9C, D). Legs unarmed; femora thickened; dorsal surface of tibiae each with a wide longitudinal furrow. Hemelytra macropterous, not reaching or slightly surpassing apex of abdomen (1A, C, 2A, 3A, C, 7A, D, 8A, D); costal margin emarginated, nearly straight, R and M branch from ca. middle of corium, membrane with ~ 10 longitudinal veins; hamus of hind wing very short. ***Pregenital abdomen.*** Connexival segments distinctly raised above tergum, posterolateral angles sometimes acute; sterna without impression or furrow ventrally; spiracles circular, small, close to lateral margin, situated before middle of sterna; spiracle II not visible. Posterior margin of female abdominal tergum VII sinuate, concave in middle, sternum VII of female with middle longitudinal cleft, plica triangular, indistinct, covered by sternum VI (Fig. 14). ***External male genitalia.*** Genital capsule near prolate spheroidal, opening dorsally (Figs 4E, F, 5D, 9E, F, 10D), ventral outline distally concave in lateral view, posterior margin of genital capsule broadly sinuate with median ventroposterior process (Fig. 14); dorsal margin of base of paramere nearly straight, distal portion of paramere sickle-shaped (Figs 5E–G, 10E–G); phallus with a sclerotized articulatory apparatus, phallotheca barrel-shaped, unarmed, conjunctiva rigid and complex, aedeagus coiled, strongly sclerotized (Figs 5A–C, 10A–C). ***External female genitalia.*** Laterotergite VIII subtriangular, spiracles present; laterotergites IX subtriangular, inner margin contact (Fig. 15). Valvifers VIII nearly triangular (Figs 6C,

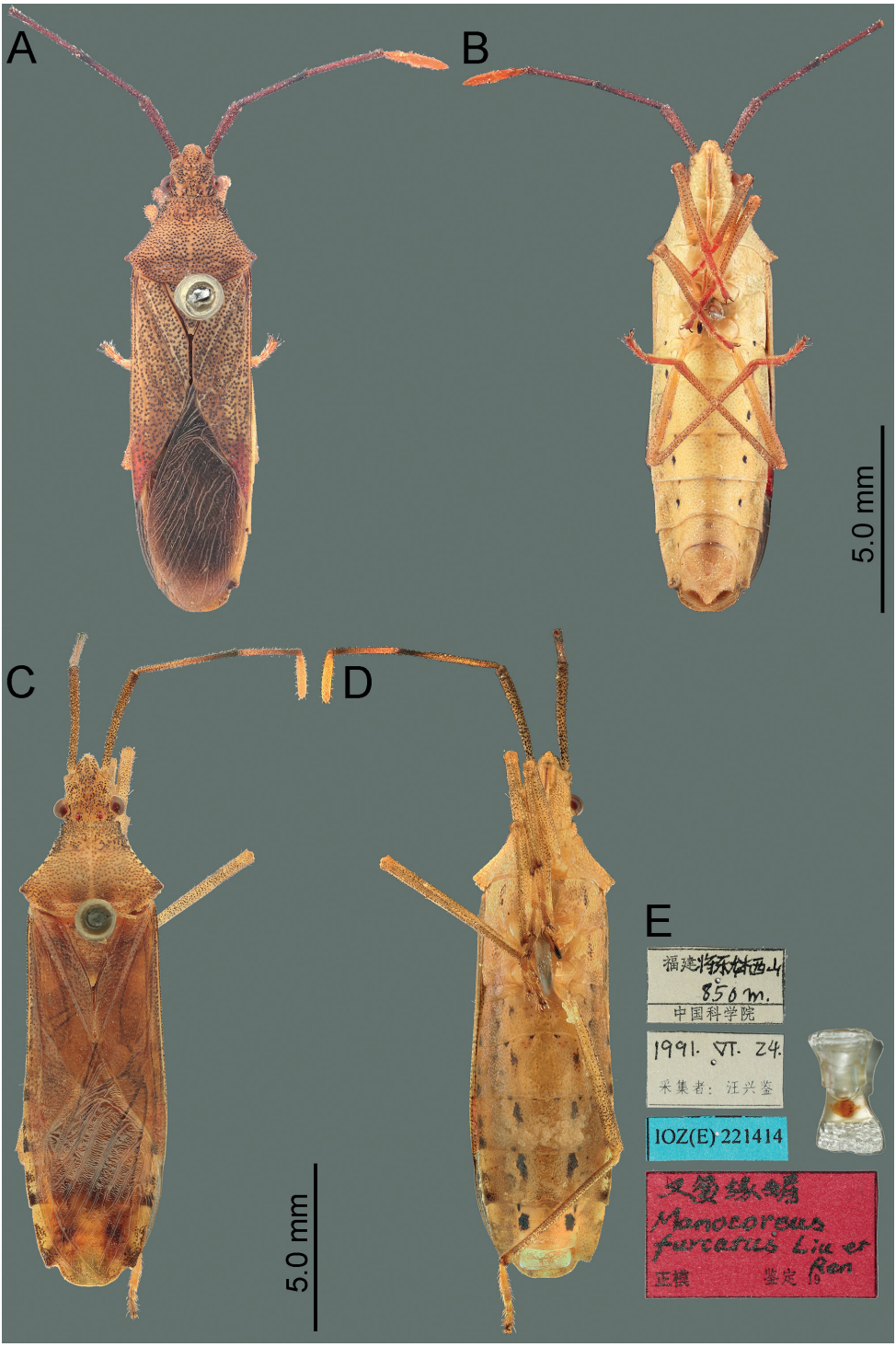

Figure 1. Habitus of *Manocoreus* spp. **A, B** *M. astinus* male non-type specimen **A** dorsal view **B** ventral view **C–E** *M. furcatus* male holotype **C** dorsal view **D** ventral view **E** labels.

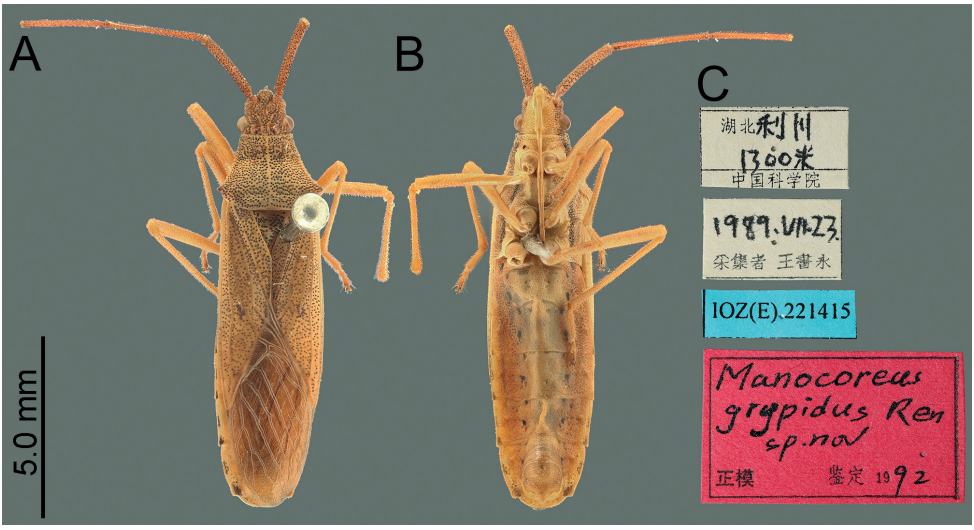

Figure 2. Habitus of *Manocoreus grypidus* male holotype. **A** dorsal view **B** ventral view **C** labels.

11B: vf8); valvulae VIII moderately membranous, with posterior distal portions slightly sclerotized (Figs 6C, 11B: va8); gonangulum elongate (Figs 6A, 11A: ga); valvifers IX separated, slender (Figs 6A, 11A: vf9); valvulae IX membranous, with posterior distal portions strongly sclerotized (Figs 6A, 11A: va9); valvulae VIII and IX interlocking through sclerotized rami VIII and IX (Figs 6A, 11A, C); gynatrium with one large ring sclerite (Figs 6A, 11A: rs); spermatheca with a long coiled duct, basal portion of duct slightly expanding, subapical with a conspicuous ampulla (Figs 6B, D, 11C, D: am); distal region with a long flexible zone (Figs 6B, D, 11C, D: fz), tightly coiled duct (Figs 6B, D, 11C, D: cd), and seminal receptacle globose (Figs 6B, D, 11C, D: sr).

Distribution. The genus currently contains eight species, all species distributed in southwestern and southern China (Fig. 16).

Manocoreus astinus Ren, 1983

Figs 1A, B, 12A, 14A, 15A, 16

Manocoreus astinus Ren, 1983: 322. Holotype: ♂, China, Yunnan, Lushui; IZCAS. Ren (1992): 140 (catalogue, distribution); Dolling (2006): 87 (catalogue, distribution).

Material examined. China. Yunnan: Lushui City, Pianma, 2300 m a.s.l., 26.v.1981, leg. S.Y. Wang (1♂ 1♀ NKUM), same but 29.v.1981 (1♂ NKUM), same but 31.v.1981 (1♂ 3♀♀ NKUM); Dehong Prefecture, Yingjiang County, 1300 m a.s.l., 13.iv.1980, leg. S. M. Song (1♂ NKUM).

Remarks. This species is similar to *M. vulgaris* in habitus, size, and color, but differs in the following characters: labium surpassing anterior margin of metacoxae (Fig. 1B); male median ventroposterior process of genital capsule triangular (Fig. 14A).

Notes. The type series of *M. astinus* was not in IZCAS rather than as Ren (1983) stated. Therefore, the authors of this paper examined all specimens which were collected in the type locality with similar dates, and other specimens deposited in NKUM and confirmed their identification as *M. astinus*.

Distribution. China. Yunnan: Lushui, Dehong (Fig. 16).

***Manocoreus furcatus* Liu & Ren, 1993**
Figs 1C–E, 12B, 14B, 15B, 16

Manocoreus furcatus Liu & Ren, 1993: 147. Holotype: ♂, China, Fujian, Jiangle; IZCAS.

Type material examined. ***Holotype*** male "Fujian [printed in Chinese] Jiangle [handwritten in Chinese] Longqishan [handwritten in Chinese] / 850 m. [handwritten] / Chinese Academy of Sciences [printed in Chinese] // 1991. VI. 24 [handwritten] / collector: Wang Xingjian [printed in Chinese] // IOZ(E) 221414 [printed] // Chamanyuanchun [handwritten in Chinese] / Manocoreus [handwritten] / furcatus Liu et [handwritten] / Ren [handwritten] / holotype [printed in Chinese] identified [printed in Chinese] 19 [printed]"; IZCAS. ***Paratype*** female, labelled: "Fujian [printed in Chinese] Longqishan [handwritten in Chinese] / 87 [handwritten] year [printed] 7 [handwritten] month [printed] 17 [handwritten] day [printed] / collector [printed in Chinese] Chen Shunli [handwritten in Chinese] // Chamanyuanchun [handwritten in Chinese] / Manocoreus [handwritten] / furcatus Liu et [handwritten] / Ren [handwritten] / paratype [printed in Chinese]"; NKUM.

Other material examined. China. Jiangxi: Jinggangshan Xiaoxidong Forest Farm, 24.vii.2002, leg. H.J. Xue (1♂ NKUM); **Zhejiang:** Lin'an volcano Dashi Valley, 400–750 m a.s.l., 9.viii.2007, leg. W. B. Zhu (1♂ 1♀ NKUM), Lin'an Qingliangfeng Botanical Garden, 900–990 m a.s.l., 13.viii.2007, leg. G. P. Zhu (3♂♂ NKUM).

Remarks. *Manocoreus furcatus* can be recognized from all other species of *Manocoreus* by the following characteristics: distinctly bigger size (Fig. 1C, D, body length 16.0–17.2 mm); middle of both sides of sterna III to VII with large irregular black spots (Fig. 1D); median ventroposterior process of genital capsule bifurcate (Fig. 14B).

Distribution. China. Fujian: Jiangle; **Jiangxi:** Jianggangshan; **Zhejiang:** Lin'an (Fig. 16).

***Manocoreus grypidus* Ren, 1993**
Figs 2A–C, 12C, 14C, 15C, 16

Manocoreus grypidus Ren, 1983: 347. Holotype: ♂, China, Hubei, Lichuan; IZCAS.
Ren and Xiong (1993): 189 (catalogue, distribution).

Type material examined. ***Holotype*** male "Hubei [printed in Chinese] Lichuan [handwritten in Chinese] / 1300 m [handwritten in Chinese] / Chinese Academy of Sciences [printed in Chinese] // 1989.VII.23 [handwritten in Chinese] / collector Wang

Shuyong [printed in Chinese] // IOZ(E) 221415 [printed] // Manocoreus [handwritten] / grypidus Ren [handwritten] / holotype [printed in Chinese] identified [printed in Chinese] 19 [printed] 92 [handwritten in Chinese]"; IZCAS.

Other material examined. China. Guizhou: Zunyi City Suiyang County Kuankuangshui National Nature Reserve Rangshui, 900 m a.s.l., 13.viii.2010, leg. X. Sun, Y.H. Wang (2♂♂ 5♀♀ NKUM); Fanjingshan Tongkuangchang, 700 m a.s.l., 28.vii.2001, leg. W.B. Zhu (2♀♀ NKUM), same but leg. W.J. Bu (1♂ NKUM).

Remarks. This species can be recognized from all other species of *Manocoreus* by the following characteristics: pronotum with dense black punctures, but lateral margin not black (Fig. 12D); the middle portion of corium with small black spot (Fig. 2A); male median ventroposterior process of genital capsule triangular in ventral view, lateral processes on posterior margin of genital capsule smaller than median process, directed backward and slightly inward in ventral view (Fig. 14C).

Distribution. China. Guizhou: Tongren, Zunyi; **Hubei**: Hefeng (Ren 1993), Lichuan (Fig. 16).

***Manocoreus hsiaoi* sp. nov.**

https://zoobank.org/00EB1E86-DA91-4E1C-91BE-20846F1C02D8

Figs 3–6, 12D, 14D, 15D, 16

Type material. ***Holotype*** (♂) **China: Guangxi Province**, Xing'an County, Maoershan: 900–1320 m a.s.l., 2009-VII-10, leg. Zhong-Hua FAN, mounted on card (NKUM). ***Paratypes*** (1♂, 1♀) same data as holotype, mounted on cards (NKUM); (5♂♂, 3♀♀) **China: Guangxi Province**, Xing'an County, Maoershan: 900–1320 m a.s.l., 2009-VII-10, leg. Qing ZHAO, mounted on cards (NKUM); (1♂) **China: Guangxi Province,** Xing'an County, Maoershan: 900–1320 m a.s.l., 2009-VII-10, leg. Xi SUN, mounted on cards (NKUM).

Diagnosis. *Manocoreus hsiaoi* sp. nov. can be recognized from all other species of *Manocoreus* by the following characters: lateral margin of pronotum black (Figs 4A, 12D); punctures on the discal region of pronotum not black (Fig. 12D); connexivum with black spots (Fig. 3A, C); the middle portion of corium with large black spots (Fig. 3A, C); male median ventroposterior process of genital capsule long and tuberculate (Figs 4E, 5D, 14D).

Description. Body elongate, ~ 3.76–3.94× as long as humeral width (Fig. 3A–D). ***Color, integument, and vestiture.*** Body brownish yellow, dorsum of head with dense black punctures, underside of head with dense punctures concolorous with body surface (Fig. 4B), compound eyes dark red, ocelli reddish; labium yellow, distal one fourth of segment IV black; antennomeres I–III brownish yellow, antennomere IV paler, apical portion of antennomeres II and III blackish, antennomere I with moderately dense small black tubercles, small tubercles on antennomeres II and III more scattered and paler, each segments with short semi-erect setae; lateral margin of pronotum black (Fig. 4A); collar, callus area, area near lateral margin and posterior margin with black

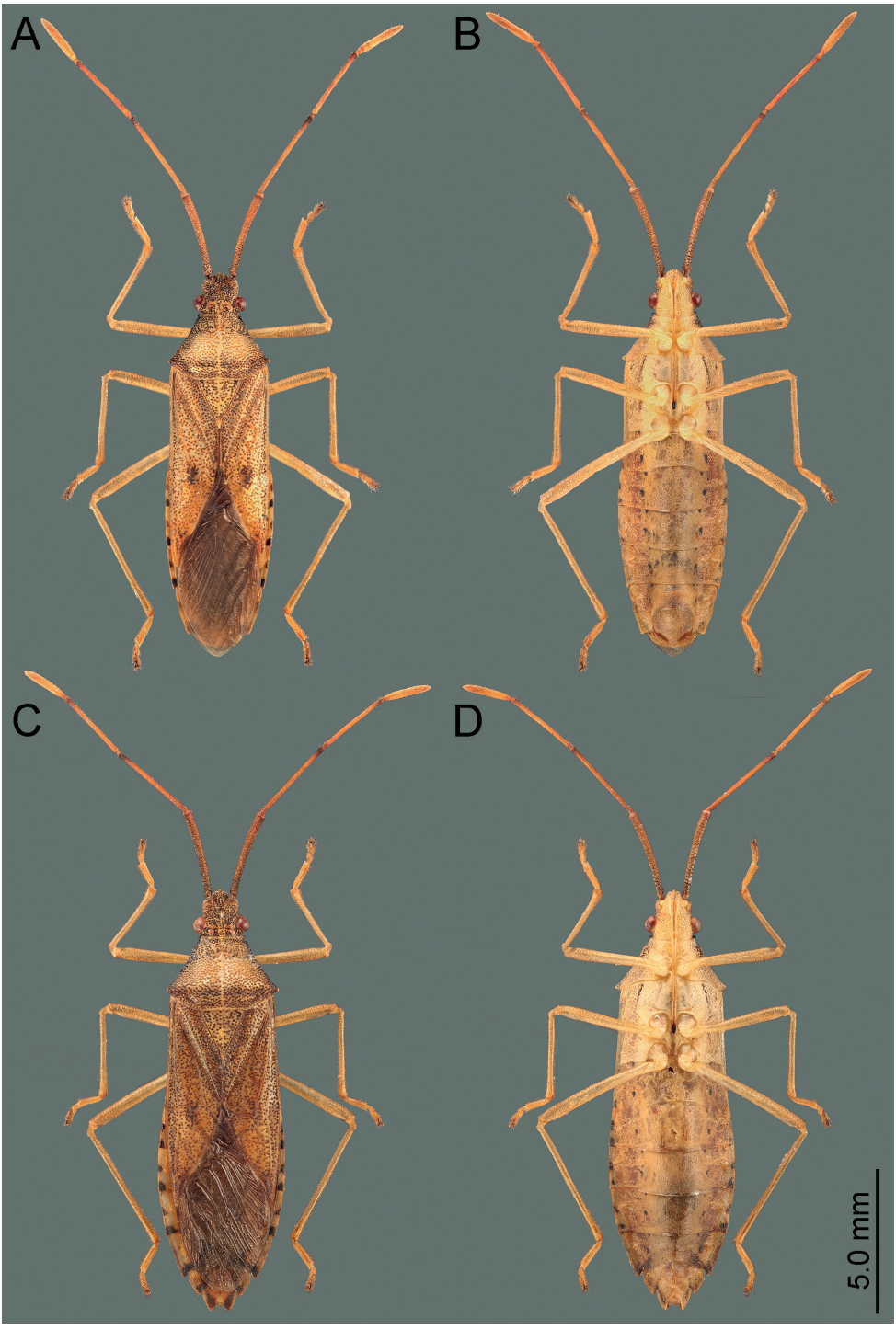

Figure 3. Habitus of *Manocoreus hsiaoi* sp. nov. **A, B** male holotype **A** dorsal view **B** ventral view **C, D** female paratype **C** dorsal view **D** ventral view.

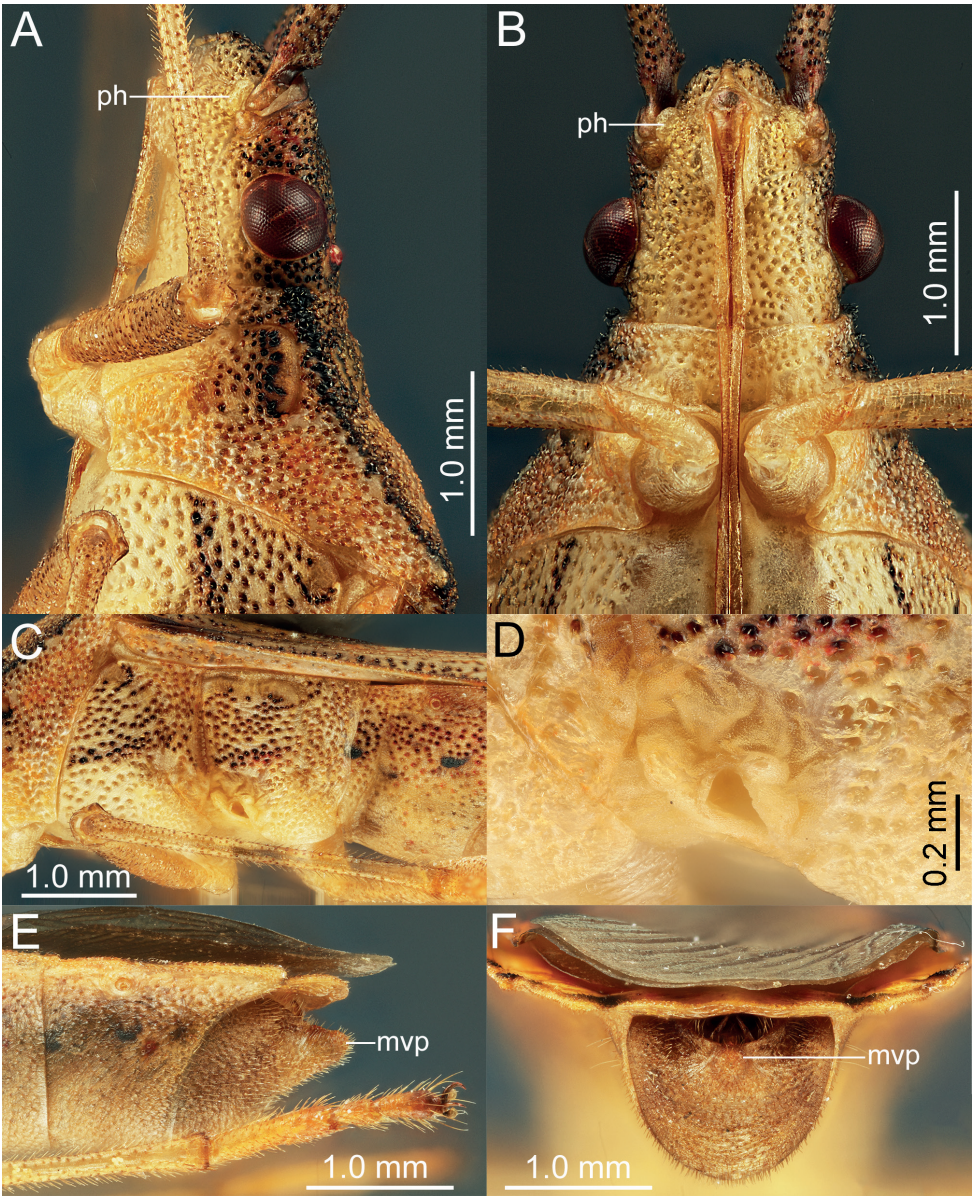

Figure 4. *Manocoreus hsiaoi* sp. nov., male holotype **A, B** head and prothorax A lateral view **B** ventral view **C** meso- and metathorax, lateral view **D** scent gland ostiole and peritreme, lateral view **E, F** terminalia **E** lateral view **F** posterior view. Abbreviations: mvp = median ventroposterior process; ph = process on head in front of antenniferous tubercles.

punctures, central discal region of pronotum with yellow punctures; propleura and prosternum yellow, propleura with black punctures (Fig. 4C); scutellum and corium brownish yellow, with brown to black punctures, meso- and metapleura, and meso- and metasternal yellow, meso- and metapleura with black punctures; legs yellow, only

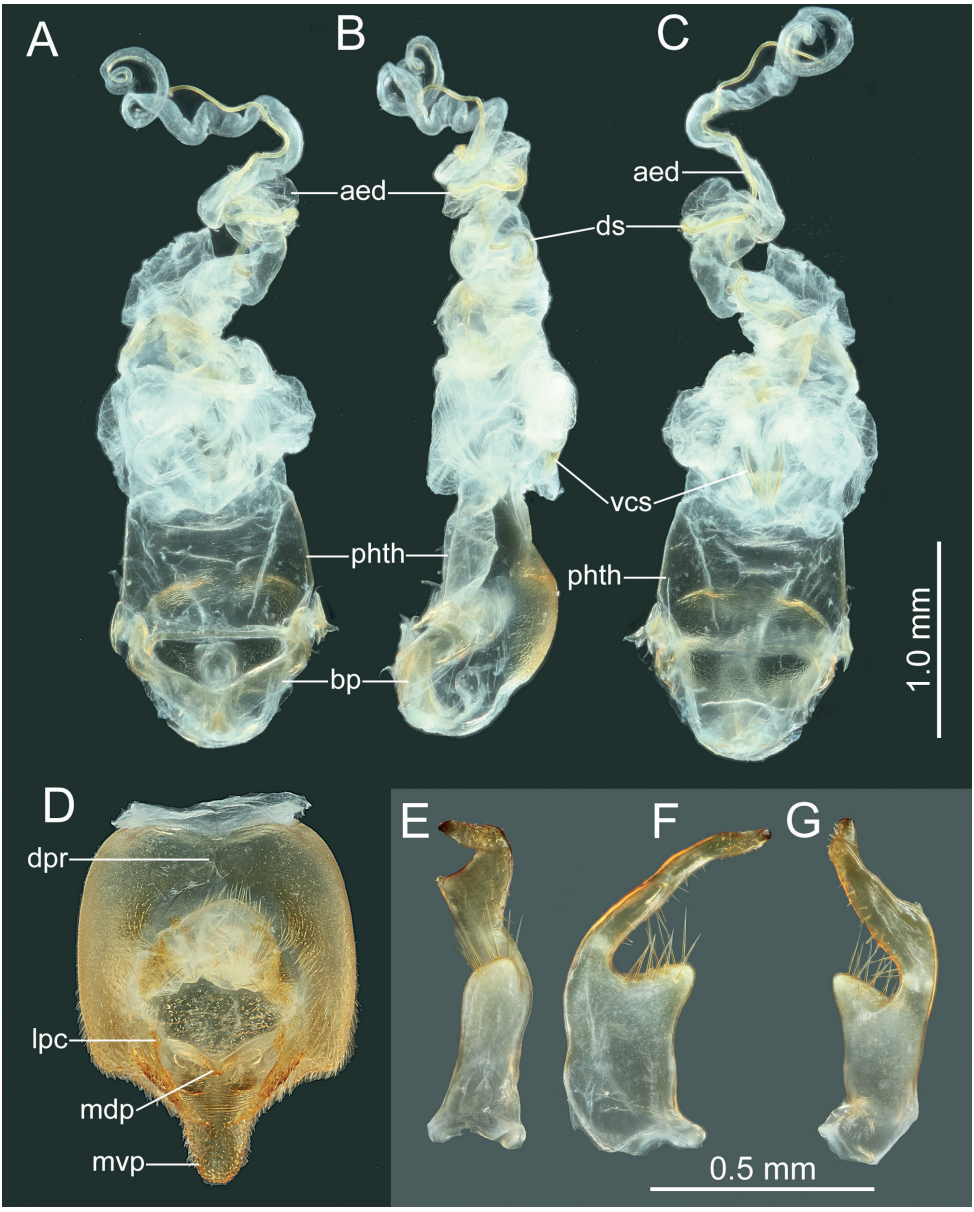

Figure 5. *Manocoreus hsiaoi* sp. nov., male genitalia **A–C** phallus **A** dorsal view **B** lateral view **C** ventral view **D** genital capsule, dorsal view **E–G** right paramere in three different aspects. Abbreviations: aed = aedeagus; bp = basal plates; dpr = dorsoposterior rim; lpc = lateroposterior convexes; mdp = median projection; mvp = median ventroposterior process; phth = phallotheca; vcs = ventral conjunctival sclerites.

apical area of tarsal segment III blackish brown, femora and tibiae of each leg with moderately dense small brownish tubercles, femora, tibiae and tarsi of each leg with short semi-erect setae, setae on apical half of tibiae and tarsi denser; corium with a large and more or less central black spot, membrane grey, basal area darker; middle

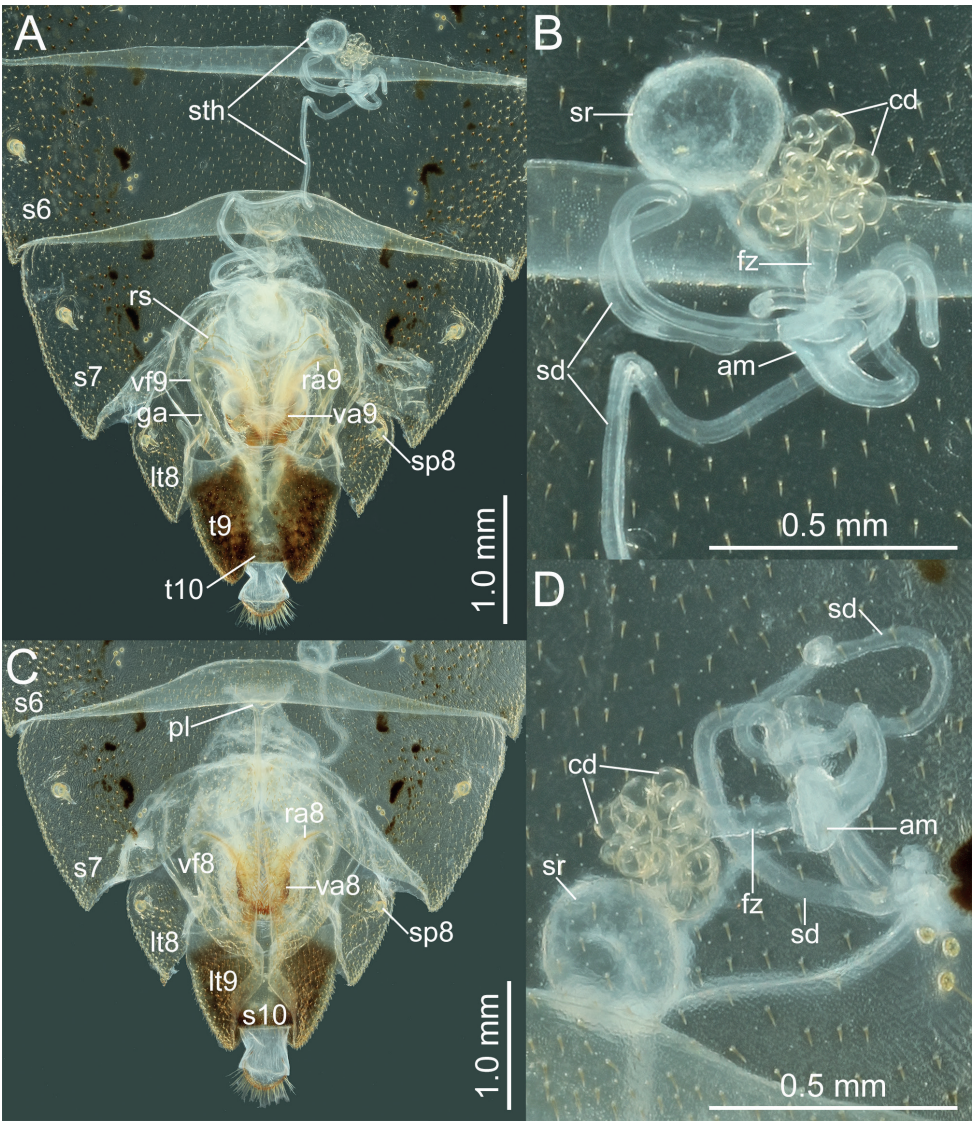

Figure 6. *Manocoreus hsiaoi* sp. nov., female genitalia **A, C** terminalia **A** dorsal view **C** ventral view **B, D** spermatheca in two different aspects. Abbreviations: am = ampulla; cd = coiled duct; ds = duct seminist; fz = flexible zone; ga = gonangulum; lt8, 9 = laterotergites VIII, IX; ra8, 9 = ramus of valvula VIII, IX; rs = ring sclerite; s6, 7, 10 = sternites VI, VII, X; sd = spermathecal duct; sp8 = spiracle VIII; sr = seminal receptacle; sth = spermatheca; t9, 10 = tergites IX, X; va8, 9 = valvulae VIII, IX; vf8, 9 = valvifers VIII, IX.

and apical portion of connexivum of each segment black, venter of abdomen yellowish brown, abdominal terga with a median black spot on each side of segments II–VII; a pair of smaller black spots located near anterior margin of segments III to VII (Fig. 3).

Structures. ***Head.*** Width of head ~ 1.07–1.26× as wide as median length of head, ~ 1.71–1.80 time as wide as interocular distance; antennomere I slightly shorter than antennomere II, ratio of antennomeres I:II:III:IV = 1:1.03:0.84:0.62; apex of labium

surpassing posterior margin of mesocoxae, not reaching to anterior margin of metacoxae. ***Pronotum*** ~ 1.43–1.60× as width across humeral angles as its median length; scutellum ~ 0.96–1.16× as long as its width. Anterior peritreme of metathoracic scent gland slightly larger than protruding posterior peritreme, gyrification of evaporatorium deep (Fig. 4C, D). ***Pregenital abdomen.*** Abdomen oblong, spiracles situated near lateral margin of abdominal sterna III–VII (segments III to VIII in female), before middle line of each segment; sternum VII of male strongly concave medially, length of concave part ~ 1/2 length of sternum VIII in ventral view; in female plica triangular, and partly exposed out of sternum VI, posterior margin of sternum VII sinuated. ***External male genitalia.*** Genital capsule opening dorsally (Fig. 4E, F), dorsoposterior rim wide, median projection conspicuous, triangular (Fig. 5D: mdp), posterior margin of genital capsule broadly sinuate and ventroposterior process median (Fig. 5D: mvp), lateral portion of posterior margin roundly produced on each side (Fig. 5D); dorsal margin of base of paramere near straight, ventral region of base of paramere with triangular lobe (Fig. 5E–G), distal portion sickle-shaped (Fig. 5E–G); phallus with a sclerotized articulatory apparatus (Fig. 5A–C), phallotheca barrel-shaped, unarmed (Fig. 5A–C: phth), conjunctiva rigid and complex, with one pair of membranous processes and a pair of slender, triangular adjacent ventral conjunctival sclerites (Fig. 5B, C: vcs), aedeagus coiled, strongly sclerotized, distal portion tubular, obliquely truncate apically (Fig. 5A–C: aed). ***External female genitalia.*** Laterotergite VIII subtriangular, with sinuate inner margin, spiracles nearer to basal margin than to lateral margin; laterotergites IX subtriangular, posterior portion of inner margin concave (Figs 6C, 14D). Valvifers VIII nearly triangular, posterior portion of outer margin slightly convex (Fig. 6C: vf8); posterior distal portions of valvulae VIII with dense hair-like setae (Fig. 6C: va8); valvifers IX slightly sclerotized (Fig. 6A: vf9); distal portions of valvulae IX strongly sclerotized, sheath-like, downcurved (Fig. 6A: va9); ring sclerite of gynatrium large, slender and curved (Fig. 6A: rs); spermatheca with a conspicuous ampulla subapically, distal area of ampulla expanded, body of ampulla elongate (Fig. 6B, D: am); distal region with relatively long flexible zone (Fig. 6B, D: fz), with sclerotized, tightly tangled coiled duct (Fig. 6B, D: cd), and not distinctly sclerotized seminal receptacle globose (Fig. 6B, D: sr).

Measurements (in mm). Male holotype / male paratypes (n = 5) / female paratypes (n = 4): total body length 13.57 / 12.02–13.64 / 13.65–14.95; head length 1.50 / 1.53–1.66 / 1.55–1.74, maximum width of head across eyes 1.89 / 1.79–1.96 / 1.83–1.99, interocular distance 1.10 / 1.03–1.11 / 1.07–1.11, preocular distance 0.82 / 0.82–0.92 / 0.83–1.00, postocular distance 0.14 / 0.13–0.21 / 0.12–0.22, interocellar distance 0.51 / 0.42–0.53 / 0.51–0.52; length of antennomere I 3.18 / 2.82–3.26 / 2.96–3.16, II 3.28 / 3.00–3.33 / 3.08–3.21, III 2.68 / 2.43–2.70 / 2.44–2.58, IV 1.89 / 1.90–2.02 / 1.74–1.83; pronotum middle length 2.25 / 2.05–2.51 / 2.34–2.53, maximum width across frontal angles 1.57 / 1.43–1.59 / 1.52–1.66, maximum width across humeral angles 3.59 / 3.16–3.58 / 3.58–3.92; scutellum length 1.76 / 1.50–1.58 / 1.60–1.81, scutellum width 1.52 / 1.30–1.58 / 1.52–1.59

Etymology. This specific epithet is dedicated to the memory of Prof. Hsiao Tsai-Yu (1903–1978), founder of the modern Heteroptera research in China (Zheng et al. 1979).

Distribution. China. Guangxi: Xing'an (Fig. 16).

***Manocoreus marginatus* Hsiao, 1964**
Figs 7A–C, 13A, 14E, 15E, 16

Manocoreus marginatus Hsiao, 1964: 92. Holotype: ♂, China, Yunnan, Jinghong; IZCAS. Hsiao (1977): 244 (description, in key, photo), 245 (description, distribution); Ren (1983): 321 (in key), 323, 324 (figs); Zhu and Bu (2005): 182 (catalogue, distribution, description).

Type material examined. ***Holotype*** male labelled: "Xishuangbanna • Yuanjinghong [handwritten in Chinese] / Shihuichang [handwritten in Chinese] /1958.7.1 NO73H [handwritten] // Manocoreus [handwritten] / marginatus [handwritten] / HSIAO [handwritten] / holotype [printed] Hsiao Tsaiyu identified [printed in Chinese] 19 [printed] 63 [handwritten in Chinese]"; NKUM. ***Allotype*** female, labelled: "Xishuangbanna • Damenglong [handwritten in Chinese] / No. 94H [handwritten] /195-VIII-4 [handwritten] // Manocoreus [handwritten] / marginatus [handwritten] / HSIAO [handwritten] / allotype [printed] Hsiao Tsaiyu identified [printed in Chinese] 19 [printed] 63 [handwritten in Chinese]"; NKUM.

Other material examined. China. Yunnan: Xishuangbanna Damenglong, 650 m a.s.l., 6.v.1958, leg. C.P. Hong (1♀ IZCAS), Mengla County Shangyong town, 1–3. viii.2007, leg. L. Shi (1♀ SYSBM).

Remarks. This species is similar to *M. yunnanensis* in habitus, size, and color, but differs in the following characters: lateral margin of pronotum black (Fig. 13A); subcostal margin of forewing black (Fig. 7A); distal portion of median ventroposterior process of the genital capsule with a round upward hook-shaped process in lateral view (see Ren 1983: fig. 29); middle of female sternum VII sharply concave, both sides with round process backward (Fig. 15E).

Distribution. China. Guizhou: Daozhen (Zhu and Bu 2005); **Yunnan:** Xishuangbanna (Fig. 16).

***Manocoreus montanus* Hsiao, 1964**
Figs 7D–F, 13B, 14F, 15F, 16

Manocoreus montanus Hsiao, 1964: 90. Holotype: ♂, China, Sichuan, Mount Emei; NKUM. Hsiao (1977): 244 (description, distribution, in key, photo); Ren (1983): 321 (in key), 323, 324 (figures).

Type material examined. ***Holotype*** male labelled: "Sichuan Emeishan [handwritten in Chinese] / Jiulaodong [handwritten in Chinese] /57.6.15 [handwritten] // Manocoreus [handwritten] / montanus [handwritten] / HSIAO [handwritten] / holotype [printed] Hsiao Tsaiyu identified [printed in Chinese] 19 [printed] 63 [handwritten in Chinese]"; NKUM. ***Allotype*** female, labelled: "Sichuan Emeishan [printed in Chinese] / Jiulaodong [printed in Chinese] 1800 m [printed] / 1957.7.8 [handwritten]

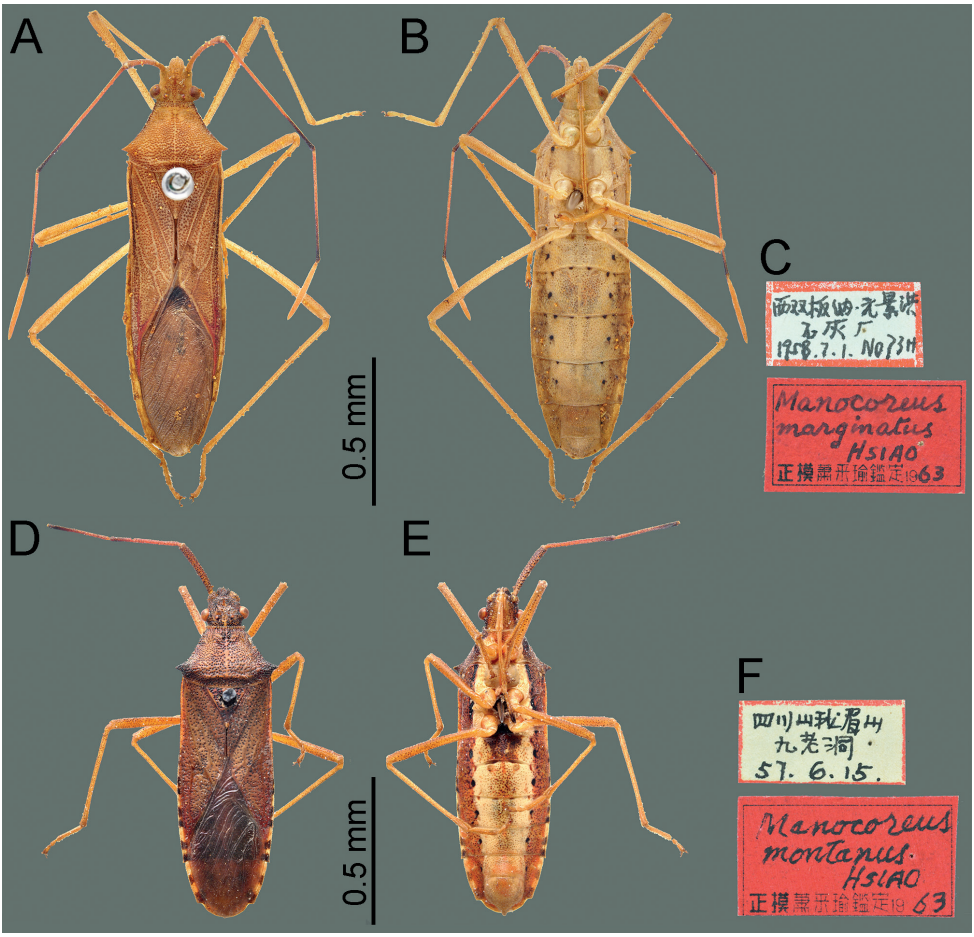

Figure 7. Habitus of *Manocoreus* spp. **A–C** *M. marginatus* male holotype **A** dorsal view **B** ventral view **C** labels **D–F** *M. montanus* male holotype **D** dorsal view **E** ventral view **F** labels.

/Zheng Leyi • Cheng Hanhua [printed in Chinese] // Manocoreus [handwritten] / marginatus [handwritten] / HSIAO [handwritten] / allotype [printed] Hsiao Tsaiyu identified [printed in Chinese] 19 [printed] 63 [handwritten in Chinese]"; NKUM.

Other material examined. China. Sichuan: Emeishan Jiulaodong 1800–1900 m a.s.l., 9.vii.1957, leg. F.X. Zhu (1♂ IZCAS), same but 17.viii.1957, leg. Z.Y. Wang (1♀ IZCAS), same but 19.viii.1957, leg. Z.Y. Wang (1♂ IZCAS), Chudian, 1783 m a.s.l., 28.vi.1957, leg. Z.Y. Wang (1♂ IZCAS), Xixiangchi, 1800–2000 m a.s.l., 30.viii.1957, leg. Y.C. Lu (1♀ IZCAS).

Remarks. This species can be recognized from all other species of *Manocoreus* by the following characteristics: antennomere III dilated apically; lateroventral side of the head, thorax, and abdomen with wide, dark reddish to brownish longitudinal stripe (Fig. 7E); lateral process on posterior margin of genital capsule round (Fig. 14F).

Distribution. China. Sichuan: Emeishan (Fig. 16).

***Manocoreus vulgaris* Hsiao, 1964**
Figs 8A–C, 9, 10, 11, 13C, 14G, 15G, 16

Manocoreus vulgaris Hsiao, 1964: 91. Holotype: ♂, China, Fujian, Chong'an; IZCAS. Hsiao (1977): 244 (description, distribution, in key, photo); Ren (1983): 321 (in key), 323, 324 (figures); Chen et al. (1993): 411 (catalogue, distribution); Ren and Xiong (1993): 189 (catalogue, distribution); Bu et al. (1995): 128 (catalogue, distribution); Liu (1998): 89 (catalogue, distribution); Chen and Li (1999): 128 (catalogue, distribution, description, host plant); Bu and Zheng (2001): 276 (catalogue, distribution); Zhu and Bu (2006): 239 (catalogue, distribution, description);

Manocoreus valgaris: Ren (1983): 321, 323, 324 (in key, figures) [incorrect subsequent spelling].

Type material examined. ***Holotype*** male labelled: "Fujian: Chong'an Xingcun Sangang [printed in Chinese] / 800 [printed] Gongchi [printed in Chinese] / Chinese Academy of Sciences [printed in Chinese] // 196 [printed] •VI•30 [handwritten] / collector: Pu Fuji [printed in Chinese] // IOZ(E) 221824 [printed] // ***Holotype*** [printed] // Manocoreus [handwritten] / vulgaris [handwritten] / HSIAO [handwritten] / holotype Hsiao Tsaiyu identified [printed in Chinese] 19 [printed] 63 [handwritten]"; IZCAS. ***Paratype*** male, labelled: "Fujian: Chong'an Xingcun Sangang [printed in Chinese] / 720–800 [printed] Gongchi [printed in Chinese] / Chinese Academy of Sciences [printed in Chinese] // 196 [printed] 0•VI•30 [handwritten] / collector: Jiang Qiaoyun [printed in Chinese] // ***Paratype*** [printed] / Manocoreus [handwritten] / vulgaris [handwritten] / HSIAO [handwritten]"; NKUM.

Other material examined. China. Fujian: Chong'an Xingcun Sangang, 900–1000 m a.s.l., 7.vii.1960, leg. Y.R. Zhang (1♂ IZCAS), same but 740–910 m a.s.l., 25.v.1960, leg. C.L. Ma (1♂ IZCAS), Chong'an Xingcun Tongmuguan, 850–970 m a.s.l., 8.vii.1960, leg. Y.R. Zhang (1♂ IZCAS), same but 900–1150 m a.s.l., 10.vii.1960, leg. C.L. Ma (1♂ IZCAS), Chong'an Xingcun Guadun, 950–1210 m a.s.l., 12.vi.1960, leg. Y. Zuo (1♀ IZCAS), same but 840–1210 m a.s.l., 21.vi.1960, leg. Y.R. Zhang (1♂ IZCAS), same but 900–1160 m a.s.l., 8.vii.1960, leg. C.L. Ma (1♂ IZCAS), Meihuashan Sanhuicun, 3.v.2004, leg. C.X. Yuan, J. Li (1♂ NKUM); **Guangdong:** Lianzhou City Dadongshan Nature Reserve, 18.vii.2004, leg. X.M. Li (1♀ NKUM), Lianzhou Dadongshan, 13–16.vi.2007, leg. L.L. Huang (1♀ SYSBM), Lianxian [= Lianzhou City] Dadongshan, 30.vii.2007, leg. H.D. Chen (1♀ SYSBM), same but leg. Z.Y. Chen (1♂ SYSBM), same but 3–9.vii.2008, leg. H.D. Chen (1♂ 2♀♀ SYSBM), same but 3–9.vii.2008 leg. Z.Y. Chen (1♂ 2♀♀ SYSBM), same but 3–6.viii.2010, leg. H.D. Chen (2♀♀ SYSBM), same but 3–6.viii.2010, leg. Z.Y. Chen (1♂ 6♀♀ SYSBM), same but 3–6.viii.2010, leg. Z.Y. Chen (1♂ 6♀♀ SYSBM), same but 3–6.viii.2010, leg. W.C. Xie (1♂ 1♀ SYSBM), Nanling Dadongshan, 24.vi.2009, leg. D.D. Fang (1♂ SYSBM), same but 25.vi.2009, leg. X.L. Han (1♂ 2♀♀ SYSBM), same but 22.vi.2009, leg. F.L. Jia (1♂SYSBM); **Guangxi:** Jinxiu Dayaoshan Nature

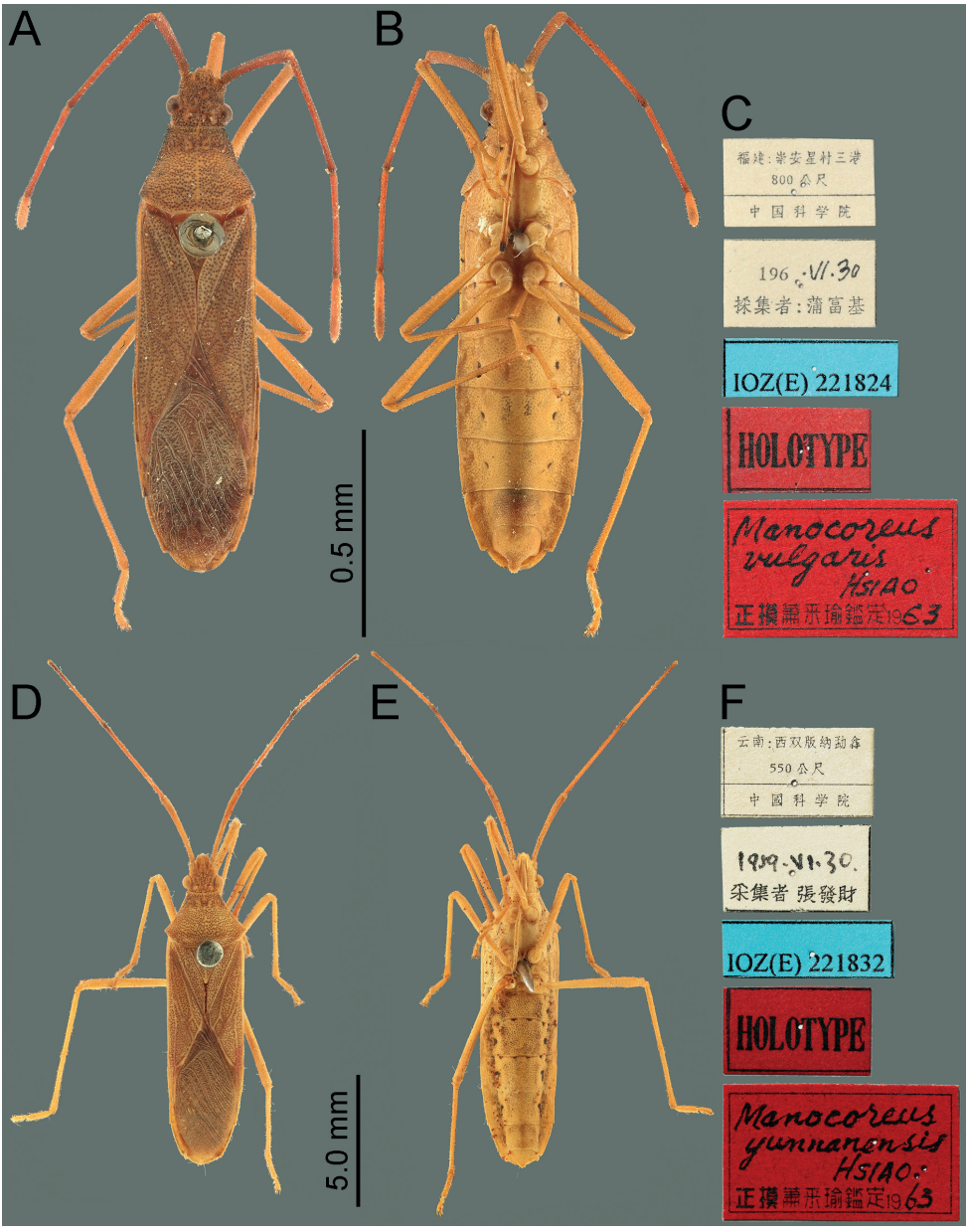

Figure 8. Habitus of *Manocoreus* spp. **A–C** *M. vulgaris* male holotype **A** dorsal view **B** ventral view **C** labels **D–F** *M. yunnanensis* male holotype **D** dorsal view **E** ventral view **F** labels.

Reserve Shengtangshan Protection Station, 780–1200 m a.s.l., 22.vii.2009, leg. Z.H. Fan (1♂ 1♀ NKUM), same but leg. Q. Zhao (1♂ NKUM), same but 1200 m a.s.l., 23.vii.2009, leg. X. Sun (1♀ NKUM), same but 1200 m a.s.l., 23.vii.2009, leg. K. Dang (1♀ NKUM), Jinxiu Dayaoshan Nature Reserve Yinshan Station, 1150 m

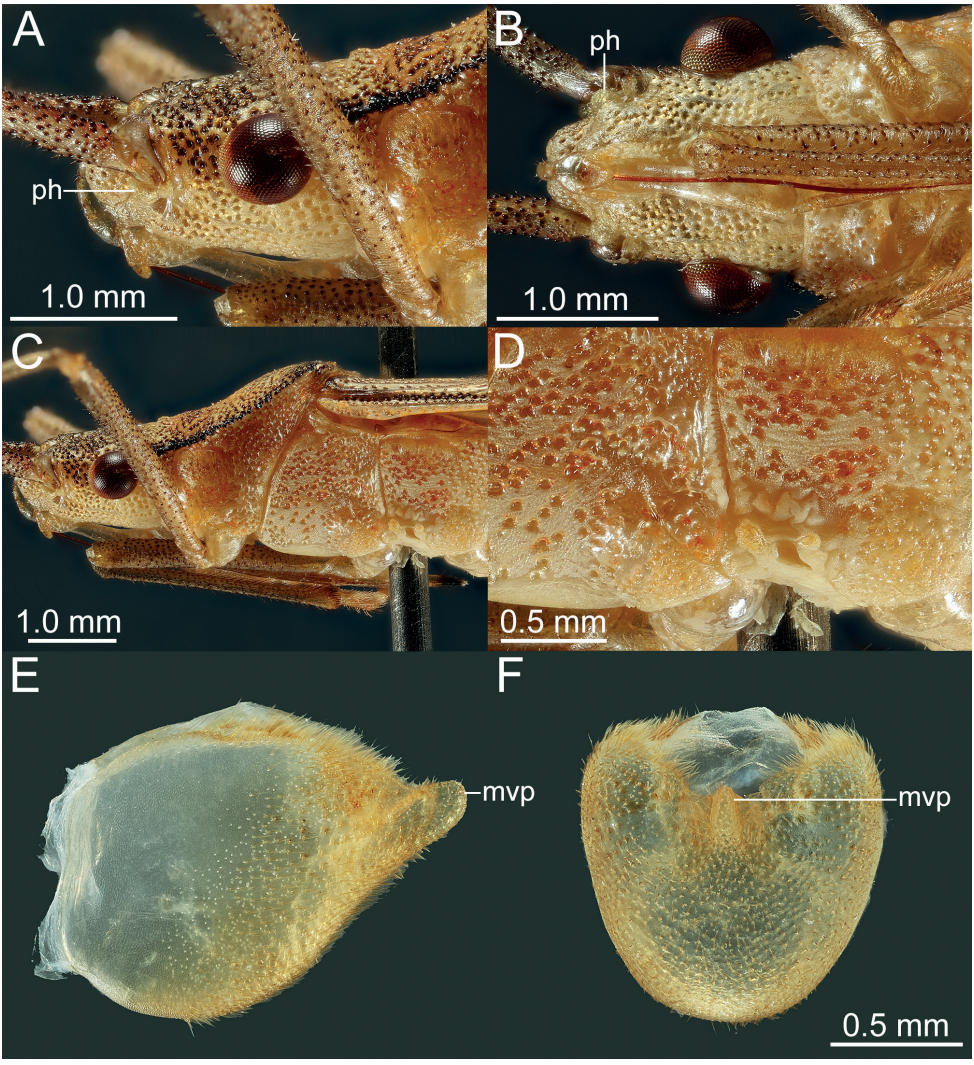

Figure 9. *Manocoreus vulgaris* male non-type specimen **A, B** head **A** lateral view **B** ventral view **C** head and thorax, lateral view **D** scent gland ostiole and peritreme, lateral view **E, F** genital capsule **E** lateral view **F** posterior view. Abbreviations: mvp = median ventroposterior process; ph = process on head in front of antenniferous tubercles.

a.s.l., 25.vii.2009, leg. K. Dang (1♀ NKUM), same but leg. Z.H. Fan (1♂ NKUM), Longsheng Huaping Nature Reserve, 800–1280 m a.s.l., 17.vii.2009, leg. X. Sun (1♀ NKUM), Tianlin Langping Linaoshan, 1400 m a.s.l., 28.v.2002, leg. G.F. Jiang (1♀ NKUM), Tianlin Laoshanlinchang, 1.vi.2002, leg. X.J. Yang (1♂ NKUM); **Guizhou:** Yanhe County Mayanghe Nature Reserve Huangtu township, 607 m a.s.l., 29.vii.2014, leg. X.J. Peng et al. (2♂♂ 2♀♀ IZCAS); **Hunan:** Yizhang Mangshan 1100–1270 m a.s.l., 22.vii.2004, leg. W.B. Zhu (1♂ 4♀♀ NKUM), same but leg. J.L. Li (2♂♂

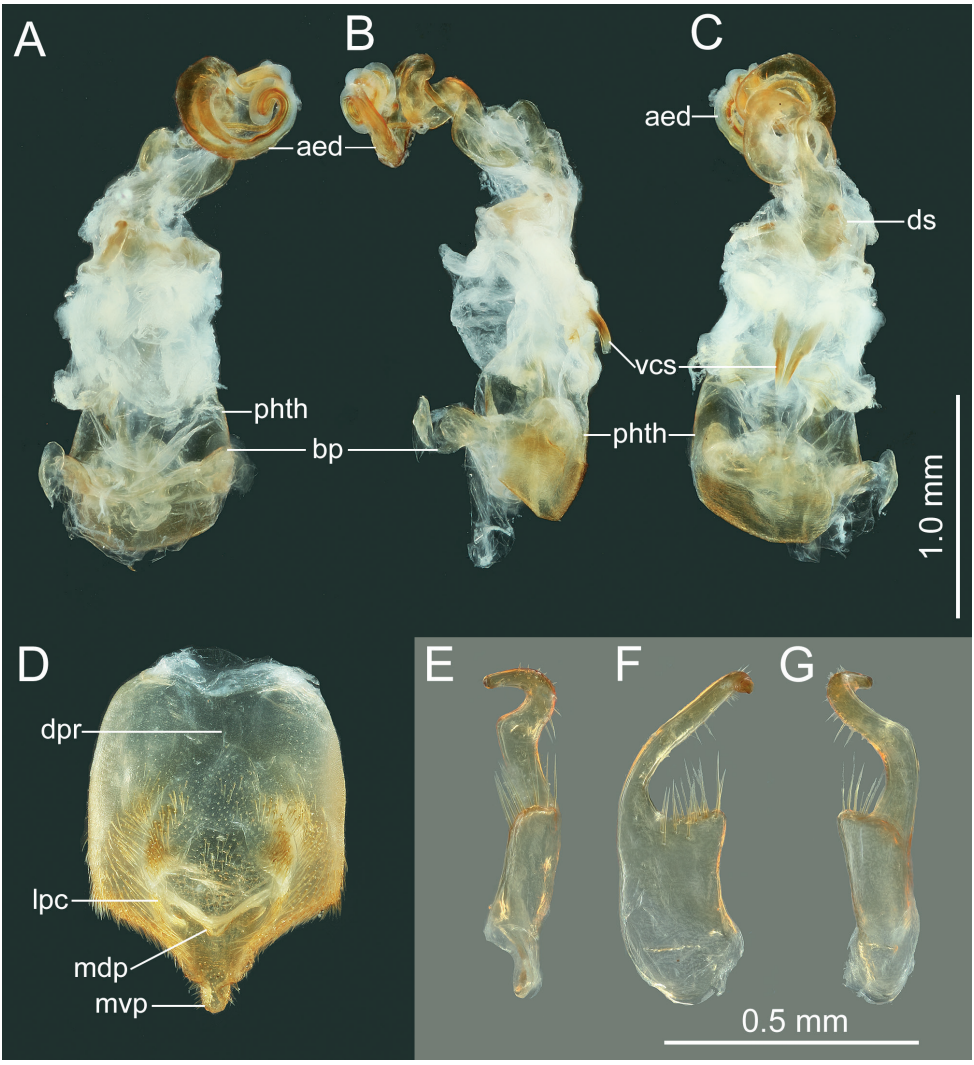

Figure 10. *Manocoreus vulgaris* male non-type specimen, male genitalia **A–C** phallus **A** dorsal view **B** lateral view **C** ventral view **D** genital capsule, dorsal view **E–G** right paramere in three different aspects. Abbreviations: aed = aedeagus; bp = basal plates; dpr = dorsoposterior rim; lpc = lateroposterior convexes; mdp = median projection; mvp = median ventroposterior process; phth = phallotheca; vcs = ventral conjunctival sclerites.

NKUM), same but leg. J.Y. Xu (2♂♂ 1♀ NKUM), same but 1050–1300 m a.s.l., 23.vii.2004, leg. W.B. Zhu (1♀ NKUM), Yizhang County Mangshan Nature Reserve Xuzichong, 487 m a.s.l., 22.viii.2014, leg. H.Q. Yin et al. (2♂♂ IZCAS), Yizhang County Mangshan Nature Reserve Yiping, 750 m a.s.l., 18.viii.2014, leg. H.Q. Yin et al. (1♀ IZCAS), Yanling County Taoyuandong, 660–800 m a.s.l., 16.vii.2004, leg. W.B. Zhu (1♂ NKUM), same but leg. Y.L. Ke (1♀ NKUM), same but 1000

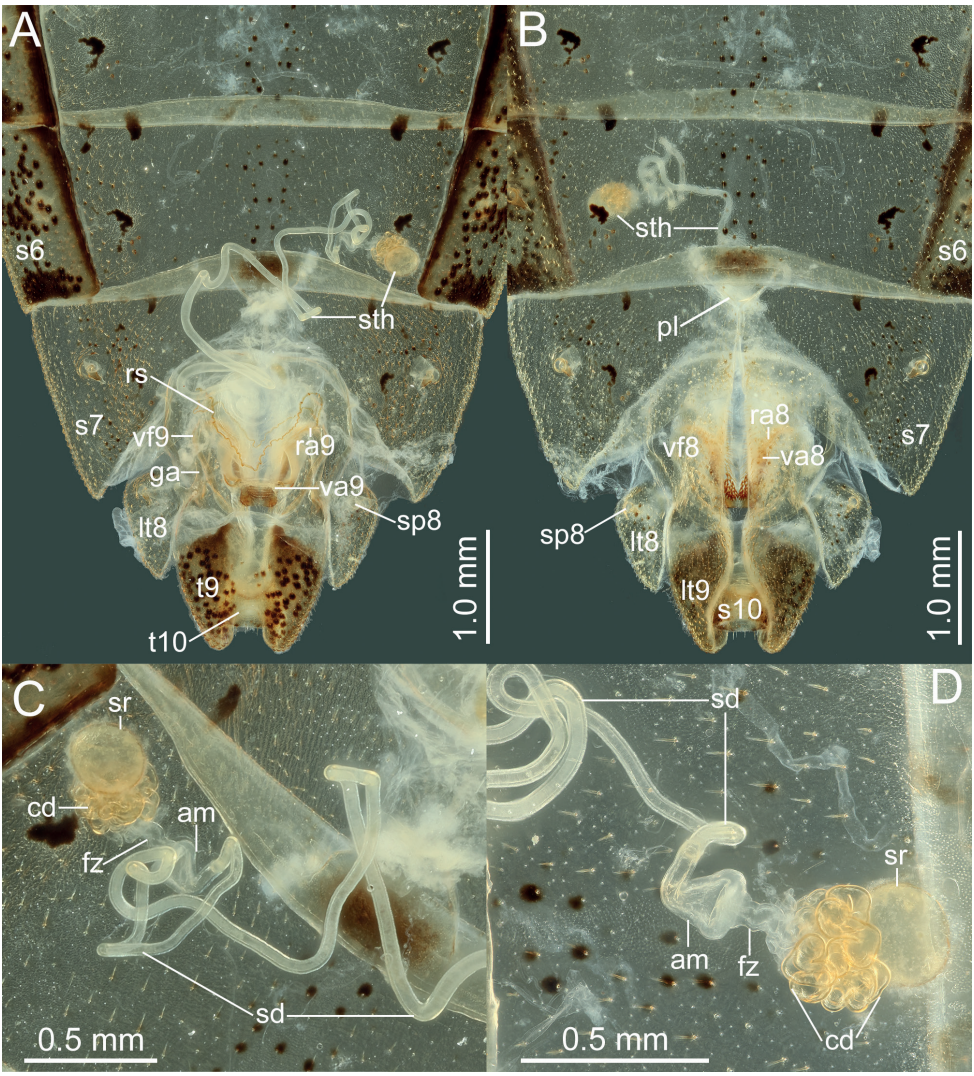

Figure 11. *Manocoreus vulgaris* female non-type specimen, female genitalia **A, C** terminalia **A** dorsal view **B** ventral view **C, D** spermatheca in two different aspects. Abbreviations: am = ampulla; cd = coiled duct; ds = duct seminist; fz = flexible zone; ga = gonangulum; lt8, 9 = laterotergites VIII, IX; ra8, 9 = ramus of valvula VIII, IX; rs = ring sclerite; s6, 7, 10 = sternites VI, VII, X; sd = spermathecal duct; sp8 = spiracle VIII; sr = seminal receptacle; sth = spermatheca; t9, 10 = tergites IX, X; va8, 9 = valvulae VIII, IX; vf8, 9 = valvifers VIII, IX.

m a.s.l., 26.vii.2004, leg. J.L. Li (1♂ NKUM), Hengyang Hengshan, 1030 m a.s.l., 20.vii.2004, leg. J.Y. Xu (1♂ 1♀ NKUM), same but leg. J.L. Li (1♂ NKUM), same but leg. Y. Tian (1♂ NKUM), same but 335–610 m a.s.l., leg. J.Y. Xu (1♂ NKUM), same but leg. J.L. Li (1♀ NKUM), Hengyang Hengshan Tianzhufeng, 1030 m a.s.l., 26.vii.2004, leg. W.B. Zhu (1♂ NKUM), Dong'an County Shunhuangshan, 470–900

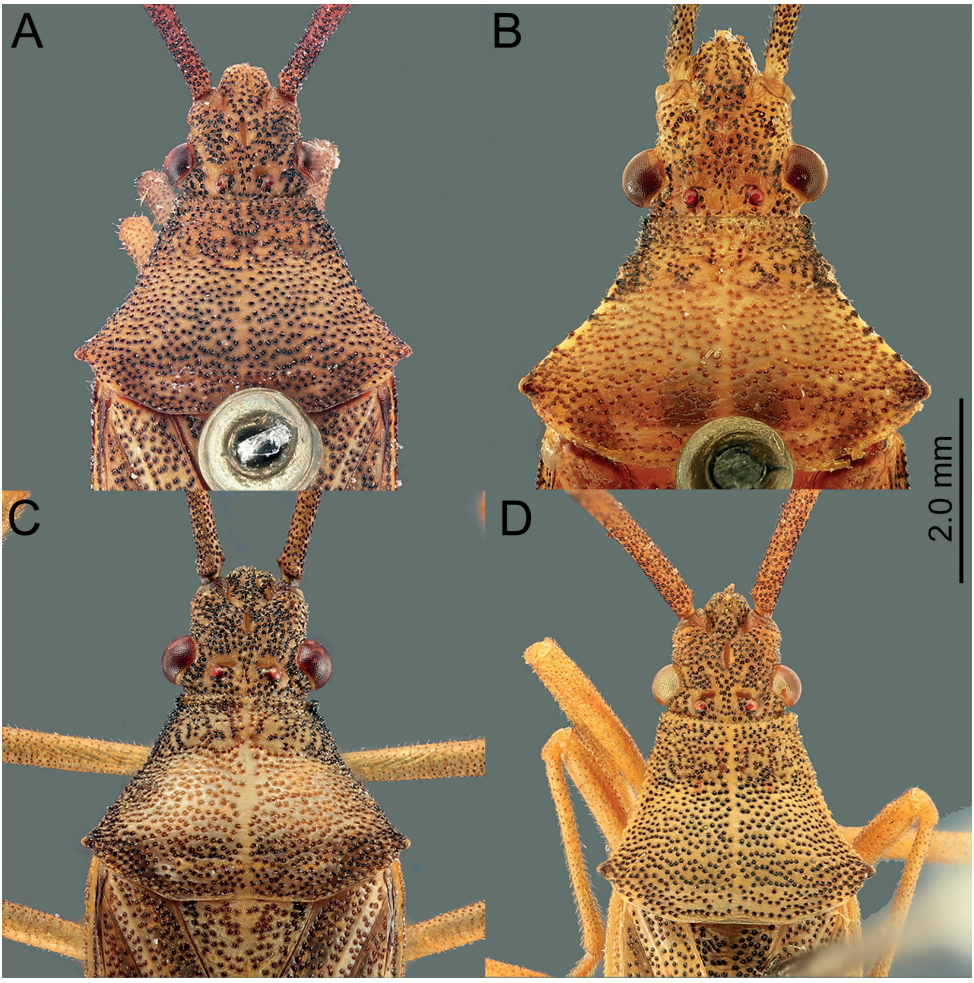

Figure 12. *Manocoreus* spp., head and pronotum, dorsal view **A** *M. astinus* (Ren, 1983) **B** *M. furcatus* (Liu & Ren, 1993) **C** *M. grypidus* (Ren, 1993) **D** *M. hsiaoi* sp. nov.

m a.s.l., 27.vii.2004, leg. J.Y. Xu (1♂ NKUM), Sangzhi County Badagongshan Xiaozhuangping, 1420 m a.s.l., 18.vi.2015, leg. H.B. Liang (1♂ IZCAS), Zhangjiajie City Wulingyuanqu Magongting, 700 m a.s.l., 9.vi.2015, leg. H.B. Liang (1♂ IZCAS); **Jiangxi:** Yifeng Yuanqian, 15.v.1959, (1♂ IZCAS), same but 19.v.1959, (1♀ IZCAS), same but 15.vi.1959, (1♀ IZCAS), same but 21.vi.1959, (1♂ IZCAS), Jinggangshan Zaohemu, 22.vii.2002, leg. H.J. Xue (2♂♂ 1♀ NKUM), Jinggangshan Xiaoxidong, 24.vii.2002, leg. H.J. Xue (1♂ NKUM), Jinggangshan Wuzhifeng Xiaoxidong, 24.vii.2002, leg. X. Yu (1♀ NKUM), Jinggangshan Dabali Forest Farm, 26.vii.2002, leg. J.H. Ding (1♀ NKUM), Jiulianshan Xiagongtang, 5.vii.2002, leg. W.L. Zhang, J.H. Ding (2♂♂ NKUM), Jiulianshan Xiagongtang Pingkeng, 14–15.vii.2002, leg. X. Yu (1♀ NKUM), Jiulianshan Pingkeng, 16.vii.2002, leg. H.J. Xue

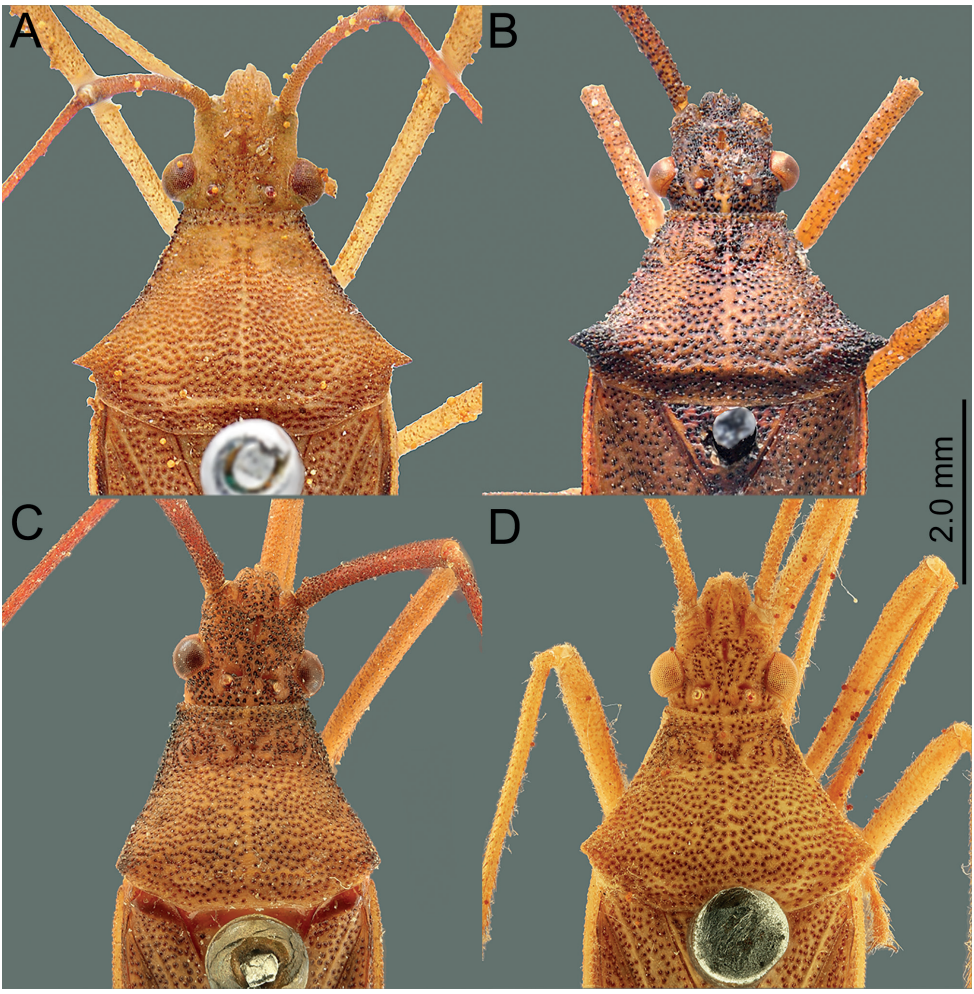

Figure 13. *Manocoreus* spp., head and pronotum, dorsal view **A** *M. marginatus* (Hsiao, 1964) **B** *M. montanus* (Hsiao, 1964) **C** *M. vulgaris* (Hsiao, 1964) **D** *M. yunnanensis* (Hsiao, 1964).

(1♀ NKUM); **Zhejiang:** Lin'an Tianmushan, 300–700 m a.s.l., 8.viii.2007, leg. W.B. Zhu (4♂♂ 5♀♀ NKUM), same but leg. Z.H. Fan (2♂♂ 2♀♀ NKUM), Lin'an Huoshan Dashigu, 400–750 m a.s.l., 9.viii.2007, leg. W.B. Zhu (1♂ 2♀♀ NKUM), Wuyanling, 700 m a.s.l., 3.viii.2007, leg. G.P. Zhu (1♂ 1♀ NKUM).

Remarks. This species can be recognized from all other species of *Manocoreus* by the following characteristics: humeral angles of pronotum rectangular or slightly acute (Fig. 13C); lateral side of head and thorax without black spots or stripes (Figs 8B, 9A–D); median ventroposterior process of genital capsule subtriangular in ventral view (Fig. 14G), lateral processes on posterior margin of genital capsule round in ventral view (Fig. 14G). Based on the examination of a series of specimens distributed from seven provinces of southern China, the morphological characteristics of *Manocoreus vulgaris* has a moderate degree of geographical variation in body

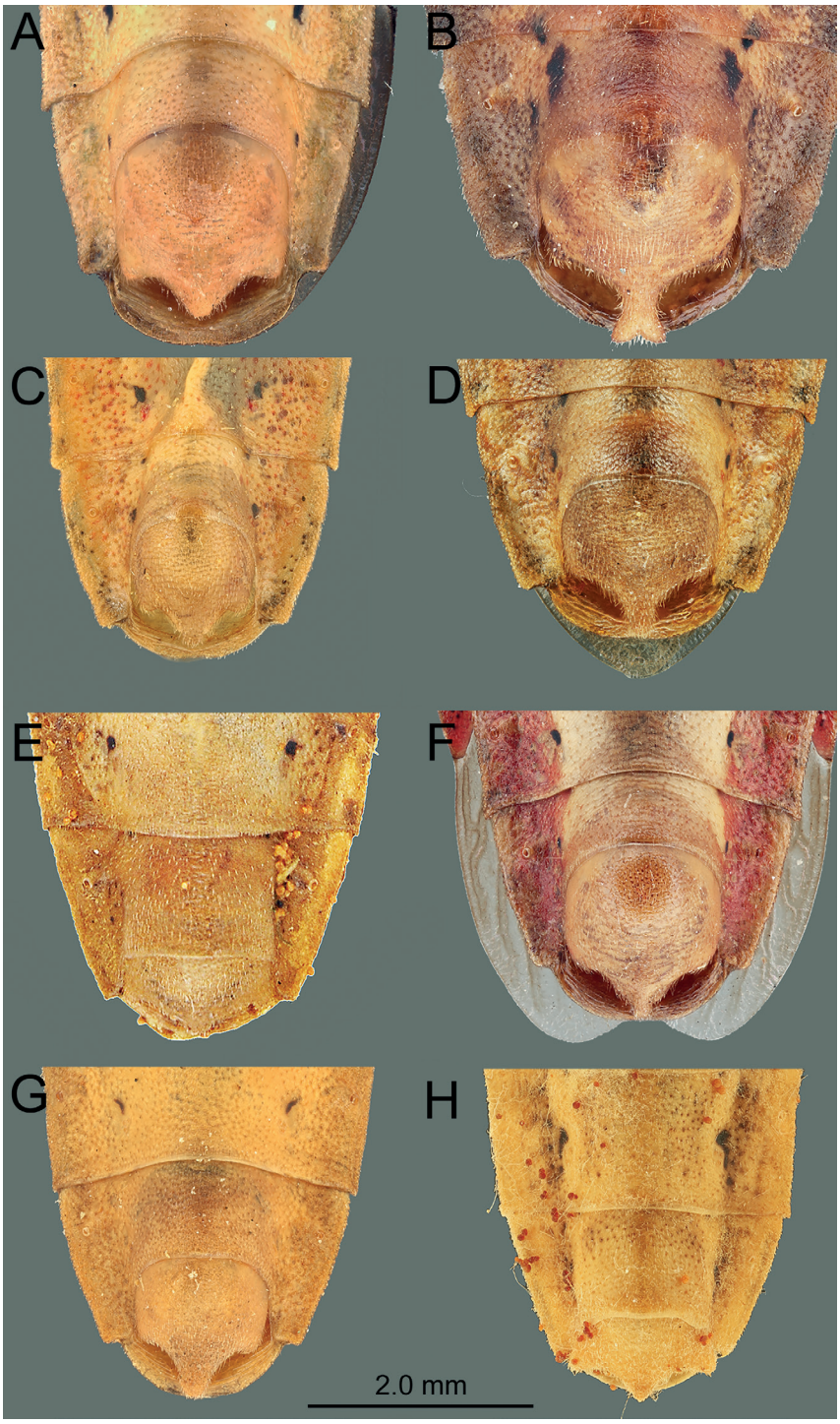

Figure 14. *Manocoreus* spp., male terminalia, ventral view **A** *M. astinus* (Ren, 1983) **B** *M. furcatus* (Liu & Ren, 1993) **C** *M. grypidus* (Ren, 1993) **D** *M. hsiaoi* sp. nov. **E** *M. marginatus* (Hsiao, 1964) **F** *M. montanus* (Hsiao, 1964) **G** *M. vulgaris* (Hsiao, 1964) **H** *M. yunnanensis* (Hsiao, 1964).

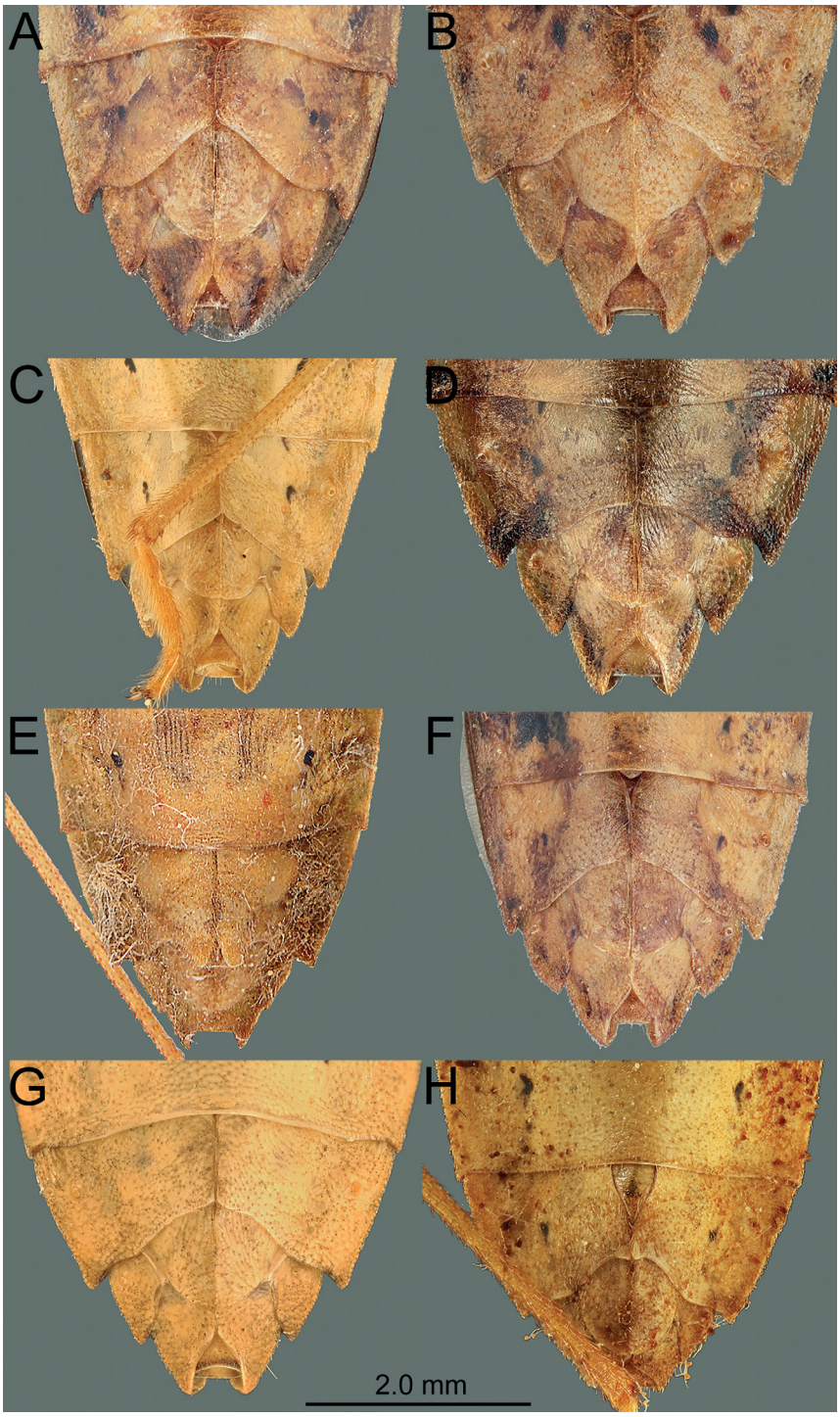

Figure 15. *Manocoreus* spp., female terminalia, in ventral view **A** *M. astinus* (Ren, 1983) **B** *M. furcatus* (Liu & Ren, 1993) **C** *M. grypidus* (Ren, 1993) **D** *M. hsiaoi* sp. nov. **E** *M. marginatus* (Hsiao, 1964) **F** *M. montanus* (Hsiao, 1964) **G** *M. vulgaris* (Hsiao, 1964) **H** *M. yunnanensis* (Hsiao, 1964).

size, coloration, and shape of spine of humeral angles, and all of them are considered in intraspecific range.

Distribution. China. Fujian: Chong'an, Jianyang (Chen et al. 1993, Chen and Li 1999), Longyan, Meihuashan, Shunchang (Chen and Li 1999), Wuyishan (Chen and Li 1999), Youxi (Chen and Li 1999); **Guangdong:** Lianzhou; **Guangxi:** Jinxiu, Longsheng, Tianlin; **Guizhou:** Fanjingshan (Zhu and Bu 2006); **Hunan:** Dong'an, Hengyang, Sangzhi, Yanling, Yizhang, Yongshun (Ren and Xiong 1993), Zhangjiajie; **Jiangxi:** Jinggangshan, Jiulianshan, Yifeng, **Zhejiang:** Baishanzu (Bu, Zheng and Ren 1995), Lin'an, Longwangshan (Liu 1998), Tianmushan, Wuyanling (Fig. 16).

***Manocoreus yunnanensis* Hsiao, 1964**
Figs 8D–F, 13D, 14H, 15H, 16

Manocoreus yunnanensis Hsiao, 1964: 91. Holotype: ♂, China, Yunnan, Xishuangbanna; IZCAS. Hsiao (1977): 244 (description, distribution, in key, photo); Ren (1983): 321 (in key), 323, 324 (figures); Zhu and Bu (2006): 239 (catalogue, distribution, description).

Type material examined. ***Holotype*** male labelled: "Yunnan: Xishuangbanna Mengna [printed in Chinese] / 550 [printed] Gongchi [printed in Chinese] / Chinese Academy of Sciences [printed in Chinese] // 1959•VI•30 [handwritten] / collector Zhang Facai [printed in Chinese] // IOZ(E) 221832 [printed] // HOLOTYPE [printed] // Manocoreus [handwritten] / yunnanensis [handwritten] / HSIAO [handwritten] / holotype Hsiao Tsaiyu identified [printed in Chinese] 19 [printed] 63 [handwritten]"; IZCAS. ***Paratype*** female, labelled: "NO. 59H [handwritten] Xishuangbanna [handwritten in Chinese] / Mengban [handwritten in Chinese] / 1958-6-9 [handwritten] // PARATYPE [printed] / Manocoreus [handwritten] / yunnanensis [handwritten] / HSIAO [handwritten]"; NKUM.

Other material examined. China. Yunnan: Xishuangbanna Damenglong, 650 m a.s.l., 14.iv.1958, leg. Y.R. Zhang (1♂ IZCAS), same but 17.iv.1958, leg. F.J. Pu (1♂ IZCAS), Yunjinghong [= Jinghong], 650 m a.s.l., 8.viii.1958, leg. X.W. Meng (1♂ IZCAS), Jinghong, 30.ix.1979, leg. J.X. Cui (3♂♂ NKUM), Damenglong, 30.ix.1979, leg. H.G. Zou (1♀ NKUM).

Remarks. This species is similar to *M. marginatus* in habitus, size, and color, but differs in the following characters: lateral margin of pronotum not black (Fig. 13D); punctures on the dorsum of head, pronotum, scutellum, and forewings not black (Fig. 8D); forewing concolorous; lateral side of the head, thorax and abdomen with blackish longitudinal stripe (Fig. 8E); distal portion of median ventroposterior process of the genital capsule with a small upward hook-shaped process in lateral view (see Ren 1983: fig. 26); plica of sternite VII not exposed out of sternite VI (Fig. 15H).

Distribution. China. Guizhou: Fanjingshan (Zhu and Bu 2006); **Yunnan:** Xishuangbanna (Fig. 16).

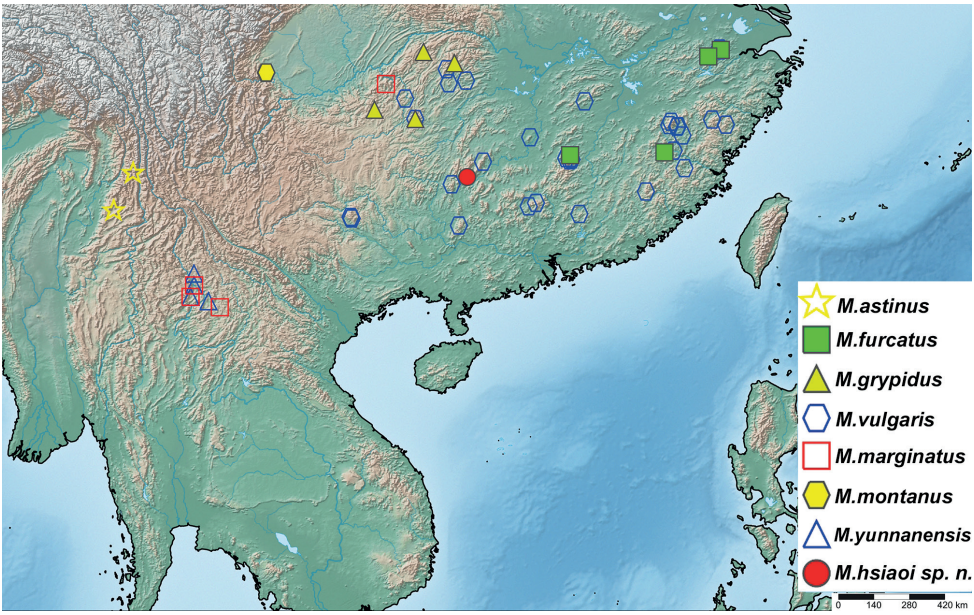

Figure 16. Distribution records of all species of *Manocoreus*.

Key to species of *Manocoreus* Hsiao, 1964

1 Connexivum without black spots (Fig. 7A) **2**
– Connexivum with black spots (Fig. 2C) **3**
2 Subcostal margin of forewing black (Fig. 7A) (body length 13.5–15.5 mm) ..... ***M. marginatus***
– Subcostal margin of forewing not black (Figs 8A) (body length 12.1–14.2 mm) ..... ***M. yunnanensis***
3 Bigger body size, > 15 mm (Fig. 1C–D) (body length 16.0–17.2 mm) ..... ***M. furcatus***
– Smaller body size, ≤ 16 mm **4**
4 Middle of corium without black spot (Fig. 1A) **5**
– Middle of corium with black spot (Fig. 3A, C) **6**
5 Labium surpassing anterior margin of metacoxae (Fig. 1B); median ventroposterior process of genital capsule triangular from ventral view (Fig. 14A) (body length 13.5–15.0 mm) ..... ***M. astinus***
– Labium not reaching anterior margin of metacoxae (Fig. 8B); median ventroposterior process of genital capsule long triangular from ventral view (Fig. 14G) (body length 12.5–14.0 mm) ..... ***M. vulgaris***
6 Lateral margin of pronotum black (Figs 4A, 12D) (body length 12.02–14.95 mm) ..... ***M. hsiaoi* sp. nov.**
– Lateral margin of pronotum pale (Fig. 2A) **7**
7 Antennomere III not dilated apically (body length 11.5–13.0 mm) ..... ***M. grypidus***
– Antennomere III dilated apically (body length 11.1–12.5 mm) ..... ***M. montanus***

Discussion

According to the only cladistic analysis based on morphological data which included Manocoreini, Manocoreini was the sister group of Gonocerini (Li 1997). Based on our examinations of specimens of these two tribes, Manocoreini has the following characteristics that are significantly different from the latter: (1) head with a small dentate or plate-like process in front of antenniferous tubercles, whereas without such process in Gonocerini; (2) plica of female sternum VII with triangular, or rectangular depression, covered by sternum VI, whereas the posterior margin of plica depressed and near the anterior margin of sternum VII in Gonocerini; (3) genital capsule has median ventroposterior process, whereas the posterior margin of genital capsule concave in Gonocerini; (4) basiconjunctivum moderately sclerotized, whereas strongly sclerotized in Gonocerini. According to recent seminal research on the morphology of spermatheca in Coreidae (Pluot-Sigwalt and Moulet 2020), the spermatheca of coreids was divided into three types (I, II, III), and type III could be subdivided into four subtypes (A, B, C, D). Based on our study, the spermatheca of Manocoreini belongs to type III, subtype A, and is closely related to Dasynini, Gonocerini, and Homoeocerini. Some recent molecular phylogenetic studies show that Manocoreini is closely related to Dasynini, Homoeocerini, Mictini, and Coreini (Ye et al. 2022) or Gonocerini and Coreini (Tian et al. 2023). Although Manocoreini can be clearly distinguished morphologically, their phylogenetic relationship still needs to be further verified by adding more molecular and biological evidences.

In the genus *Manocoreus*, *M. marginatus* and *M. yunnanensis* are closer in morphology than other species, such as having slender antenna (Figs 7A, B, 8D–F), posterior margin of male sternum VII concave ~ 1/3 in ventral view (Fig. 13E, H), and middle of female sternum VII sharply concave, both sides with process backward (Fig. 14E, H). More morphological and molecular evidences are needed to figure out the phylogenetic relationship and phylogeographical pattern of the species in this genus.

Acknowledgements

We express our sincere thanks to Prof. Jun Chen, Ms. Hong Liu, and Dr. Chunyan Jiang (IZCAS) for providing access to specimens and Dr. Jiuyang Luo (SYSU) for the warm help in examining specimens and preparing the manuscript. We are also grateful to Dr. Pierre Moulet (Muséum Requien, Avignon) Dr. Hélcio R Gil-Santana (IOC), and Dr. Petr Kment (NMPC) for reviewing the manuscript and providing valuable comments and constructive suggestions. This study was supported by the GDAS Special Project of Science and Technology Development (grant nos. 2021GDASYL-20210103055, 2020GDASYL-20200301003, 2020GDASYL-20200102021).

References

Bergroth E (1913) Supplementum catalogi Heteropterorum bruxellensis (II). Coreidae, Pyrrhocoridae, Colobathristidae, Neididae. Mémoires de la Société Entomologique de Belgique 22: 125–183.

Brailovsky H (2007a) A revision of the tribe Gonocerini from Australia (Hemiptera: Heteroptera: Coreidae: Coreinae). Zootaxa 1530(1): 1–18. https://doi.org/10.11646/zootaxa.1530.1.1

Brailovsky H (2007b) A new genus and two new species of Dasynini (Hemiptera: Heteroptera: Coreidae) from Madagascar. Proceedings of the Entomological Society of Washington 109(4): 847–855.

Bu WJ, Zheng LY (2001) Hemiptera: Coreidae, Rhopalidae, Alydidae. In: Wu H, Pan CW (Eds) Insects of Tianmushan National Nature Reserve. Science Press, Beijing, 274–277. [in Chinese]

Bu WJ, Zheng LY, Ren SZ (1995) Hemiptera: Coreidae, Alydidae and Rhopalidae. In: Wu H (Ed.) The Series of the Bioresources Expedition to the Baishanzu Mountain Nature Reserve: Insects of Baishanzu Mountain, Eastern China. China Forestry Publishing House, Beijing, 127–129. [in Chinese]

Chen SL, Li YG (1999) Coreidae. In: Huang BK (Ed.) Fauna of Insects of Fujian Province of China (Vol. 2). Fujian Science & Technology Publishing House, Fuzhou, 113–136. [in Chinese]

Chen SL, Li YG, Lin QY (1993) Coreidae. In: Zhao XF (Ed.) Collection of Scientific Investigation Reports of Wuyishan Nature Reserve (Wuyishan Ziran Baohuqu Kexue Kaocha Baogaoji). Fujian Science & Technology Publishing House, Fuzhou, 409–412. [in Chinese]

Dolling WR (2006) Coreidae. In: Aukema B, Rieger C (Eds) Catalogue of Palearctic Heteroptera Pentatomomorpha II. Netherlands Entomological Society, Amsterdam, 43–101.

Hsiao TY (1964) New Coreidae (Hemiptera, Heteroptera) from China II. Acta Zoologica Sinica 16(1): 89–100. [in Chinese, with English summary]

Hsiao TY (1977) Coreinae. In: Hsiao TY, Ren SZ, Zheng LY (Eds) A Handbook for the Determination of the Chinese Hemiptera-Heteroptera (Vol. 1). Science Press, Beijing, 214–252. [in Chinese, with English summary]

Li XZ (1996) Comparative morphological study of Coreidae (Heteroptera, Coreoidea) II. Zoological Research 17(2): 97–102. [in Chinese]

Li XZ (1997) Cladistic analysis of the phylogenetic relationships among the tribal rank taxa of Coreidae (Hemiptera, Heteroptera, Coreoidea). Acta Zootaxonomica Sinic 22(1): 60–68. [in Chinese, with English Abstract]

Liu Q (1998) Hemiptera. In: Wu H (Ed.) The Series of the Bioresources Expedition to the Longwangshan Nature Reserve: Insects of Longwangshan Nature Reserve. China Forestry Publishing House, Beijing, 86–94. [in Chinese]

Liu GQ, Ren SZ (1993) Hemiptera: Coreoidea. In: Huang CM (Ed.) The Series of the Bioresources Expedition to the Longqi Mountain Nature Reserve: Animals of Longqi Mountain. China Forestry Publishing House, Beijing, 106–139. [in Chinese]

Pluot-Sigwalt D, Moulet P (2020) Morphological types of spermatheca in Coreidae: bearing on intra-familial classification and tribal-groupings (Hemiptera: Heteroptera). Zootaxa 4834(4): 451–501. https://doi.org/10.11646/zootaxa.4834.4.1

Ren SZ (1983) Notes on the genus *Manocoreus* Hsiao from China (Heteroptera: Coreidae). Entomotaxonomia 5(4): 321–325. [in Chinese, with English summary]

Ren SZ (1992) Hemiptera: Coreoidea. In: Chen SX (Ed.) The Series of the Scientific Expedition to the Hengduan Mountains, Qinghai-Xizang Plateau: Insects of the Hengduan Mountains Region (Vol. 1). Science Press, Beijing, 135–146. [in Chinese]

Ren SZ (1993) New species of Coreidae from Wuling Mountains, China (Hemiptera: Heteroptera). Acta Zootaxonomica Sinica 18(3): 344–352. [in Chinese, with English summary]

Ren SZ, Xiong J (1993) Hemiptera: Coreidae. In: Huang FS (Ed.) Serial Publications of the Bioresources Survey and Evaluation Conducted by Chinese Academy of Sciences: Insects of Wuling Mountains area, southwestern China. Science Press, Beijing, 186–190. [in Chinese]

Tian XK, Li YQ, Chen Q, Chen QQ (2023) Mitogenome of the leaf-footed bug *Notobitus montanus* (Hemiptera: Coreidae) and a phylogenetic analysis of Coreoidea. PLoS ONE 18(2): e0281597. https://doi.org/10.1371/journal.pone.0281597

Ye F, Kment P, Rédei D, Luo JY, Wang YH, Kuechler SM, Zhang W-W, Chen P-P, Wu H-Y, Wu Y-Z, Sun X-Y, Ding L, Wang Y-R, Xie Q (2022) Diversification of the phytophagous lineages of true bugs (Insecta: Hemiptera: Heteroptera) shortly after that of the flowering plants. Cladistics 38(4): 403–428. https://doi.org/10.1111/cla.12501

Yi WB, Bu WJ (2015) Contributions to the tribe Leptocorisini, with descriptions of *Planusocoris schaeferi* gen. & sp. nov. (Hemiptera: Alydidae). Zootaxa 4040(3): 401–420. https://doi.org/10.11646/zootaxa.4040.4.1

Zheng LY, Ren SZ, Zou HG (1979) Reminiscences of Dr. Hsiao Tsai-Yu. Entomotaxonomia (02): e141. [120] [in Chinese]

Zhou YY, Rédei D (2020) From lanceolate to plate-like: Gross morphology, terminology, and evolutionary trends of the trichophoran ovipositor. Arthropod Structure & Development 54: e100914. https://doi.org/10.1016/j.asd.2020.100914

Zhu WB, Bu WJ (2005) Hemiptera: Coreidae, Rhopalidae and Alydidae. In: Yang MF, Jin DC (Eds) Insects from Dashahe Nature Reserve of Guizhou. Guizhou Peoples Publishing House, Guiyang, 181–184. [in Chinese]

Zhu WB, Bu WJ (2006) Coreidae, Rhopalidae and Alydidae. In: Li ZZ, Jin DC (Eds) Fanjingshan Jingguan Kunchong. Guizhou Science and Technology Publishing House, Guiyang, 236–241. [in Chinese]

ZooKeys 1152: 163–204 (2023)
doi: 10.3897/zookeys.1152.96058
https://zookeys.pensoft.net

RESEARCH ARTICLE

A peer-reviewed open-access journal
ZooKeys
Launched to accelerate biodiversity research

A new genus and a new species of wasp-mimicking Harpactorini (Hemiptera, Heteroptera, Reduviidae, Harpactorinae), with an updated key to the Neotropical genera

Hélcio R. Gil-Santana[1], Jader Oliveira[2,3]

1 *Laboratório de Diptera, Instituto Oswaldo Cruz, Av. Brasil, 4365, 21040-360, Rio de Janeiro, RJ, Brazil* **2** *Universidade de São Paulo, Faculdade de Saúde Pública, Laboratório de Entomologia em Saúde Pública, São Paulo, SP, Brazil* **3** *Laboratório de Parasitologia, Universidade Estadual Paulista "Julio de Mesquita Filho", Faculdade de Ciências Farmacêuticas UNESP/FCFAR, Rodovia Araraquara Jaú, KM 1, 14801-902, Araraquara, SP, Brazil*

Corresponding author: Hélcio R. Gil-Santana (helciogil@uol.com.br; helciogil@ioc.fiocruz.br)

Academic editor: Nikolay Simov | Received 6 October 2022 | Accepted 22 December 2022 | Published 9 March 2023

https://zoobank.org/F2B80B9C-09A8-41F8-9E09-A31E58928A75

Citation: Gil-Santana HR, Oliveira J (2023) A new genus and a new species of wasp-mimicking Harpactorini (Hemiptera, Heteroptera, Reduviidae, Harpactorinae), with an updated key to the Neotropical genera. ZooKeys 1152: 163–204. https://doi.org/10.3897/zookeys.1152.96058

Abstract

Quasigraptocleptes maracristinae **gen. nov.**, **sp. nov.** (Hemiptera, Heteroptera, Reduviidae, Harpactorinae, Harpactorini) is described based on male and female specimens from Brazil. Photographs and comments about the syntypes of *Myocoris nigriceps* Burmeister, 1835, *Myocoris nugax* Stål, 1872, *Myocoris tipuliformis* Burmeister, 1838 and *Xystonnytus ichneumoneus* (Fabricius, 1803) are presented. The intra-specific variability and sexual dimorphic characteristics among specimens of *Q. maracristinae* **sp. nov.** are recorded. General characteristics of *Hiranetis* Spinola, 1837, *Graptocleptes* Stål, 1866, *Quasigraptocleptes* **gen. nov.** and *Parahiranetis* Gil-Santana, 2015, which seem to be closer genera, are compared, including those of the male genitalia of some species. A key to the species of *Myocoris* Burmeister, 1835, and an updated key to Neotropical wasp-mimicking Harpactorini genera are provided.

Keywords

Graptocleptes, *Hiranetis*, *Parahiranetis*, sexual dimorphism, wasp mimicry

Introduction

The subfamily Harpactorinae has the largest number of genera and species of Reduviidae (Hemiptera, Heteroptera) and is represented by the tribes Apiomerini and Harpactorini in the Neotropical region (Gil-Santana et al. 2015). Harpactorini is the most diverse group within Reduviidae with about 52 genera in the Neotropics (Forero 2011; Gil-Santana 2015; Gil-Santana et al. 2015, 2017; Forero and Mejía-Soto 2021). Several taxa of this tribe are recognized as being involved in mimicry systems with Hymenoptera, resembling bees or wasps in general body and wing coloration as well as characteristics of physical proportions (Champion 1899; Haviland 1931; Elkins 1969; Maldonado and Lozada 1992; Hogue 1993; Leathers and Sharkey 2003; Gil-Santana 2008, 2015, 2016, 2022; Gil-Santana et al. 2013, 2015, 2017; Castro-Huertas and Forero 2021). Maldonado and Lozada (1992) presented a key to Neotropical wasp-mimicking Harpactorinae genera, which in their view helps to quickly sort out specimens from unidentified material, although this is a somewhat artificial way of grouping genera. Gil-Santana (2015) has updated their key, including two additional genera to it, *Coilopus* Elkins, 1969 and *Parahiranetis* Gil-Santana, 2015. Among the genera presented in this key, while *Coilopus* is regarded as mimicking species of Vespidae (Elkins 1969; Forero and Giraldo-Echeverry 2015), the remaining genera are considered as mimetic of Braconidae and/or Ichneumonidae and in need of a comprehensive revision in order to clarify their systematics (Gil-Santana et al. 2015). For most of the genera included in this group, more recent works have described or redescribed them or at least some of their species, providing figures and more comprehensive descriptions, allowing a better knowledge of their characteristics as follows: *Acanthischium* Amyot & Serville, 1843 (Castro-Huertas and Forero 2021), *Coilopus* (Elkins 1969; Gil-Santana and Forero 2009; Forero and Giraldo-Echeverry 2015), *Graptocleptes bicolor* (Burmeister, 1838) (Gil-Santana et al. 2013), *Hiranetis* Spinola, 1837 (Gil-Santana 2016), *Neotropiconyttus* Kirkaldy, 1909 (Maldonado and Lozada 1992), and *Parahiranetis* Gil-Santana, 2015 (Gil-Santana 2015; Gil-Santana et al. 2017). However, in regard to *Myocoris* Burmeister, 1835 and *Xystonyttus* Kirkaldy, 1909, there are no published images of their species, and the information about their characteristics are restricted to short original descriptions or their mentioning in diagnosis or keys (e.g., Stål 1872; Maldonado and Lozada 1992). It is noteworthy that among other genera of Harpactorini, such as *Zelus* Fabricius, 1803, there are some species that are considered as being similar to braconids, e.g., *Zelus vespiformis* Hart, 1987 and *Z. errans* Fabricius, 1803, while most of the other numerous species of the same genus are not (Zhang et al. 2016). Therefore, only those genera mentioned before, in which all or most of the known included species have been recognized as wasp-mimetic (Maldonado and Lozada 1992; Gil-Santana 2015), will be considered as such for the purpose of our study.

Most authors have only mentioned or given attention to the pattern of yellowish or straw-colored hemelytra with a median transverse black band, in relation to the alleged mimicry between Harpactorini and certain Ichneumonidae and Braconidae, as models (Champion 1899; Haviland 1931; Maldonado and Lozada 1992; Hogue

1993; Leathers and Sharkey 2003; Hespenheide 2010; Zhang et al. 2016). However, Gil-Santana (2015) and Gil-Santana et al. (2017) emphasized that other wasp-mimicking Harpactorini, like *Parahiranetis salgadoi* Gil-Santana, 2015, show a pattern of darkened to reddish general coloration with yellowish 'pterostigmata' on the hemelytra, which is similar to the similar coloration exhibited in the forewings by several other species of Ichneumonidae and Braconidae. This pattern was also observed for instance in *Graptocleptes bicolor* (Burmeister, 1838), *G. haematogaster* (Stål, 1860), and an undescribed species of *Hiranetis* Spinola, 1840 (Gil-Santana 2016; Gil-Santana et al. 2017). Yet, in some other species of wasp-mimicking Harpactorini, the hemelytra are almost or completely dark, such as in *Hiranetis atra* Stål, 1872 (Gil-Santana 2016). Another common feature among all these species with a darkened general coloration on the hemelytra, with or without yellowish 'pterostigmata', is the presence of pale bands on the middle and hind femora (Gil-Santana 2015, 2016).

A variable degree of intraspecific variation in color, occasionally at extreme range, was documented in many harpactorines (e.g., Stål 1872; Champion 1899; Gil-Santana 2008, 2022; Zhang et al. 2016; Forero and Mejía-Soto 2021), including in some wasp-mimicking Harpactorini (Champion 1899; Gil-Santana et al. 2013, 2017). However, at least in the species with the pattern of darkened or blackish hemelytra with yellowish pterostigmata, there is no variation in this pattern. The yellowish pterostigmata are always present (e.g., Gil-Santana et al. 2013, 2017).

Numerous species of Harpactorini have shown sexual dimorphism. In several species belonging to *Zelus* Fabricius, 1803, for example, males and females differ drastically in size, body configuration, and coloration (Zhang et al. 2016). In *Acanthischium* Amyot & Serville, 1843 the pattern of coloration was found as being sexually dimorphic in most species of the genus (Castro-Huertas and Forero 2021). In addition to the bigger size and larger abdomen of females, males in several genera have larger eyes and/or a basally thickened antennal basiflagellomere. The latter has been considered to be among the diagnostic features at the generic level (Stål 1872; Champion 1899; Martin-Park et al. 2012; Gil-Santana et al. 2013, 2017; Gil-Santana 2016). However, sexual dimorphism may also be limited to minor differences in coloration and size, as in many species of *Zelus* (Zhang et al. 2016).

The male genitalia has been found to provide useful diagnostic characteristics for distinguishing species within the genera of Harpactorini by diverse authors (e.g. Elkins 1954a, b; Hart 1975, 1986, 1987; Forero et al. 2008; Zhang et al. 2016; Gil-Santana et al. 2017; Castro-Huertas and Forero 2021). Among wasp-mimicking Neotropical Harpactorini, they have been described for *Graptocletes bicolor* (Burmeister, 1838) (Gil-Santana et al. 2013), *Hiranetis atra* Stål, 1872 (Gil-Santana 2016), *Parahiranetis salgadoi* Gil-Santana, 2015 (Gil-Santana et al. 2017) and species of *Acanthischium* Amyot & Serville, 1843 (Castro-Huertas and Forero 2021). The genera to which the former three species belong, *Graptocleptes* Stål, 1866, *Hiranetis* and, *Parahiranetis* Gil-Santana, 2015, are considered to be closely related to each other (Stål 1872; Champion 1899; Gil-Santana 2015, 2016; Gil-Santana et al. 2017), allowing for important comparisons of several diagnostic traits of male genitalia.

Besides describing a new genus and new species, *Quasigraptocleptes maracristinae* gen. nov., sp. nov., photographs of the syntypes of *Myocoris nigriceps* Burmeister, 1835, *Myocoris nugax* Stål, 1872, *Myocoris tipuliformis* Burmeister, 1838 and *Xystonyttus ichneumoneus* (Fabricius, 1803) are provided to record the main characteristics of the genera to which they belong. An improved and updated version of the key to Neotropical wasp-mimicking Harpactorini genera, previously presented by Maldonado and Lozada (1992) and Gil-Santana (2015), is also provided.

Materials and methods

Syntypes of *Myocoris nigriceps* Burmeister, 1835 (catalog numbers MfN URI http://coll.mfn-berlin.de/u/915662 and MfN URI http://coll.mfn-berlin.de/u/bc0135) and *Myocoris tipuliformis* Burmeister, 1838 (catalog number MfN URI http://coll.mfn-berlin.de/u/f1f08c) deposited in the Hemimetabola Collection of the Museum für Naturkunde Berlin, Leibniz Institute for Evolution and Biodiversity Science, Berlin, Germany (**MFNB**), were directly examined by the first author (HRG-S), while their images (Figs 1–8, 13–16) were provided by Birgit Jaenicke and the copyright of these images is property of the MFNB. Images of a syntype [sex not determined] of *Myocoris nugax* Stål, 1872 (Figs 9–12), deposited in the Swedish Museum of Natural History, Stockholm, Sweden (**NHRS**) were provided by Gunvi Lindberg and are copyright (2022) of the NHRS. The photographs of the female syntypes of *Zelus ichneumoneus* Fabricius, 1803, deposited in the Natural History Museum of Denmark (**ZMUC**), Copenhagen, Denmark, were taken by Sree Gayathree Selvantharan (Figs 101–103, 106–108) and Anders Alexander Illum (Figs 104, 105), and provided by Lars Vilhelmsen.

The original photographs were cropped, their lighting and contrast slightly adjusted but without modifying their characteristics, while the numbered scales of Figs 1–3, 5–7, 13–15, 101, 102, 104–107 were reduced or modified to similar simple scale bars in order to standardize them.

Photographs of paratypes of *Quasigraptocleptes maracristinae* sp. nov. (Figs 20–24, 26, 34, 36, 38, 39, 42, 47–50, 55–72, 89–97) were taken by the second author (JO) using a stereoscope microscope (Leica 205A) with a digital camera. Scanning electron microscopy images (Figs 27, 28, 30–33, 35, 37, 40, 41, 43–46, 51–54, 73–76, 98–100) were also obtained by JO. Two males and a female paratypes of *Quasigraptocleptes maracristinae* sp. nov. were cleaned in an ultrasound machine. Subsequently, the samples were dehydrated in alcohol, dried in an incubator at 45 °C for 20 min, and fixed in small aluminum cylinders with transparent glaze. Sputtering metallization was then performed on the samples for 2 min at 10 mA in an Edwards sputter coater. After this process, the samples were studied and photographed using a high-resolution field emission gun scanning electron microscope (SEM; JEOL, JSM-6610LV), similarly as described by Rosa et al. (2010, 2014). All remaining figures were produced by the first author (HRG-S). The fixed adults, microscopic preparations, and genitalia were photographed using digital cameras (Nikon D5600 with a Nikon Macro Lens 105 mm and Sony DSC-W830). Drawings were made using a camera lucida. For clarity,

the vestiture (setation) was omitted in the ink drawings of Figs 25, 29, 77. Images were edited using Adobe Photoshop CS6.

Observations were made using a stereoscope microscope (Zeiss Stemi) and a compound microscope (Leica CME). Measurements were made using a micrometer eyepiece. The total length of the head was measured excluding the neck, for better uniformity of this measurement. Dissections of the male genitalia were made by first removing the pygophore from the abdomen with a pair of forceps and then clearing it in 20% NaOH solution for 24 hours. The dissections were carried out on the genitalia of different males presenting the range of color variation recorded among them (e.g., Figs 17–19). The dissected structures were studied and photographed in glycerol.

General morphological terminology mainly follows Schuh and Weirauch (2020). Currently, there is a lack of consensus about the terminology to be applied to female and male genitalia in Reduviidae (e.g., Rédei and Tsai 2011). Therefore, in order to maintain uniformity with previous works about species of Harpactorini, the terminology of the male and female genitalia structures generally follows Gil-Santana et al. (2013, 2017) and Gil-Santana (2016).

The type specimens of *Quasigraptocleptes maracristinae* gen. nov., sp. nov. will be deposited as follows: male holotype, 2 male paratypes and 1 female paratype in the Entomological Collection of the "Museu Nacional da Universidade Federal do Rio de Janeiro", Rio de Janeiro, Brazil (**MNRJ**); 6 male paratypes and 1 female paratype in the Dr Jose Maria Soares Barata Triatominae Collection (**CTJMSB**) of the São Paulo State University Julio de Mesquita Filho, School of Pharmaceutical Sciences, Araraquara, São Paulo, Brazil.

When describing label data, a slash (/) separates the lines and a double slash (//) different labels, and comments or translations to English of the label data are provided in square brackets ([ ]). All measurements are in millimeters (mm).

Taxonomy

Subfamily Harpactorinae
Tribe Harpactorini

Myocoris Burmeister, 1835

Myocoris Burmeister, 1835: 221 [key], 226 [description], 1838: 104 [diagnostic characteristics]; Stål 1859: 367 [key], 370 [diagnostic characteristics], 1866: 294 [key], 1872: 69 [key], 83 [catalog]; Walker 1873a: 49 [key], 63 [key], 1873b: 128 [catalog]; Lethierry and Severin 1896: 178 [catalog]; Wygodzinsky 1949: 42 [catalog]; Putshkov and Putshkov 1985: 52 [catalog]; Maldonado 1990: 236 [catalog]; Maldonado and Lozada 1992: 165 [key]; Forero 2011: 15 [checklist]; Gil-Santana 2015: 36 [key], 2016: 92 [citation]; Gil-Santana et al. 2017: 41 [citation]. Type species: *Myocoris nigriceps* Burmeister, 1835: 226, by subsequent designation, Wygodzinsky 1949: 42.

Cosmonyttus Stål 1866: 295 [key, in part, including *M. nigriceps*]; synonym proposed by Kirkaldy 1909: 388. Type species: *Myocoris nigriceps* Burmeister, 1835: 226, by monotypy.

Morphological remarks. Head cylindrical, elongated, with sparse thin setae on ventral and anteocular portions; postantennal spines short, curved forward, apices acute or somewhat rounded. Legs: fore femora thickened, narrowing at apices and somewhat curved at basal half; fore tibia curved at apical third; middle and hind legs elongated, slender; hind femora curved approximately at basal half.

Burmeister (1835) described *Myocoris* and two new species included in this genus: *M. nigriceps* and *M. braconiformis*. In his subsequent paper, "Some account of the Genus *Myocoris*…" (Burmeister 1838), he considered ten species as included in the genus, some of which were described as new in this occasion, such as *M. tipuliformis*. While several of these ten species were transferred to other genera or considered as synonyms of other species (Maldonado 1990), Stål (1872) described *M. nugax* and maintained only two other species included in *Myocoris*: *M. nigriceps* and *M. tipuliformis*. With exception of Walker (1873b), who considered 26 species as belonging to *Myocoris*, all other subsequent authors (Lethierry and Severin 1896; Wygodzinsky 1949; Putshkov and Putshkov 1985; Maldonado 1990) followed Stål (1872). The three species currently included in *Myocoris* were described from Brazil and accordingly with Stål (1872) may be separated by the following key:

1 Humeral angles acutely spined (Figs 5, 13) **2**
– Humeral angles not acute, rounded (Fig. 9) ..... ***M. nugax* Stål, 1872**
2 Only the basal portion of the first visible labial segment blackish (Fig. 3) .... ***M. nigriceps* Burmeister, 1835**
– First visible labial segment entirely blackish (Fig. 14) .... ***M. tipuliformis* Burmeister, 1838**

Stål (1872) stated that *M. nigriceps* and *M. tipuliformis* were very related and similar species, while *M. nugax* although similar to *M. tipuliformis*, differed from the latter by the somewhat shorter neck, shorter postantennal spines, and humeral angle without acute prominence. Another difference in coloration between *M. nigriceps* and *M. tipuliformis* is in their legs. In *M. tipuliformis* the apical portion of the femora and basal portion of tibiae are blackish, while in *M. nigriceps* these portions are pale.

Myocoris nigriceps Burmeister, 1835

Figs 1–8

Myocoris nigriceps Burmeister, 1835: 226 [description], 1838: 105 [redescription]; Stål 1859: 370 [citation], 1872: 83 [catalog]; Walker 1873b: 128 [catalog]; Lethierry and Severin 1896: 178 [catalog]; Wygodzinsky 1949: 42 [catalog]; Maldonado 1990: 236 [catalog].

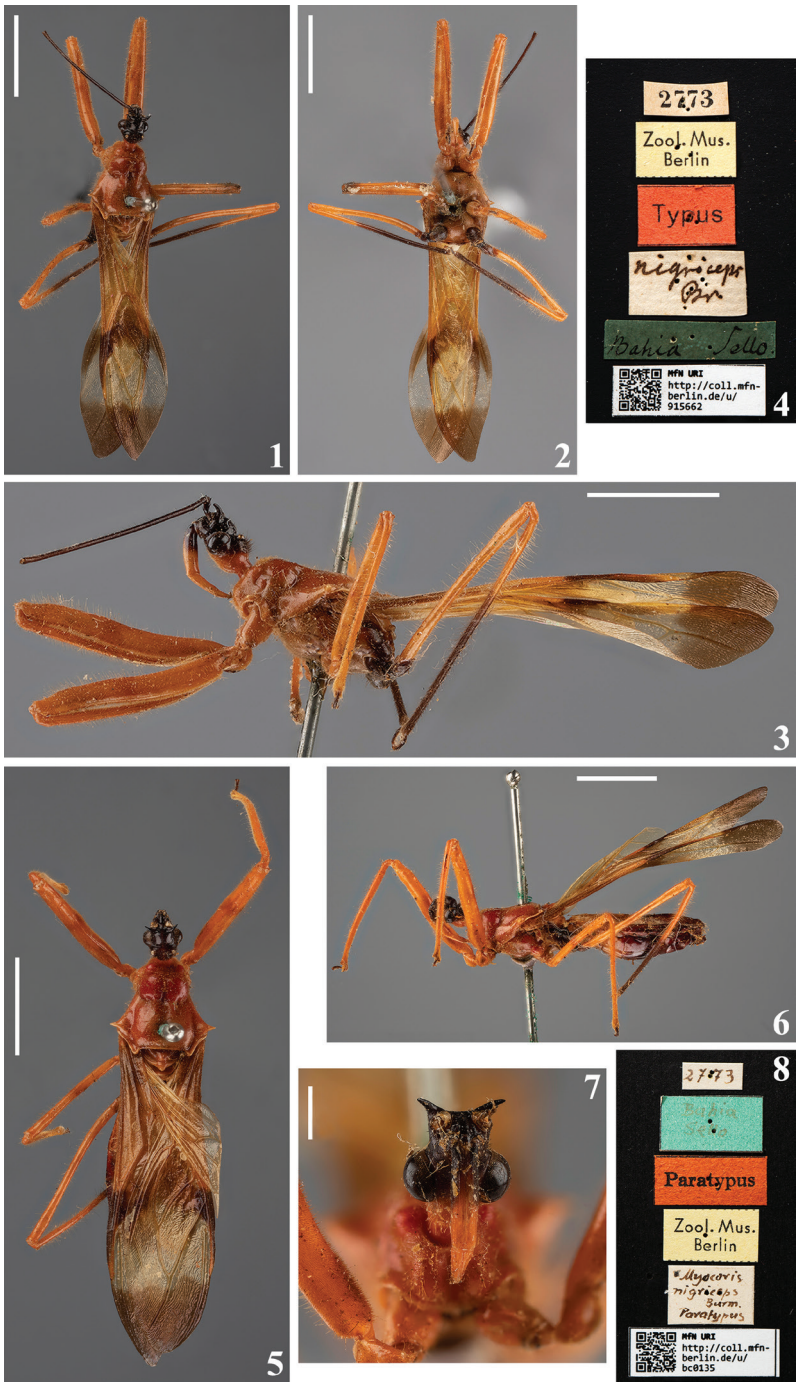

Figures 1–8. *Myocoris nigriceps* Burmeister, 1835, syntypes deposited in MFNB **1–4** sex not determined, catalog number MfN URI http://coll.mfn-berlin.de/u/915662 **1** dorsal view **2** ventral view **3** lateral view **4** labels **5–8** female, catalog number MfN URI http://coll.mfn-berlin.de/u/bc0135 **5** dorsal view **6** lateral view **7** head, anterior view **8** labels. The copyright of these images is property of the MFNB. Scale bars: 5.0 mm (**1–3, 5, 6**); 1.0 mm (**7**).

Type material examined. *Myocoris nigriceps*. ***Syntype*** [sex not determined; abdomen absent]: [printed label]: 2773 // [printed label]: Zool. Mus. / Berlin // [printed red label]: Typus // [handwritten label]: *nigriceps* / Br // [handwritten green label]: Bahia Sello. // [printed label]: [at left side]: QR CODE, [at right side]: MfN URI / http://coll.mfn- / berlin.de/u/ / 915662; **Female syntype**: [handwritten label]: 2773 // [printed label]: Zool. Mus. / Berlin // [printed red label]: Paratypus // [handwritten label]: *Myocoris* / *nigriceps* / Burm. / Paratypus // [handwritten green label]: Bahia / Sello // [printed label]: [at left side]: QR CODE, [at right side]: MfN URI / http:// coll.mfn- / berlin.de/u/ / bc0135 (MFNB).

In the Hemimetabola Collection of the Museum für Naturkunde Berlin, Leibniz Institute for Evolution and Biodiversity Science, Berlin, Germany (MFNB) there are two type specimens of *M. nigriceps*. A specimen without abdomen, and sex not determined, labeled as "Typus", catalog number MfN URI http://coll.mfn-berlin.de/u/915662 (Figs 1–4), and a female labeled as "paratypus", catalog number MfN URI http://coll.mfn-berlin.de/u/bc0135 (Figs 5–8). Both of them are considered here as syntypes, following Art. 73.2 of the ICZN.

Myocoris nugax Stål, 1872

Figs 9–12

Myocoris nugax Stål, 1872: 83 [description]; Lethierry and Severin 1896: 178 [catalog]; Wygodzinsky 1949: 42 [catalog]; Maldonado 1990: 236 [catalog].

Xystonyttus nugax (Burm.); Haviland 1931: 150 [wrong combination and authorship; record from Guyana; comments on difficulties of determination: possible misidentification].

Note. Stål (1872) described *M. nugax* based on an unspecified number of female specimens from Brazil and cited "Mus. Holm." (NHRS) as the depository of the type specimen(s). Currently, only one type specimen of *M. nugax* was found there and it is without its abdomen (G. Lindberg pers. comm.) (Figs 9–11). Consequently, it is not possible to be sure about its gender, but possibly it is a female taking into account that Stål (1872) mentioned only the female of the species in his description. It is considered a syntype accordingly to Art. 73.2 of the ICZN. Photographs of this specimen allow observing the shorter postantennal spine and the humeral angle without acute prominence, as described by Stål (1872) (Figs 9, 11).

Myocoris tipuliformis Burmeister, 1838

Figs 13–16

Myocoris tipuliformis Burmeister, 1838: 105 [description]; Stål 1859: 370 [citation], 1872: 83 [catalog]; Walker 1873b: 128 [catalog]; Lethierry and Severin 1896: 178 [catalog]; Wygodzinsky 1949: 42 [catalog]; Maldonado 1990: 236 [catalog].

Hiranetis tipuliformis; Stål 1860: 76 [catalog].

Type material examined. Male syntype: [printed label]: 2774 // [printed label]: Zool. Mus. / Berlin // [printed red label]: Typus // [handwritten label]: *tipulifor-* / *mis** ♂. // [handwritten green label]: Rio Bescke // [printed label]: [at left side]: QR CODE, [at right side]: MfN URI / http://coll.mfn- / berlin.de/u/ / f1f08c (MFNB).

The male type specimen deposited in the MFNB (Figs 13–15), labeled as "Typus" (Fig. 16), is herewith considered as a syntype, accordingly with Art. 73.2 of the ICZN.

Figures 9–12. *Myocoris nugax* Stål, 1872, syntype, sex not determined, deposited in NHRS, catalog number NHRS-GULI000000052, photographs provided by Gunvi Lindberg, 2022 Naturhistoriska riksmuseet. Made available by the Swedish Museum of Natural History under Creative Commons Attribution 4.0 International Public License, CC-BY 4.0, https://creativecommons.org/licenses/by/4.0/legalcode **9** dorsal view **10** ventral view **11** lateral view **12** labels.

Figures 13–16. *Myocoris tipuliformis* Burmeister, 1838, male syntype deposited in MFNB, catalog number MfN URI http://coll.mfn-berlin.de/u/f1f08c **13** dorsal view **14** lateral view **15** head, anterior view **16** labels. The copyright of these images is property of the MFNB. Scale bars: 5.0 mm (**13, 14**); 1.0 mm (**15**).

Comments. The characteristics stated by Stål (1872) to separate the species of *Myocoris* were confirmed in their respective type specimens (Figs 1–3, 5–7, 9–11, 13–15). However, it is necessary to study more specimens, with a more profound taxonomical approach, to ascertain their value to this separation, and more importantly, to confirm the validity of these species, such as the case of *M. nigriceps* and *M. tipuliformis*, separated only by color differences, which may be subject of intraspecific variation, as commented above.

***Quasigraptocletes* gen. nov.**
https://zoobank.org/9A9CBC12-B6B9-4B67-B9D3-3134D0A9978E

Type species. *Quasigraptocleptes maracristinae* sp. nov., by present designation.

Diagnosis. *Quasigraptocletes* gen. nov. can be separated from other genera of wasp-mimicking Harpactorini by the combination of the characteristics presented in the key below, and specially by the postantennal spines, which are strongly curved backwards.

Description. Integument mostly shiny, smooth. ***Head*** gibbous, large, approximately as long as wide across eyes (neck excluded); with sparse long and short, straight or somewhat curved blackish setae; the latter much denser, forming pubescence of long blackish thick setae on postocular portion and gula. Clypeus straight in dorsal view, curved in lateral view. Antenna inserted at level of upper third of eye; scape and pedicel straight with shiny and smooth integument; flagellomeres with opaque integument; basiflagellomere variably curved; in males conspicuously thickened approximately in basal half; distiflagellomere thinner than the other segments and slightly curved. Postantennal spines strongly curved backwards and variably directed medially. Eyes globose, glabrous, projecting laterally, prominent in dorsal view, reaching closer to dorsal margin of head at interocular sulcus slightly behind its midportion; not reaching ventral margin of head, which is far from inferior margin of the eye. Interocular sulcus thin and shallow, curved laterally; just anterior to it, on midline, a small oval fossa, followed anteriorly by a very short thin shallow median sulcus, which sometimes is not evident. Ocelli and portion between them elevated, the former much closer to eyes than to each other. Labium stout, curved, reaching prosternum approximately at proximal part of its distal third; segment II (first apparent) thickest and longest, straight, surpassing level of posterior portion of eyes; segment IV shortest, triangular, tapering. Neck thin. ***Thorax.*** Anterior collar inconspicuous; anterolateral angles moderately prominent. Transverse sulcus not very deep, interrupted before middle by a pair of submedian shallow carina. Midlongitudinal sulcus on fore lobe of pronotum shallow or not evident at basal half, deeper at distal half, above transverse sulcus, almost or forming a narrow depression; disc of hind lobe smooth; lateral longitudinal sulci well marked at posterior half to posterior two-thirds of hind lobe of pronotum. Humeral angle moderately elevated, rounded at lateral margin. Scutellum with margins elevated, apex thin, acutely pointed or sometimes rounded at its tip. Mesosternum somewhat elevated laterally, with a median U-shaped carina posteriorly. ***Legs*****:** coxae

globose, slightly constricted apically; femora and tibiae slender, elongate and generally straight. Fore femur shorter than head and pronotum together, slightly thickened at basal portion and somewhat curved at midportion; middle and hind femora slightly dilated subapically and slightly narrower at the portion where submedian distal pale annuli are located; apices of all femora with a pair of lateral small tubercles. Fore and middle tibiae thickened apically, the former more than the latter; at apex of fore tibiae a dorsal spur and a mesal comb. Hemelytra long, surpassing abdomen by about half length of membrane. ***Abdomen*:** elongate; spiracles rounded.

Distribution. Brazil, States of Minas Gerais and Paraná.

Etymology. The name of the new genus was composed by the Latin word *quasi*, meaning almost, nearly, like, and *Graptocleptes*, in reference to its apparent proximity to the latter genus. The gender is neutral.

***Quasigraptocleptes maracristinae* sp. nov.**
https://zoobank.org/83AC7695-DE84-4133-8E8C-1FE932D55CF5
Figs 17–100

Type material. **Brazil**, Minas Gerais, Juiz de Fora Municipality, x. 1997, J. da Silva leg.: 1 male holotype (MNRJ), 2 males, 1 female paratypes (MNRJ), 6 male paratypes (CTJMSB); Paraná, Londrina Municipality, 25.ii.2004, Malaise trap, Rafael Barros leg.: 1 female paratype (CTJMSB).

Description. Male. Figs 17–87. Measurements are given in Table 1.

Coloration: general coloration black, brownish or reddish (Figs 17–19). ***Head*** black or reddish; antennal segments black, dark brownish or reddish; labium completely dark or with distal half of second visible segment and last segment pale or entirely reddish; neck black, mostly or completely dark yellow or reddish (Figs 17–24, 26, 34, 36, 38, 39, 42). ***Thorax*** completely blackish, dark brown, brownish or reddish, sometimes blackish on fore lobe and brownish on hind lobe; sometimes humeral angles and/or posterior margin of hind lobe of pronotum slightly paler (Figs 17–24). Scutellum with similar coloration of thorax, sometimes with the apex of the process, in variable extension paler or whitish (Figs 17–19, 47–50). Hemelytra generally black with veins concolorous or paler, brownish to dark gray with the veins of the corium darker; a yellowish spot on external and mid-distal portions of corium reaching adjacent part of membrane, especially in basal portion of distal cell of membrane and just posterior to it; in paler specimens, the portion medial to the yellowish spot slightly paler (Figs 17–19). ***Legs*.** All coxae blackish (Fig. 55) or with fore coxae pale on posterior surface (Fig. 56), or completely pale (Figs 57, 58), or all coxae almost or completely pale or reddish (Fig. 59). All trochanters blackish or dark brownish (Figs 55, 56), or fore or the latter and middle trochanters partially or completely pale (Figs 57, 58) or all of them almost or completely pale or reddish (Fig. 59). Femora generally blackish, brownish or reddish. Fore femora frequently with dorsal surface paler, with dark yellowish tinge or generally reddish or dark yellowish in variable extent along the segment (Figs 17–19). Middle and hind femora with one

Table 1. Measurements (mm) of male type specimens (n = 9) of *Q. maracristinae* sp. nov.

	Holotype	Mean	SD	Maximum	Minimum
Body length to tip of hemelytra	12.2	13.45	0.55	14.0	12.2
Body length to tip of abdomen	9.5	10.47	0.47	11.0	9.5
Head length (excluding neck)	1.3	1.42	0.19	1.7	1.0
Anteocular portion length[1]	0.32	0.43	0.08	0.5	0.32
Postocular portion length[1]	0.35	0.44	0.06	0.5	0.35
Head width across eyes	1.4	1.34	0.16	1.5	1.1
Interocular distance (synthlipsis)	0.8	0.8	0.08	0.9	0.6
Transverse width of eye	0.32	0.33	0.02	0.38	0.3
Length of eye	0.5	0.5	0.05	0.6	0.4
Ocellar tubercle width	0.9	0.82	0.09	0.9	0.6
Scape length	3.4	3.43	0.1	3.5	3.2
Pedicel length	1.0	0.97	0.04	1.0	0.9
Basiflagellomere length (n = 8)[2]	6.5	5.48	0.43	6.5	5.1
Basiflagell. max. width (n = 8)[2]	0.2	0.26	0.07	0.4	0.2
Distiflagellomere length (n = 3)[2]	–	1.5	0.00	1.5	1.5
Labial segment II length[1]	0.9	0.95	0.07	1.0	0.8
Labial segment III length[1]	0.8	0.82	0.08	0.9	0.7
Labial segment IV length[1]	0.2	0.21	0.03	0.3	0.2
Pronotum length (at midline)	2.0	2.27	0.11	2.4	2.0
Pronotum maximum width	1.9	2.37	0.19	2.5	1.9
Scutellum length	0.9	0.96	0.05	1.0	0.9
Fore femur length	3.2	3.39	0.16	3.7	3.2
Fore tibia length	3.5	3.6	0.15	4.0	3.5
Fore tarsus length (n = 7)[2]	0.4	0.4	0.06	0.5	0.3
Middle femur length	2.6	2.9	0.16	3.1	2.6
Middle tibia length	3.2	3.45	0.21	3.7	3.0
Middle tarsus length	0.5	0.52	0.03	0.6	0.5
Hind femur length	3.9	4.26	0.20	4.5	3.9
Hind tibia length	5.1	5.85	0.36	6.2	5.1
Hind tarsus length	0.5	0.57	0.05	0.65	0.5
Abdomen length[3]	5.3	5.58	0.35	6.5	5.3
Abdomen maximum width	1.2	1.52	0.13	1.7	1.2

[1] Measured in lateral view; [2] Segments or portions broken or missing in some specimens; [3] Measured on ventral view, at midline, from anterior margin of sternite II to posterior border of genitalia.

pale or yellowish submedian distal annulus or also with an additional pale or yellowish subbasal or basal annulus (Figs 17, 60, 64, 65); sometimes the subbasal annulus is fainter, darker and/or incomplete, and as such, only evident on hind leg (Fig. 17); in specimens with reddish general coloration, the portion proximal to the submedian distal annuli is sometimes variably darker (Figs 19, 63, 66); additionally, in some specimens with a pair of annuli, the apex of these femora are also paler (Figs 18, 61, 62, 65). Tibiae completely dark or variably pale brownish or reddish on its basal or distal portion, or almost completely or completely pale brownish to pale reddish (Figs 17–19, 64–66). Tarsi in general with a similar coloration to the apex of the respective tibia. ***Abdomen.*** Sternites generally pale reddish, reddish or dark reddish with some or most segments partially or entirely darkened to blackish (Figs 67–71).

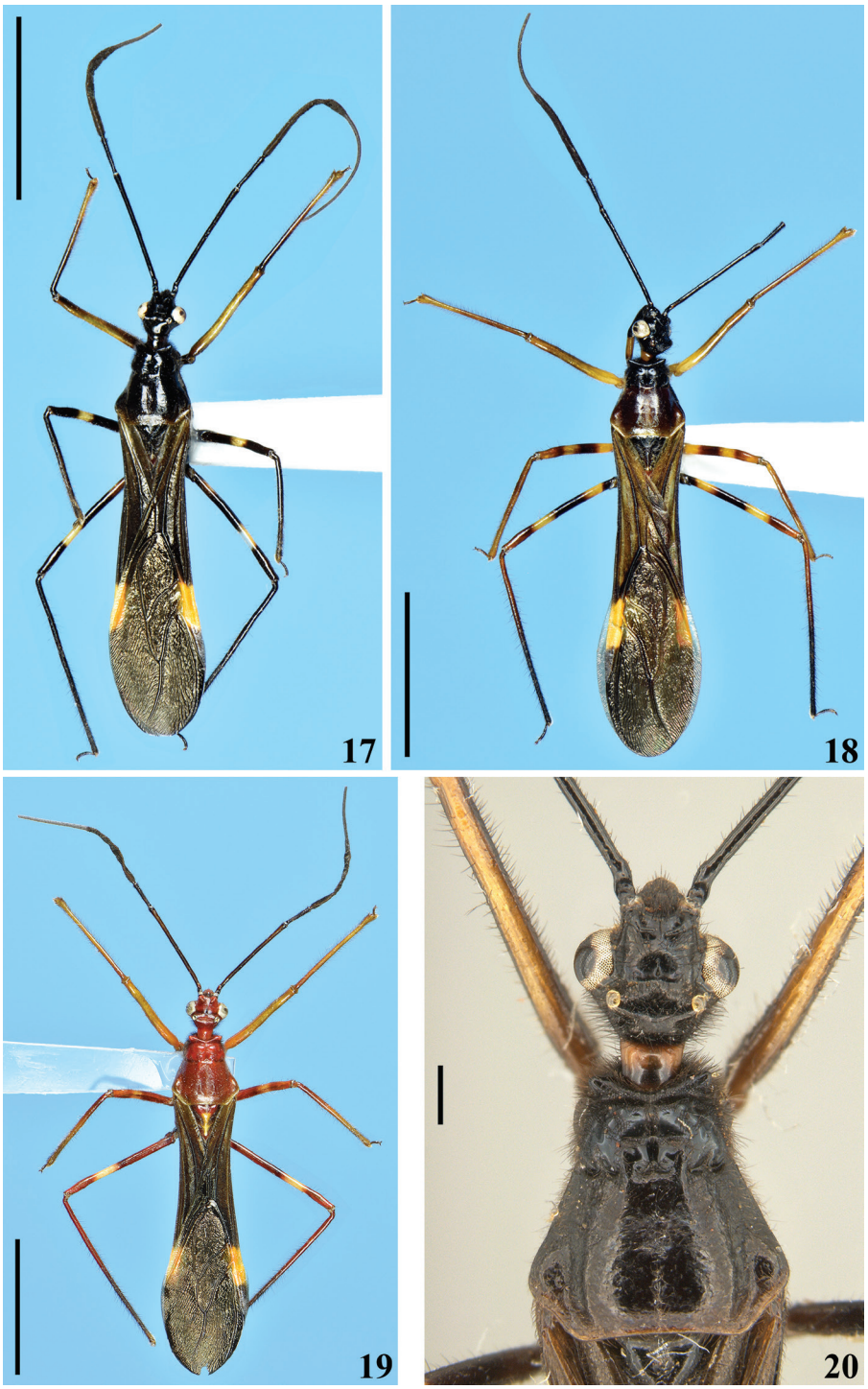

Figures 17–20. *Quasigraptocleptes maracristinae* gen. nov., sp. nov., males, dorsal view **17** holotype **18–20** paratypes **20** head and pronotum. Scale bars: 5.0 mm (**17–19**); 0.5 mm (**20**).

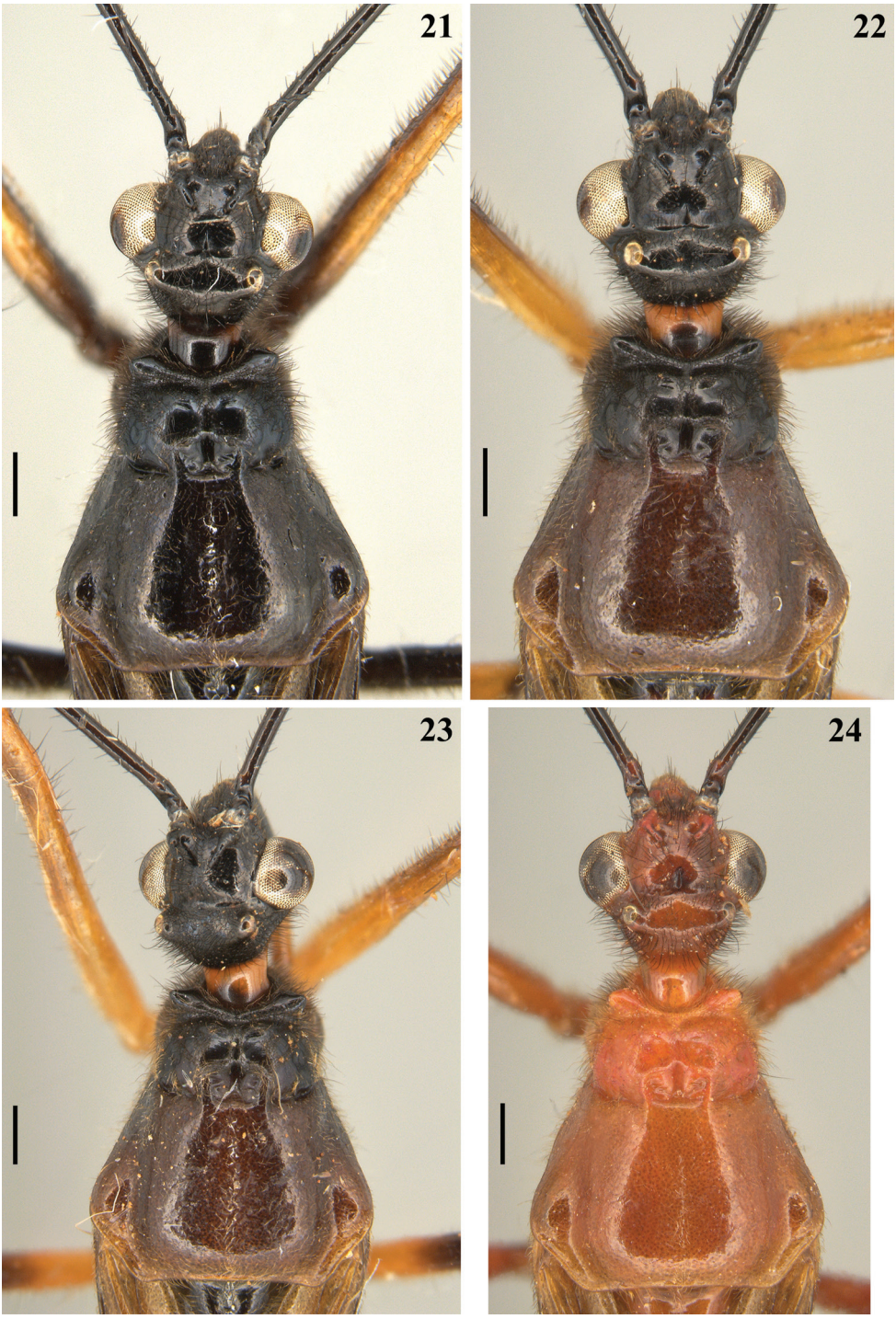

Figures 21–24. *Quasigraptocleptes maracristinae* gen. nov., sp. nov., males, head and pronotum, dorsal view. Scale bars: 0.5 mm (**21–24**).

Vestiture. ***Head*** covered by long and short, straight or somewhat curved blackish setae, which are denser, forming pubescence of long blackish thick setae on postocular portion, even more numerous on gula, and sparser or absent in the area anterior to transverse sulcus (Figs 20–24, 26–28, 30–33). Antenna: scape with sparse short, stiff, slightly curved, dark setae, which become more numerous on mesal surface, approximately in distal two-thirds (Figs 34, 35) and a few longer blackish thin setae scattered along the segment; pedicel, except at glabrous base, covered with numerous short, stiff, obliquely semi-erect dark setae (Figs 36, 37), and a few (about eight to ten) very much thinner isolated elements (interpreted as trichobothria), which are present laterally on basal two-thirds of external surface and dorsally on distal third; thickened portion of basiflagellomere, except at extreme base (which is glabrous), completely covered with short, stiff, dark, adpressed setae, and with scattered stiff, darkened, semi-erect setae and a pubescence formed by longer, very thin, pale setae, which are almost imperceptible in this portion (Figs 38–40); distal (not thickened) portion of basiflagellomere and distiflagellomere covered with dense pubescence formed by short, thin, pale to whitish setae and with scattered short, darkened, stiff, semi-erect setae; the latter somewhat less numerous or not evident on distiflagellomere (Figs 38, 39, 41–43). Labium with scattered and somewhat curved, longer and thinner dark setae (Figs 28, 44). Eyes and ocelli glabrous (Figs 27, 28, 30). Neck almost completely or completely glabrous (Figs 20–24, 26–28, 30). ***Thorax.*** Prothorax covered with very numerous blackish thick setae on fore lobe of pronotum, anterior portions of propleura and hind lobe of pronotum; the latter with sparse long setae at dorsal portion or, almost glabrous, except on midline, where thinner, somewhat shorter and light yellowish to whitish setae form a faint midlongitudinal line on hind lobe; median portion of posterior margin of pronotum with some long thin darkened setae (Figs 20–24, 45, 52). Scutellum with scattered thin dark or pale long setae more or less numerous; sometimes with midlongitudinal line of whitish setae on approximately its basal third, which may be a continuation of the line of whitish setae on hind lobe, or may be present only on the scutellum, while absent on pronotum (Figs 46–52). The pale setae which form the midlongitudinal line on hind lobe of pronotum and/or scutellum are sometimes partially or completely covered by a small amount of white wax-like substance (e.g. Figs 21, 23, 47, 49). Posterior portion of propleura, mesopleura, metapleura and thoracic sterna with less numerous long darkened setae, which are shorter and thinner at center of mesosternum and metasternum (Figs 52, 55–59). In some specimens, there is a group of thin whitish setae basally covered with rounded, flocky patches of white wax-like substance, extending along midline of mesosternum and metasternum and sometimes extending to basal half of first visible sternite (Figs 55, 56, 58, 59). Dorsal sclerite below scutellum covered by numerous minute spiny setae (Figs 53, 54). ***Legs*****:** coxae with numerous long thin setae on posterior and lateral surfaces, which are less numerous or absent on basal third; fore trochanters densely covered with pale long setae ventrally and with some scattered even longer thinner pale setae; middle and hind trochanters progressively less setose. All femora covered with scattered, long, straight, erect or semi-erect

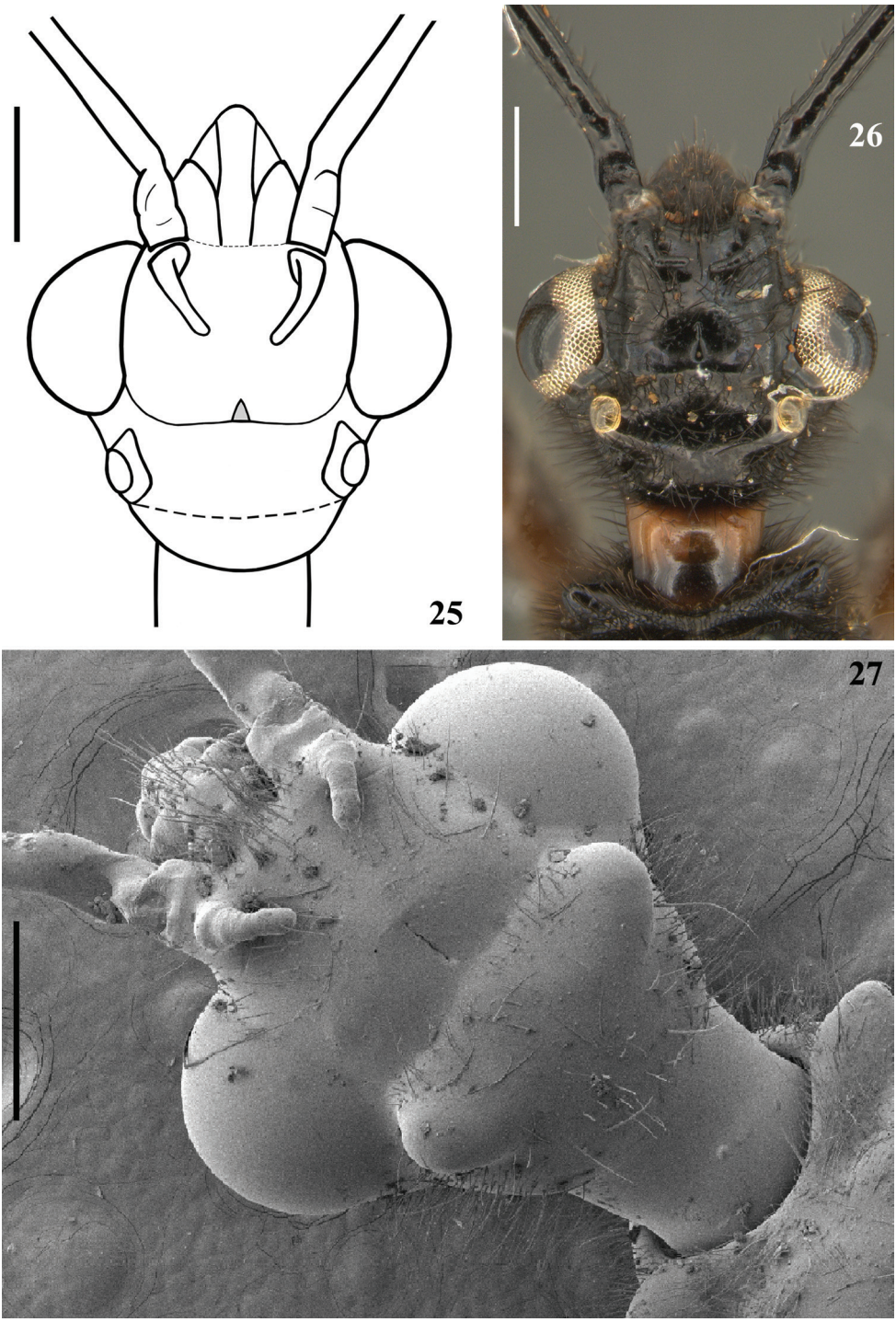

Figures 25–27. *Quasigraptocleptes maracristinae* gen. nov., sp. nov., males, head, dorsal view. Scale bars: 0.5 mm (**25–27**).

darkened setae and dense, erect, mostly pale, brush-like setae ventrally, which are even more numerous on basal portion and absent on hind femur. All tibiae with scattered long thick blackish setae and covered with shorter dark setae on ventral surface, which become progressively more numerous towards apex, where they also cover lateral and dorsal surfaces. Tarsi covered with shorter dark setae. Hemelytron: clavus and corium generally covered by numerous curved, short, very thin, pale setae, which become much less numerous, adpressed and even shorter on distal half of corium; membrane glabrous. ***Abdomen*:** number of setae on sternites varying among individuals, generally with scattered long thin setae, which are light on reddish portions and dark on the blackish segments, and thicker, longer, and also more numerous on parts adjacent to genitalia and on the latter (Figs 67–71). In some specimens, median portion of basal half of first visible sternite with whitish setae covered by white wax-like substance (Figs 56, 59); in one individual, a pair of lateral narrow stripes of sparse whitish setae on distal half of sternite VII, extending to basal exposed portion of pygophore (Fig. 69). ***Structure*.** Antennal basiflagellomere variably slightly curved, from 1.6 to 1.8 times longer than scape, conspicuously thickened approximately in basal half, which is clearly separated in relation to the distal thinner portion (Figs 38–40). Postantennal spines variable in length and thickness among individuals; slightly or strongly directed medially towards their apices, which are blunt to subacute (Figs 20–33). Abdominal segment VIII with only its distal margin of ventral surface visible externally (Figs 72, 73); sclerotized only on ventral portion, which is subrectangular in shape and has both basal and distal margins curved, the latter more than the former, and more prominent laterally.

Male genitalia (Figs 67–87). Pygophore darkened, blackish; paler or reddish at proximal portion, in paler specimens (Figs 67–72); suboval in ventral view, somewhat enlarged laterally just below the insertions of the parameres (Fig. 73); with an enlarged, somewhat arrow-shaped apex (medial process, mp), in which lateral margins are acutely pointed and the median portion is rounded (Figs 72–75, 77); between anterior and posterior genital openings, a relatively narrow dorsal (transverse) bridge (db) (Fig. 77); ventrolateral margins of exposed portion of pygophore with numerous, long, erect setae (Figs 72, 73, 75, 76). Parameres (pa) symmetrical, rod-like in shape; apices rounded, paler at basal third, becoming darker to blackish in apical half; glabrous in basal two-thirds and with long, stout, dark setae in apical third (Figs 72, 73, 75, 76). Phallus (Figs 78–80): articulatory apparatus with basal plate arms (ba) and basal plate bridge (bb) narrow and forming a subsquared set, except in apical portion, where the arms are curved (Fig. 82); pedicel (pd) (= basal plate extension) short (Figs 78, 80, 82). Dorsal phallothecal plate (dp) weakly sclerotized (Figs 78, 81); subrectangular in dorsal view, somewhat expanded laterally at basal portion and with small acute spines on lateral margins (Figs 78, 79, 81); medially to the latter, a pair of somewhat depressed subrectangular areas on the disc; struts (st) with curved lateral arms, which are thicker basally, and subparallel median arms slightly converging towards apices (Fig. 81). Endosoma wall smooth on basal half, becoming progressively more densely, minutely, spiny towards apex; at distal third: a pair of small more sclerotized lateral portions (sp); an apical pair of prominent sclerotized subtriangular lobes (sl), between which, ventrally, a shallower not sclerotized lobe (sn) (Figs 78–80, 85, 86). The fol-

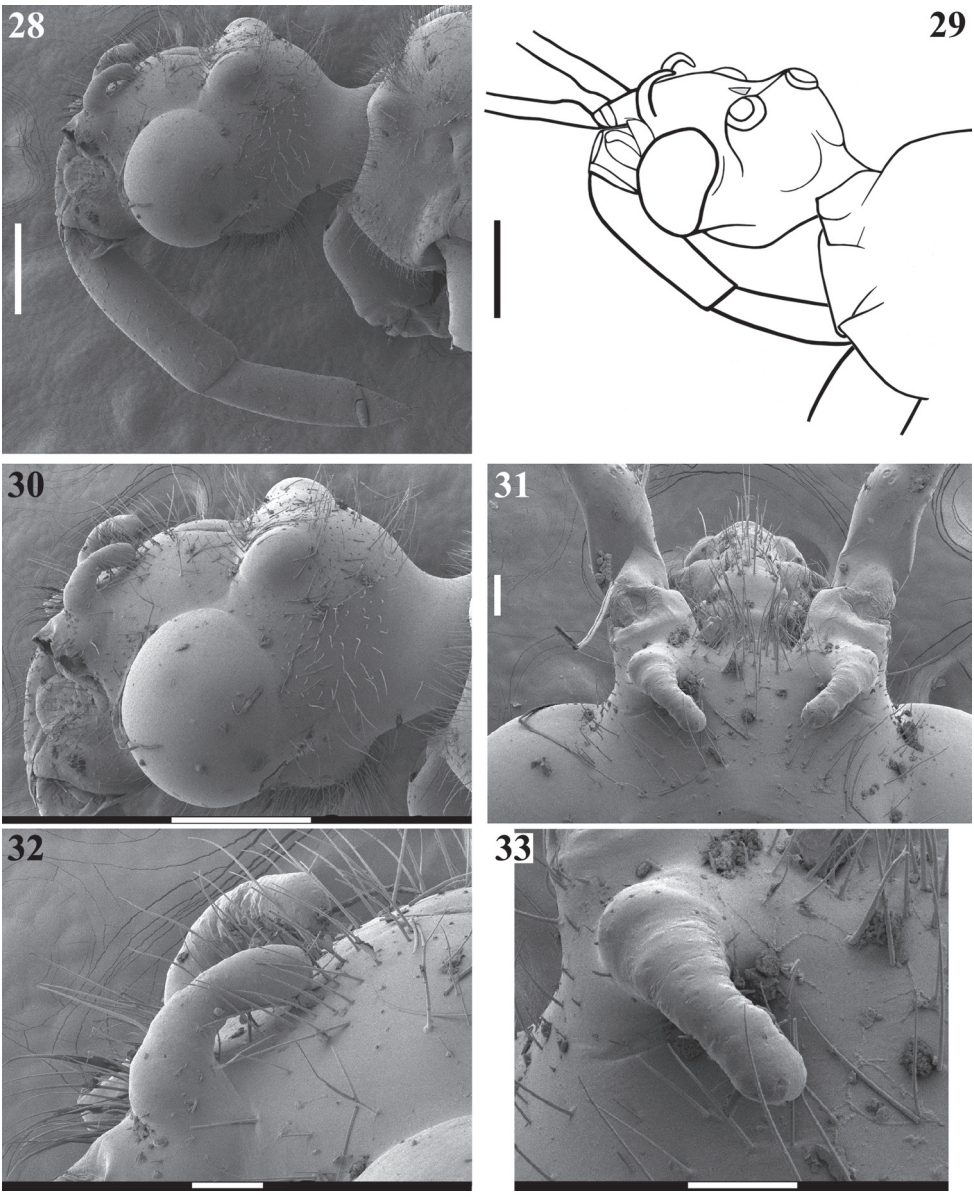

Figures 28–33. *Quasigraptocleptes maracristinae* gen. nov., sp. nov., males, head **28–30** posterolateral view **30** upper portion **31** anterior portion, including postantennal spines, dorsal view **32** postantennal spines, laterodorsal view **33** left postantennal spine, dorsal view. Scale bars: 0.5 mm (**28–30**); 0.1 mm (**31–33**).

lowing endosomal processes were observed: 1 - a pair of elongate, parallel, flat, medial and weakly sclerotized processes (fp), wrapped in a smooth portion of endosoma wall, dorsally (Figs 78, 79, 83–85); 2 - a larger U-shaped basal process (u) formed by diffuse thickening (Figs 80, 87); 3 - a median subspherical process (m), situated between the lateral arms of the basal process and formed by a dense grouping of small thickenings (Figs 80, 83, 87).

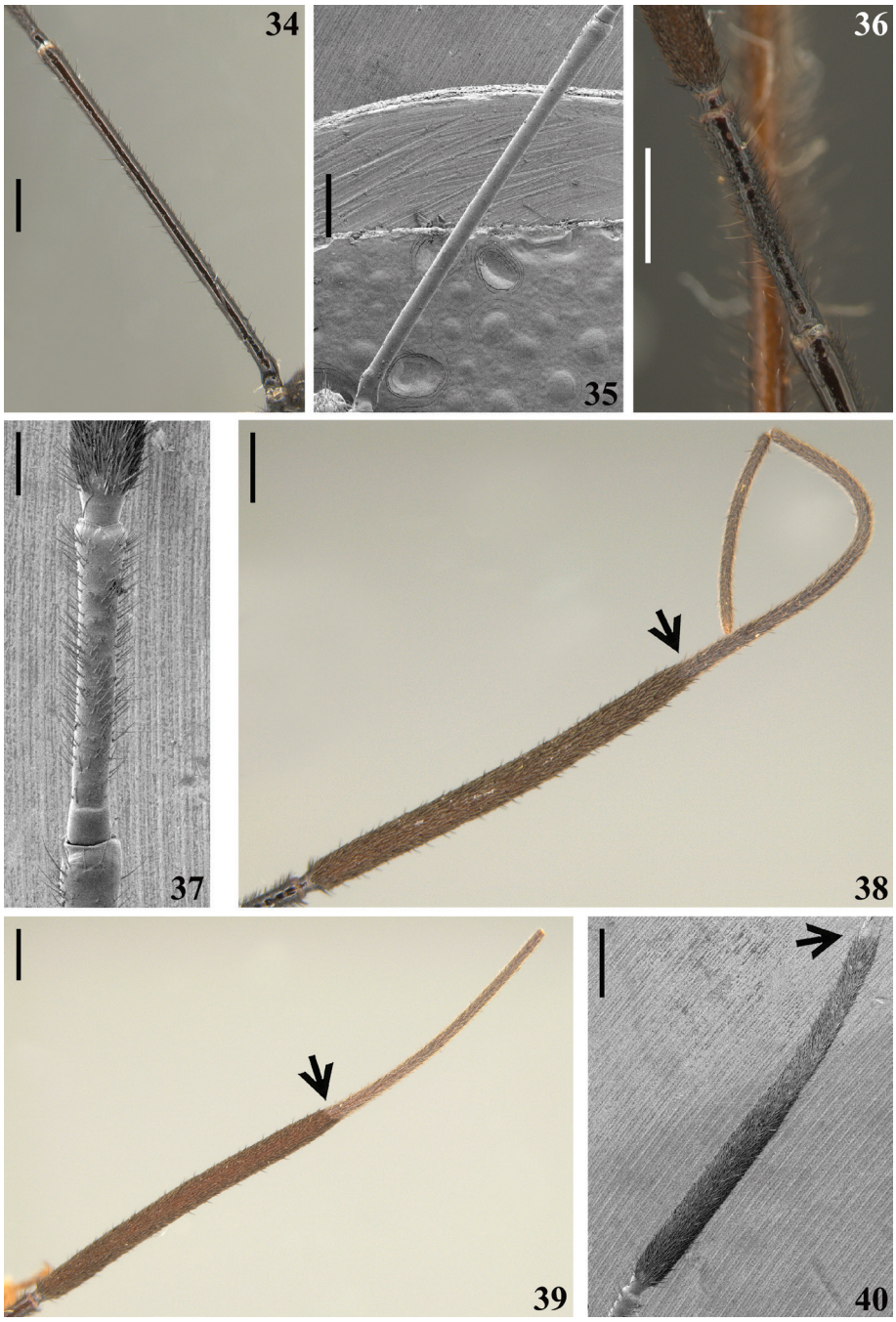

Figures 34–40. *Quasigraptocleptes maracristinae* gen. nov., sp. nov., males, antenna, dorsal view **34, 35** scape **36, 37** apex of scape, pedicel and basal portion of basiflagellomere **38–40** arrows point to the portion of clear separation between the thickened and thinner portions of basiflagellomere **38** apex of pedicel and flagellomeres **39** apex of pedicel and basiflagellomere **40** apex of scape and approximately basal half of basiflagellomere. Scale bars: 0.5 mm (**34–36, 38–40**); 0.2 mm (**37**).

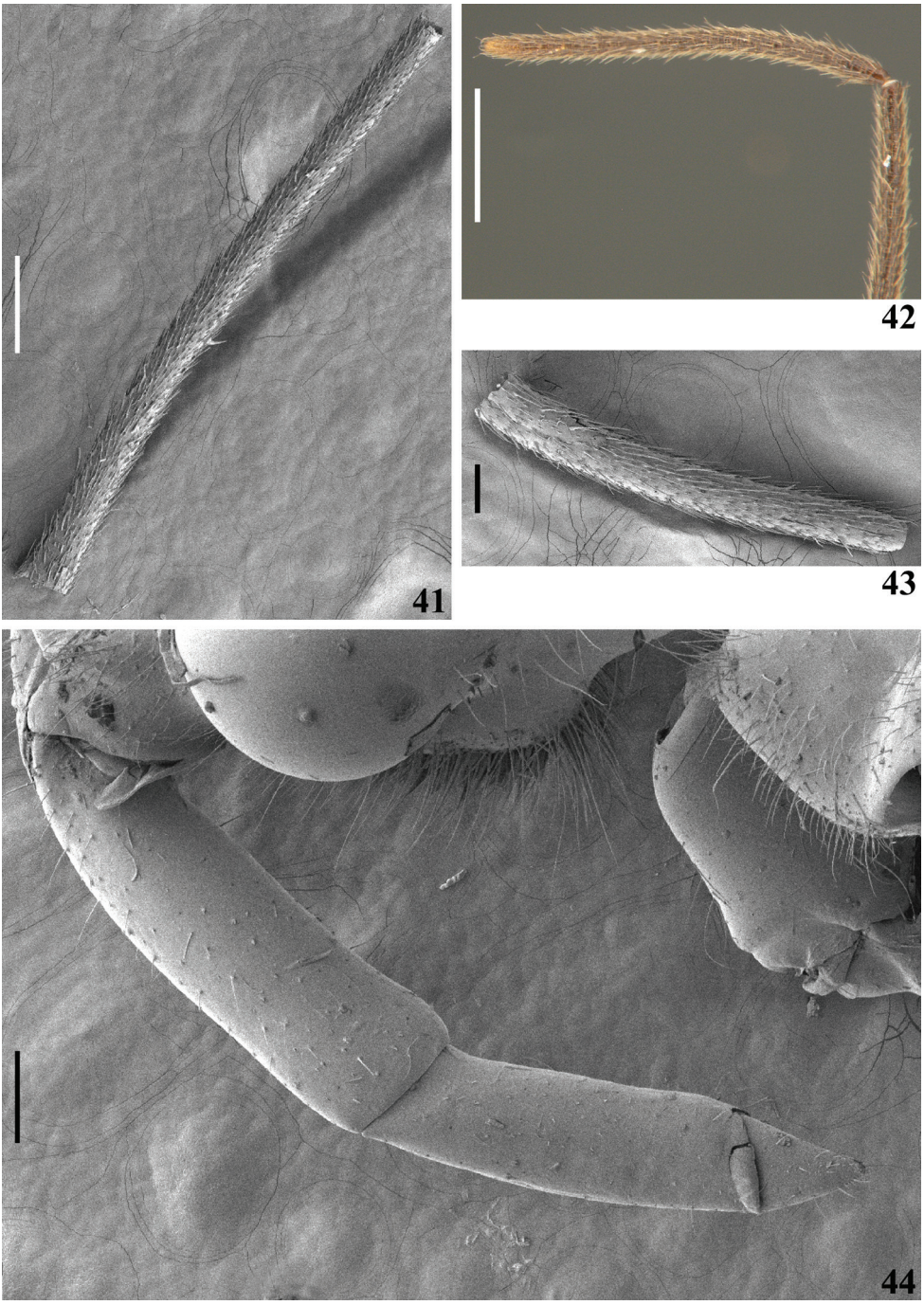

Figures 41–44. *Quasigraptocleptes maracristinae* gen. nov., sp. nov., male **41** basiflagellomere, distal half, dorsal view **42** distal portion of basiflagellomere and distiflagellomere, lateral view **43** distiflagellomere, dorsal view **44** lower portion of head and labium, lateral view. Scale bars: 0.5 mm (**42**); 0.3 mm (**41**); 0.2 mm (**44**); 0.1 mm (**43**).

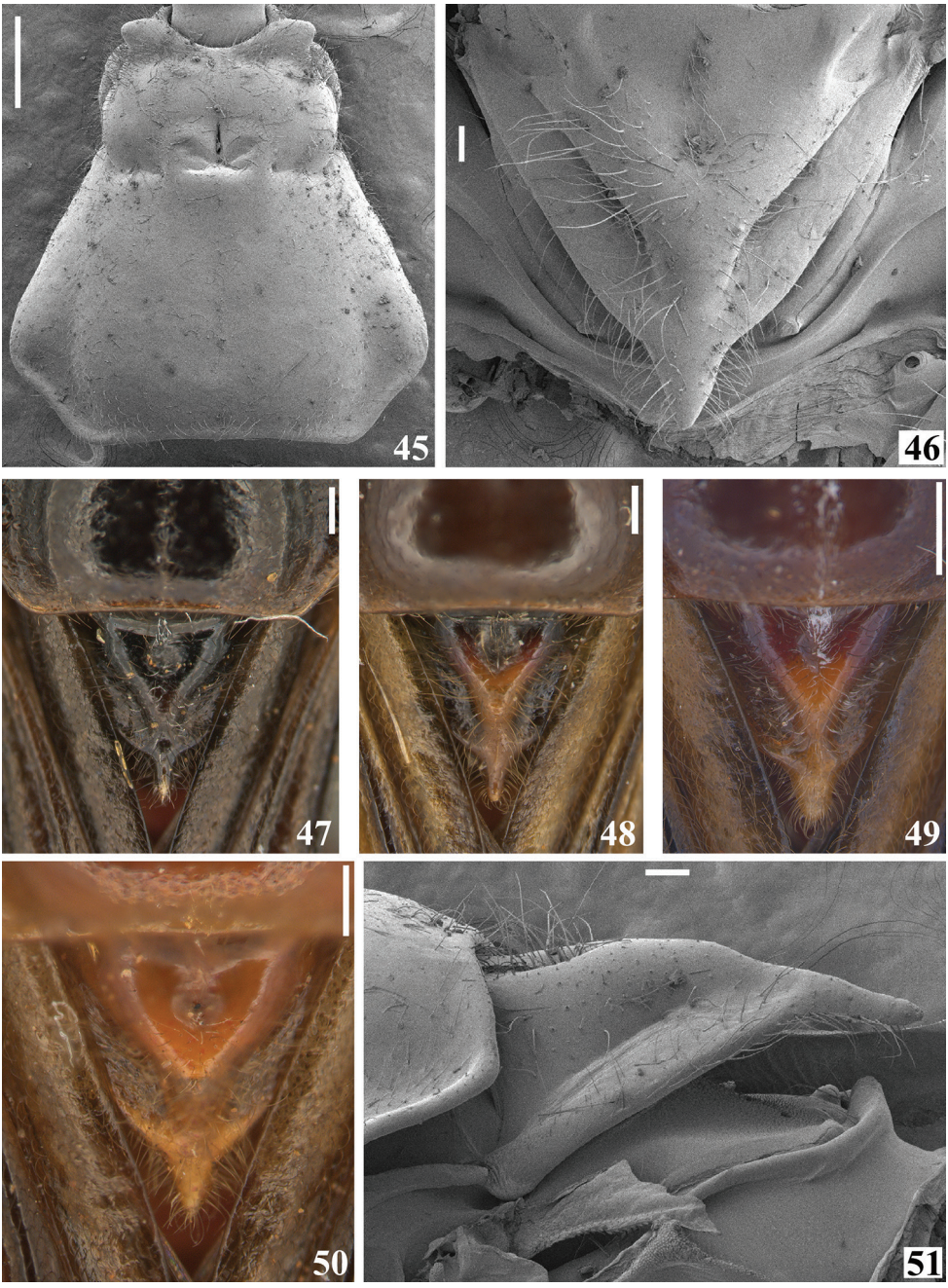

Figures 45–51. *Quasigraptocleptes maracristinae* gen. nov., sp. nov., males, thorax **45–50** dorsal view. **45** pronotum **46–51** scutellum **51** lateral view. Scale bars: 0.5 mm (**45, 49**); 0.25 mm (**47, 48, 50**); 0.1 mm (**46, 51**).

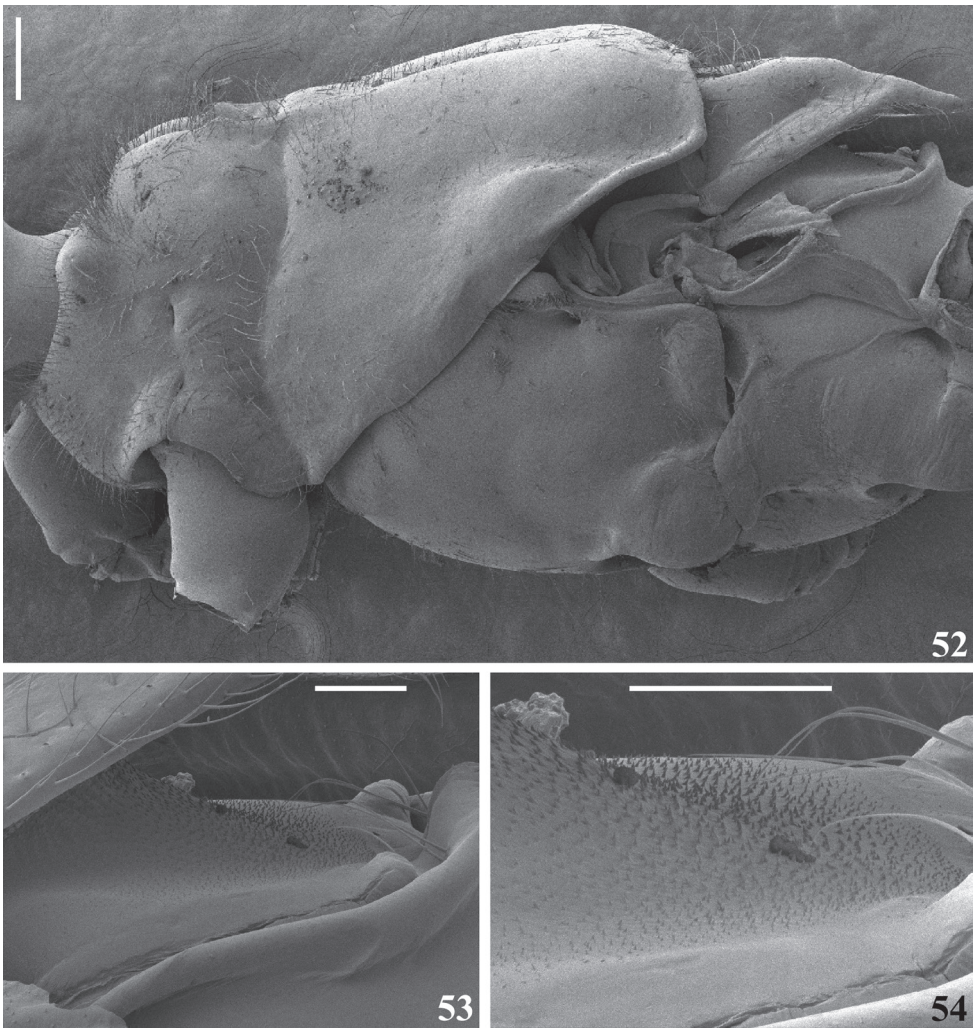

Figures 52–54. *Quasigraptocleptes maracristinae* gen. nov., sp. nov., male, thorax, lateral view **52** legs and wings extracted **53, 54** sclerite below scutellum **54** under higher magnification. Scale bars: 0.3 mm (**52**); 0.1 mm (**53, 54**).

Female. Figs 88–100. Measurements are given in Table 2. Similar to male in general. One specimen with a general dark coloration (Fig. 88) and other with reddish general coloration (Figs 89–97); both with only the submedian distal yellowish annuli on middle and hind femora evident. **Structure.** ***Head*:** basiflagellomere slightly thicker in basal portion (Fig. 94), but much thinner as a whole than that in males, and becoming progressively thinner toward apex, without a clear separation between more or less thickened portions (Fig. 94), uniformly covered with pubescence formed by thin, pale setae (blackish, stiff, adpressed, short setae that completely cover thicker portion in male are absent); approximately 1.2 times longer than scape. Sternites IV–VII with

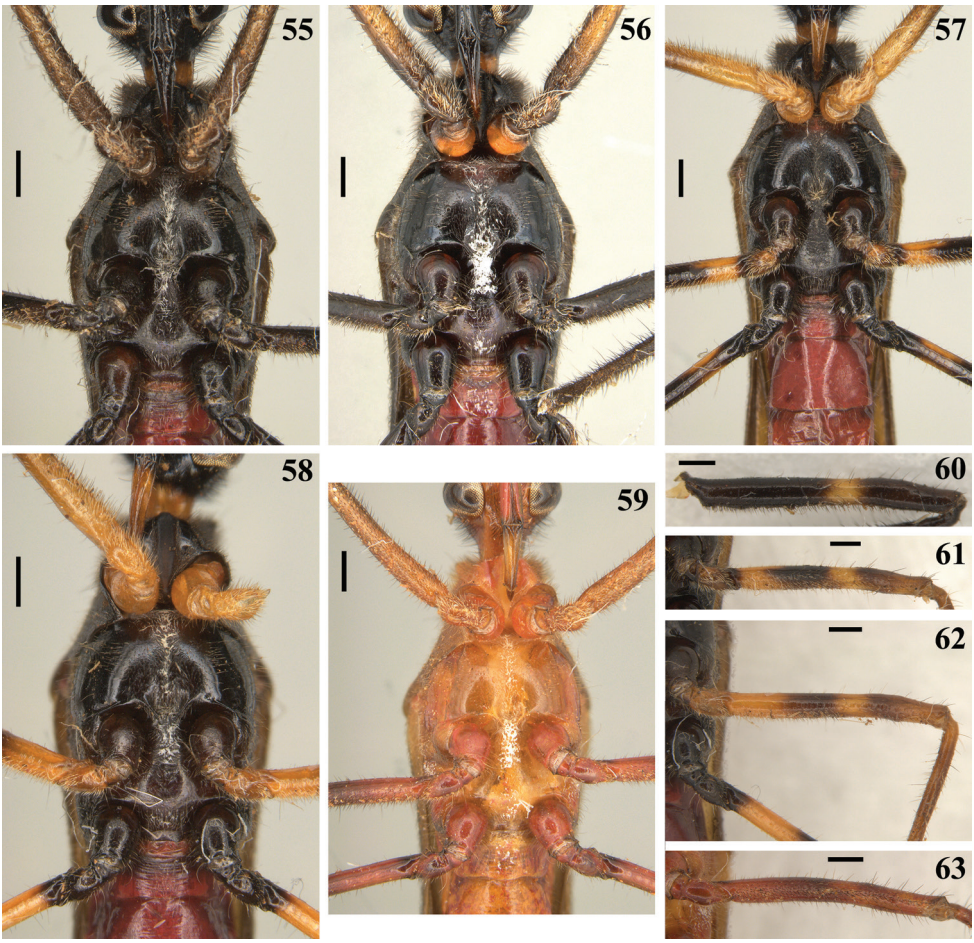

Figures 55–63. *Quasigraptocleptes maracristinae* gen. nov., sp. nov., males **55–59** thorax and first visible (s) sternite (s), ventral view **60–63** middle femur **60–62** lateral view **63** ventral view. Scale bars: 0.5 mm (**55–59**); 0.4 mm (**60–63**).

fusiform or elongated patches of minute, short, adpressed, thin, whitish setae, covered with a variable amount of white wax, present on midlateral portions of basal half (sternites IV, V) or, although with more numerous setae on basal portions, extending along the segment on sternites VI and VII; in one specimen, also sparsely on basal portion of the genital tergite 9 (Figs 97–99). External genitalia in posterior view (Fig. 100): tergite 9 with very long, sparse, strong blackish setae at median and lateral portions and numerous shorter, thinner setae at distal margin; tergite 10 with sparse short setae; gonocoxite 8 and gonapophysis 9 with numerous short to somewhat longer setae.

Comments. The genitalia of different males presenting a range of color variation (e.g. Figs 17–19) showed to have the same characteristics of structure (Figs 72–87). The females were slightly larger than the males (Tables 1, 2).

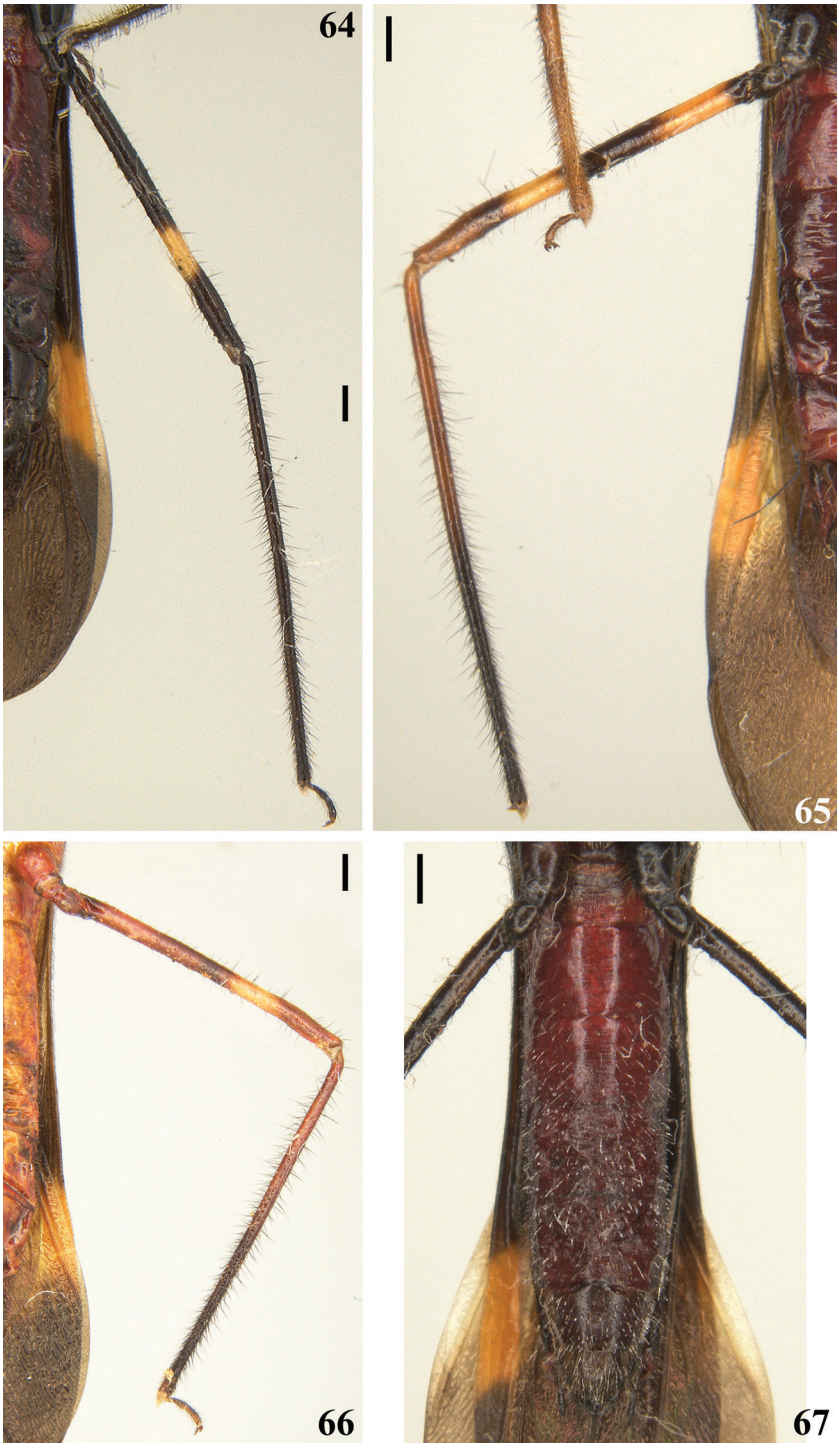

Figures 64–67. *Quasigraptocleptes maracristinae* gen. nov., sp. nov., males **64–66** hind leg, lateral view. **67** abdomen, ventral view. Scale bars: 0.5 mm (**64–67**).

Table 2. Measurements (mm) of female type specimens (n = 2) of *Q. maracristinae* sp. nov.

	Mean	SD	Maximum	Minimum
Body length to tip of hemelytra	15.3	0.28	15.5	15.1
Body length to tip of abdomen	12.1	0.14	12.2	12.0
Head length (excluding neck)	1.45	0.07	1.5	1.4
Anteocular portion length[1]	0.55	0.62	0.6	0.5
Postocular portion length[1]	0.55	0.62	0.6	0.5
Head width across eyes	1.45	0.07	1.5	1.4
Interocular distance (synthlipsis)	0.8	–	0.8	0.8
Transverse width of eye	0.34	0.01	0.35	0.33
Length of eye	0.5	–	0.5	0.5
Ocellar tubercle width	0.9	–	0.9	0.9
Scape length	4.25	0.07	4.3	4.2
Pedicel length	1.35	0.07	1.4	1.3
Basiflagellomere length	5.25	0.07	5.3	5.2
Basiflagell. max. width	0.15	0.07	0.2	0.1
Distiflagellomere length (n = 1)[2]	–	–	1.5	1.5
Labial segment II length[1]	1.2	–	1.2	1.2
Labial segment III length[1]	0.9	–	0.9	0.9
Labial segment IV length[1]	0.25	0.07	0.3	0.2
Pronotum length (at midline)	2.65	0.07	2.7	2.6
Pronotum maximum width	2.9	–	2.9	2.9
Scutellum length	1.2	–	1.2	1.2
Fore femur length	3.65	0.07	3.7	3.6
Fore tibia length	4.1	0.14	4.2	4.0
Fore tarsus length	0.5	-	0.5	0.5
Middle femur length	3.1	0.14	3.2	3.0
Middle tibia length	3.85	0.07	3.9	3.8
Middle tarsus length (n = 1)[2]	–	–	0.8	0.8
Hind femur length	4.8	0.14	4.9	4.7
Hind tibia length	5.25	0.07	5.3	5.2
Hind tarsus length	0.65	0.07	0.7	0.6
Abdomen length[3]	7.1	0.14	7.2	7.0
Abdomen maximum width	1.85	0.07	1.9	1.8

[1] Measured in lateral view; [2] Segments or portions broken or missing in some specimens; [3] Measured on ventral view, at midline, from anterior margin of sternite II to posterior border of genitalia.

The minimum body length in females (to tip of hemelytra/tip of abdomen: 15.1/12.0) is greater than the maximum body length in males (14.0/11.0). Many of the other measurements are proportionally greater in females, in accordance with their bigger size (Tables 1, 2), including the antennal scape and pedicel, slightly longer than in males. One apparent exception is the basiflagellomere, which was longer in most males (5.1 to 6.5 mm in length; n = 8) than in females (5.2 to 5.3 mm in length; n = 2) and showed to be generally thicker approximately in basal half in males (maximum width: 0.2–0.4 mm) (Figs 17–19, 38–40), but thinner in females (maximum width: 0.1–0.2 mm) (Figs 88, 94). This thickened region in males is completely covered by blackish, stiff, adpressed, and short setae (Figs 38–40), which are absent in females

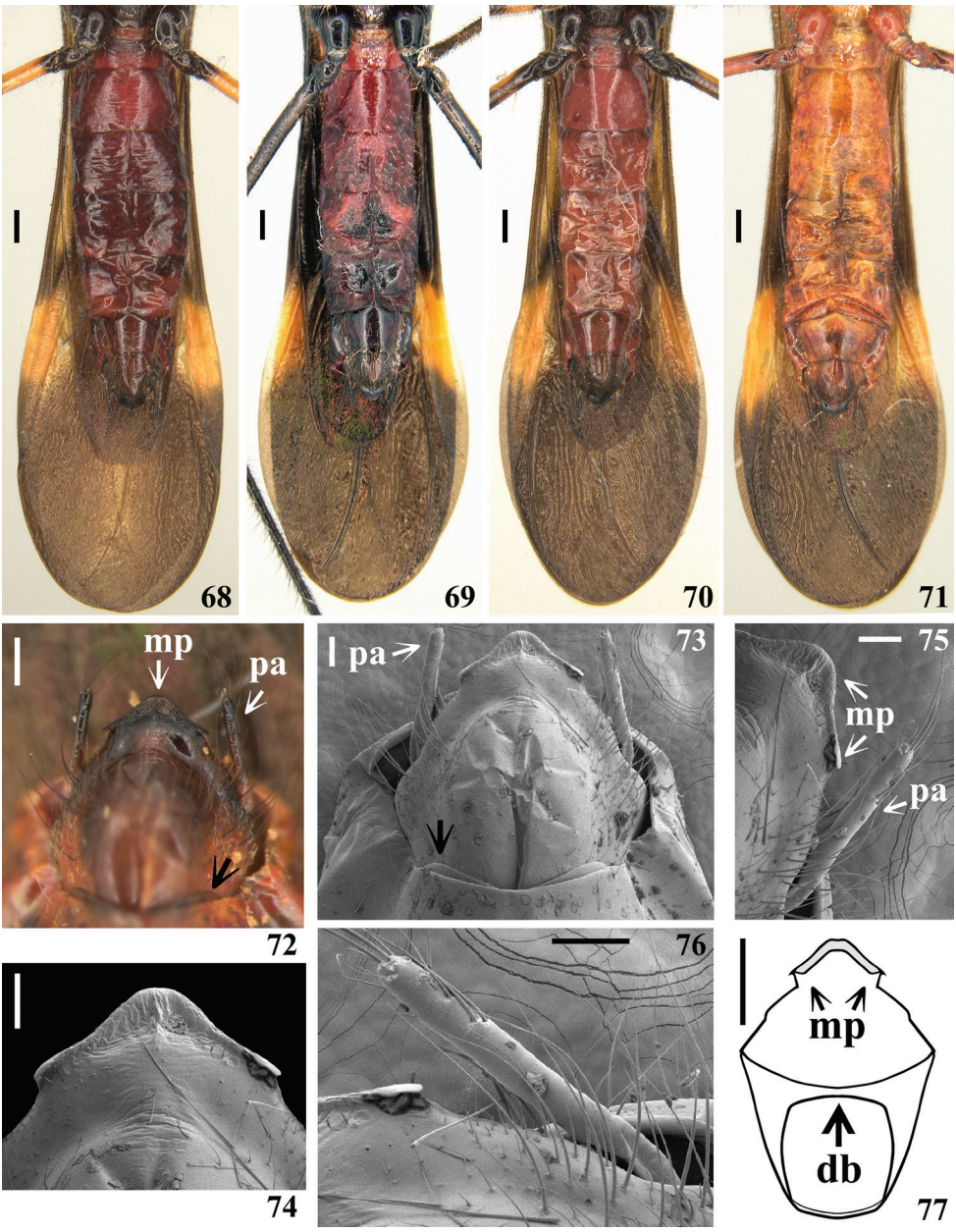

Figures 68–77. *Quasigraptocleptes maracristinae* gen. nov., sp. nov., males **68–71** abdomen and apical portion of membrane of hemelytra, ventral view **72–76** ventral view **72, 73** apex of abdomen with pygophore in situ, black arrows point to distal margin of segment VIII **74** medial process of pygophore **75, 76** lateral portion of pygophore and left paramere **77** pygophore without parameres, schematic outline, dorsal view. Abbreviations: **db**: dorsal bridge; **mp**: medial process of pygophore; **pa**: paramere. Scale bars: 0.5 mm (**68–71, 77**); 0.2 mm (**72**); 0.1 mm (**73–76**).

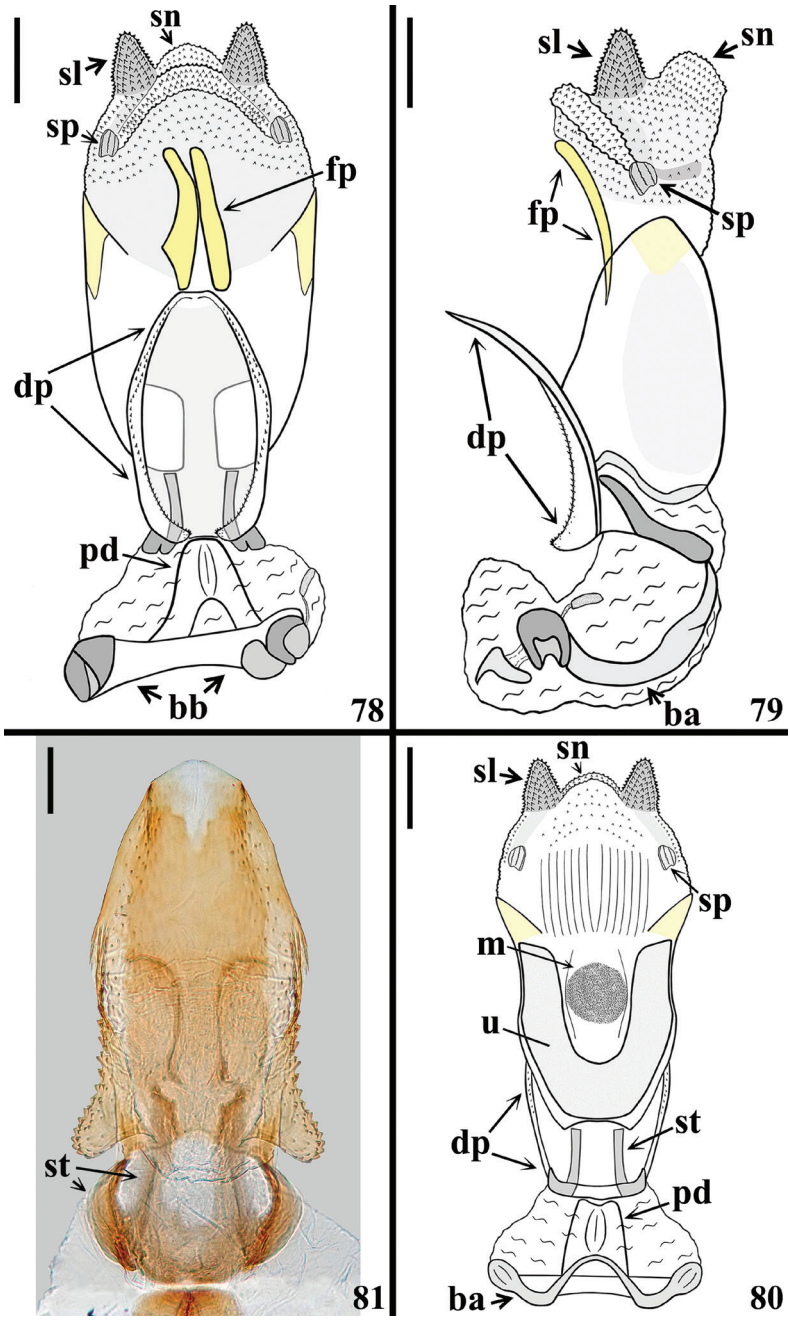

Figures 78–81. *Quasigraptocleptes maracristinae* gen. nov., sp. nov., male genitalia **78–80** phallus **78** dorsal view **79** lateral view **80** ventral view **81** dorsal phallothecal plate and struts, dorsal view. Abbreviations: **ba**: basal plate arm; **bb**: basal plate bridge; **dp**: dorsal phallothecal plate; **fp**: flat process of endosoma; **m**: median process of endosoma; **pd**: pedicel; **sl**: sclerotized subtriangular lobe of endosoma wall; **sn**: not sclerotized lobe; **sp**: small sclerotized portion; **st**: strut; **u**: U-shaped process of endosoma. Scale bars: 0.2 mm (**78–80**); 0.1 mm (**81**).

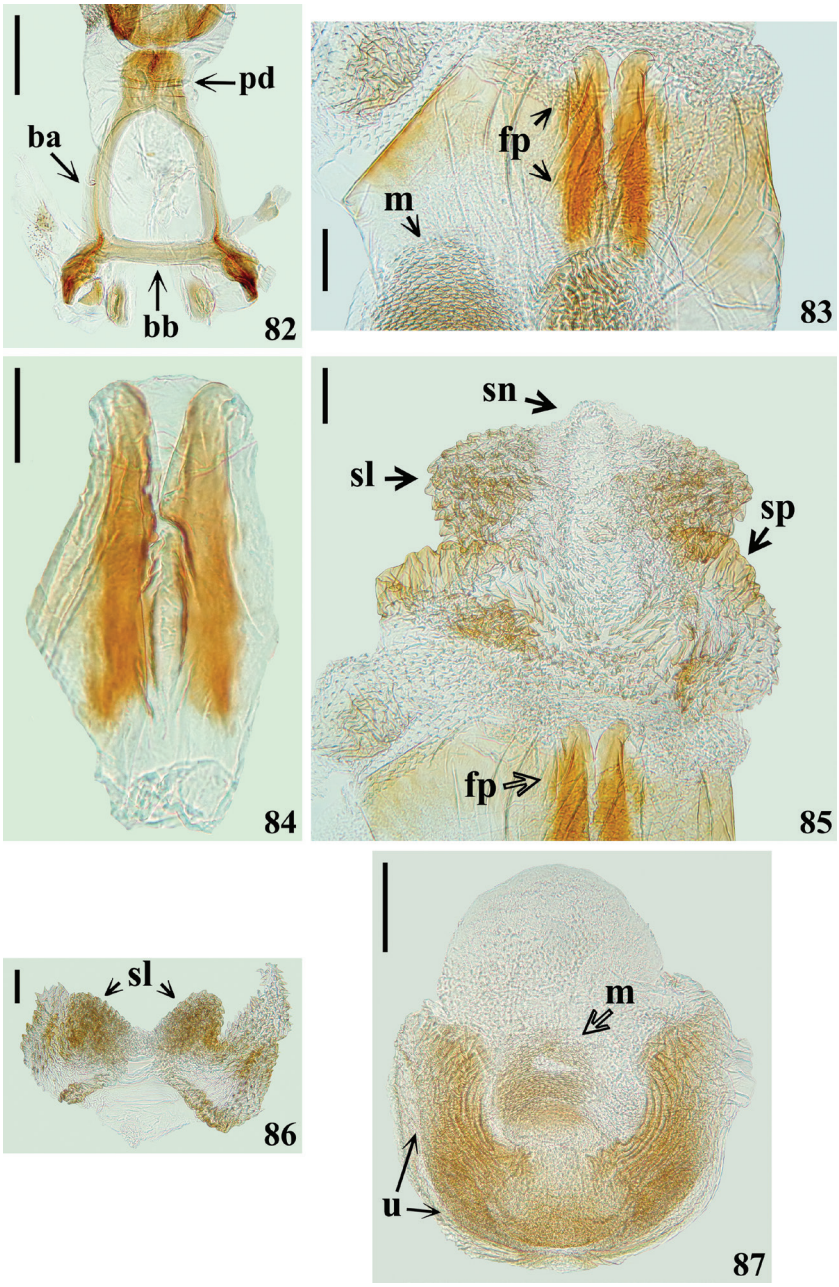

Figures 82–87. *Quasigraptocleptes maracristinae* gen. nov., sp. nov., male genitalia **82–86** dorsal view **82** articulatory apparatus **83** phallus, middle portion **84** flat processes of endosoma **85** phallus, apical portion **86** apical subtriangular lobes of endosoma wall; **87** U-shaped and median processes of endosoma, ventral view. Abbreviations: **ba**: basal plate arm; **bb**: basal plate bridge; **fp**: flat process of endosoma; **m**: median process of endosoma; **pd**: pedicel; **sl**: sclerotized subtriangular lobe of endosoma wall; **sn**: not sclerotized lobe; **sp**: small sclerotized portion; **u**: U-shaped process of endosoma. Scale bars: 0.2 mm (**82, 87**); 0.1 mm (**83–86**).

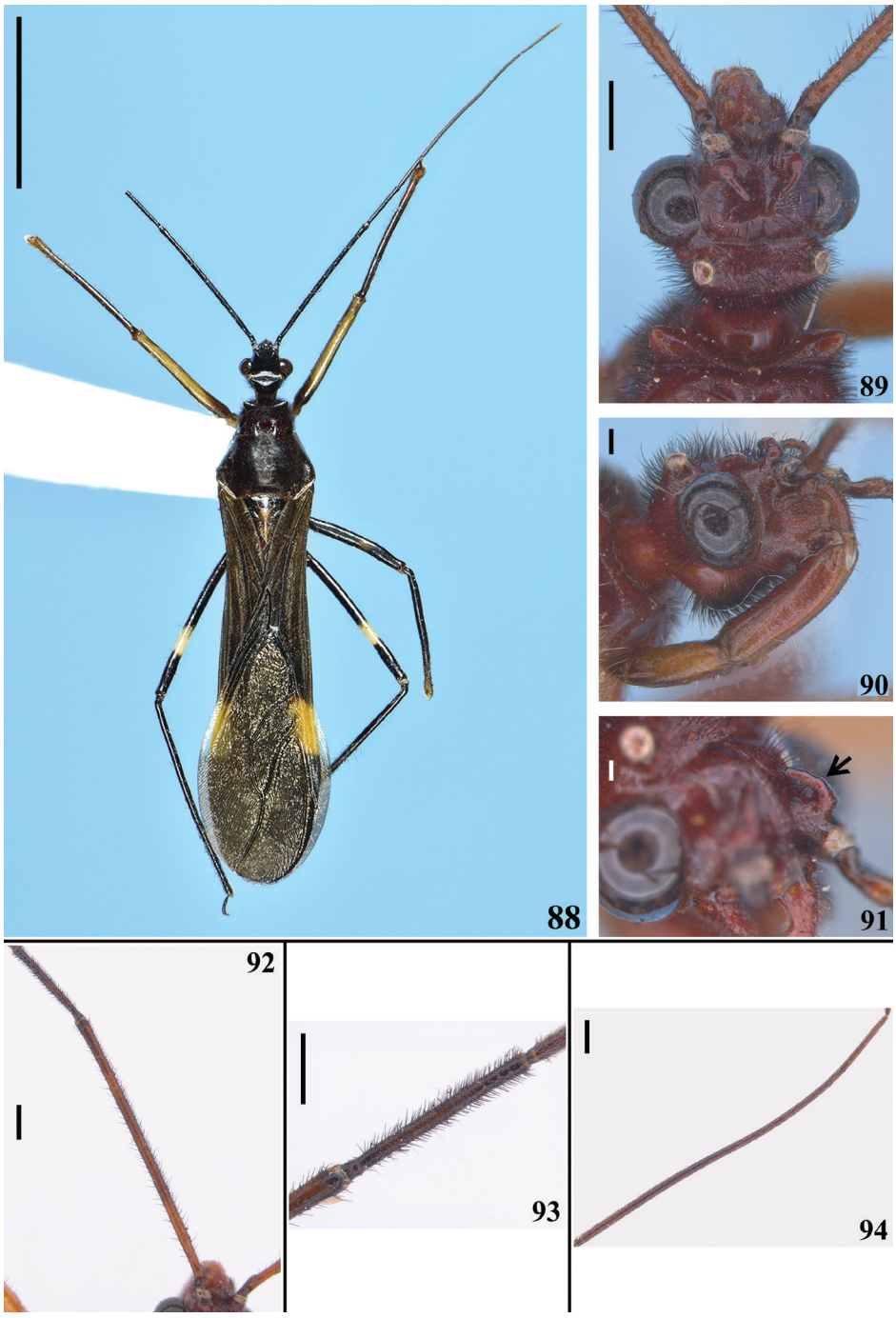

Figures 88–94. *Quasigraptocleptes maracristinae* gen. nov., sp. nov., females **88–89** dorsal view. **89** head and anterolateral angles of pronotum **90** head, anterolateral view **91** left postantennal spine (pointed by an arrow), inner surface, lateral view **92–94** antennal segments, dorsal view **92** scape and pedicel **93** apex of scape, pedicel and basal portion of basiflagellomere **94** basiflagellomere. Scale bars: 5.0 mm (**88**); 0.5 mm (**89, 92–94**); 0.2 mm (**90**); 0.1 mm (**91**).

(Fig. 94). While the males presented a wide range of variation in coloration and markings, the two females examined presented different patterns of coloration, but similar to some of the males. Also, the patches of minute, short, adpressed, thin, whitish setae, covered with a variable amount of white wax, present on sternites IV–VII and even on the basal portion of the genitalia (Fig. 97), were absent in the males, with the exception of the record of a narrow stripe of whitish setae on distal half of sternite VII, extending to the basal portion of the exposed portion of pygophore in a single male (Fig. 69). However, because the relatively low number of specimens examined, especially of females (only two), it is not possible to be sure in what extent most of these differences are intraspecific or sexually dimorphic characteristics. Similarly, in relation to coloration, only the examination of more specimens of both sexes will allow ascertaining the range of variation and if there is any sexual dimorphism.

Distribution. Brazil, in states of Minas Gerais and Paraná.

Etymology. The new species is named in honor of Dr. Mara Cristina Pinto (Faculty of Pharmaceutical Sciences, UNESP, Araraquara, São Paulo, Brazil), a friend and eternal mentor of the second author (JO), as a tribute and recognition for her contributions to the studies of Medical Entomology, especially those on sandflies and also for all her meritorious performance as a teacher and knowledge as a transforming agent. The taxon's homage is a way of rewarding all her remarkable contributions to Brazilian entomology which she has been studying for more than 33 years.

Comments. The variation in color and number and extension of pale markings recorded among the specimens of *Q. maracristinae* sp. nov. studied here are considered as intra-specific variability. It is in accordance with the intraspecific variation in color, occasionally at extreme range, previously documented in many harpactorines (e.g., Stål 1872; Champion 1899; Gil-Santana 2008, 2022; Zhang et al. 2016), including in some wasp-mimicking Harpactorini (Champion 1899; Gil-Santana et al. 2013, 2017).

The wax-like substance was sometimes absent from portions where it was observed on other specimens. It may be lost during the manipulation of the individuals, which may also include loss of the thin fragile setae associated with it (HRG-S pers. obs.; Gil-Santana et al. 2017). Body parts covered with patches of setae with whitish wax-like material have been registered in some Harpactorini species, such as *Cosmoclopius curacavensis* Cobben & Wygodzinsky, 1975 (Cobben and Wygodzinsky 1975), *Harpactor angulosus* (Lepeletier & Serville, 1825) (Pikart et al. 2014), various species of *Heza* Amyot & Serville, 1843 (Maldonado 1976), *Sphedanolestes zhengi* Zhao, Ren, Wang & Cai, 2015 (Zhao et al. 2015), and *Parahiranetis salgadoi* (Gil-Santana et al. 2017). It is noteworthy that the wax-like substance may be absent when specimens are examined and described, and thus the extent of their existence may remain unknown (Gil-Santana et al. 2017). Similarly, records of the presence or absence of a wax-like substance may be an additional feature of systematic or taxonomic importance, in the same way as suggested for the "extensive sericeous areas on the abdominal sterna" of *Heza ventralis* Stål, 1872 (Maldonado 1976). Therefore, as stressed by Gil-Santana et al. (2017), future studies on Harpactorini should include careful handling of the specimens after collection, to avoid unintentional removal of these substances from their bodies. It is also recommended that this information should be included in the records and/or descriptions whenever present.

Figures 95–100. *Quasigraptocleptes maracristinae* gen. nov., sp. nov., female **95** postocular portion of head, pronotum and basal portion of scutellum, dorsal view **96–99** ventral view **96** thorax and first visible sternites **97** abdomen **98** patches of minute, short, adpressed, thin, whitish setae, covered with a variable amount of white wax on left side of sternites VI–VII **99** main portion of the patch of left side of sternite VI in higher magnification **100** female genitalia, posterior view. Scale bars: 0.5 mm (**95–97**); 0.1 mm (**98–100**).

Differences in the structure and vestiture of the basiflagellomere were clear-cut enough to be considered sexually dimorphic in *Q. maracristinae* sp. nov. Despite the small number of females, adults can be sexed readily with the naked eye, by observing the basiflagellomeres of their antennae. The females examined were larger than males in many of the morphological characteristics measured, what can be confirmed by

studying more specimens in the future. In any case, the two sexual differences pointed out in *Q. maracristinae* sp. nov. (i.e., females larger than males and the latter with basiflagellomere thickened) are concordant with several observations in the literature (Champion 1899; Martin-Park et al. 2012; Gil-Santana et al. 2013, 2017; Gil-Santana 2016). Additionally, the thickened portion of the basiflagellomere in males was completely covered by short, stiff, adpressed, blackish setae, which were absent in females. Although fewer females were examined, their coloration showed similar patterns of variation of some of the males, therefore only with the examination of more specimens will be possible to ascertain possible sexual variation in coloration patterns. Yet, in the females, patches of minute, short, adpressed, thin, whitish setae, covered with a variable amount of white wax, were present on sternites IV–VII and even on the basal portion of the genitalia, while in the males they were absent (with the exception of a single male in which only a narrow stripe of whitish setae was present on distal half of sternite VII, extending to the basal portion of the exposed portion of pygophore). In other wasp-mimicking harpactorines, such as *Parahiranetis salgadoi*, similar patches of setae covered with white wax on sternites were observed in both sexes (Gil-Santana et al. 2017). Therefore, it is necessary to examine more specimens in order to ascertain if the absence/presence of these patches on sternites in males and females of *Q. maracristinae* sp. nov., respectively, expresses another sexual dimorphism or if it is merely an inter-individual variation.

In the male genitalia, while the variation in color of the pygophore (Figs 67–72) is compatible with the general intra-specific variability in coloration, the uniformity of the other characteristics (Figs 72–87) is in accordance with the assumption that all specimens belong to the same species.

Yet, the male genitalia of *Q. maracristinae* sp. nov. showed similarities to those of *G. bicolor* (Gil-Santana et al. 2013), *H. atra* (Gil-Santana 2016), and *P. salgadoi* (Gil-Santana et al. 2017), such as: - parameres similar in shape and somewhat similar in vestiture; - pygophore with a somewhat large medial process that is medially rounded at the apex, but in *G. bicolor* and *H. atra* it is subtriangular in shape, while in *P. salgadoi* and *Q. maracristinae* sp. nov. it is somewhat arrow-shaped, with the lateral margins acutely pointed (Figs 72–74); - pedicel (pd) (= basal plate extension) short; - struts with subparallel median arms and curved basal lateral arms, although with different shapes in each species; - a pair of elongate, parallel, flat, weakly sclerotized endosomal processes, although with different locations and shapes in each of these species.

The presence of a somewhat laterally expanded basal portion with small acute spines on lateral margins of the dorsal phallothecal plate was recorded in *P. salgadoi* and *Q. maracristinae* sp. nov. U-shaped and median subspherical endosomal processes very similar to those of *Q. maracristinae* sp. nov. (Figs 80, 87) were recorded in *H. atra* and *P. salgadoi*. Yet, variable, different, or not well evident spiny lobes or portions of endosoma wall were recorded in each of these species, making their comparison difficult.

On the other hand, the general shape and peculiarities of the dorsal phallothecal plate were different in all species (Gil-Santana et al. 2013; Gil-Santana 2016; Gil-Santana et al. 2017; this study).

Thus, in agreement with previous studies (Elkins 1954a, b; Hart 1975, 1986, 1987; Forero et al. 2008; Zhang et al. 2016), the features of the male genitalia of *Q. maracristinae* sp. nov. that should especially be taken into consideration for comparative purposes are the shape of the medial process of the pygophore and the features of the dorsal phallothecal plate.

Xystonyttus Kirkaldy, 1909

Cosmonyttus Stål, 1868: 103; Stål 1872: 83 (not Stål 1866: 295); Lethierry and Severin 1896: 178 [catalog; including erroneously Stål 1866: 295]. Type species: *Zelus ichneumoneus* Fabricius 1803: 286, by monotypy.

Xystonyttus Kirkaldy, 1909: 388 [as a new name for "*Cosmonyttus*, Stål, 1872 (not 1866)"]; Wygodzinsky 1949: 48 [catalog]; Putshkov and Putshkov 1985: 66 [catalog]; Maldonado 1990: 324 [catalog]; Maldonado and Lozada 1992: 165 [key]; Forero 2011: 16 [checklist]; Gil-Santana 2015: 37 [key], 2016: 92 [citations]; Gil-Santana et al. 2017: 41 [citation]. Type species: *Zelus ichneumoneus* Fabricius 1803: 286, by original designation.

Morphological remarks. Head gibbous, large, as long as wide across eyes, densely covered with long setae on ventral and postocular portions; postantennal spines elongated, curved forward, apices acute. Legs: fore and hind femora curved at median portion; fore femora thickened, narrowing at apices; fore tibia curved at apical third; middle and hind legs elongated, slender. Hemelytra long, surpassing the abdomen by somewhat more than half of the length of the membrane.

Xystonyttus ichneumoneus (Fabricius, 1803)

Figs 101–108

Zelus ichneumoneus Fabricius, 1803: 286 [description; "Habitat in America meridionali"].

Cosmonyttus ichneumoneus Stål, 1868: 103–104 [redescription; color varieties "a", "b" and "c"; record from Suriname]; Stål 1872: 83 [catalog]; Lethierry and Severin 1896: 178 [catalog; cited as being from Guyana].

Myocoris ichneumoneus Walker, 1873b: 129 [catalog; record from Brazil].

Xystonyttus ichneumoneus Kirkaldy, 1909: 388 [type species to *Xystonyttus*, new name to *Cosmonyttus* Stål, 1872]; Haviland 1931: 150 [record from Guyana]; Wygodzinsky 1949: 48 [catalog; cited as being from [British] Guyana]; Maldonado 1990: 324 [catalog; cited as being originally described from [British] Guyana]; Gil-Santana et al. 2003: 12 [comment on its etymology].

Notes. The general similarity of *X. ichneumoneus* (Figs 101, 102, 104, 105) with ichneumonids certainly led Fabricius (1803) to name it as such (Gil-Santana et al. 2003).

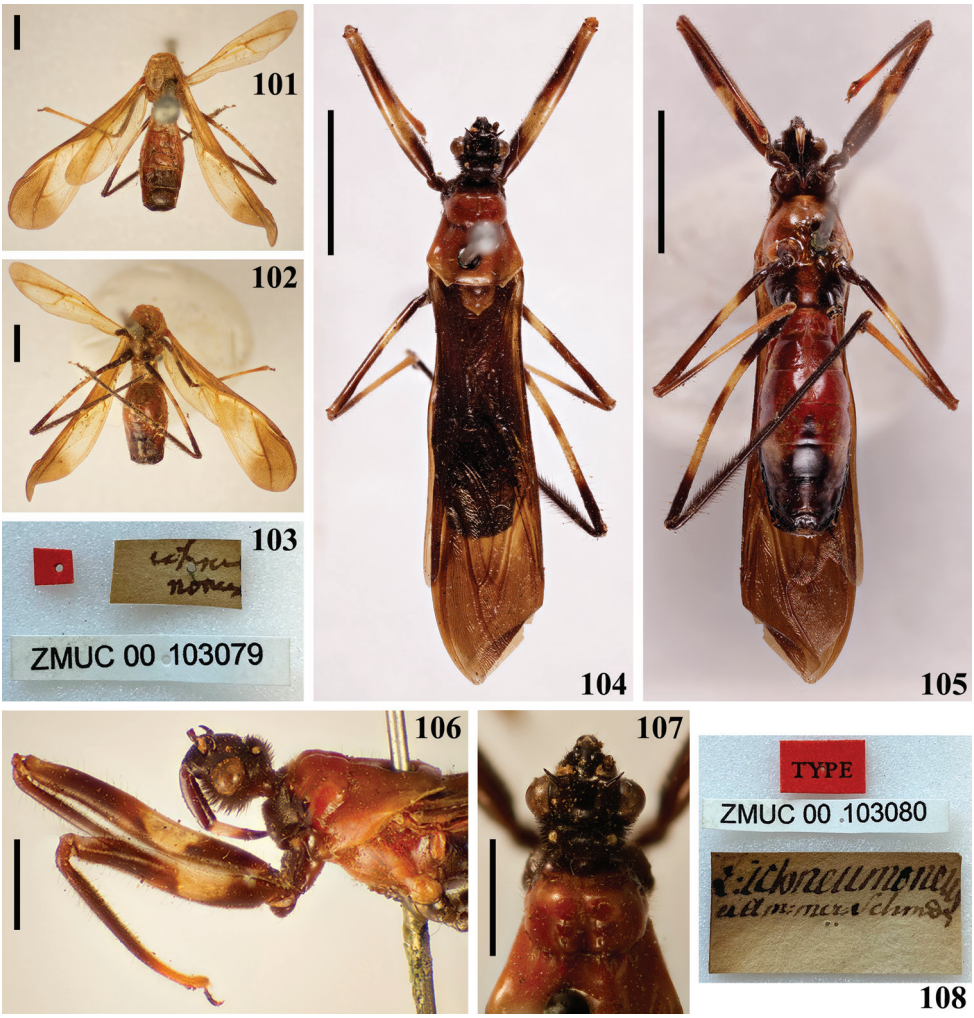

Figures 101–108. *Zelus ichneumoneus* Fabricius, 1803, female syntypes deposited in ZMUC **101–103** syntype catalog number ZMUC 00 103079 **101** dorsal view **102** ventral view **103** labels **104–108** syntype catalog number ZMUC 00 103080 **104** dorsal view **105** ventral view **106** head, pronotum, fore legs, lateral view **107** head and most part of pronotum, dorsal view **108** labels. Scale bars: 5.0 mm (**104, 105**); 2.0 mm (**101, 102, 106, 107**).

Fabricius (1803) recorded the species from South America ("America meridionali") without specifying a country or location. The citations of Guyana ("British Guiana") as the country from which the species was described, apparently were first stated by Lethierry and Severin (1896). Possibly, it was assumed because Fabricius (1803) cited "Dom. Smidt. Mus. Dom. de Sehestedt" when stating about the specimens of *Zelus ichneumoneus* examined by him. In fact, "most of the numerous South American species that Fabricius described and for which a certain Smidt is cited as a collector are found

only in the Copenhagen Museum, in Tönder Lund's and Sehestedt's famous collections (…). The only information (…) on Smidt is that he visited besides several West Indian islands, certain places on the South American mainland, such as Essequibo and Demerara in the present British Guiana; therefore all of the South American species cited as having been collected by Smidt can with certainty be considered as coming from the vicinity of the named localities, and this is just what one who is familiar with American Hemiptera and their distribution immediately perceives" (Stål 1868: 3, translation by G. C. Steyskal in Papavero 1971: 21). Stål (1868: 104), however, when recording the distribution of *X. ichneumoneus* maintained the original statement of Fabricius (1803) ("America meridionalis. Dom Smidt. (Mus. Sehestedt)"), adding: "Surinam. (Mus. Holm.)". The latter refers to the specimen(s) examined and considered as belonging to *X. ichneumoneus* by himself in Stockholm Museum (currently, Swedish Museum of Natural History, Stockholm, Sweden), while Stål (1872) restricted the occurrence of the species to Suriname only. In any case, Haviland (1931) recorded *X. ichneumoneus* from Kartabo, Bartica District, Guyana, confirming the presence of the species in this country.

In the Natural History Museum of Denmark (ZMUC), Copenhagen, Denmark, there are two type specimens of *X. ichneumoneus*, both of them females, and considered here as syntypes, following Art. 73.2 of ICZN. In the syntype catalogued as ZMUC 00 103079, the head, fore legs, and a portion of the prothorax are missing (Figs 101, 102), while the other syntype, numbered as ZMUC 00 103080, is quite well preserved, with only the antennae and most tarsi missing (Figs 104–107). In the original label attached to the latter syntype (Fig. 108) the word "*ichneumoneus*" is clearly legible. Both specimens seem to belong to the same species judging by the remaining portions of the syntype ZMUC 00 103079 (Figs 101, 102), while the characteristics observed in the syntype ZMUC 00 103080 (Figs 104–107) agree very well with the original description (Fabricius 1803: 286). The photographs presented here are helpful to ascertain not only the characteristics of the species but also those regarded as establishing limits between the recognized genera of Neotropical wasp-mimicking Harpactorini.

The concise description of the coloration of the specimens of *X. ichneumoneus*, as recorded by Haviland (1931), without mention of any variation, was quite similar not only with the original description of the species (Fabricius 1803) but also with that observed in the syntypes (Figs 101, 102, 104–107). The color variations attributed to *X. ichneumoneus* by Stål (1866), however, are in need to be reviewed by examining series of specimens with more comprehensive approaches, since they may be variations of this single species or may represent two or more different species.

Discussion

Among the Neotropical Harpactorini, *Quasigraptocleptes* gen. nov. seems closer to *Graptocleptes* and *Hiranetis*, while the latter have been considered allied genera (Stål 1872; Champion 1899) and also close to *Parahiranetis* (Gil-Santana 2015; Gil-Santana et al. 2017).

The main diagnostic characteristics that separate *Hiranetis*, *Graptocleptes*, *Parahiranetis* and *Quasigraptocleptes* gen. nov. according to Spinola (1840a, b), Stål (1866, 1872), Maldonado and Lozada (1992), Gil-Santana et al. (2013, 2017), Gil-Santana (2015, 2016) and this work, are the following:

1. *Graptocleptes*: head elongate, approximately 1.1 to 1.3 times as long as width across eyes; legs thicker; fore femur shorter than head and pronotum together, somewhat thicker basally or with uniform thickness.
2. *Hiranetis*: head gibbous, swollen ventrally, approximately as long as width across eyes; legs elongated, slender; fore femur subequally longer than head and pronotum together, thicker basally.
3. *Parahiranetis*: head elongate, approximately 1.3–1.7 times as long as width across eyes; legs elongated, slender; fore femur subequally longer than head and pronotum together, thicker basally.
4. *Quasigraptocleptes* gen. nov.: head gibbous, swollen ventrally, approximately as long as width across eyes; legs thicker; fore femur shorter than head and pronotum together, somewhat thicker basally.

Additionally, while *Quasigraptocleptes* gen. nov. has conspicuous postantennal spines strongly curved backwards and completely or partially directed medially (Figs 20–33), in most species of the other three genera mentioned above, these spines are absent or present as small postantennal tubercles or in some species of *Graptocleptes* as straight vertical or semivertical spines (Stål 1872; Maldonado and Lozada 1992; Gil-Santana et al. 2013, 2017; Gil-Santana 2015, 2016, 2022).

Historically, only the pattern of yellowish or straw-colored hemelytra with a median transverse black band has received attention in regard to the supposed mimicry between Harpactorini and species of hymenopteran Ichneumonidae and Braconidae (Champion 1899; Haviland 1931; Maldonado and Lozada 1992; Hogue 1993; Leathers and Sharkey 2003; Hespenheide 2010). However, some species that have similar patterns of blackish wings with yellowish 'pterostigmata' and pale bands on the middle and hind femora arise as possible candidates for mimetic complexes, including *Q. maracristinae* sp. nov. As suggested by Gil-Santana et al. (2017), these would be the wasp-mimicking harpactorines *Graptocleptes bicolor*, *G. haematogaster* (Stål, 1860), an undescribed species of *Hiranetis* and *Parahiranetis salgadoi* as well as ichneumonoid wasps and a species of the cerambycid beetle, all of them recorded from southeastern Brazil.

Although there are records of color variation in some wasp-mimicking Harpactorini, at least in the species with the pattern of darkened or blackish hemelytra with yellowish pterostigmata, there is no variation in this pattern. The yellowish pterostigmata are always present (e.g., Gil-Santana et al. 2013, 2017). The specimens of *Q. maracristinae* sp. nov. studied here were concordant with this assumption, taking into account that, in spite of a considerable range of variation in color, the mentioned pattern of the hemelytra was present in all of them.

Additionally, as emphasized by Gil-Santana (2015) and Gil-Santana et al. (2017), it is necessary to elucidate which species or groups of insects share the same color pattern as in *Q. maracristinae* sp. nov. (i.e., blackish to reddish coloration with yellowish 'pterostigmata' on wings and/or yellowish markings on legs) are involved in possible mimicry complexes.

Key to the Neotropical genera of wasp-mimicking Harpactorini

Based on Stål 1866, 1872; Elkins 1969; Maldonado and Lozada 1992; Gil-Santana 2015; Castro-Huertas and Forero 2021.

1 Pronotum greatly inflated and covering scutellum posteriorly ..... ***Coilopus*** **Elkins, 1969**

– Pronotum not inflated; scutellum not covered by the posterior portion of pronotum and visible from above **2**

2 Hind lobe of pronotum with a pair of elevated submedial longitudinal carinae and spines on its posterior margin; fore trochanter with a ventral spine in most species ..... ***Acanthischium*** **Amyot & Serville, 1843**

– Hind lobe of pronotum different; fore trochanter without spines..... **3**

3 Postantennal spines curved and directed forward **4**

– Postantennal spines absent, as tubercles, straight directed vertically, semivertically or strongly curved backwards **6**

4 Head generally sparsely setose (Figs 3, 11, 14) .. ***Myocoris*** **Burmeister, 1835**

– Head quite setose to very densely setose, especially on ventral and post-ocular portions **5**

5 Fore femora almost entirely thickened, somewhat narrowing at apex only; fore tibiae curved at apical third (Fig. 106) ..... ***Xystonyttus*** **Kirkaldy, 1909**

– Fore femora thicker only basally; fore tibiae straight..... ***Neotropiconyttus*** **Kirkaldy, 1909**

6 Postantennal spines strongly curved backwards and completely or partially directed medially (Figs 20–33)..... ***Quasigraptocleptes*** **gen. nov.**

– Postantennal spines absent, or straight directed vertically, semivertically, or as tubercles **7**

7 Fore femora slender, elongated; clearly thicker basally..... **8**

– Fore femora stouter; not or only slightly thicker basally ..... ***Graptocleptes*** **Stål, 1866**

8 Head gibbous, swollen ventrally, subequally as long as wide across eyes; in dorsal view, postocular portion clearly separated from a distinct neck ..... ***Hiranetis*** **Spinola, 1837**

– Head elongate, not swollen ventrally, approximately 1.3 to 1.7 times as long as wide across eyes; in dorsal view, postocular portion narrowing gradually to form neck ..... ***Parahiranetis*** **Gil-Santana, 2015**

Acknowledgements

We thank the "Laboratório de Microscopia Avançada LMA, Instituto de Química, Unesp", Araraquara, São Paulo, Brazil" for allowing the use of the scanning electron microscope facility. The first author (HRG-S) thanks Jürgen Deckert, former curator of MFNB, for allowing him to examine specimens of this institution. The second author (JO) thanks FAPESP ("Fundação de Amparo à Pesquisa do Estado de São Paulo") and Dr João Aristeu da Rosa for support and for providing the facilities of the Parasitology Laboratory, and is very grateful to the Brazilian entomologist Rafael Barros for donating a female paratype of *Q. maracristinae* sp. nov. We also especially thank the Natural History Museum of Denmark, Anders Alexander Illum, Sree Gayathree Selvantharan, and Lars Vilhelmsen (ZMUC), Gunvi Lindberg (NHRS), as well as Birgit Jaenicke (MFNB), for the photographs that they provided. We are also grateful to an anonymous reviewer, Manuel Baena, and Nikolay Simov for their valuable comments and suggestions.

References

Burmeister H (1835) Handbuch der Entomologie. Zweiter Band. Erste Abtheilung. Schnabelkerfe. Rhynchota. Theodor Christian Friedrich Enslin, Berlin, 400 pp.

Burmeister H (1838) Some account of the genus *Myocoris*, of the family Reduvini. Transactions of the Entomological Society of London 2(2): 102–107. https://doi.org/10.1111/j.1365-2311.1836.tb00303.x

Castro-Huertas V, Forero D (2021) Revision and phylogenetic analysis of the genus *Acanthischium* Amyot & Serville, 1843 (Hemiptera: Reduviidae: Harpactorinae). Insect Systematics & Evolution 52(5): 524–574. https://doi.org/10.1163/1876312X-bja10018

Champion GC (1899) Insecta Rhynchota. Hemiptera-Heteroptera, Vol II. In: Godman FD, Salvin O (Eds) Biologia Centrali Americana. Taylor and Francis, London, 193–304.

Cobben RH, Wygodzinsky P (1975) The Heteroptera of the Netherlands Antilles – IX. Reduviidae (Assassin Bugs). Studies on the Fauna of Curaçao and other Caribbean Islands 48: 1–62.

Elkins JC (1954a) A new American Harpactorine genus (Hemiptera, Reduviidae). Texas Reports on Biology and Medicine 12: 39–48.

Elkins JC (1954b) A synopsis of *Atrachelus* (Hemiptera, Reduviidae). Proceedings of the Entomological Society of Washington 56: 97–120.

Elkins JC (1969) A new genus of hemipteran wasp mimics (Reduviidae, Harpactorinae). Journal of the Kansas Entomological Society 42: 456–461.

Fabricius JC (1803) Systema Rhyngotorum secundum ordines, genera, species: adiectis synonymis, locis, observationibus, descriptionibus. Carolum Reichard, Brunsvigae, 314 pp. https://doi.org/10.5962/bhl.title.11644

Forero D (2011) Classification of Harpactorinae, assassin bugs Hemiptera: Heteroptera: Reduviidae. Boletín del Museo Entomológico Francisco Luís Gallego 1: 9–24.

Forero D, Giraldo-Echeverry N (2015) First record of the assassin bug genus *Coilopus* Elkins, 1969 (Hemiptera: Heteroptera: Reduviidae) from Colombia. Check List 11(3): 1634. https://doi.org/10.15560/11.3.1634

Forero D, Mejía-Soto A (2021) A striking sexually dimorphic new species of *Castolus* (Hemiptera: Heteroptera: Reduviidae) from Colombia, with new records from Neotropical countries and taxonomic notes on the genus. Zootaxa 5048(4): 538–560. https://doi.org/10.11646/zootaxa.5048.4.4

Forero D, Gil-Santana HR, van Doesburg PH (2008) Redescription of the Neotropical genus *Aristathlus* (Heteroptera, Reduviidae, Harpactorinae). In: Grozeva S, Simov N (Eds) Advances in Heteroptera research: festschrift in honor of 80th anniversary of Michail Josifov. Pensoft, Sofia-Moscow, 85–103.

Gil-Santana HR (2008) New records, and nomenclatural and biological notes on Reduviidae (Hemiptera: Heteroptera) from Bolivia and Brazil. Zootaxa 1785(1): 43–53. https://doi.org/10.11646/zootaxa.1785.1.2

Gil-Santana HR (2015) *Parahiranetis salgadoi*, a new genus and species of Harpactorini (Hemiptera: Heteroptera: Reduviidae), with a key to Neotropical wasp-mimicking harpactorine genera. Acta Entomologica Musei Nationalis Pragae 55: 29–38.

Gil-Santana HR (2016) First description of the male of *Hiranetis atra* Stål and new country records, with taxonomic notes on other species of *Hiranetis* Spinola (Hemiptera, Heteroptera, Reduviidae, Harpactorinae). ZooKeys 605: 91–111. https://doi.org/10.3897/zookeys.605.8797

Gil-Santana HR (2022) New records, taxonomic notes, and the description of a new species of Harpactorinae (Hemiptera: Heteroptera: Reduviidae) from French Guiana. Zootaxa 5105(3): 381–400. https://doi.org/10.11646/zootaxa.5105.3.3

Gil-Santana HR, Forero D (2009) A new species of *Notocyrtus*, a new synonym of *Coilopus*, and new records and notes on other Harpactorini (Hemiptera: Heteroptera: Reduviidae: Harpactorinae) from South America. Zootaxa 2148(1): 55–67. https://doi.org/10.11646/zootaxa.2148.1.5

Gil-Santana HR, Costa LAA, Forero D, Zeraik SO (2003) Sinopse dos Apiomerini, com chave ilustrada para os gêneros (Hemiptera-Heteroptera, Reduviidae, Harpactorinae). Publicações Avulsas do Museu Nacional 97: 1–24.

Gil-Santana HR, Davranoglou L-R, Neves JA (2013) A new synonym of *Graptocleptes bicolor* (Burmeister), with taxonomical notes (Hemiptera: Heteroptera: Reduviidae: Harpactorini). Zootaxa 3700: 348–360. https://doi.org/10.11646/zootaxa.3700.3.2

Gil-Santana HR, Forero D, Weirauch C (2015) Assassin bugs (Reduviidae excluding Triatominae). In: Panizzi AR, Grazia J (Eds) True bugs (Heteroptera) of the Neotropics, Entomology in Focus 2. Springer Science+Business Media, Dordrecht, 307–351. https://doi.org/10.1007/978-94-017-9861-7_12

Gil-Santana HR, Salomão AT, Oliveira J (2017) First description of the male and redescription of the female of *Parahiranetis salgadoi* Gil-Santana (Hemiptera, Reduviidae, Harpactorinae). ZooKeys 671: 19–48. https://doi.org/10.3897/zookeys.671.11985

Hart ER (1975) A new species of *Ischnoclopius* Stål, with notes on the systematic position of the genus (Hemiptera: Reduviidae). Proceedings of the Entomological Society of Washington 94: 162–165.

Hart ER (1986) Genus *Zelus* Fabricius in the United States, Canada, and Northern Mexico (Hemiptera: Reduviidae). Annals of the Entomological Society of America 77(3): 419–425. https://doi.org/10.1093/aesa/79.3.535

Hart ER (1987) The genus *Zelus* Fabricius in the West Indies (Hemiptera: Reduviidae). Annals of the Entomological Society of America 80(2): 293–305. https://doi.org/10.1093/aesa/80.2.293

Haviland MD (1931) The Reduviidae of Kartabo, Bartica District, British Guiana. Zoologica 7(5): 129–154. https://doi.org/10.5962/p.203764

Hespenheide HA (2010) New *Agrilus* Curtis (Coleoptera: Buprestidae) from México and Costa Rica mimicking parasitic wasps. Zootaxa 2545(1): 39–46. https://doi.org/10.11646/zootaxa.2545.1.4

Hogue CL (1993) Latin American Insects and Entomology. University of California Press, Los Angeles, USA, 536 pp.

ICZN [International Comission on Zoological Nomenclature] (1999) International code of zoological nomenclature. 4th edn. The International Trust for Zoological Nomenclature, London. https://www.iczn.org/the-code/

Kirkaldy GW (1909) Hemiptera, old and new, No. 2. Canadian Entomologist 41(11): 388–392. https://doi.org/10.4039/Ent41388-11

Leathers JW, Sharkey MJ (2003) Taxonomy and life history of Costa Rican *Alabagrus* (Hymenoptera: Braconidae), with a key to World species. Contributions in Science 497: 1–78. https://doi.org/10.5962/p.214390

Lethierry L, Severin G (1896) Catalogue général des Hémiptères. Tome III. Hétéroptères. R. Friedländer & Fils, Libraires-Éditeurs, Berlin, 275 pp.

Maldonado CJ (1976) The genus *Heza* (Hemiptera: Reduviidae). The Journal of Agriculture of the University of Puerto Rico 60: 403–433. https://doi.org/10.46429/jaupr.v60i3.10533

Maldonado CJ (1990) Systematic catalogue of the Reduviidae of the World. Caribbean Journal of Science, Special publication No. 1, University of Puerto Rico, Mayagüez, 694 pp.

Maldonado CJ, Lozada RPW (1992) Key to the group of neotropical wasp-mimetic harpactorine genera and the description of a new species (Hemiptera: Reduviidae). Proceedings of the Entomological Society of Washington 94: 162–165.

Martin-Park A, Delfín-González H, Coscarón MC (2012) Revision of genus *Repipta* Stål, 1859 (Hemiptera: Heteroptera: Reduviidae: Harpactorinae) with new species and distribution data. Zootaxa 3501(1): 1–54. https://doi.org/10.11646/zootaxa.3501.1.1

Papavero N (1971) Essays on the history of Neotropical Dipterology, with special reference to collectors (1750–1905). Vol. 1. Universidade de São Paulo, São Paulo, 216 pp. https://doi.org/10.5962/bhl.title.101715

Pikart TG, Souza GK, Ribeiro RC, Zanuncio JC, Serrão JE (2014) Epidermis associated with wax secretion in the *Harpactor angulosus* (Hemiptera: Reduviidae). Annals of the Entomological Society of America 107(1): 227–233. https://doi.org/10.1603/AN13003

Putshkov VG, Putshkov PV (1985) A catalogue of the Assassin-bugs genera of the World (Heteroptera, Reduviidae). Published by the authors, Kiev, 137 pp.

Rédei D, Tsai J-F (2011) The assassin bug subfamilies Centrocnemidinae and Holoptilinae in Taiwan (Hemiptera: Heteroptera: Reduviidae). Acta Entomologica Musei Nationalis Pragae 51: 411–442.

Rosa JA, Mendonça VJ, Rocha CS, Gardim S, Cilense M (2010) Characterization of the external female genitalia of six species of Triatominae (Hemiptera, Reduviidade) by scanning electron microscopy. Memorias do Instituto Oswaldo Cruz 105(3): 286–292. https://doi.org/10.1590/S0074-02762010000300007

Rosa JA, Mendonça VJ, Gardim S, Carvalho DB, Oliveira J, Nascimento JD, Pinotti H, Pinto MC, Cilense M, Galvão C, Barata JMS (2014) Study of the external female genitalia of 14 *Rhodnius* species (Hemiptera, Reduviidae, Triatominae) using scanning electron microscopy. Parasites & Vectors 7(1): 17. https://doi.org/10.1186/1756-3305-7-17

Schuh RT, Weirauch C (2020) True Bugs of the World (Hemiptera: Heteroptera). Classification and natural history, 2nd edn. Siri Scientific Press, Manchester, 767 pp. [32 pls]

Spinola M (1840a) [1837] Essai sur les genres d'insectes appartenants à l'ordre des Hémiptères, Lin. ou Rhyngotes, Fab. et à la section des Hétéroptères, Dufour. Yves Gravier, Gènes, 383 pp. https://doi.org/10.5962/bhl.title.65481

Spinola M (1840b) Essai sur les Insectes Hémiptères Rhyngotes ou Hétéroptères. Chez J.-B. Baillière, Paris, France, 383 pp. https://doi.org/10.5962/bhl.title.48511

Stål C (1859) Till kännedomen om Reduvini. Öfversigt af Kongliga Vetenskaps-Akademiens Förhandlingar 16(8): 363–386.

Stål C (1860) Bidrag till Rio de Janeiro-Traktens Hemipter-Fauna. Kongliga Svenska Vetenskaps-Akademiens Handlingar 2(7): 1–84.

Stål C (1866) Bidrag till Reduviidernas kännedom. Öfversigt af Kongliga Vetenskaps-Akademiens Förhandlingar 23(9): 235–302.

Stål C (1868) Hemiptera Fabriciana. Kongliga Svenska Vetenskaps-Akademiens Handlingar 7: 93–131.

Stål C (1872) Enumeratio Hemipterorum. Bidrag till en företeckning öfver alla hittils kända Hemiptera, jemte systematiska meddelanden. 2. Kongliga Svenska Vetenskaps-Akademiens Handlingar 10(4): 1–159.

Walker F (1873a) Catalogue of the specimens of Hemiptera Heteroptera in the Collection of the British Museum (Part VII). Printed for the Trustees of the British Museum, London, 213 pp.

Walker F (1873b) Catalogue of the specimens of Hemiptera Heteroptera in the Collection of the British Museum (Part VIII). Printed for the Trustees of the British Museum, London, 220 pp.

Wygodzinsky P (1949) Elenco sistematico de los reduviiformes americanos. Instituto de Medicina Regional de la Universidad Nacional de Tucumán. Monografia 1: 1–102.

Zhang G, Hart ER, Weirauch C (2016) A taxonomic monograph of the assassin bug genus *Zelus* Fabricius (Hemiptera: Reduviidae): 71 species based on 10,000 specimens. https://doi.org/10.3897/BDJ.4.e8150

Zhao P, Ren S, Wang B, Cai W (2015) A new species of the genus *Sphedanolestes* Stål, 1866 (Hemiptera: Reduviidae: Harpactorinae) from China, with a key to Chinese species. Zootaxa 3985(4): 591–599. https://doi.org/10.11646/zootaxa.3985.4.8